

UNIVERSITÉ DU LITTORAL CÔTE D' OPALE
CENTRE NATIONAL DE LA RECHERCHE SCIENTIFIQUE
U.M.R. 8101

THÈSE

pour obtenir le grade de
Docteur de l' Université du Littoral Côte d'Opale
Discipline
Physique

présentée et soutenue publiquement par
Konstantinos EFSTATHIOU
le 11 mars 2004

**Métamorphoses de systèmes Hamiltoniens
avec symétries**

Directeur de thèse Boris Zhilinskií

Jury

Charles-Michel Marle	Professeur émérite Université de Paris VI	Président
Yves Colin de Verdière	Professeur Université Grenoble I	Rapporteur
Richard Cushman	Professeur Universiteit Utrecht	Rapporteur
Nikolaií Nekhoroshev	Professeur Université de Milan	Examineur
Dmitrií Sadovskii	Maître de Conférences Co-directeur de thèse Université du Littoral	Examineur
Boris Zhilinskií	Professeur Directeur de thèse Université du Littoral	Examineur

Résumé

Dans ce travail, quatre systèmes hamiltoniens classiques présentant des symétries discrètes ou continues ont été étudiés à l'aide de méthodes et de techniques qui ont été développées au cours des dernières décennies. Trois de ces systèmes sont des familles d'hamiltoniens modélisant des systèmes moléculaires et atomiques. Ces systèmes sont d'une part le mode vibratoire triplement dégénéré des molécules tétraédriques, d'autre part l'atome d'hydrogène dans des champs électriques et magnétiques croisés et enfin la molécule LiCN. L'atome d'hydrogène est naturellement décrit à partir d'une famille à deux paramètres où les paramètres sont les forces des deux champs. Les deux autres systèmes physiques sont décrits comme membres spécifiques de familles paramétriques plus générales. La normalisation (si approprié) et la réduction ont été utilisées afin de réduire le nombre de degrés de liberté de ces familles. Nous nous sommes particulièrement concentrés sur certaines caractéristiques qualitatives de ces systèmes, à savoir, les équilibres relatifs, les bifurcations de Hopf et la monodromie hamiltonienne ainsi que les métamorphoses de ces caractéristiques pour différentes gammes de paramètres. Le quatrième système étudié porte sur la perturbation de deux oscillateurs harmoniques en résonance 1: – 2. Un tel système permet de décrire la dynamique d'un hamiltonien à deux degrés de liberté à proximité d'un équilibre. Pour ce système nous apportons notamment une preuve analytique de l'existence d'une monodromie fractionnaire, qui est une généralisation de la monodromie ordinaire.

Mots clés : Systèmes hamiltoniens, Équilibres relatifs, Monodromie, Monodromie fractionnaire, Symétrie, Réduction, Bifurcation hamiltonienne de Hopf.

Μεταμορφώσεις Χαμιλτονιανών συστημάτων με συμμετρίες

Περίληψη

Σε αυτήν την εργασία μελετάμε τέσσερα κλασικά Χαμιλτονιανά συστήματα με διακριτές ή συνεχείς συμμετρίες χρησιμοποιώντας μεθόδους και τεχνικές που αναπτύχθηκαν τις τελευταίες δεκαετίες. Τρία από αυτά τα συστήματα είναι οικογένειες Χαμιλτονιανών συναρτήσεων οι οποίες μοντελοποιούν μοριακά και ατομικά συστήματα. Αυτά τα συστήματα είναι ο τριπλά εκφυλισμένος τρόπος ταλάντωσης τετραεδρικών μορίων, το άτομο του υδρογόνου σε κάθετα τεμνόμενα ηλεκτρικό και μαγνητικό πεδίο και το μόριο LiCN. Το άτομο του υδρογόνου περιγράφεται εκ φύσεως ως διαπαραμετρική οικογένεια όπου οι παράμετροι είναι οι εντάσεις των δύο πεδίων. Τα άλλα δύο φυσικά συστήματα περιγράφονται σαν συγκεκριμένα μέλη πιο γενικών παραμετρικών οικογενειών. Χρησιμοποιούμε κανονικοποίηση (όπου είναι απαραίτητο) και αναγωγή για να μειώσουμε τους βαθμούς ελευθερίας αυτών των οικογενειών. Εστιάζουμε σε συγκεκριμένα ποιοτικά χαρακτηριστικά αυτών των συστημάτων, όπως, σχετικά σημεία ισορροπίας, Χαμιλτονιανές Χοφ διακλαδώσεις και μονοδρομία, καθώς και στις μεταμορφώσεις αυτών των χαρακτηριστικών σε διαφορετικές περιοχές των παραμέτρων. Το τέταρτο σύστημα είναι μία διαταραχή δύο αρμονικών ταλαντωτών σε συντονισμό 1: -2. Ένα τέτοιο σύστημα μπορεί να περιγράψει την δυναμική σε μια γειτονιά ενός σημείου ισορροπίας μιας Χαμιλτονιανής δύο βαθμών ελευθερίας. Για αυτό το σύστημα δίνουμε μια αναλυτική απόδειξη της ύπαρξης κλασματικής μονοδρομίας, η οποία είναι μια δραστική γενίκευση της συνηθισμένης μονοδρομίας.

Λέξεις κλειδιά: Χαμιλτονιανά συστήματα, Σχετικά σημεία ισορροπίας, Μονοδρομία, Κλασματική μονοδρομία, Συμμετρία, Αναγωγή, Χαμιλτονιανή Χοφ διακλάδωση.

Metamorphoses of Hamiltonian systems with symmetries

Summary

In this work we study four classical Hamiltonian systems with discrete or continuous symmetries using methods and techniques that have been developed in the last decades. Three of these systems are Hamiltonian families which model molecular and atomic systems. These systems are the triply degenerate vibrational mode of tetrahedral molecules, the hydrogen atom in crossed electric and magnetic fields and the floppy molecule LiCN. The hydrogen atom is described naturally as a two parameter family where the parameters are the strengths of the two fields. The other two physical systems are described as specific members of more general parametric families. We use normalization (when appropriate) and reduction in order to reduce the number of degrees of freedom of these families. We focus on certain qualitative characteristics of these systems, namely, relative equilibria, Hamiltonian Hopf bifurcations and monodromy and the metamorphoses of these characteristics in different parameter regions. The fourth system is a perturbation of two harmonic oscillators in 1:-2 resonance. Such a system may describe the dynamics in the neighbourhood of an equilibrium of a two degree of freedom Hamiltonian. For this system we give an analytic proof of the existence of fractional monodromy, which is a radical generalization of standard monodromy.

Keywords: Hamiltonian systems, Relative equilibria, Monodromy, Fractional monodromy, Symmetry, Reduction, Hamiltonian Hopf bifurcation.

Acknowledgments

It is with great pleasure that I have the opportunity to thank many people without whose contribution this work would have never been possible.

Boris Zhilinskiĭ for giving me the opportunity to do this work under his supervision, and the freedom to follow my own path. He has kept me alert throughout this work by marking subtle mistakes and asking difficult questions.

Richard Cushman for sharing with me many of his ideas, answering many questions, having an almost zero turn-around time for corrections to my texts and welcoming me many times at his house in Dordrecht which he made feel warmer than it really was.

Yves Colin de Verdière for his interest in this work and for examining it as a referee.

Charles-Michel Marle for his kind participation in the jury and for assuming the duty of being its president.

Nikolaiĭ Nekhoroshev for his participation in the jury.

Dmitriĭ Sadovskii for helping me immensely during the course of this work while guiding me firmly along the right path. Dmitriĭ has supported and encouraged me along every step and I doubt that without his clarity of thought and sense of organization this work would have finished in a timely manner.

Furthermore, I would like to thank some people whose help although not so evident has been important. I would like to thank James Montaldi for accepting my application to the first Mechanics and Symmetry Summer School that took place in Peyresq, since it was there that I got in touch for the first time with the MASIE network.

I want to thank the European Union without the financial support of which, through the Mechanics And Symmetry In Europe Research Training Network (MASIE RTN)¹, nothing would have been possible and Mark Roberts for coordinating the MASIE network.

In MREID, I would like to thank Frédéric Roussel and Agnès Noyer for their considerable help in preparing my defense. I would also like to thank Chantal Dessailly and Renée Vérove for their administrative assistance and their efforts to understand my French.

Dans MREID, je voudrais remercier Frédéric Roussel et Agnès Noyer pour leur aide considérable dans la préparation de ma soutenance. Je voudrais aussi remercier Chantal Dessailly et Renée Vérove pour leur assistance administrative et leurs efforts à comprendre mon français.

I would like to thank my former supervisors George Contopoulos and Nikos Voglis, whose interest in my current work has been a constant source of encouragement.

Θα ήθελα να ευχαριστήσω τους πρώην επιβλέποντές μου Γεώργιο Κοντόπουλο και Νίκο Βόγγλη, το ενδιαφέρον των οποίων για την τρέχουσα έρευνά μου υπήρξε διαρκής πηγή ενθάρρυνσης.

¹HPRN-CT-2000-00113

I would also like to thank Christos Eftymiopoulos, Panos Patsis, Charis Skokos, Costas Kalapotharakos, Ioannis Stavropoulos, Dora Gaga and Maro Markoulaki for supporting my decision to come to Dunkerque.

Θα ήθελα επίσης να ευχαριστήσω τους Χρίστο Ευθυμιόπουλο, Πάνο Πάτση, Χάρη Σκόκο, Κώστα Καλαποθαράκο, Γιάννη Σταυρόπουλο, Δώρα Γκάγκα και Μάρω Μαρκουλάκη για την υποστήριξή τους στην απόφασή μου να έρθω στην Δουνκέρκη.

Finally, I would like to thank my parents who supported me during my studies and who taught me the respect for intellectual achievement and the relative disrespect for material possessions, both of which I believe are essential for following a scientific career.

Θα ήθελα τέλος να ευχαριστήσω τους γονείς μου οι οποίοι με υποστήριξαν στην διάρκεια των σπουδών μου και οι οποίοι μου δίδαξαν τον σεβασμό για τα πνευματικά επιτεύγματα και την σχετική έλλειψη εκτίμησης για τα υλικά αγαθά, χαρακτηριστικά τα οποία πιστεύω ότι είναι αμφότερα απαραίτητα για μια επιστημονική καριέρα.

Contents

Introduction	15
0 Four Hamiltonian systems	21
0.1 Small vibrations of tetrahedral molecules	21
0.1.1 Description	21
0.1.2 The 2-mode	23
0.1.3 The 3-mode	25
0.2 The hydrogen atom in crossed fields	27
0.2.1 Perturbed Kepler systems	27
0.2.2 Description	27
0.2.3 Normalization and reduction	28
0.2.4 Energy momentum map	29
0.3 Quadratic spherical pendula	31
0.3.1 A spherical pendulum model for floppy triatomic molecules	31
0.3.2 The family of quadratic spherical pendula	32
0.4 Oscillators in $m:-n$ resonance	35
0.4.1 Reduction	35
0.4.2 Fractional monodromy in the $1:-2$ resonance	37
1 Small vibrations of tetrahedral molecules	41
1.1 Introduction	41
1.1.1 The Hamiltonian family	41
1.1.2 Dynamical symmetry. Relative equilibria	43
1.1.3 Symmetry and topology	46
1.2 One-parameter classification	48
1.3 Normalization and reduction	51
1.4 Relative equilibria corresponding to critical points	51
1.5 Relative equilibria corresponding to non-critical points	55
1.5.1 Existence and stability of the $C_s \wedge \mathcal{T}_2$ relative equilibria	56
1.5.2 Configuration space image of the $C_s \wedge \mathcal{T}_2$ relative equilibria	59
1.6 Bifurcations	60
1.7 The 3-mode as a 3-DOF analogue of the Hénon-Heiles Hamiltonian	61
2 The hydrogen atom in crossed fields	63
2.1 Review of the Keplerian normalization	63
2.1.1 Kustaanheimo-Stiefel regularization	63
2.1.2 First normalization	64
2.1.3 First reduction	64

2.2	Second normalization and reduction	67
2.2.1	Second normalization	67
2.2.2	Second reduction	68
2.2.3	Fixed points	68
2.3	Discrete symmetries and reconstruction	69
2.4	The Hamiltonian Hopf bifurcations	71
2.4.1	Local chart	72
2.4.2	Flattening of the symplectic form	72
2.4.3	S^1 symmetry	73
2.4.4	Linear Hamiltonian Hopf bifurcation	74
2.4.5	Nonlinear Hamiltonian Hopf bifurcation	77
2.5	Hamiltonian Hopf bifurcation and monodromy	78
2.6	Description of the Hamiltonian Hopf bifurcation on the fully reduced space	82
2.6.1	The standard situation	82
2.6.2	The hydrogen atom in crossed fields	83
2.6.3	Degeneracy	86
3	Quadratic spherical pendula	87
3.1	Generalities	87
3.1.1	Constrained equations of motion	87
3.1.2	Reduction of the axial symmetry	89
3.2	Classification of quadratic spherical pendula	91
3.2.1	Critical values of the energy-momentum map	91
3.2.2	Reconstruction	93
3.3	Monodromy in the family of quadratic spherical pendula	97
3.3.1	Monodromy in type O and type II systems	98
3.3.2	Non-local monodromy	98
3.4	Quantum monodromy in the quadratic spherical pendula	99
3.5	Geometric Hamiltonian Hopf bifurcations	101
3.6	The LiCN molecule	104
4	Fractional monodromy	107
4.1	The 1:-1 resonance	107
4.2	The 1:-2 resonance	108
4.2.1	The energy-momentum map	108
4.2.2	The integrable foliation	108
4.3	Fractional monodromy in the 1:-2 resonance	112
4.3.1	From regular to fractional monodromy	112
4.3.2	Rotation angle and first return time	115
4.3.3	The period lattice	116
4.3.4	Going through the critical line with the period lattice	117
4.3.5	Quantum fractional monodromy	121
4.3.6	Technical proofs	122
4.4	Fractional monodromy in other resonances	125

5	Conclusions	127
5.1	Triply degenerate vibrational mode of tetrahedral molecules . . .	127
5.2	The hydrogen atom in crossed fields	128
5.3	Quadratic spherical pendula	128
5.4	Fractional monodromy	129
A	The tetrahedral group	131
A.1	Action of the group $T_d \times \mathcal{T}$ on the spaces \mathbf{R}^3 and $T^*\mathbf{R}^3$	131
A.2	Fixed points of the action of $T_d \times \mathcal{T}$ on \mathbf{CP}^2	132
A.3	Subspaces of \mathbf{CP}^2 invariant under the action of $T_d \times \mathcal{T}$	133
A.4	Action of $T_d \times \mathcal{T}$ on the projections of nonlinear normal modes in the configuration space \mathbf{R}^3	134
B	Local properties of equilibria	137
B.1	Stability of equilibria	137
B.2	Morse inequalities and the Euler characteristic	138
B.3	Linearization near equilibria on \mathbf{CP}^2	139
C	Classical and quantum monodromy	141
C.1	Classical monodromy	141
C.2	Quantum monodromy	142
	Personal papers	145
	Bibliography	147

Introduction

V. I. Arnol'd writes in [12] that

The two hundred year interval from the brilliant discoveries of Huygens and Newton to the geometrization of mathematics by Riemann and Poincaré seems a mathematical desert, filled only by calculations.

Although not everyone agrees with this aphorism, Arnol'd has managed to point out in a provocative manner the significance of Poincaré's contribution to modern mathematics. In 1899, Poincaré published the third volume of *Les méthodes nouvelles de la mécanique céleste* [76] where he introduced qualitative methods to the study of problems in classical mechanics and dynamics in general. Poincaré's view of a dynamical system is that of a vector field whose integral curves are tangent to the given vector at each point. He is not interested in the exact solutions of the dynamical equations, which in any case can not be obtained except for a few systems, but in uncovering basic qualitative features, such as the asymptotic behaviour of orbits.

Poincaré's contribution to classical mechanics revolutionized the field. Nevertheless, its impact on the physics community, which would soon go through a different revolution itself, was minimal. In the 1920's quantum mechanics, through the work of Bohr, Schrödinger, Heisenberg, Dirac and many others became the predominant theory for explaining nature. The role of classical mechanics was reduced to that of an introduction to 'real physics' and the field was not considered by physicists to have any scientific interest by itself. H. Goldstein writes characteristically in the preface of the 1950 edition² of [41], trying to justify the necessity of a course in classical mechanics

Classical mechanics remains an indispensable part of the physicist's education. It has a twofold role in preparing the student for the study of modern physics. . .

The effect of Poincaré's contribution was much more apparent in the mathematics community, whose attitude towards classical mechanics was completely different. In a sense, this is justified. When a physical problem is stated in a mathematically precise form, it becomes a problem in mathematics. The time period between Poincaré and the mid-1970's is marked by mathematicians like Lyapunov, Birkhoff, Smale, Arnol'd Moser and Nekhoroshev who follow

²But note that in the preface of the second edition in 1980 the attitude is completely different.

Poincaré's lead in using qualitative methods to tackle difficult questions in dynamical systems theory. They obtain new significant results, like Birkhoff's twist theorem [15], the celebrated KAM theorem [10, 69] and Nekhoroshev's stability estimates [71].

The symplectic formulation of classical mechanics was developed by the mid-60's by many mathematicians among which we mention Ehresmann, Souriau, Lichnerowicz and Reeb. According to the symplectic formulation, a Hamiltonian system is given by a function H defined on a manifold M with a closed non-degenerate two-form ω . This formulation is later popularized in [9, 11, 83].

Two major advances brought classical mechanics back into the physics mainstream. The first of them is the rediscovery in the mid-1960's of deterministic chaos in both conservative [51] and dissipative [57] systems. Even then, more than a decade passed before physicists took notice and finally in the 1980's there was an explosion in the study of nonlinear dynamics and deterministic chaos. This exceedingly complex behaviour of very simple systems fascinated physicists who saw its relevance to real world problems. The fact that a completely deterministic system can behave in an apparently random fashion—an idea taken almost for granted today—changed considerably our view of nature (and in some cases became the source of major philosophical confusion). Moreover the new theory under the more general guise of dynamical systems theory had many applications ranging from galaxies and dynamical astronomy to plasma containment and the stock exchange. One should not forget that classical mechanics is the physical theory that describes mesoscopic scales and therefore it can never become irrelevant.

The second advance happened in the understanding of the relation between the quantum and classical theories. One important postulate of quantum physics is the notion that in the limit $\hbar \rightarrow 0$, classical and quantum mechanics should give quantitatively the same results. But there is a stronger point of view, championed initially by Dirac, according to which the classical theory provides much more than something to which to compare the results of quantum mechanics. Classical mechanics provides a framework for understanding the new mechanics. In this tradition, physicists tried to clarify how the quantum theory is obtained from classical mechanics.

The original Bohr-Sommerfeld quantization condition is generalized by Einstein, Brillouin and Keller (EBK) to integrable systems with two or more degrees of freedom. Keller, Maslov, Leray, Hörmander, de Verdière worked on the linear partial differential equations side of quantum mechanics. In particular Maslov uncovered the topological meaning of the correction term that gives the energy levels of the quantum harmonic oscillator. In the 1970's Kostant and Souriau laid the foundations for geometric quantization [93].

The first semi-classical approximation to quantum mechanics is the WKB series method developed in the 1930's. In the 1970's Gutzwiller discovered his famous trace formula [44], that relates the behaviour of a quantum system to its classical orbits. The importance of Gutzwiller's formula is that it also applies to chaotic systems while the previous methods deal only with the quantization of integrable systems. This opened the field to a series of semi-classical methods that try to increase the understanding of a quantum system by looking at its underlying classical system. The EBK and Gutzwiller methods are based on a thorough knowledge of the classical dynamics that can often be obtained using the qualitative methods introduced by Poincaré in the 1890's.

In these notes we study concrete physical systems from a purely classical viewpoint using mathematical methods that have been developed in the last few decades. Specifically we study the triply degenerate vibrational mode of tetrahedral molecules, the hydrogen atom in crossed electric and magnetic fields, quadratic spherical pendula which model certain floppy molecules and oscillators in $m: -n$ resonance.

Our purpose is to analyze the dynamics of these physical systems in order to uncover their basic qualitative features. For this reason we do not insist on the details of each specific system. Instead we treat these physical systems as specific members of parametric families and consider the *metamorphoses* of the family as the parameters change.

We briefly describe here some notions and techniques that are central to our approach.

Symmetry, continuous (Lie) or discrete, is the common thread that binds together the systems studied in this work. By Noether's theorem, continuous symmetries correspond to the existence of first integrals of the Hamiltonian system. Taking advantage of first integrals we define *reduced* Hamiltonians with fewer degrees of freedom.

Reduction of continuous symmetries, goes at least back to Jacobi and the elimination of the nodes in the restricted three body problem. The modern version of regular reduction (also called Marsden-Weinstein reduction) was introduced in [59]. In order to do regular reduction the group action must be free and proper. If this is not true, we perform singular reduction which was developed by Cushman in order to deal with exactly these cases. In this work we do reduction using *algebraic invariant theory*.

Relative equilibria are periodic orbits of the original symmetric system which are also group orbits of an \mathbf{S}^1 action. These basic objects play an important role in the study of a system since they serve as organizing centers of its dynamical behavior.

Normalization is used to make exact some otherwise approximate dynamical symmetries. We use the standard Lie series algorithm [27, 43]. There are three different types of normalization used in this work. The first is the standard oscillator normalization, in which the unperturbed Hamiltonian describes an oscillator. The second type is normalization in a Poisson algebra. In our case the algebra $\mathfrak{so}(3) \times \mathfrak{so}(3)$ appears in the study of the hydrogen atom in crossed fields. The third type is nilpotent normalization in the proof of the Hamiltonian Hopf bifurcations in the hydrogen atom and the quadratic spherical pendula.

Monodromy is a common characteristic of most of these systems. Monodromy, introduced in [29], is the crudest topological obstruction to the existence of global action-angle variables in an integrable Hamiltonian system with two or more degrees of freedom. In this work we have three qualitatively different types of monodromy namely standard, non-local and fractional. The first two appear in the hydrogen atom in crossed fields and the quadratic spherical pendula while the third appears in the 1:-2 resonance.

Hamiltonian Hopf bifurcations are related to standard and non-local monodromy. We explore this relation in detail in the hydrogen atom in crossed fields and in the quadratic spherical pendula.

We describe now in more detail the physical systems that we study in this work.

Tetrahedral molecules. The first system that we study is the triply degenerate vibrational mode of tetrahedral molecules of type X_4 , e.g. P_4 . This system is invariant with respect to the tetrahedral group T_d extended by the time reversal symmetry \mathcal{T} . It is described by a three degree of freedom Hamiltonian which is a perturbation of the 1:1:1 resonant harmonic oscillator.

Instead of considering specific tetrahedral molecules we consider a three degree of freedom Hamiltonian family in which the potential is the most general T_d invariant polynomial up to terms of order 4 defined in \mathbf{R}^3 with coordinates x, y, z . This Hamiltonian family depends on parameters that are not physically tunable because they depend on quantities like the atom masses that are fixed for each molecule. Nevertheless, we study the whole family in order to uncover all possible qualitatively different types of tetrahedral molecules and observe the metamorphoses that happen when the parameters change.

Models of this kind have been widely studied in molecular applications [50, 75]. They are 3-DOF analogues of the 2-DOF Hamiltonians that were used to describe the doubly degenerate vibrational modes of molecules whose equilibrium configuration has one or several threefold symmetry axes [78] like H_3^+ , P_4 , CH_4 and SF_6 . Such two degree of freedom systems with threefold symmetry are described by the 2-DOF Hénon-Heiles Hamiltonian [51]. Therefore, we can consider our Hamiltonian as a natural 3-DOF analogue of the latter. One should also draw attention to [2] where the vibrational and rotational modes of a tetrahedral molecule are studied together, and [1] where critical points of discrete subgroups of $SO(3) \times \mathcal{T}$, including $T_d \times \mathcal{T}$, are classified in terms of their possible types of linear stability.

The hydrogen atom in crossed fields. The second system is the hydrogen atom in perpendicular electric and magnetic homogeneous fields. This is a perturbed Kepler system. This and similar systems, have been studied extensively [23, 33, 38, 39, 80, 81] (see also [24] and references therein). In [24] it was proven that the system has *monodromy* for a range of the relative field strengths. The approach in [24] uses second normalization and reduction, in the spirit of [19, 86]. Our work is a continuation of [24]. Specifically, we prove the existence of two *Hamiltonian Hopf* bifurcations and we show in detail that the appearance of monodromy is related to these bifurcations.

The Hamiltonian Hopf bifurcation was first discovered in the \mathcal{L}_4 Lagrange point of the planar restricted three body problem. It was studied analytically and numerically in a series of papers [16, 28, 74] and proved finally in [61]. Certainly, the most influential work on this type of bifurcation is [85] where it was studied in detail and a systematic method for proving its existence was given. When an equilibrium of a Hamiltonian system with two degrees of freedom is elliptic-elliptic, by a theorem of Weinstein [90] there exists a family of periodic orbits emanating from this point. In the standard Hamiltonian Hopf

bifurcation, the equilibrium becomes complex hyperbolic. Then two different things may happen to the attached family of periodic orbits. It either detaches from the equilibrium or it disappears completely. The two scenarios are called respectively *supercritical* and *subcritical* Hamiltonian Hopf bifurcation.

It is known [31, 85] that the supercritical Hamiltonian Hopf bifurcation is related to the existence of monodromy. We show here, how the *subcritical* Hamiltonian Hopf bifurcation in our system is related to a generalized type of monodromy, that we call *non-local monodromy*.

Floppy molecules. The third system that we study was introduced [5] as a model of ‘floppy molecules’ like HCN or LiCN. We model such a system as a point mass constrained to move on the surface of a sphere. The whole system is placed inside an axisymmetric potential field $V(z) = \frac{1}{2}bz^2 + cz$ where b, c are parameters. Notice that this is a generalization of the *linear* spherical pendulum where $V(z) = z$. We call this parametric Hamiltonian family *quadratic spherical pendula*. The family of quadratic spherical pendula is a simple system that brings together Hamiltonian Hopf bifurcations, standard monodromy and non-local monodromy.

In the case of standard monodromy we consider a closed path Γ in the set of regular values of the energy-momentum map \mathcal{EM} which goes around a critical value c of \mathcal{EM} . In the linear spherical pendulum c lifts to a singly pinched torus and The bundle $\mathcal{EM}^{-1}(\Gamma) \rightarrow \Gamma$ is a regular \mathbf{T}^2 bundle. Generalizations of this case appeared over time. Thus, systems with more than one critical values or critical values that lift to doubly or more generally k -pinched tori [14] and systems with three degrees of freedom such as the Lagrange top [25] were studied. All these generalizations are within the context of Duistermaat’s original proposal to consider \mathbf{T}^2 bundles over a closed path in the set of regular values of the \mathcal{EM} . Non-local monodromy [89] generalizes even more such examples of systems with monodromy in the sense that we consider paths that go around a *curve segment* of singular values of the \mathcal{EM} map in a way that is explained in detail in chapter 3. Nevertheless, notice that the essence of non-local and standard monodromy is the same since in both cases we consider the monodromy of a regular \mathbf{T}^2 bundle.

In the family of quadratic spherical pendula the two equilibria at the ‘north’ and ‘south’ poles of the sphere can change linear stability type from degenerate elliptic (two identical imaginary frequencies) to degenerate hyperbolic (two identical real frequencies). This situation is due to the rotational symmetry around the z -axis and the time-reversal symmetry. This is a generalized kind of Hamiltonian Hopf bifurcation [46], that we call *geometric Hamiltonian Hopf* bifurcation. It is qualitatively indistinguishable from the standard one in terms of the behaviour of short period orbits near the equilibria although the linear behaviour, i.e. the motion of the frequencies, is different.

Resonant oscillators. The fourth and final system that we study is oscillators in $m:n$ resonance, where m, n can be any non-zero integers with $\gcd(m, n) = 1$. These systems do not model a specific physical system but are usually used as models of the dynamics near resonant equilibria.

For certain values of $m:n$, e.g. $1: -2$ we find that in the image of the energy-momentum map \mathcal{EM} there is a curve \mathcal{C} of critical values of \mathcal{EM} that

we can not enclose with a path because it joins at one end the boundary of the image of \mathcal{EM} . Points on \mathcal{C} lift to singular curled tori in the phase space. Nevertheless, we can consider a path Γ that crosses \mathcal{C} and we prove that in this case it is possible to define another generalized type of monodromy that we call *fractional monodromy*. The concept of fractional monodromy is a radical departure from the original notion of monodromy in [29] since $\mathcal{EM}^{-1}(\Gamma)$ is not a regular \mathbf{T}^2 bundle over Γ .

Fractional monodromy was proposed by Zhilinskií for the 1: – 2 resonance. It was proven geometrically by Nekhoroshev, Sadovskii and Zhilinskií [72, 73]. In this work we give, an alternative and more ‘traditional’ analytic proof of fractional monodromy using the notion of the period lattice, introduced in the study of monodromy by Duistermaat and Cushman.

0

Four Hamiltonian systems

We describe the four Hamiltonian systems that we study in this work and state our objectives for each system.

0.1 Small vibrations of tetrahedral molecules

The first Hamiltonian system is a model of the triply degenerate vibrational mode of a four atomic molecule of type X_4 with tetrahedral symmetry. The model has certain similarities with the two degree of freedom Hénon-Heiles Hamiltonian that has been used in order to model the doubly degenerate vibrational mode. In this section we describe X_4 molecules in general and then we concentrate on the doubly and triply degenerate vibrational modes.

0.1.1 Description

Consider a molecule of type X_4 which at equilibrium has the shape of a tetrahedron. The symmetry of the equilibrium configuration is given by the tetrahedral group T_d which we describe in detail in appendix A.

A molecule rotates as a whole about its center of mass and its atoms vibrate around the equilibrium positions. We assume here that the vibrations of the atoms are small compared to the dimensions of the molecule. In order to make this point clear one can forget the molecule altogether and think of a system of point masses on the vertices of a tetrahedron that are connected by very stiff identical springs. All the standard approximations apply to our model (the springs do not have any mass, they do not bend etc.).

The most central notion in the study of small vibrations of a molecule is that of linear normal modes. The theory of small vibrations can be found in many introductory books on classical mechanics and so we will be brief. Consider small vibrations of the atoms and describe the positions of all the atoms by a displacement vector x that has 12 components; 3 for each one of the 4 atoms. Then the linearized equations of motion for the small vibrations can be put into the form $\ddot{x} = M \cdot x$ where M is a constant matrix. Diagonalization of M gives the eigenvalues $0(\times 6)$, $-4\omega^2(\times 1)$, $-\omega^2(\times 2)$ and $-2\omega^2(\times 3)$. Here $\omega^2 = k/m$ where k is the spring constant for the atom-atom bonds and m is the mass of the atoms.

The six 0 eigenvalues correspond to translational and rotational motions of the molecule. The eigenvalue $-4\omega^2$ corresponds to a *breathing* motion of the molecule. The linear space spanned by the corresponding eigenvector ρ_1 realizes the one-dimensional representation A_1 of T_d .

Of considerably more interest are the doublet and triplet of eigenvalues of M . The space spanned by the eigenvectors ρ_2, ρ_3 corresponding to the pair of eigenvalues $-\omega^2$ realizes the two-dimensional irreducible representation E of T_d . Notice here that we always choose the vectors ρ_2 and ρ_3 so that they are orthonormal, i.e. we use unitary representations. In an appropriate system of coordinates the image of T_d on the representation spanned by the E mode is D_3 (the dihedral group of order 3 or the group of all symmetries of an equilateral triangle).

Finally, the eigenvectors of the triplet of eigenvalues $-2\omega^2$ span a linear space that realizes the F_2 irreducible representation of T_d . F_2 is a vector representation and this means in particular that the action of T_d on this space is identical to the action of T_d on the physical 3-space. We use coordinates q_1, \dots, q_6 to describe the 3 modes so the most general vibrational displacement can be expressed as a sum $r = \sum_{j=1}^6 q_j \rho_j$.

Separation of the rotating and vibrating motions is not trivial. One way to achieve this is by the method of Eckart frames which works very well in the case of small vibrations of a nonlinear molecule [58,92]. The result of this method is a Hamiltonian of the form

$$H(q, p; j) = \frac{1}{2} \sum_j p_j^2 + \frac{1}{2} (\ell - \pi)^\dagger \mathcal{I}(q) (\ell - \pi) + U(q) \quad (0.1)$$

Here ℓ is the total angular momentum of the molecule, π is a vibrationally induced angular momentum—its three components being expressions of (q, p) —and $\mathcal{I}(q)$ is the inverse of the modified inertia matrix.

$U(q)$ is the potential energy of the molecule. As in our simple model we choose a harmonic two-center interaction between the atoms. Notice though that this does not mean that the potential is quadratic in q . Specifically, we have that

$$U = \frac{k}{2} \sum_{\alpha\beta} (|r_\alpha + R_\alpha - r_\beta - R_\beta| - |R_\alpha - R_\beta|)^2 \quad (0.2)$$

where the sum runs over pairs $\alpha\beta$ of atoms. In particular $U(q)$ is not polynomial. In order to have a polynomial form for U we Taylor expand in terms of q and we truncate the resulting series at the desired order. This procedure introduces nonlinear terms in the potential and interaction terms between the different linear modes. The general form of these nonlinear terms can be predicted using symmetry arguments.

In the following sections we will consider each vibrational mode independently. This means that we ‘freeze’ the other modes by setting the respective coordinates equal to zero and study only one particular mode. Alternatively, we can normalize the complete six degree of freedom system which is the perturbation of a six-oscillator. This system is composed of two parts which are not in resonance between them. The first part corresponds to the F_2 representation and represents a 3-oscillator in 1:1:1 resonance. The second part corresponds to the $A \oplus E$ representation and represents a 3-oscillator in 1:1:2 resonance. Notice that in this way we can isolate the 3-mode F_2 from the rest,

but we can not do the same for the 2-mode E which is in resonance with the 1-mode A .

0.1.2 The 2-mode

The image of $T_d \times \mathcal{T}$ in the E representation spanned by the E mode coordinates q_2, q_3 is the dihedral group D_3 (the group of all symmetries of an equilateral triangle). Therefore, the Hamiltonian that describes the E mode must be a D_3 invariant perturbation of the two degrees of freedom harmonic oscillator in 1:1 resonance.

Such a Hamiltonian was considered in [51] by Michel Hénon and Carl Heiles in an attempt to study the existence of a third integral of motion in galactic dynamics. Because it is D_3 invariant (a feature that was probably unintended) it can serve (and has been used, see [17, 18]) as a model of the E mode. The concrete Hamiltonian is

$$H(x, y, p_x, p_y) = \frac{1}{2}(p_x^2 + p_y^2 + x^2 + y^2) + 2y(x^2 - \frac{1}{3}y^2) \quad (0.3)$$

and it is known as the Hénon-Heiles Hamiltonian (we use the notation x, y instead of q_2, q_3).

One of the most important consequences of the $D_3 \times \mathcal{T}$ symmetry is the existence of 8 *nonlinear normal modes* (usually denoted $\Pi_{1, \dots, 8}$) for the Hénon-Heiles Hamiltonian and indeed for every $D_3 \times \mathcal{T}$ invariant perturbation of the 1:1 resonance (see figure 0.3). In order to gain some understanding on the origin of the nonlinear normal modes and some appreciation of the methods that we will use later for the 3-mode case we show how we can predict the existence of these modes using only symmetry arguments.

The reduced phase space for the 1:1 resonance is a sphere \mathbf{S}^2 parametrized by the invariants j_1, j_2, j_3 subject to the relation $j_1^2 + j_2^2 + j_3^2 = j^2$ (see [20]).

Nonlinear normal modes correspond to equilibria of the reduced system and by virtue of Michel's theorem [62] every critical point of the action of $D_3 \times \mathcal{T}$ on \mathbf{S}^2 is an equilibrium of the reduced system. Therefore, in the search for the equilibria of the reduced Hamiltonian our first stop must be the critical points of the $D_3 \times \mathcal{T}$ action.

Lemma 0.1. *The action of $D_3 \times \mathcal{T}$ on \mathbf{S}^2 has 8 isolated critical points.*

Isotropy group	Coordinates
$C_3 \wedge T_2$	$(0, \pm j, 0)$
$C_2 \times \mathcal{T}$	$(0, 0, j), \frac{j}{2}(\pm\sqrt{3}, 0, -1)$
$C_2' \times \mathcal{T}$	$(0, 0, -j), \frac{j}{2}(\pm\sqrt{3}, 0, 1)$

Proof. $D_3 \times \mathcal{T}$ has generators C_3, C_2 and T which act on j_1, j_2, j_3 in the following way. C_3 is rotation by $2\pi/3$ about the j_2 axis, C_2 sends $j_1 \rightarrow -j_1$ and T sends $j_2 \rightarrow -j_2$. It is now easy to check that the only critical points of the $D_3 \times \mathcal{T}$ action on \mathbf{S}^2 are the ones given in the lemma. \square

The points given in the last lemma are equilibria of any $D_3 \times \mathcal{T}$ invariant Hamiltonian on \mathbf{S}^2 . In order to simplify the rest of the analysis and determine the type of these equilibria (maxima, minima or saddle points) we take into account the discrete symmetry.

Lemma 0.2. *The ring $\mathbf{R}[j_1, j_2, j_3]^{D_3 \times \mathcal{T}}$ of $D_3 \times \mathcal{T}$ invariant polynomials in the variables j_1, j_2 and j_3 is generated freely by $j, \mu_2 = j_2^2$ and $\mu_3 = j_3(3j_1^2 - j_3^2)$.*

Proof. The Molien generating function for the action of $D_3 \times \mathcal{T}$ on (j_1, j_2, j_3) is

$$g(\lambda) = \frac{1}{(1 - \lambda^2)(1 - \lambda^3)} \quad (0.4)$$

Therefore the ring $\mathbf{R}[j_1, j_2, j_3]^{D_3 \times \mathcal{T}}$ is generated freely by two invariants of orders 2 and 3 in $j_i, i = 1, 2, 3$ respectively. \square

Notice here that the terms j and μ_2 have a higher symmetry than $D_3 \times \mathcal{T}$. Specifically, j is $O(3)$ invariant (it remains invariant under any rotation of the sphere \mathbf{S}^2 and inversion through the origin), while μ_2 is $O(2)$ invariant (it remains invariant under any rotation of the sphere around the j_2 -axis and inversion).

The last lemma allows to conclude that normalization and reduction of the Hénon-Heiles Hamiltonian (0.3) gives a reduced Hamiltonian which is a function of j, μ_2 and μ_3 . Since normalization up to order ϵ^2 can only contain the term j of degree 2, and μ_2, j^2 of degree 4 which have a higher symmetry than $D_3 \times \mathcal{T}$ we need to normalize up to order ϵ^4 in order to reproduce completely the symmetry of the original Hamiltonian. For this reason, normalization only up to order ϵ^2 gives a circle of degenerate equilibria on \mathbf{S}^2 . The resolution of this rather obvious degeneracy (which was known as the problem of critical inclination) puzzled astronomers that studied the Hénon-Heiles Hamiltonian until the 80's when it was finally resolved [18].

More concretely, consider the reduced Hénon-Heiles Hamiltonian which up to order ϵ^4 has the general form

$$\widehat{H} = j + \epsilon^2(a j^2 + b \mu_2) + \epsilon^4(c j \mu_2 + d \mu_3) \quad (0.5)$$

where a, b, c, d are real nonzero numbers. Subtracting constant terms, gathering together the term $b + \epsilon^2 c j = e$ and dividing by ϵ^2 we write

$$\widehat{H} = e \mu_2 + \epsilon^2 d \mu_3 \quad (0.6)$$

This is the most general form of the ϵ^4 reduced Hamiltonian. Notice that we wrote this expression taking into account only the symmetry of the Hamiltonian (0.3) and without explicit normalization. Of course this latter step is needed if we want to compute the exact values of d and e .

Lemma 0.3. *The orbit space $\mathbf{S}^2 / (D_3 \times \mathcal{T})$ is a two dimensional semialgebraic variety which can be represented as the closed subset of \mathbf{R}^2 with coordinates (μ_3, μ_2) enclosed between the curves $s \mapsto ((2s - 1)j^3, 0)$, $s \mapsto (s^3 j^3, (1 - s^2)j^2)$ and $s \mapsto (-s^3 j^3, (1 - s^2)j^2)$ where $s \in [0, 1]$ in all cases (see figure 0.1).*

Proof. Find the image of \mathbf{S}^2 under the reduction map $(j_1, j_2, j_3) \mapsto (\mu_3, \mu_2)$. \square

In figure 0.2 we see the two types of reduced Hamiltonians (0.6) in general position, i.e. when d and e are non zero. The straight curves represent the level curves of the reduced Hamiltonian, i.e. they are solutions of the equation $h = e \mu_2 + \epsilon^2 d \mu_3$ for different h . In the first case the function has one minimum,

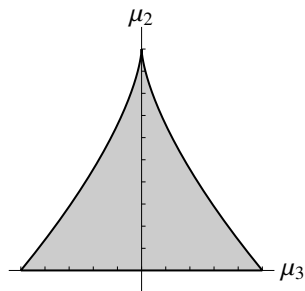


Figure 0.1: Fully reduced space $\mathbf{S}^2/(D_3 \times T)$.

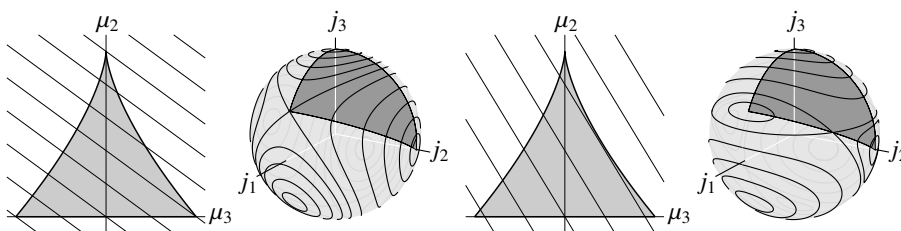


Figure 0.2: Types of $D_3 \times T$ invariant Hamiltonians on \mathbf{S}^2 . For each type we show the level curves of the Hamiltonian $e\mu_2 + \epsilon^2 d\mu_3$ on the fully reduced space and the intersections of the level sets of the Hamiltonian with the reduced phase space \mathbf{S}^2 . There is an 1-1 mapping between the dark gray patch on \mathbf{S}^2 and the fully reduced phase space $\mathbf{S}^2/(D_3 \times T)$.

one maximum and one saddle point in the fully reduced space. On \mathbf{S}^2 they lift back to three minima, three saddle points and two maxima. The reduced Hénon-Heiles system falls in this case since for small ϵ the lines defined by $\mu_2 = \frac{1}{e}(h - d\epsilon^2\mu_3)$ have small slope.

The equilibria of the reduced Hamiltonian correspond to nonlinear normal modes. Therefore in this case we have three stable modes $\Pi_{1,2,3}$ with stabilizer $C_2 \times T$, three unstable modes $\Pi_{4,5,6}$ with stabilizer $C_2' \times T$ and two more stable modes $\Pi_{7,8}$ with stabilizer $C_3 \wedge T_2$. These normal modes are described in more detail in [17, 18, 66, 78] (figure 0.3).

In the second case the function has two maxima, one minimum and one saddle point on the fully reduced space. These lift back to five maxima, six saddle points and three minima on \mathbf{S}^2 . Notice that when we pass from one type to the other we have a pitchfork bifurcation where each saddle point spawns two new saddle points while itself becomes stable.

0.1.3 The 3-mode

We now turn our attention to the triply degenerate vibrational linear mode F_2 . In this section we ‘freeze’ again all the other modes of the molecule. The action of T_d on its irreducible representation F_2 is identical to the T_d action on the physical space. This is again described in detail in appendix A.

The action of T_d on the phase space $T^*\mathbf{R}^3 = \mathbf{R}^6$ is induced by the cotangent lift of each element of T_d . Specifically, if R is the image of an element of T_d in

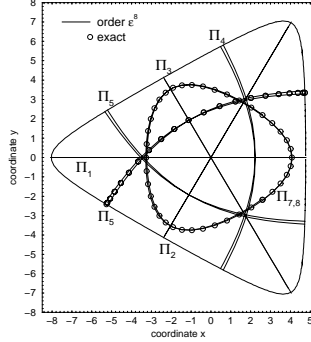


Figure 0.3: Nonlinear normal modes of the Hénon-Heiles Hamiltonian.

the representation F_2 , then its action on \mathbf{R}^6 is given by the matrix $\begin{pmatrix} R & 0 \\ 0 & R \end{pmatrix}$.

We change notation for the coordinates in the F_2 mode from (q_4, q_5, q_6) to (x, y, z) . The Taylor expanded potential $U(q)$ restricted to this mode becomes a function $U(x, y, z)$ that we denote by the same letter. The Taylor expansion of the potential $U(x, y, z)$ is a T_d invariant function. The following lemma gives information on the form of $U(x, y, z)$.

Lemma 0.4. *The ring of T_d invariant polynomials $\mathbf{R}[x, y, z]^{T_d}$ is freely generated by $\mu_2 = x^2 + y^2 + z^2$, $\mu_3 = xyz$ and $\mu_4 = x^4 + y^4 + z^4$.*

Proof. The Molien function for the action of T_d on $\mathbf{R}_{x,y,z}^3$ is

$$M(\lambda) = \frac{1}{|T_d|} \sum_{g \in T_d} \frac{1}{\det(1 - \lambda g)} = \frac{1}{(1 - \lambda^2)(1 - \lambda^3)(1 - \lambda^4)} \quad (0.7)$$

The meaning of this Molien function is that $\mathbf{R}[x, y, z]^{T_d}$ is freely generated by invariant polynomials in x, y, z of degrees 2, 3 and 4. The specific expressions for these polynomials can be computed by acting with the projection operator $\frac{1}{|T_d|} \sum_{g \in T_d} g$ on the spaces of polynomials of order 2, 3 and 4 respectively. \square

This means that the most general form of the Taylor expansion of the potential is

$$U(x, y, z) = \frac{1}{2}\mu_2 + \epsilon K_3 \mu_3 + \epsilon^2 K_4 \mu_4 + \epsilon^2 K_0 \mu^2 + \dots \quad (0.8)$$

The coefficients K_0, K_3, K_4 are real numbers of order 1. The positive number ϵ is a smallness parameter that we use to keep track of the degree of each term.

The ‘rotational’ part $\frac{1}{2}\pi^t \mathcal{I}(q) \pi$ (remember that we consider that we have no rotation i.e. $\ell = 0$) of the complete Hamiltonian of the molecule (0.1) also contributes to the terms of degree 4 of the F_2 mode Hamiltonian with the term $[(x, y, z) \times (p_x, p_y, p_z)]^2$. The symmetry of this term is $O(3)$.

Therefore the most general (modulo a time rescaling that sets the frequency to 1) F_2 mode Hamiltonian that we can have up to terms of degree 4 is

$$H(x, y, z, p_x, p_y, p_z) = \frac{1}{2}(p_x^2 + p_y^2 + p_z^2) + \epsilon^2 K_R [(x, y, z) \times (p_x, p_y, p_z)]^2 + \frac{1}{2}\mu_2 + \epsilon K_3 \mu_3 + \epsilon^2 K_4 \mu_4 + \epsilon^2 K_0 \mu^2 \quad (0.9)$$

The last equation defines a 4 parametric family of Hamiltonian systems. We have now reached the point where we can state the first of our objectives.

Objective *Classify generic members of family (0.9) in terms of their nonlinear normal modes and their types of linear stability. Describe the different forms of these generic members.*

0.2 The hydrogen atom in crossed fields

The second Hamiltonian system is the hydrogen atom in crossed electric and magnetic fields. This is only one system of the class of perturbed Kepler systems. All systems in this class can be studied using the same techniques.

0.2.1 Perturbed Kepler systems

The Kepler problem is perhaps the single most important, influential and paradigmatic problem of classical mechanics. Most of the questions that are studied in classical mechanics arose studying this problem and its perturbations.

In its simplest integrable form the Kepler problem is the problem of the motions of a body in a central potential field of type $1/r$. There are two well known incarnations of the problem. The first is the two-body problem in which two bodies of mass m_1 and m_2 move under the mutual influence of their gravitational fields. The second is the classical non-relativistic model of the hydrogen atom in which an electron moves around a proton. The Hamiltonian in both cases (considering appropriate systems of units and moving to the center of mass frame) is

$$H_0(Q, P) = \frac{1}{2}\mathbf{P}^2 - \frac{1}{|\mathbf{Q}|} \quad (0.10)$$

where $\mathbf{Q} = (Q_1, Q_2, Q_3)$ are coordinate functions in \mathbf{R}^3 and $\mathbf{P} = (P_1, P_2, P_3)$ their conjugate momenta.

We work with a class of perturbed Kepler systems for which the perturbation is polynomial in Q, P . One such example is the lunar problem which is essentially the restricted three body problem for a large value of the Jacobi constant. Another one is dust orbiting around a planet under the influence of radiation pressure and a third is the artificial satellite problem [19].

A completely different field in which we have the same types of perturbed Keplerian problems is atomic physics. The hydrogen atom in electric and/or magnetic fields can be modeled as a perturbed Kepler system. Notable variations on this theme are the hydrogen atom in homogeneous electric field (Stark effect), in weak homogeneous magnetic field (linear Zeeman effect), in strong magnetic field (quadratic Zeeman effect), and in parallel or perpendicular electric and magnetic fields.

0.2.2 Description

We consider the classical motion of the electron of the hydrogen atom in homogeneous perpendicularly crossed electric and magnetic fields. We work in a

system of units in which the electric charge of the electron is -1 and its mass is 1 . By ‘classical’ we mean that we ignore all relativistic effects and spin. Moreover, we assume that because the proton mass is much larger than that of the electron, the proton stays fixed at the origin of our coordinate system (Q_1, Q_2, Q_3) in \mathbf{R}^3 .

The electric field points along the Q_2 -axis, and is given by $\mathbf{E} = (0, F, 0)$. The corresponding potential energy is $\phi_e = FQ_2$. The magnetic field is given by $\mathbf{B} = (G, 0, 0)$. The corresponding vector potential is

$$\mathbf{A} = \frac{1}{2}\mathbf{B} \times \mathbf{Q} = \frac{1}{2}G(0, -Q_3, Q_2) \quad (0.11)$$

The motion of the electron is described by the Hamiltonian

$$H(Q, P) = \frac{1}{2}(\mathbf{P} + \mathbf{A})^2 + \phi_c + \phi_e \quad (0.12)$$

where $\phi_c = -\frac{1}{|\mathbf{Q}|}$ is the Coulomb potential. Direct substitution of the expressions for \mathbf{A} , ϕ_e and ϕ_c into (0.12) and some algebra gives

$$H(Q, P) = \frac{1}{2}\mathbf{P}^2 - \frac{1}{|\mathbf{Q}|} + FQ_2 + \frac{1}{2}G(Q_2P_3 - Q_3P_2) + \frac{1}{8}G^2(Q_2^2 + Q_3^2) \quad (0.13)$$

The last two terms in (0.13) describe the linear and quadratic Zeeman effect. If the magnetic field is weak the last term may be omitted. Then, the resulting Hamiltonian is identical to the Hamiltonian that describes the orbiting dust problem [86].

0.2.3 Normalization and reduction

The treatment of all systems in the class of perturbed Kepler systems is very similar. We concentrate here on the hydrogen atom in crossed fields but one should keep in mind that the same techniques can be applied to other systems in this class. The whole procedure consists of regularization of the Kepler problem, first normalization and reduction, second normalization and reduction and reduction of the discrete symmetry of the problem. We explain these steps in more detail. Note here that second normalization may not be necessary or may not be applicable in other systems. We come back to this point later.

The first step in the study of the hydrogen atom in crossed fields is *Keplerian normalization* which consists of regularization of the singularity of the Kepler potential and normalization of the resulting system [33–35, 53, 55, 80, 81]. Different types of regularization have been used for this type of problems. Indicatively we mention, Levi-Civita regularization [56] and Delaunay regularization in [19, 86].

In this work we use Kustaanheimo-Stiefel (KS) regularization [54]. The result of KS regularization is a Hamiltonian that is a perturbation of the harmonic oscillator in 1:1:1:1 resonance. The regularized system has a first integral of motion (except the energy) that we call the KS integral ζ . This means that it has an extra \mathbf{S}^1 symmetry due to the flow of the Hamiltonian vector field associated to ζ .

Moreover, the system has an approximate dynamical \mathbf{S}^1 symmetry induced by the 1:1:1:1 resonance i.e. the unperturbed part of the regularized Hamiltonian. The normalization of the regularized system with respect to this symmetry can then be easily performed using standard techniques from normal form theory, like the Lie series algorithm [27].

The next step is the reduction of the first normalized Hamiltonian in terms of the $\mathbf{S}^1 \times \mathbf{S}^1 = \mathbf{T}^2$ oscillator and KS symmetry. This first reduction gives a Poisson system defined on $\mathbf{S}^2 \times \mathbf{S}^2$. The dynamical variables on $\mathbf{S}^2 \times \mathbf{S}^2$ span the algebra $\mathfrak{so}(4) = \mathfrak{so}(3) \times \mathfrak{so}(3)$.

The important property of the crossed fields system is that the first reduced system has yet another approximate \mathbf{S}^1 axial symmetry. Note that other systems in the class of perturbed Kepler problems, for example the hydrogen atom in homogeneous electric field, have an exact \mathbf{S}^1 symmetry. In both cases we proceed in essentially the same way. The only difference is that in the case studied here we first have to do the second normalization in order to turn the approximate dynamical symmetry into an exact one. Obviously such normalization is not necessary in the case that the \mathbf{S}^1 symmetry is exact. Moreover, note that in many cases there is no extra \mathbf{S}^1 symmetry, neither exact nor approximate. In that case we can not do the second normalization and reduction and we have to work on the first reduced space $\mathbf{S}^2 \times \mathbf{S}^2$.

To continue, we perform a second normalization and reduction with respect to the axial \mathbf{S}^1 symmetry. We perform the second normalization using the Lie series algorithm [27, 43] for the standard Poisson structure on $\mathfrak{so}(3) \times \mathfrak{so}(3)$. The result is an one degree of freedom integrable Poisson system. Let us denote by n the value of the oscillator integral with respect to which we did the first normalization and by c the value of the generator of the \mathbf{S}^1 symmetry with respect to which we did the second normalization. The reduced phase space $V_{n,c}$ is diffeomorphic to a 2-sphere except for two cases. First, for $c = 0$ where $V_{n,0}$ is only homeomorphic to a sphere and has two conical singularities. Second, for $c = \pm n$ where $V_{n,\pm n}$ are each a single point. The singular points of $V_{n,0}$ and the single points that constitute $V_{n,\pm n}$ correspond to equilibria of the second normalized system on $\mathbf{S}^2 \times \mathbf{S}^2$.

The last step is to reduce the discrete symmetry of the system. One can easily see that the original perturbed Kepler system has a $\mathbf{Z}_2 \times \mathbf{Z}_2$ symmetry, generated by reflections

$$(Q_1, Q_2, Q_3, P_1, P_2, P_3) \rightarrow (-Q_1, Q_2, Q_3, -P_1, P_2, P_3)$$

and reflections-time reversals

$$(Q_1, Q_2, Q_3, P_1, P_2, P_3) \rightarrow (Q_1, Q_2, -Q_3, -P_1, -P_2, P_3)$$

These discrete symmetries are system specific. Therefore, this step may not apply to other perturbed Keplerian systems. The orbit space of this discrete symmetry is depicted in figure 0.4.

0.2.4 Energy momentum map

The \mathcal{EM} map of the system is defined on $\mathbf{S}^2 \times \mathbf{S}^2$ as

$$\mathcal{EM}(p) = (\tilde{\mathcal{H}}(p), \tilde{\mathcal{H}}_1(p)) \tag{0.14}$$

where $\tilde{\mathcal{H}}$ is the second normalized Hamiltonian, and $\tilde{\mathcal{H}}_1$ is the generator of the axial \mathbf{S}^1 symmetry with respect to which we perform the second normalization.

The hydrogen atom in crossed fields can be tuned between the Stark and Zeeman limits by varying the strengths of the electric and magnetic field. The

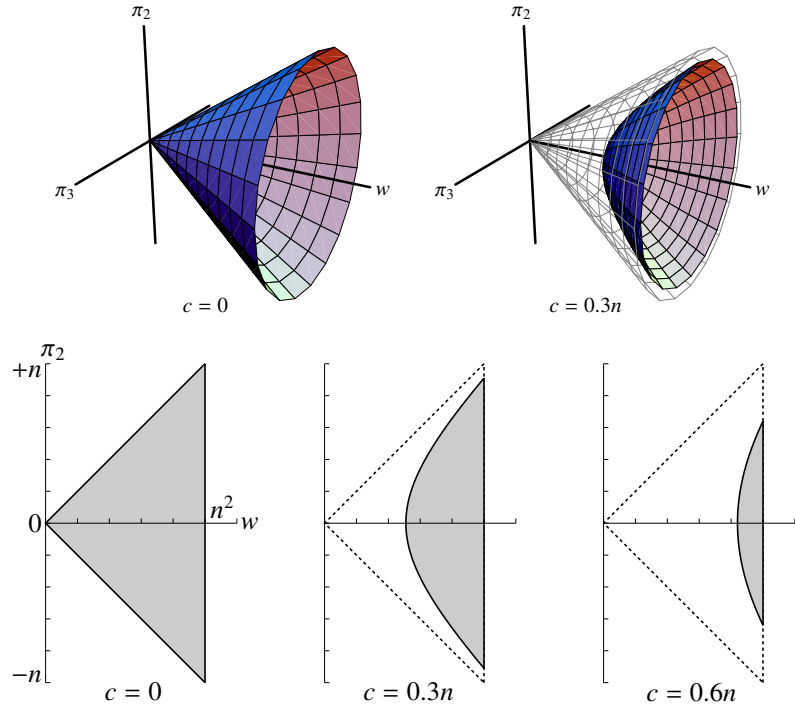


Figure 0.4: Fully reduced spaces $V_{n,c}$ and their projections $V_{n,c}^0$ to the (π_2, w) plane.

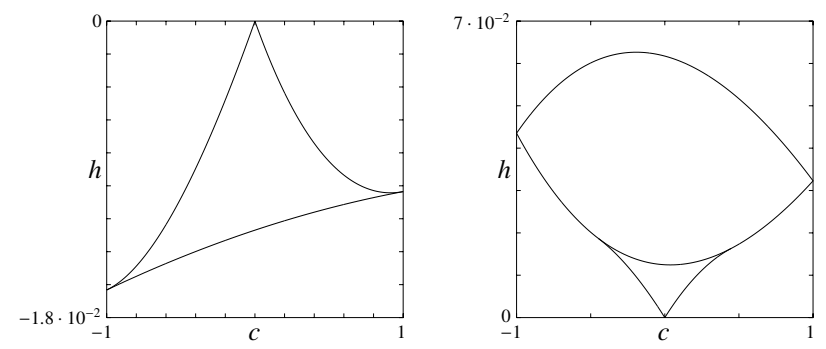


Figure 0.5: Image of the \mathcal{EM} map in the Stark and Zeeman limits.

image of the \mathcal{EM} map at the two limits is shown in figure 0.5. In the figure we observe that the two limits are qualitatively different. The question that is posed is what happens exactly as we tune the atom between the two limits and what kind of qualitative changes appear when we pass from the image at the left to the image at the right:

Objective *Prove that as we tune the hydrogen atom in crossed fields between the Stark and Zeeman limits we have two qualitatively different Hamiltonian Hopf bifurcations. Illustrate and discuss the geometric manifestation of these bifurcations in the reduced phase space and explain their relation to monodromy.*

0.3 Quadratic spherical pendula

A very simple model of a floppy triatomic molecule with two stable linear equilibria is the constrained motion of a particle on the unit sphere in \mathbf{R}^3 under the influence of a potential that is a quadratic polynomial in z . This model is a deformation of the spherical pendulum.

0.3.1 A spherical pendulum model for floppy triatomic molecules

We consider floppy molecules of type XAB in which X is a light atom (H, Li) and AB is a rather rigid and heavy diatom. Molecules of this type include HCN, LiCN, HCP and HClO. The XAB system has six degrees of freedom, ignoring electronic motions and bringing the system in its center of mass frame. Two of these degrees are the stretching mode r of the AB bond and the distance R between the light X atom and the diatom fragment AB. One degree is described by the bending angle γ of the hydrogen atom with respect to the AB axis. Finally, there are three rotational degrees of freedom, one of which describes rotations around the AB axis and the other two describe rotations around axes that are approximately perpendicular to the AB axis.

A first approximation in the study of XAB is to ignore the latter two rotational degrees of freedom. Moreover, the XAB fragment is rigid and we can consider r to be fixed. Ignoring R is more difficult. The first major obstruction is that R oscillates. In many molecules there is a 1:2 resonance between the oscillation of R and the bending mode oscillations in γ . In that case we can not ignore the interaction between the two modes. Nevertheless, this resonance does not exist in HCN or LiCN. In these cases we can normalize the system, and arrive at a system in which R does not oscillate but has a specific average value at each direction γ . This however leaves the problem that R is not constant but changes for different γ . In order to simplify the problem we are going to assume that R is constant, i.e. that X is moving on the surface of a sphere. This approximation gives the correct qualitative description of LiCN but, as we show later, modifies the qualitative characteristics of HCN. In reality, since R is not constant the X atom is not moving on a sphere, but on a more general surface of revolution, and therefore the kinetic energy of the system is modified.

Without any further assumptions we have a particle moving on the surface of a sphere under the influence of an unspecified axisymmetric potential. Spec-

troscopists have found that the potential that describes the LiCN molecule has two minima; one for each pole of the sphere. Moreover the potential is clearly axisymmetric. Therefore we can describe it using a function

$$V(z) = \frac{1}{2}b_{\text{LiCN}}z^2 + c_{\text{LiCN}}z + d_{\text{LiCN}} \quad (0.15)$$

where the values $b_{\text{LiCN}} < 0$, c_{LiCN} are chosen in such a way such as to give the experimentally determined values of the minima and maxima of the potential.

0.3.2 The family of quadratic spherical pendula

As we mentioned in the introduction we study not only the particular Hamiltonian that models LiCN but also the whole family of systems defined as a particle moving on the surface of the unit sphere in a quadratic potential

$$V(z) = \frac{1}{2}bz^2 + cz + d \quad (0.16)$$

We call this family *quadratic spherical pendula*. Since these systems are invariant under rotations about the vertical axis of the sphere, there is a conserved quantity, the vertical component J of the angular momentum. This means in particular that these systems (and all systems with a potential $V(z)$) are Liouville integrable.

Notable members of this family are the linear spherical pendulum for which $V(z) = z$, and two quadratic spherical pendula with $V(z) = z^2$ and $V(z) = -z^2$. We discuss these systems in some detail.

The linear spherical pendulum

The linear spherical pendulum is one of the classical integrable systems [20]. It has been studied, as early as 1673, by Huygens who found its relative equilibria which are horizontal circular periodic orbits. In more recent times the linear spherical pendulum has served as the first concrete example of a Hamiltonian system with *monodromy* [29].

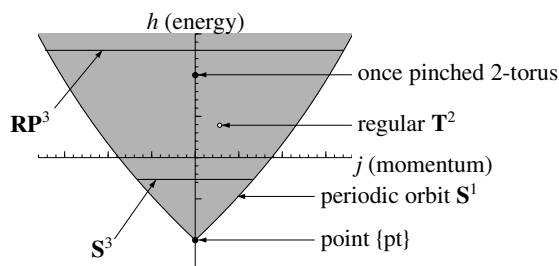


Figure 0.6: Image and fibers of the energy-momentum map \mathcal{EM} of the spherical pendulum, see Chap. IV.3 of [20].

For our purposes, the spherical pendulum is the motion of a particle on a sphere under the influence of gravity. The image of the energy-momentum map of the spherical pendulum is depicted in figure 0.6. The fiber $\mathcal{EM}^{-1}(1, 0)$ is a singly pinched torus. Therefore by the *geometric monodromy theorem* [21, 97], the system has monodromy and the monodromy matrix is $\begin{pmatrix} 1 & 1 \\ 0 & 1 \end{pmatrix}$.

Quadratic spherical pendulum with $V(z) = z^2$

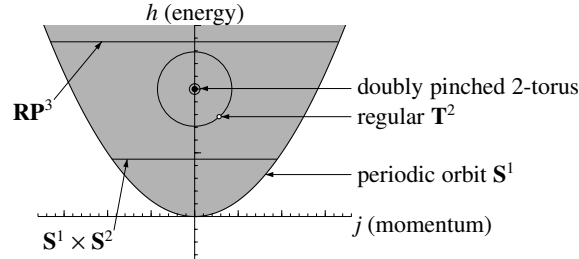


Figure 0.7: Image and fibers of the energy-momentum map \mathcal{EM} of the quadratic spherical pendulum with $V(z) = z^2$.

This system is studied in [14, 26]. I learned about the quadratic spherical pendulum with $V(z) = z^2$ from a ‘homework’ of R. Cushman at the first Peyresq school [65]. The image of \mathcal{EM} for this quadratic spherical pendulum is depicted in figure 0.7. Here the fiber $\mathcal{EM}^{-1}(1, 0)$ corresponds to a *doubly pinched* torus. This system has monodromy, but in this case the monodromy matrix is $\begin{pmatrix} 1 & 2 \\ 0 & 1 \end{pmatrix}$.

Quadratic spherical pendulum with $V(z) = -z^2$

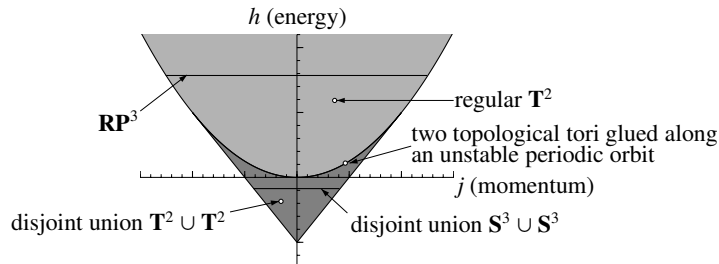


Figure 0.8: Image and fibers of the energy-momentum map \mathcal{EM} of the quadratic spherical pendulum with $V(z) = -z^2$.

As far as I know the quadratic spherical pendulum with $V(z) = -z^2$ has not been studied before. Its \mathcal{EM} map is depicted in figure 0.8. Points in the interior of the dark gray area correspond to two disjoint tori in phase space. Points in the interior of the light gray area correspond to a single torus. Points on the line that separates the two regions correspond to two tori joined along an X_J orbit. I do not know of any way to define monodromy for this system although the question remains open.

General situation

As we change the parameters b, c of the potential the system goes through different regimes. These regimes can be classified as follows in terms of the image of \mathcal{EM} .

Type O. \mathcal{EM} has one isolated critical value that lifts to a singly pinched torus whose pinch point is the unstable equilibrium. The linear spherical pendulum $V(z) = z$ belongs in this category.

Type I. The image of \mathcal{EM} consists of two leaves. The smaller of these leaves covers part of the larger leaf. Each point inside each leaf lifts to a regular 2-torus. The leaves join at a line of critical values of \mathcal{EM} . The image of one stable equilibrium is attached to the boundary of each leaf. A special case is $V(z) = -z^2$ in which the smaller leaf touches the boundary of the \mathcal{EM} image and the images of the two equilibria coincide.

Type II. The \mathcal{EM} has two isolated critical values. Each of them lifts to a singly pinched torus. The case $V(z) = z^2$ is a special subcase in which the images of the two singly pinched tori merge to one doubly pinched torus.

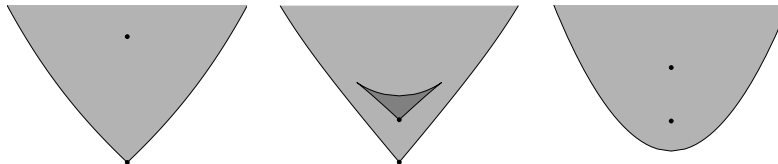


Figure 0.9: Type O, I and II systems.

Note that from now on when we refer to type I and II systems we do not include the special cases $V(z) = \pm z^2$ unless explicitly mentioned.

Type O systems are qualitatively identical to the spherical pendulum, which we already discussed. Monodromy in type II systems can be characterized in two ways. If we consider a path in the image of \mathcal{EM} that encloses only one of the two isolated critical values, then we find the monodromy matrix $\begin{pmatrix} 1 & 1 \\ 0 & 1 \end{pmatrix}$. If on the other hand, we consider a path that encloses both critical values then we find the monodromy matrix $\begin{pmatrix} 1 & 2 \\ 0 & 1 \end{pmatrix}$. When the two equilibria join for $V(z) = z^2$ the latter matrix is the monodromy matrix around the isolated critical value of \mathcal{EM} that lifts to a doubly pinched torus.

Monodromy in type I systems is different. As we mentioned before, in this case the image of \mathcal{EM} contains two leaves that join along a curve segment \mathcal{C} of critical values. We define monodromy in this case by considering paths that stay on one of the leaves and go around \mathcal{C} . In chapter 3 we use a *deformation* argument to show that the monodromy matrix is the same as in type O systems, i.e. $\begin{pmatrix} 1 & 1 \\ 0 & 1 \end{pmatrix}$. The argument is based on the fact that we can smoothly deform the small leaf in type I systems to the isolated critical value in type O systems.

Two of the changes between the different regimes are of particular interest. The first case is when we go from a type O to a type II system. In this case one equilibrium detaches from the boundary of the \mathcal{EM} image and becomes isolated. This case corresponds exactly to the nonlinear character of a supercritical Hamiltonian Hopf bifurcation.

The second is when we go from a type I to a type O system. In this case the small leaf shrinks to an isolated equilibrium. This case corresponds to a

subcritical Hamiltonian Hopf bifurcation. We see in quadratic spherical pendula just as in the hydrogen atom in crossed fields that non-local monodromy is related to a subcritical Hamiltonian Hopf bifurcation.

Objective *Study the different types of monodromy that appear in the family (0.16) and the passage between them. Especially, study the Hamiltonian Hopf bifurcations of the equilibria P_{\pm} as the system goes through different parameter regions.*

0.4 Oscillators in $m:-n$ resonance

We consider 2 degrees of freedom oscillators in resonance either $m:n$ or $m:-n$ where m, n are positive integers with $\gcd(m, n) = 1$. We reduce the \mathbf{S}^1 action induced in each case by the oscillator flow. Although we are interested mainly in $m:-n$ resonances we do also the reduction of the $m:n$ resonances.

0.4.1 Reduction

We do the reduction of the $m:n$ and $m:-n$ oscillator symmetry.

Reduction of the $m:n$ resonance

The flow of the $m:n$ resonant oscillator generates an \mathbf{S}^1 action

$$\Phi_{m:n} : \mathbf{S}^1 \times \mathbf{R}^4 \rightarrow \mathbf{R}^4 : (q_1, q_2, p_1, p_2) \mapsto (\exp(imt)z_1, \exp(int)z_2) \quad (0.17)$$

Lemma 0.5. *The algebra $\mathbf{R}[q, p]^{\Phi_{m:n}}$ of $\Phi_{m:n}$ invariant polynomials in q, p is generated by*

$$\begin{aligned} J &= \frac{1}{2}(m(q_1^2 + p_1^2) + n(q_2^2 + p_2^2)) \\ \pi_1 &= \frac{1}{2}(m(q_1^2 + p_1^2) - n(q_2^2 + p_2^2)) \\ \pi_2 &= (n^m m^n)^{1/2} \operatorname{Re}((q_1 + ip_1)^n (q_2 - ip_2)^m) \\ \pi_3 &= (n^m m^n)^{1/2} \operatorname{Im}((q_1 + ip_1)^n (q_2 - ip_2)^m) \end{aligned}$$

which satisfy

$$\Psi_{m:n} = \pi_2^2 + \pi_3^2 - (J + \pi_1)^n (J - \pi_1)^m = 0 \text{ and } J \geq 0 \text{ and } |\pi_1| \leq J$$

The Poisson structure for the invariants is

$$\begin{aligned} \{\pi_1, \pi_2\} &= -2mn\pi_3 \\ \{\pi_3, \pi_1\} &= -2mn\pi_2 \\ \{\pi_2, \pi_3\} &= -mn(J + \pi_1)^{n-1} (J - \pi_1)^{m-1} ((m+n)\pi_1 + (m-n)J) \end{aligned}$$

or more concisely

$$\{\pi_i, \pi_j\} = -mn \sum_k \varepsilon_{ijk} \frac{\partial \Psi_{m:n}}{\partial \pi_k}$$

The reduced phase space $P_j = J^{-1}(j)/\mathbf{S}^1$ is the semialgebraic variety defined by

$$\Psi_{m:n} = \pi_2^2 + \pi_3^2 - (j + \pi_1)^n(j - \pi_1)^m = 0, j \geq 0 \text{ and } |\pi_1| \leq j \quad (0.18)$$

In this case P_j is compact. This is easy to deduce from (0.18).

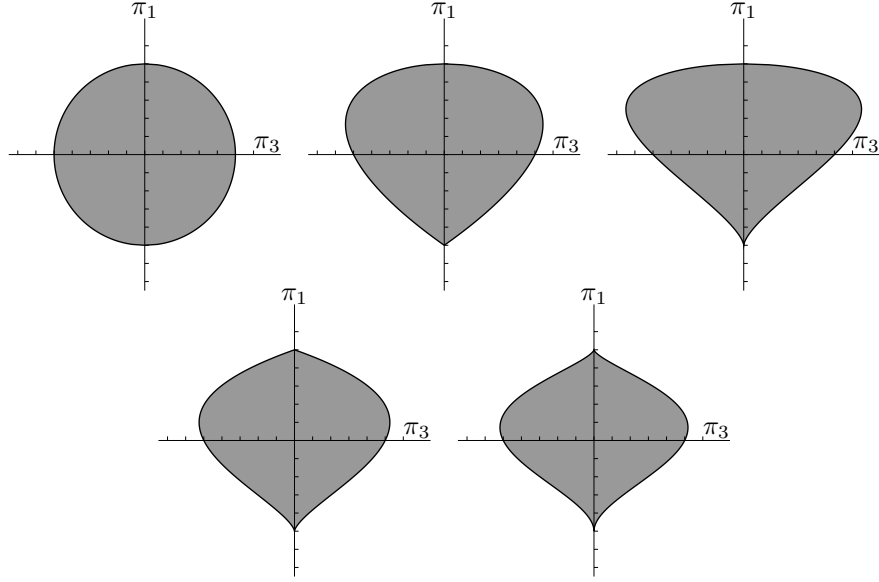


Figure 0.10: Projections of the reduced phase spaces of the $m:n$ resonances 1:1, 1:2, 1:3, 2:3 and 3:4 on the (π_3, π_1) plane.

Notice that the points $(\pi_1, \pi_2, \pi_3) = \pm(j, 0, 0)$ are always on P_j and they correspond to the minimum and maximum values of π_1 . When $n = 1$, P_j is smooth at $(-j, 0, 0)$, when $n = 2$ it has a conical singularity and for $n \geq 3$ it has a cusp-like singularity. The behaviour of P_j at $(j, 0, 0)$ depends on the values of m , and for $m = 1$, $m = 2$ and $m \geq 3$ we have that P_j is smooth, has a conical singularity or has a cusp-like singularity respectively. These are depicted in figure 0.10.

Reduction of the $m: -n$ resonance

The flow of the $m: -n$ resonant oscillator generates an \mathbf{S}^1 action

$$\Phi_{m:-n} : \mathbf{S}^1 \times \mathbf{R}^4 \rightarrow \mathbf{R}^4 : (q_1, q_2, p_1, p_2) \mapsto (\exp(imt)z_1, \exp(-int)z_2) \quad (0.19)$$

Lemma 0.6. *The algebra $\mathbf{R}[q, p]^{\Phi_{m:-n}}$ of $\Phi_{m:-n}$ invariant polynomials in q, p is generated by*

$$\begin{aligned} J &= \frac{1}{2}(m(q_1^2 + p_1^2) - n(q_2^2 + p_2^2)) \\ \pi_1 &= \frac{1}{2}(m(q_1^2 + p_1^2) + n(q_2^2 + p_2^2)) \\ \pi_2 &= (n^m m^n)^{1/2} \operatorname{Re}((q_1 + ip_1)^n (q_2 + ip_2)^m) \\ \pi_3 &= (n^m m^n)^{1/2} \operatorname{Im}((q_1 + ip_1)^n (q_2 + ip_2)^m) \end{aligned}$$

which satisfy

$$\Psi_{m:-n} = \pi_2^2 + \pi_3^2 - (\pi_1 + J)^n (\pi_1 - J)^m = 0 \text{ and } \pi_1 \geq |J|$$

The Poisson structure for the invariants is

$$\begin{aligned} \{\pi_1, \pi_2\} &= -2mn\pi_3 \\ \{\pi_3, \pi_1\} &= -2mn\pi_2 \\ \{\pi_2, \pi_3\} &= -mn(\pi_1 + J)^{n-1}(\pi_1 - J)^{m-1}((m+n)\pi_1 + (m-n)J) \end{aligned}$$

or more concisely

$$\{\pi_i, \pi_j\} = -mn \sum_k \varepsilon_{ijk} \frac{\partial \Psi_{m:-n}}{\partial \pi_k}$$

The reduced phase space $P_j = J^{-1}(j)/\mathbf{S}^1$ is the semialgebraic variety defined by

$$\Psi_{m:-n} = \pi_2^2 + \pi_3^2 - (j + \pi_1)^n (\pi_1 - j)^m = 0 \text{ and } \pi_1 \geq |j| \quad (0.20)$$

In this case P_j is not compact.

Notice that the point $(\pi_1, \pi_2, \pi_3) = (|j|, 0, 0)$ is always on P_j and corresponds to the minimum value of π_1 . P_j at $(|j|, 0, 0)$ for $j < 0$ is smooth when $n = 1$, has a conical singularity when $n = 2$ and has a cusp-like singularity for $n \geq 3$. The same hold for $j > 0$ but with n replaced by m . The reduced phase spaces P_j are depicted in figure 0.11.

0.4.2 Fractional monodromy in the 1:-2 resonance

We consider the 1:-2 resonance. The Hamiltonian is defined as

$$H = \pi_3 + \epsilon(\pi_1^2 - J^2) \quad (0.21)$$

where $\pi_{1,2,3}$ and J are polynomials of (q, p) defined in lemma 0.6 for $m = 1$, $n = 2$. The energy-momentum map is $\mathcal{EM}(q, p) = (H(q, p), J(q, p))$.

The image of \mathcal{EM} is depicted in figure 0.12. The set of critical values of \mathcal{EM} consists of the boundary of the image of \mathcal{EM} , and a line \mathcal{C} along the j axis that joins the boundary at one side and ends at $(0, 0)$ at the other side (we do not consider end points as parts of \mathcal{C}). Each point on this line corresponds to a ‘curled’ torus in the phase space \mathbf{R}^4 (figure 0.13).

The set of regular values \mathcal{R} of \mathcal{EM} is simply connected. This means that for any closed path Γ that we consider inside \mathcal{R} the monodromy is trivial. As we mentioned in the introduction, the idea of Zhilinskií was that if we find a meaningful way in which a path Γ that goes around $(0, 0)$ could cross \mathcal{C} then we would be able to define a generalized notion of monodromy. In [73] the authors announce that such a way exists and give the sketch of a geometric proof. The complete geometric proof is given in [72].

Our approach to the proof of existence of generalized monodromy is analytic and follows the period lattice approach of Duistermaat [29]. The period lattice on a regular torus is the set of pairs of ‘times’ (t_1, t_2) after which a point on the torus returns to itself after following the flow of X_J for time t_1 and the flow of X_H for time t_2 . Duistermaat proves that for a closed path Γ in the set

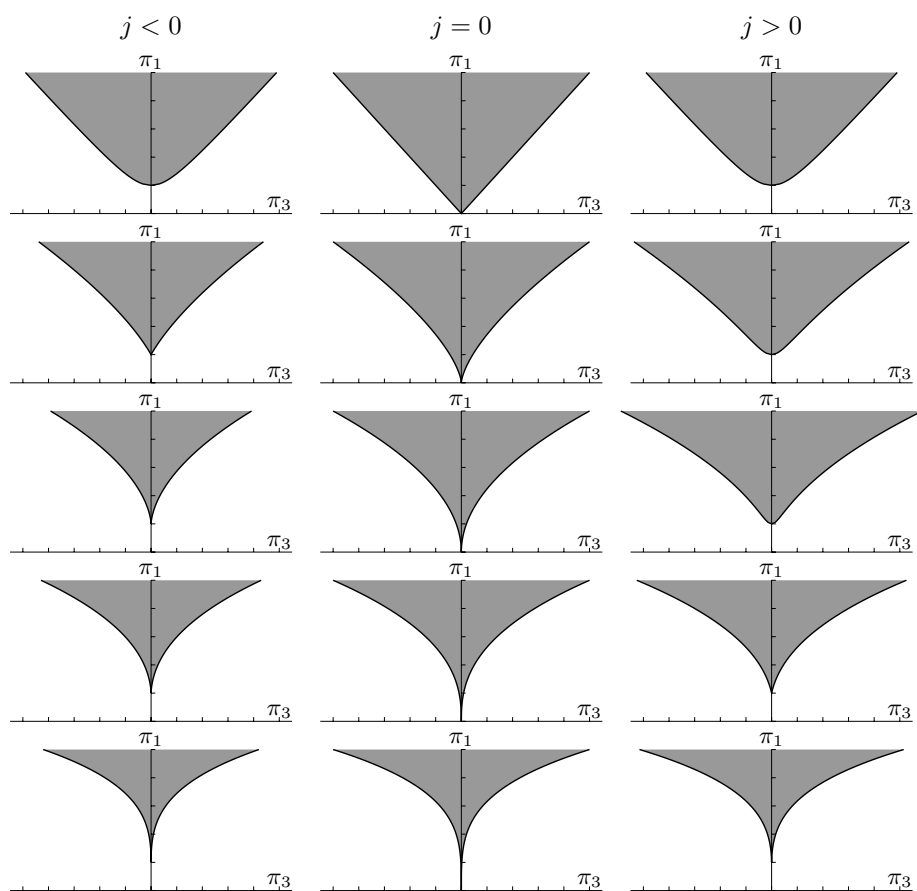


Figure 0.11: Projections of the reduced phase spaces of the $m: -n$ on the (π_3, π_1) plane. From top to bottom: 1: - 1, 1: - 2, 1: - 3, 2: - 3, 3: - 4.

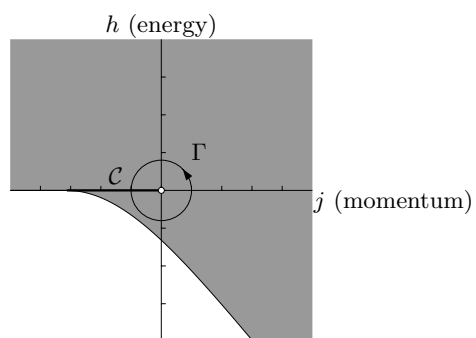


Figure 0.12: Image of the energy-momentum map of the 1:-2 resonance.

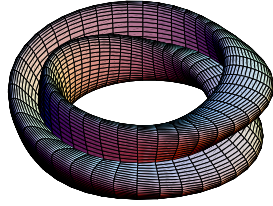


Figure 0.13: Curled torus.

of regular values of \mathcal{EM} , the period lattice bundle over Γ is isomorphic to the first homology group bundle over Γ . This means that the non-triviality of the \mathbf{T}^2 bundle over Γ appears as a variation of the period lattice as we go once around Γ . This variation can be computed using analytic methods.

In the 1:-2 resonance system consider a path Γ that encircles the origin and crosses \mathcal{C} at a point p . Since $\mathcal{EM}^{-1}(p)$ is not a \mathbf{T}^2 we no longer have a \mathbf{T}^2 bundle over Γ . We show in chapter 4 that we have to consider a sublattice of the period lattice. Specifically, if the period lattice is spanned by vectors v_1, v_2 then the sublattice we consider is spanned by $v_1, 2v_2$. We can then prove that the variation of the sublattice is given by the linear automorphism with matrix $\begin{pmatrix} 1 & 1 \\ 0 & 1 \end{pmatrix}$. If we express this automorphism *formally* in the original basis we obtain the matrix

$$M = \begin{pmatrix} 1 & \frac{1}{2} \\ 0 & 1 \end{pmatrix} \in \mathrm{SL}(2, \mathbf{Q})$$

For this reason this type of monodromy is called *fractional monodromy*.

Objective *Prove analytically that a generalized type of monodromy can be defined for the 1 : -2 resonance using the notion of the period lattice and compute the monodromy matrix.*

1

Small vibrations of tetrahedral molecules

1.1 Introduction

1.1.1 The Hamiltonian family

In § 0.1.3 we introduced the most general quartic Hamiltonian (0.9) that can model the triply degenerate vibrational mode of a tetrahedral molecule. Recall here that the Hamiltonian (0.9) is defined as

$$H(x, y, z, p_x, p_y, p_z) = \frac{1}{2}(p_x^2 + p_y^2 + p_z^2) + \epsilon^2 K_R [(x, y, z) \times (p_x, p_y, p_z)]^2 + \frac{1}{2}\mu_2 + \epsilon K_3 \mu_3 + \epsilon^2 K_4 \mu_4 + \epsilon^2 K_0 \mu_2^2 \quad (1.1)$$

where x, y, z are Cartesian coordinates in \mathbf{R}^3 , and p_x, p_y, p_z are the corresponding conjugate momenta. The invariants μ_2, μ_3 and μ_4 are functions of (x, y, z) defined in lemma 0.4. (x, y, z) transform according to the *vector representation* of the orthogonal group $O(3)$ of transformations of \mathbf{R}^3 . The zero-order Hamiltonian in (1.1)

$$H_0(x, y, z, p_x, p_y, p_z) = \frac{1}{2}(p_x^2 + p_y^2 + p_z^2) + \frac{1}{2}(x^2 + y^2 + z^2) \quad (1.2)$$

represents three harmonic oscillators with equal frequencies, that is, the 1:1:1 resonant (isotropic) harmonic oscillator. The dimensionless smallness parameter ϵ characterizes the magnitude of the perturbation, while parameters K_0, K_3, K_4 and K_R give the relative strength of each perturbation term. We assume that these parameters are of the order of 1. Note that we use K_3 in order to keep track of the contribution of the cubic potential term; in principle, this parameter can be absorbed into ϵ .

The Hamiltonian system (1.1) is non-integrable for typical values of the parameters. We do not give a proof of the nonintegrability since such a proof is not really necessary in our context. However, direct computations for high degree $T_d \times \mathcal{T}$ invariant polynomials $F(x, y, z, p_x, p_y, p_z)$ show that $\{H_\epsilon, F\}$ does not vanish. Furthermore, numerical integration also reveals chaotic dynamics.

The natural starting point of the analysis of the family of systems with Hamiltonian (1.1) is near the linearization limit $\epsilon \rightarrow 0$. According to a theorem

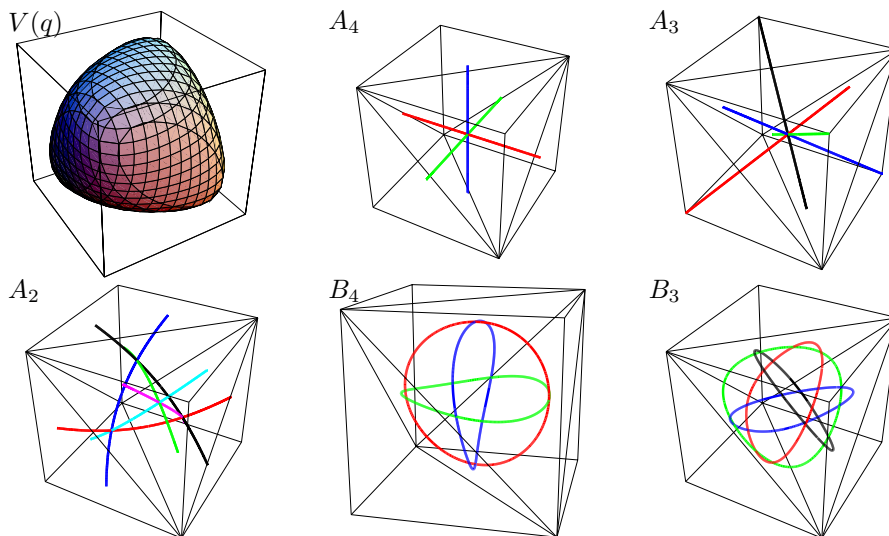


Figure 1.1: Qualitative representation of the equipotential surface of H (top left). Configuration space representation of the periodic orbits of the system with Hamiltonian H_ϵ (1.1) that correspond to the critical points of $\mathbb{T}_d \times \mathcal{T}$. These periodic orbits have been computed for appropriate values of the parameters ϵ, K_3, K_4, K_0 in (1.1).

by Weinstein [90], a perturbed non-resonant k -oscillator near this limit has k families of short periodic orbits called *nonlinear normal modes*. In the presence of resonances, the oscillator can have more than k such families. The number and the properties of the modes depend primarily on the resonance and the symmetry of the perturbing nonlinear terms. The discrete symmetry gives the existence of a minimum number of nonlinear normal modes of the Hamiltonian system (1.1) which are special periodic solutions characterized by a nontrivial *isotropy group* \mathcal{G} , or *stabilizer*. \mathcal{G} is a subgroup of the total symmetry group of the system $\mathbb{T}_d \times \mathcal{T}$. Description of the subgroups \mathcal{G} is given in A.1 and in more detail in [1].

In [66] Montaldi, Roberts, and Stewart study special short period solutions for a system which near $\epsilon \rightarrow 0$ is equivalent to ours. Using their results we immediately obtain

Theorem 1.1. *The system with Hamiltonian (1.1) has at least 27 nonlinear normal modes which can be classified according to their stabilizers $G \subset \mathbb{T}_d \times \mathcal{T}$ as follows.*

conjugacy class of stabilizers	shorthand notation	number of modes
$\mathcal{D}_{2d} \times \mathcal{T}$	A_4	3
$\mathcal{C}_{3v} \times \mathcal{T}$	A_3	4
$\mathcal{C}_{2v} \times \mathcal{T}$	A_2	6
$\mathcal{S}_4 \wedge \mathcal{T}_2$	B_4	6
$\mathcal{C}_3 \wedge \mathcal{T}_s$	B_3	8

The description of these stabilizers is given in A.2.

Remark 1.2. We can also use the approach of [66, 67] to reconstruct qualitatively the nonlinear normal modes in theorem 1.1 using their isotropy groups. Figure 1.1 shows the projection of these periodic orbits in the configuration space \mathbf{R}^3 . A detailed discussion is relegated to A.4, see also [2].

We determine the actual number of nonlinear normal modes for each member of the family (1.1) and we find situations where the Hamiltonian has more than the 27 nonlinear normal modes given by theorem 1.1. Computing the value of H_ϵ (energy) for these modes and characterizing their linear stability we give a basic qualitative description of the whole parametric family (1.1).

1.1.2 Dynamical symmetry. Relative equilibria

An alternative proof of theorem 1.1 was suggested in [79] on the basis of the earlier work by Zhilinskiĭ [95]. In order to follow this latter approach we would like to recall a number of known facts which we formulate as lemmas.

Lemma 1.3. *For all $n > 0$ the n -level set of the Hamiltonian H_0 in (1.2) is a sphere $\mathbf{S}_n^5 : \{\xi \in T^*\mathbf{R}^3, H_0(\xi) = h_0 = n > 0\} \subset T^*\mathbf{R}^3 \setminus \{0\}$. All orbits of the flow $\varphi_0 : (\mathbf{S}_n^5, t) \mapsto \mathbf{S}_n^5$ of the Hamiltonian vector field X_{H_0} are periodic with period 2π . This flow defines a symmetry group \mathbf{S}^1 . The action of this symmetry on $T^*\mathbf{R}^3 \setminus \{0\}$ and on \mathbf{S}_n^5 is free. The orbit space $\mathbf{S}_n^5/\mathbf{S}^1$ is a complex projective 2-space \mathbf{CP}^2 .*

Proof. . Identify the phase space $T^*\mathbf{R}^3$ with a complex 3-space \mathbf{C}^3 with coordinates

$$w_1 = x + ip_x, \quad w_2 = y + ip_y, \quad \text{and } w_3 = z + ip_z \quad (1.3)$$

In these coordinates the equation

$$H_0 = \frac{1}{2}(w_1\bar{w}_1 + w_2\bar{w}_2 + w_3\bar{w}_3) = h_0 = n > 0$$

defines a sphere $\mathbf{S}_n^5 \subset \mathbf{C}^3 \setminus \{0\}$ of radius $\sqrt{2n}$. The flow

$$\varphi_0 : (w, \bar{w}; t) \rightarrow (e^{it}w, e^{-it}\bar{w}) \quad (1.4)$$

is, obviously, diagonal, and all orbits are circles \mathbf{S}_n^1 of radius $\sqrt{2n}$. The quotient space $\mathbf{S}_n^5/\mathbf{S}_n^1$ is obtained by identifying points in each $\mathbf{S}_n^1 \subset \mathbf{S}_n^5$ orbit. We come to one of the standard definitions of the complex projective space. See an appropriate textbook, for example [70]. \square

We denote by $\mathbf{CP}^2(n)$ the orbit space of H_0 for the level set $H_0^{-1}(n)$, $n > 0$. A convenient way to parameterize $\mathbf{CP}^2(n)$ globally is by using polynomial invariants of the flow φ_0 .

Lemma 1.4. *The quadratic invariants of the \mathbf{S}^1 action (1.4) are*

$$\nu_1 = \frac{1}{2}w_1\bar{w}_1, \quad \nu_2 = \frac{1}{2}w_2\bar{w}_2, \quad \nu_3 = \frac{1}{2}w_3\bar{w}_3, \quad (1.5a)$$

$$\sigma_1 = \text{Re}(w_2\bar{w}_3), \quad \sigma_2 = \text{Re}(w_3\bar{w}_1), \quad \sigma_3 = \text{Re}(w_1\bar{w}_2), \quad (1.5b)$$

$$\tau_1 = \text{Im}(w_2\bar{w}_3), \quad \tau_2 = \text{Im}(w_3\bar{w}_1), \quad \tau_3 = \text{Im}(w_1\bar{w}_2), \quad (1.5c)$$

Except for the relation

$$\Sigma_0 = \nu_1 + \nu_2 + \nu_3 - n = 0, \quad (1.6a)$$

which fixes the level set $H_0^{-1}(n)$, these invariants are linearly independent. They satisfy nine algebraic relations $\Sigma_k = 0$, called syzygies of the first order, where

$$\begin{aligned} \Sigma_1 &= 4\nu_2\nu_3 - \sigma_1^2 - \tau_1^2, & \Sigma_4 &= 2\nu_1\sigma_1 - \sigma_2\sigma_3 + \tau_2\tau_3, & \Sigma_7 &= 2\nu_1\tau_1 + \sigma_2\tau_3 + \tau_2\sigma_3, \\ \Sigma_2 &= 4\nu_3\nu_1 - \sigma_2^2 - \tau_2^2, & \Sigma_5 &= 2\nu_2\sigma_2 - \sigma_3\sigma_1 + \tau_3\tau_1, & \Sigma_8 &= 2\nu_2\tau_2 + \sigma_3\tau_1 + \tau_3\sigma_1, \\ \Sigma_3 &= 4\nu_1\nu_2 - \sigma_3^2 - \tau_3^2, & \Sigma_6 &= 2\nu_3\sigma_3 - \sigma_1\sigma_2 + \tau_1\tau_2, & \Sigma_9 &= 2\nu_3\tau_3 + \sigma_1\tau_2 + \tau_1\sigma_2. \end{aligned} \quad (1.6b)$$

The syzygies (1.6) are themselves not algebraically independent.

The following two lemmas show why invariants (1.5) are used extensively in the reduction of the oscillator symmetry (1.4).

Lemma 1.5. *We can represent the points on $\mathbf{CP}^2(n)$, i.e., the orbits of the \mathbf{S}^1 action in (1.4) using $(\nu_1, \nu_2, \nu_3; \sigma_1, \sigma_2, \sigma_3; \tau_1, \tau_2, \tau_3)$ where the 9 parameters satisfy relations (1.6).*

Lemma 1.6. *Any \mathbf{S}^1 invariant smooth function $\mathbf{C}^3 \rightarrow \mathbf{R}$ is a smooth function of basic quadratic invariants (1.5). In particular, any \mathbf{S}^1 invariant polynomial can be expressed uniquely in terms of an integrity basis. One possible choice of such basis is*

$$\mathbf{R}[n, \nu_1 - \nu_2, \sigma_1, \sigma_2, \sigma_3] \bullet \{1, \nu_3, \nu_3^2, \tau_1, \tau_2, \tau_3\}.$$

Here $\mathbf{R}[\dots]$ is the ring generated freely by the principal invariants listed within the square brackets; auxiliary invariants listed within the curly brackets can enter only linearly, so that the whole ring can be represented as follows.

$$\mathbf{R}[n, \nu_1 - \nu_2, \sigma_1, \sigma_2, \sigma_3] \cdot 1 + \mathbf{R}[n, \nu_1 - \nu_2, \sigma_1, \sigma_2, \sigma_3] \cdot \nu_3 + \dots$$

Proof. This lemma follows from a standard Gröbner basis computation and Schwarz's theorem [82]. The structure of the polynomial ring is described by the following Molien generating function

$$g(\lambda) = \frac{1 + 4\lambda + \lambda^2}{(1 - \lambda)^5} \quad (1.7)$$

where λ represents any of generators in (1.5), see more in [2]. \square

Lemma 1.7. *Invariants (1.5) generate a Poisson algebra $\mathfrak{u}(3)$ with $n = \nu_1 + \nu_2 + \nu_3$ one of its Casimirs. The ring of invariant polynomials, generated multiplicatively by (1.5), can therefore be equipped with a Poisson structure. This structure is used to define Hamiltonian dynamical systems on \mathbf{CP}^2 .*

Proof. The Poisson bracket $\{, \}$ of any two invariants in (1.5) is \mathbf{S}^1 invariant. By lemma 1.6 it can be expressed in terms of (1.5). Moreover, since (1.5) are all quadratic in (x, y, z, p_x, p_y, p_z) , the brackets are linear in (1.5). The concrete Poisson structure is found straightforwardly by computing $\{, \}$ in the coordinates (x, y, z, p_x, p_y, p_z) . The brackets satisfy relations of $\mathfrak{u}(3)$. Note that if we set n to a specific value greater than 0, then the algebra spanned by the linearly independent invariants (1.5) is isomorphic to $\mathfrak{su}(3)$. \square

Near the limit of linearization $\epsilon \rightarrow 0$ the perturbed Hamiltonian H_ϵ in (1.1) is approximately invariant with respect to the flow φ_0 in lemma 1.3. Near $\epsilon \rightarrow 0$ we can *normalize* H_ϵ with respect to H_0 and make this approximate dynamical symmetry exact. After normalization we obtain a formal series \tilde{H}_ϵ such that $\{\tilde{H}_\epsilon, H_0\} = 0$. In practice we truncate \tilde{H}_ϵ at some finite order.

Definition 1.8. The relative equilibria (RE) are periodic orbits of the normalized system with Hamiltonian \tilde{H}_ϵ in $T^*\mathbf{R}^3$ which are also group orbits of the \mathbf{S}^1 action in lemma 1.3.

RE are also sometimes called *short periodic orbits*, i.e., periodic orbits with period close to 2π , or *basic orbits*.

To *reduce* the now exact \mathbf{S}^1 symmetry of \tilde{H}_ϵ , we pass from the original phase space $T^*\mathbf{R}^3$ to the space $\mathbf{CP}^2(n)$ of \mathbf{S}^1_n orbits or the *reduced space* as follows. Since $\{\tilde{H}_\epsilon, H_0\} = 0$, the value of \tilde{H}_ϵ on each orbit of H_0 is constant. This means that we can properly define a function \hat{H}_ϵ on the phase space $\mathbf{CP}^2(n)$ of H_0 by assigning to each \mathbf{S}^1_n orbit of H_0 the value of \tilde{H}_ϵ on any point of the orbit. We call the Hamiltonian \hat{H}_ϵ on $\mathbf{CP}^2(n)$ the *reduced Hamiltonian*. Reduction results in a 2-DOF system on \mathbf{CP}^2 or the *reduced system*. By lemma 1.7, this system is a Poisson dynamical system with Hamiltonian \hat{H}_ϵ expressed (uniquely) in terms of the invariants (1.5) and the integrity basis in lemma 1.6.

Lemma 1.9. *After reduction of the \mathbf{S}^1 symmetry, the RE of the normalized Hamiltonian \tilde{H}_ϵ are reduced to equilibria of the reduced system with Hamiltonian \hat{H}_ϵ on \mathbf{CP}^2 . A relative equilibrium of \tilde{H}_ϵ and the corresponding equilibrium of \hat{H}_ϵ have the same type of linear Hamiltonian stability and the same isotropy group.*

The normal form of (1.1) is a formal power series whose orders are ‘tracked’ by the degrees of the smallness parameter ϵ . Since this series diverges for typical values of parameters in (1.1), it is *truncated* at the order of interest, which is in our case the principle order ϵ^2 . At this order \hat{H}_ϵ is a Morse function on \mathbf{CP}^2 for typical values of the parameters.

As is well known (see for example Appendix 7 of [11]), the system described by such truncated normal form \tilde{H}_ϵ and the original system are profoundly different. At the same time, it is possible to use \tilde{H}_ϵ to analyze the short time average behaviour of the original system, and in particular its short periodic orbits. The adequateness (validity) of the truncated normal form approximation for the study of orbits of a given short period is clearly limited by the value of ϵ which should be sufficiently small. [Note that decreasing ϵ is equivalent to decreasing energy and approaching the equilibrium $x = y = z = 0$ of (1.1) where $H = 0$.] This makes \tilde{H}_ϵ particularly suited for the analysis of the nonlinear normal modes which exist and can be studied anywhere close to the limit $\epsilon \rightarrow 0$.

Lemma 1.10. *For small enough ϵ , RE of the normalized system with Hamiltonian \tilde{H}_ϵ correspond to the nonlinear normal modes of the original system with Hamiltonian (1.1).*

The correspondence between the RE of the normalized system and the nonlinear normal modes is used in many applications. In particular this was discussed

in detail by Duistermaat in [30] who uncovers the relation of normalization near the equilibrium and Lyapunov-Schmidt reduction.

We conclude that the study of the nonlinear normal modes of the system with Hamiltonian (1.1) becomes the study of the equilibria of the reduced system, i.e., of the stationary points of the appropriately truncated reduced Hamiltonian \widehat{H}_ϵ .

1.1.3 Symmetry and topology

In order to describe qualitatively the systems with Hamiltonian (1.1) in terms of their nonlinear normal modes, we find the equilibria of Hamiltonians \widehat{H}_ϵ on \mathbf{CP}^2 (and hence the relative equilibria of the normalized system) and characterize them in terms of their energy and linear stability type. When searching for the stationary points of \widehat{H}_ϵ we account for the action of $T_d \times \mathcal{T}$ on \mathbf{CP}^2 and the topology of this space.

Consider the action of a compact or finite group \mathcal{G} on a manifold M . The isotropy group (or *stabilizer*) of $m \in M$ is the subgroup \mathcal{G}_m of elements of \mathcal{G} that leave m fixed. A point $m \in M$ is called a *fixed point* of the \mathcal{G} action when $\mathcal{G}_m = \mathcal{G}$, that is, when it is fixed by all the elements of \mathcal{G} . The \mathcal{G} -*orbit* of m is the set $\mathcal{G} \cdot m = \{g \cdot m : g \in \mathcal{G}\}$. We are primarily interested in points $m_c \in M$ such that there is a neighbourhood of m_c in which there are no points m with isotropy group \mathcal{G}_m which belongs to the same conjugacy class in \mathcal{G} as \mathcal{G}_{m_c} . We call such points m_c and the orbit $\mathcal{G} \cdot m_c$ *critical*. For more details see, for example, [63]. The importance of the critical points is due to the following theorem by Louis Michel [62]:

Theorem 1.11 (Michel). *Critical points of the action of a group \mathcal{G} on a smooth manifold M are stationary points of every smooth, \mathcal{G} -invariant function H on M .*

Consequently, the analysis of the critical points of the $T_d \times \mathcal{T}$ group action on the reduced space \mathbf{CP}^2 provides a number of relative equilibria of the normalized system and by lemma 1.10, nonlinear normal modes of the original system with Hamiltonian (1.1). A concrete study of this action results in the following conclusion (Zhilinskiĭ [95], see also [79], [1, 2] and A.1).

Theorem 1.12. *The action of $T_d \times \mathcal{T}$ on \mathbf{CP}^2 induced by the action of $T_d \times \mathcal{T}$ on $T^*\mathbf{R}^3 \sim \mathbf{C}^3$ has 27 critical (i.e., isolated fixed) points grouped into five critical orbits with the conjugacy classes of stabilizers given in theorem 1.1. Table 1.1 presents the position of these points on $\mathbf{CP}^2(n)$ characterized by the values of the invariants (1.5).*

Remark 1.13. Table A.3 of appendix A.1 lists the isotropy groups of the 27 points in theorem 1.12. Isotropy groups of the points in the same critical orbit of the $T_d \times \mathcal{T}$ action are conjugate in $T_d \times \mathcal{T}$. These points are equivalent: dynamics in their neighborhood is identically the same, so it is usually sufficient to study one representative of each critical orbit. We denote different points of the same critical orbit by a superscript; we drop this index when referring to the entire orbit or when our results apply identically to all points in the orbit.

Point	Coordinates on \mathbf{CP}_n^2	Point	Coordinates on \mathbf{CP}_n^2
A_4^x	$n(1, 0, 0; 0, 0, 0; 0, 0, 0)$	B_4^x	$n(0, \alpha, \alpha; 0, 0, 0; 1, 0, 0)$
A_4^y	$n(0, 1, 0; 0, 0, 0; 0, 0, 0)$	$B_4^{\bar{x}}$	$n(0, \alpha, \alpha; 0, 0, 0; \bar{1}, 0, 0)$
A_4^z	$n(0, 0, 1; 0, 0, 0; 0, 0, 0)$	B_4^y	$n(\alpha, 0, \alpha; 0, 0, 0; 0, 1, 0)$
A_3^a	$\frac{2n}{3}(\alpha, \alpha, \alpha; 1, 1, 1; 0, 0, 0)$	$B_4^{\bar{y}}$	$n(\alpha, 0, \alpha; 0, 0, 0; 0, \bar{1}, 0)$
A_3^b	$\frac{2n}{3}(\alpha, \alpha, \alpha; \bar{1}, \bar{1}, \bar{1}; 0, 0, 0)$	B_4^z	$n(\alpha, \alpha, 0; 0, 0, 0; 0, 0, 1)$
A_3^c	$\frac{2n}{3}(\alpha, \alpha, \alpha; 1, \bar{1}, \bar{1}; 0, 0, 0)$	$B_4^{\bar{z}}$	$n(\alpha, \alpha, 0; 0, 0, 0; 0, 0, \bar{1})$
A_3^d	$\frac{2n}{3}(\alpha, \alpha, \alpha; \bar{1}, 1, \bar{1}; 0, 0, 0)$	B_3^a	$\frac{2n}{3}(\alpha, \alpha, \alpha; \bar{\alpha}, \bar{\alpha}, \bar{\alpha}; \beta, \beta, \beta)$
A_2^x	$n(0, \alpha, \alpha; 1, 0, 0; 0, 0, 0)$	$B_3^{\bar{a}}$	$\frac{2n}{3}(\alpha, \alpha, \alpha; \bar{\alpha}, \bar{\alpha}, \bar{\alpha}; \bar{\beta}, \bar{\beta}, \bar{\beta})$
$A_2^{\bar{x}}$	$n(0, \alpha, \alpha; \bar{1}, 0, 0; 0, 0, 0)$	B_3^b	$\frac{2n}{3}(\alpha, \alpha, \alpha; \alpha, \alpha, \alpha; \beta, \beta, \beta)$
A_2^y	$n(\alpha, 0, \alpha; 0, 1, 0; 0, 0, 0)$	$B_3^{\bar{b}}$	$\frac{2n}{3}(\alpha, \alpha, \alpha; \alpha, \alpha, \bar{\alpha}; \bar{\beta}, \bar{\beta}, \beta)$
$A_2^{\bar{y}}$	$n(\alpha, 0, \alpha; 0, \bar{1}, 0; 0, 0, 0)$	B_3^c	$\frac{2n}{3}(\alpha, \alpha, \alpha; \bar{\alpha}, \alpha, \alpha; \bar{\beta}, \beta, \beta)$
A_2^z	$n(\alpha, \alpha, 0; 0, 0, 1; 0, 0, 0)$	$B_3^{\bar{c}}$	$\frac{2n}{3}(\alpha, \alpha, \alpha; \bar{\alpha}, \alpha, \alpha; \beta, \bar{\beta}, \bar{\beta})$
$A_2^{\bar{z}}$	$n(\alpha, \alpha, 0; 0, 0, \bar{1}; 0, 0, 0)$	B_3^d	$\frac{2n}{3}(\alpha, \alpha, \alpha; \alpha, \bar{\alpha}, \alpha; \beta, \bar{\beta}, \beta)$
		$B_3^{\bar{d}}$	$\frac{2n}{3}(\alpha, \alpha, \alpha; \alpha, \bar{\alpha}, \alpha; \bar{\beta}, \beta, \bar{\beta})$

Table 1.1: Critical points of the $T_d \times \mathcal{T}$ action on $\mathbf{CP}^2(n)$. Coordinates are given as $(\nu_1, \nu_2, \nu_3; \sigma_1, \sigma_2, \sigma_3; \tau_1, \tau_2, \tau_3)$ with $\alpha = 1/2$, $\beta = \sqrt{3}/2$, $\bar{\alpha} = -1/2$, $\bar{\beta} = -\sqrt{3}/2$ and $\bar{1} = -1$.

Proof of theorem 1.1. We rely on lemma 1.10 in order to establish the correspondence of the nonlinear normal modes of the initial system with Hamiltonian (1.1) and the relative equilibria of the normalized system near the limit $\epsilon \rightarrow 0$. We then use the theorem of Michel and theorem 1.12. \square

Consider a smooth Hamiltonian function $\mathcal{H} : \mathbf{CP}^2 \rightarrow \mathbf{R}$ whose stationary points are nondegenerate. We call \mathcal{H} a *Morse type Hamiltonian*. The isotropy group of a stationary point c of \mathcal{H} restricts the possible types of linear Hamiltonian stability and Morse index of c . Recall that linear stability is given by the eigenvalues of the 4×4 Hamiltonian matrix which describes the linearized equations of motion near $c \in \mathbf{CP}^2$, while the Morse index of c is the number of negative eigenvalues of the Hessian matrix of the Hamiltonian at c . Depending on the eigenvalues of this matrix we will distinguish six linear stability types EE, HH, EH, CH, 2E, 2H, described in B.1.

Theorem 1.14. *The critical points of the $T_d \times \mathcal{T}$ action on \mathbf{CP}^2 listed in theorem 1.12 are equilibria of any $T_d \times \mathcal{T}$ -invariant Morse type Hamiltonian function on \mathbf{CP}^2 . They can have the following linear Hamiltonian stability types and Morse indices.*

	critical orbit	stability	index		critical orbit	stability	index		
$\mathcal{D}_{2d} \times \mathcal{T}$	A_4	3	2E	0, 4	$\mathcal{S}_4 \wedge \mathcal{T}_2$	B_4	6	EE	0, 2, 4
			2H	2				EH	1, 3
$\mathcal{C}_{3v} \times \mathcal{T}$	A_3	4	2E	0, 4	$\mathcal{C}_3 \wedge \mathcal{T}_s$	B_3	8	EE, CH	0, 2, 4
			2H	2					
$\mathcal{C}_{2v} \times \mathcal{T}$	A_2	6	EE	0, 2, 4					
			EH	1, 3					
			HH	2					

Proof. See [1] for the part about the possible types of linear stability and B.2 about the Morse index. \square

Theorem 1.14 is a local statement which concerns an open neighbourhood $D_c \subset \mathbf{CP}^2$ of each critical point c of the $T_d \times \mathcal{T}$ action on \mathbf{CP}^2 . This far we have no information whether the set of stationary points characterized in theorems 1.12 and 1.14 is complete. This information can only be obtained from the global (topological) analysis. Note, that we already used the topology of this space in order to find the action of $T_d \times \mathcal{T}$ (initially defined on $\mathbf{R}_{x,y,z}^3$) on \mathbf{CP}^2 and of the isotropy group G_c of c on D_c . In B.2 we summarize how *Morse theory* [64,68] is applied in order to check the consistency of any set of stationary points using the Morse inequalities (four inequalities and one equality) imposed by the topology of \mathbf{CP}^2 on the number and types of stationary points of Morse functions \mathcal{H} . In particular we can determine if it is possible for a $T_d \times \mathcal{T}$ -invariant Morse function \mathcal{H} to have stationary points solely at the critical points of the $T_d \times \mathcal{T}$ action in theorem 1.12.

Definition 1.15. A simplest (or perfect) G -invariant Morse function on a manifold M is one that has the minimal possible number of non-degenerate stationary points.

Note that there is no guarantee that all the stationary points of a perfect function lie on critical orbits of the G -action. In our case we have

Lemma 1.16. *The simplest $T_d \times \mathcal{T}$ -invariant Morse Hamiltonian \mathcal{H} on \mathbf{CP}^2 has 27 equilibria which are critical points of the $T_d \times \mathcal{T}$ action in theorems 1.12 and 1.14. In this case the six A_2 and six B_4 stationary points of \mathcal{H} are of odd Morse index and have stability EH .*

Proof. According to theorem 1.14, points A_3 , A_4 , and B_3 are of even Morse index. The 27 points can have the right Morse indexes to give the Euler characteristic of \mathbf{CP}^2 only if A_2 and B_4 are of odd Morse index. \square

The linear stability types of the nonlinear normal modes in theorem 1.1 correspond to the stability types in theorem 1.14. In the simplest possible case, the system with Hamiltonian (1.1) has exactly 27 families of periodic orbits near the limit of linearization.

Remark 1.17. Morse theory provides necessary conditions that must be satisfied by the stationary points of any Morse function on \mathbf{CP}^2 . At the same time, even when a set of known stationary points of a Morse function \mathcal{H} obeys all these conditions, \mathcal{H} can still have other stationary points.

A more complete consistency check of a known system of stationary points of a $T_d \times \mathcal{T}$ invariant Morse function \mathcal{H} on \mathbf{CP}^2 requires satisfying Morse inequalities not only for \mathbf{CP}^2 but also for all G invariant subspaces of \mathbf{CP}^2 with G a subgroup of $T_d \times \mathcal{T}$.

1.2 One-parameter classification

Theorem 1.1 has already highlighted the important consequences of the presence of the additional finite symmetry $T_d \times \mathcal{T}$. The next lemma shows that this symmetry causes important modifications of the standard \mathbf{S}^1 -invariant polynomial basis in lemma 1.6.

Lemma 1.18. *Consider the most general $(\mathbb{T}_d \times \mathcal{T}) \times S^1$ -invariant polynomials $P_k(w, \bar{w})$ of degree k in variables (w, \bar{w}) . Then $P_k = 0$ if k is odd, and*

$$P_2 = c'n = c'(\nu_1 + \nu_2 + \nu_3) \quad (1.8a)$$

$$P_4 = cn^2 + a(\sigma_1^2 + \sigma_2^2 + \sigma_3^2) + b(\tau_1^2 + \tau_2^2 + \tau_3^2) \quad (1.8b)$$

where a, b, c , and c' are arbitrary constants.

Proof. The action of $O(3) \times \mathcal{T}$ and its subgroup $\mathbb{T}_d \times \mathcal{T}$ on the polynomials (1.5) can be found by direct computation, see appendix A.1 and [1, 2]. In particular we can verify that all S^1 -invariants in (1.5) are invariant with respect to spatial inversion, and that

$$n, \quad (\tau_1, \tau_2, \tau_3), \quad \text{and} \quad \left(\sigma_1, \sigma_2, \sigma_3, \frac{3\nu_3 - n}{\sqrt{3}}, n_1 - n_2 \right)$$

transform according to the irreducible representations of $O(3)$ of indexes 0_g , 1_g and 2_g respectively. In other words, n and (τ_1, τ_2, τ_3) transform as a scalar and an axial 3-vector respectively. We can also easily verify that

$$T : (\nu, \sigma, \tau) \rightarrow (\nu, \sigma, -\tau).$$

Knowing the action of $\mathbb{T}_d \times \mathcal{T}$, we can further symmetrize the basis in lemma 1.6. In particular we obtain the generating function

$$g(\lambda) = \frac{1 + \lambda^3 + \lambda^4 + \lambda^5 + \lambda^6 + \lambda^9}{(1 - \lambda)(1 - \lambda^2)^2(1 - \lambda^3)(1 - \lambda^4)} \quad (1.9)$$

which describes the symmetrized integrity basis, see [2]. The symmetrized invariants have high degrees in generators (1.5): of the five denominator factors in (1.9), which describe principal invariants, $(1 - \lambda)$ corresponds to n , while $(1 - \lambda^2)^2$ represents two invariants of degree two in generators (1.5). Direct computation shows that τ^2 and σ^2 are $\mathbb{T}_d \times \mathcal{T}$ invariant and can be chosen as these two invariants. The function (1.9) indicates that there are no other principal or auxiliary invariants of this degree. \square

Remark 1.19. The 3-vector $\tau = (\tau_1, \tau_2, \tau_3)$ is the angular momentum vector. Both n and $\tau^2 = \tau_1^2 + \tau_2^2 + \tau_3^2$ are totally symmetric with respect to the larger group $O(3) \times \mathcal{T}$. The only term in (1.8) which represents $\mathbb{T}_d \times \mathcal{T}$ symmetry is σ^2 .

We now come to a central result which provides the basis for the classification of generic tetrahedral Hamiltonians.

Theorem 1.20. *All $\mathbb{T}_d \times \mathcal{T}$ -invariant reduced Hamiltonians on \mathbb{CP}^2 with terms of order at most ϵ^2 can be characterized using a single parameter.*

Proof. According to lemma 1.18, \tilde{H}_ϵ has the form $P_2 + \epsilon^2 P_4 + \dots$. Since $\{H_0, \tilde{H}_\epsilon\} = 0$, H_0 is replaced by its value n when we define the reduced Hamiltonian \hat{H}_ϵ . Then, up to the constant $c'n + \epsilon^2 cn^2$ and the overall scaling factor of ϵ^2 , we have

$$\hat{H} = K_s(\sigma_1^2 + \sigma_2^2 + \sigma_3^2) + K_t(\tau_1^2 + \tau_2^2 + \tau_3^2) + \dots \quad (1.10)$$

It remains to verify that the family of systems (1.1) is generic in the sense that for practically all members of this family $K_s^2 + K_t^2 \neq 0$. (For the exceptional members we would have to normalize to higher orders.) This is done in section 1.3 after computing explicitly the normal form \tilde{H}_ϵ of (1.1).

In the generic situation when $R = (K_s^2 + K_t^2)^{1/2} > 0$ we can define a one-parameter family by setting $K_s = R \sin \theta$ and $K_t = R \cos \theta$ and rescaling the reduced Hamiltonian \hat{H} in (1.10) by R . Then

$$\hat{H} = \sin \theta (\sigma_1^2 + \sigma_2^2 + \sigma_3^2) + \cos \theta (\tau_1^2 + \tau_2^2 + \tau_3^2) + \dots, \quad (1.11)$$

where in general, θ can take any value in $[0, 2\pi)$. Systems with the same value of θ but different values of R have qualitatively the same dynamics but different time scales. Specifically, for smaller R dynamics is slower. \square

Remark 1.21. Lemma 1.18 and theorem 1.20 apply, in fact, to a larger family of systems with an extended Hamiltonian $H_\epsilon + W_\epsilon(x, y, z, p_x, p_y, p_z)$, where H_ϵ is defined in (1.1), and W_ϵ is a general $T_d \times \mathcal{T}$ -invariant ϵ -series perturbation of degree 3 or higher in all dynamical variables (x, y, z, p_x, p_y, p_z) .

To continue classifying reduced systems with Hamiltonian (1.11) and respective original systems with Hamiltonian (1.1) we restrict our attention to the class of Hamiltonians (1.1) for which the truncation of the reduced system to order ϵ^2 gives accurate information about its nonlinear normal modes. We use the equivalence relation which takes into account only the families of relative equilibria and respective nonlinear normal modes.

Definition 1.22. Consider the system with Hamiltonian H_ϵ (1.1) and the respective reduced system with Hamiltonian \hat{H}_ϵ truncated at the principal order ϵ^2 . H_ϵ is called ϵ^2 -generic if its nonlinear normal modes are in 1-1 correspondence to the equilibria of \hat{H}_ϵ in terms of linear stability and isotropy group, and \hat{H}_ϵ is a Morse function on \mathbf{CP}^2 .

In this work we consider only ϵ^2 -generic systems with Hamiltonian (1.1). In order to characterize all such systems we can study all possible sets of stationary points $\xi \in \mathbf{CP}^2(n)$ of the reduced Hamiltonian (1.11). Symmetry properties of ξ can be obtained from the study of the action of $T_d \times \mathcal{T}$ on $\mathbf{CP}^2(n)$. Stability of ξ is given by the four eigenvalues $(\pm\lambda_1, \pm\lambda_2)$ of the Hamiltonian matrix of the locally linearized Hamiltonian $\hat{H}|_\xi$. We also use the eigenvalues of the Hessian matrix to compute the Morse index of ξ .

Remark 1.23. It is sufficient to study (1.11) for $\theta \in [0, \pi)$ because $\hat{H}(\theta + \pi) = -\hat{H}(\theta)$. Both Hamiltonian and Hessian matrices change signs when $\theta \rightarrow \theta + \pi$. This does not affect stability (since both λ and $-\lambda$ are eigenvalues). On the other hand, if the Morse index for θ is d then for $\theta + \pi$ it becomes $4 - d$.

We like to point out that our classification has both qualitative and quantitative aspects. We will find several different classes of ϵ^2 generic systems with Hamiltonian (1.1). At the same time we represent all systems in the same class as a continuous one-parameter family and describe quantitatively the evolution of their relative equilibria as the parameter varies.

1.3 Normalization and reduction

Normalization is the first step of the concrete study of systems with Hamiltonian H_ϵ in (1.1). This well known procedure can be performed using the Lie series method [27, 43, 60]. To the second order terms ϵ^2 we obtain the normalized Hamiltonian

$$\tilde{H}_\epsilon(w, \bar{w}) = \tilde{H}_0(w, \bar{w}) + \epsilon^2 \tilde{H}_2(w, \bar{w}), \quad (1.12a)$$

where variables (w, \bar{w}) are given in (1.3), $\tilde{H}_0(w, \bar{w}) = H_0(w, \bar{w}) = \frac{1}{2} \sum w_i \bar{w}_i$, and

$$\begin{aligned} \tilde{H}_2(w, \bar{w}) = & \frac{3}{8}(K_0 + K_4)(w_1^2 \bar{w}_1^2 + w_2^2 \bar{w}_2^2 + w_3^2 \bar{w}_3^2) \\ & + \frac{1}{24}(12K_0 - K_3^2 + 12K_R)(w_1 \bar{w}_1 w_2 \bar{w}_2 + w_2 \bar{w}_2 w_3 \bar{w}_3 + w_3 \bar{w}_3 w_1 \bar{w}_1) \\ & + \frac{1}{32}(4K_0 - K_3^2 - 8K_R)(w_1^2 \bar{w}_2^2 + \bar{w}_1^2 w_2^2 + w_2^2 \bar{w}_3^2 + \bar{w}_2^2 w_3^2 + w_3^2 \bar{w}_1^2 + \bar{w}_3^2 w_1^2) \end{aligned} \quad (1.12b)$$

Reduction of the Hamiltonian (1.12) gives

$$\hat{H}_\epsilon = \hat{H}_0 + \epsilon^2 \hat{H}_2 \quad (1.13a)$$

where

$$\hat{H}_0 = \nu_1 + \nu_2 + \nu_3 = n \quad (1.13b)$$

$$\hat{H}_2 = \frac{3}{2}(K_4 + K_0)n^2 + K_s(\sigma_1^2 + \sigma_2^2 + \sigma_3^2) + K_t(\tau_1^2 + \tau_2^2 + \tau_3^2) \quad (1.13c)$$

with

$$K_s = (-5K_3^2 - 36K_4)/48, \quad K_t = (K_3^2 - 36K_4 - 24K_0 + 48K_R)/48. \quad (1.13d)$$

Ignoring the constant terms in \hat{H}_ϵ and rescaling by ϵ^2 we arrive at the Hamiltonian \hat{H} in (1.10). Furthermore, since K_0 , K_3 , K_4 and K_R can take arbitrary values (of order 1) we can rewrite \hat{H} in the one-parameter form $\hat{H}(\theta)$ in (1.11), where $0 \leq \theta < \pi$.

Remark 1.24. There are two values of θ at which the reduced system with Hamiltonian $\hat{H}(\theta)$ has a large Lie group of symmetries and is Liouville integrable, see below.

value of θ	first integrals	symmetry
0	$n, \tau_1^2 + \tau_2^2 + \tau_3^2, \tau_3$	O(3)
$\pi/4$	ν_1, ν_2, ν_3	SU(3)

1.4 Relative equilibria corresponding to critical points

We study the equilibria of the reduced system with Hamiltonian (1.11) which are critical points of the $T_d \times \mathcal{T}$ action on $\mathbf{CP}^2(n)$.

Lemma 1.25. *The nonlinear normal modes in theorem 1.1 correspond to the relative equilibria (RE) of the normalized system with Hamiltonian (1.1). On the phase space \mathbf{CP}^2 of the corresponding reduced system, these RE are critical points of the action of the symmetry group $T_d \times \mathcal{T}$ given in theorem 1.12. The principal terms in the energy-action characteristics for these modes are given below.*

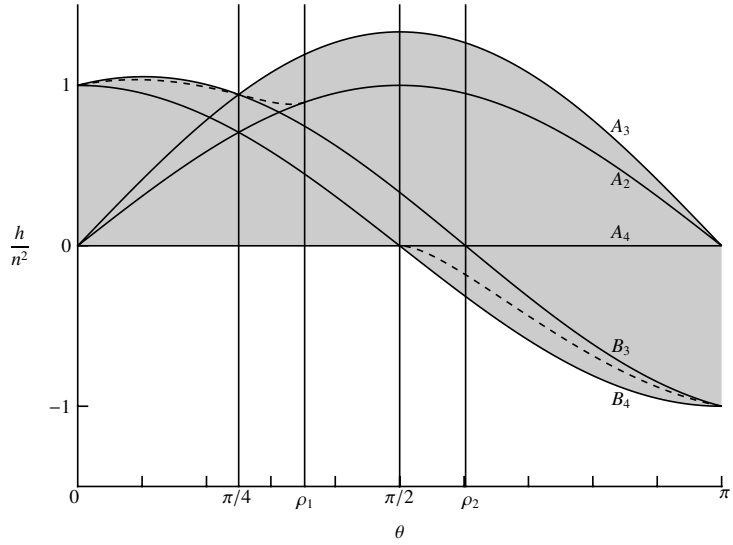


Figure 1.2: Scaled energy h/n^2 of the stationary points of \hat{H} (1.11) as a function of the parameter θ . The dashed curve marks the energy of the C_s point (see sec. 1.5).

conjugacy class of stabilizers	shorthand notation	number of modes	energy $\hat{H}(n, \theta)$
$\mathcal{D}_{2d} \times \mathcal{T}$	A_4	3	0
$\mathcal{C}_{3v} \times \mathcal{T}$	A_3	4	$\frac{4}{3}n^2 \sin \theta$
$\mathcal{C}_{2v} \times \mathcal{T}$	A_2	6	$n^2 \sin \theta$
$\mathcal{S}_4 \wedge \mathcal{T}_2$	B_4	6	$n^2 \cos \theta$
$\mathcal{C}_3 \wedge \mathcal{T}_s$	B_3	8	$\frac{1}{3}n^2(\sin \theta + 3 \cos \theta)$

Note that n is equal to the action $I = \oint pdq$ computed along the respective periodic orbit, and θ is defined in the proof of theorem 1.20. For the members of the family of systems with Hamiltonian (1.1), the absolute maximum and minimum accessible energy $E_{\max}(n)$ and $E_{\min}(n)$ for a given fixed action n can be estimated as follows: $E_{\min} = E_{A_4}$ and $E_{\min} = E_{B_4}$ in the regions $\theta \in [0, \frac{1}{2}\pi]$ and $\theta \in [\frac{1}{2}\pi, \pi]$ respectively, while $E_{\max} = E_{B_3}$ and $E_{\max} = E_{A_3}$ in the regions $\theta \in [0, \frac{1}{4}\pi]$ and $\theta \in [\frac{1}{4}\pi, \pi]$ respectively.

Proof. We find the energy for each type of RE by substituting the coordinates in table 1.1 into (1.11). Figure 1.2 and table 1.2 present the result. We now prove that \hat{H}/n^2 takes the values represented by the gray shaded region in figure 1.2. We do this in a number of steps. First, note that when $0 \leq \theta \leq \pi/2$ we have $\sin \theta \geq 0$ and $\cos \theta \geq 0$, therefore $\hat{H} \geq 0 = \hat{H}_{A_4}$ in that region.

Let $\nu^2 \equiv \nu_1^2 + \nu_2^2 + \nu_3^2$, $\sigma^2 \equiv \sigma_1^2 + \sigma_2^2 + \sigma_3^2$ and $\tau^2 \equiv \tau_1^2 + \tau_2^2 + \tau_3^2$. From (1.6a) we find that $\nu^2 \geq n^2/3$. In the region $\pi/4 \leq \theta \leq \pi$ we express \hat{H} as $\hat{H} = \sin \theta(\sigma^2 + \tau^2) + (\cos \theta - \sin \theta)\tau^2$. Using the syzygies (1.6) we find that $\sigma^2 + \tau^2 = 2(n^2 - \nu^2)$ and since $\nu^2 \geq n^2/3$ we get $\sigma^2 + \tau^2 \leq 4n^2/3$. Also when $\pi/4 \leq \theta \leq \pi$ we have $\cos \theta - \sin \theta \leq 0$. Therefore $\hat{H} \leq \sin \theta(\sigma^2 + \tau^2) \leq 4n^2 \sin \theta/3 = \hat{H}_{A_3}$.

In order to complete the argument we need to show that $\tau^2 \leq n^2$. By remark 1.19, any rotation in the original phase space $T^*\mathbf{R}^3$ leaves τ^2 unchanged. Note also that the form of the syzygies in (1.6) remains invariant under such rotation. Therefore we can rotate coordinate axes so that in the new coordinate system we have $\tau'_1 = \tau'_2 = 0$ and $\tau'^2_3 = \tau^2$. If $\tau'_3 = 0$, then what we want to prove is true. If $\tau'_3 \neq 0$ then using the syzygies we find that $\nu'_3 = \sigma'_1 = \sigma'_2 = 0$ and $\tau'^2_3 = 4\nu'_1(n - \nu'_1) - \sigma'^2_3$. It follows from the last relation that τ'^2_3 and therefore τ^2 is less or equal than n^2 .

We complete the proof. In the region $\pi/2 \leq \theta \leq \pi$ we have that $\widehat{H} = \sin \theta \sigma^2 - |\cos \theta| \tau^2$. Since $\sin \theta \geq 0$ we get $\widehat{H} \geq -|\cos \theta| \tau^2 \geq -|\cos \theta| n^2 = \widehat{H}_{B_4}$. Finally, in the region $0 \leq \theta \leq \pi/4$ we have $\widehat{H} = \sin \theta (\sigma^2 + \tau^2) + (\cos \theta - \sin \theta) \tau^2 \leq \frac{4n^2}{3} \sin \theta + n^2 (\cos \theta - \sin \theta) = \frac{n^2}{3} (\sin \theta + 3 \cos \theta) = \widehat{H}_{B_3}$. \square

We now study linear stability of the RE found in lemma 1.25 and the Morse index of the corresponding stationary points. Theorem 1.14 leaves a number of different possibilities which require a concrete study of the Hamiltonian (1.11).

Lemma 1.26. *The one-parameter family of reduced Hamiltonians (1.11) and corresponding Hamiltonians (1.1) can be separated into five qualitatively different subfamilies, which correspond to five open intervals of the values of the parameter θ . Concrete values are listed in table 1.2. Each subfamily is distinguished by a particular pattern of the linear stability of the relative equilibria in lemma 1.25.*

region	E_{\min}	E_{\max}	A_4	A_3	A_2	B_4	B_3	C_s	
I	$(0, \frac{1}{4}\pi)$	\widehat{H}_{A_4}	\widehat{H}_{B_3}	2E 0	2H 2	EH 1	EE 2	EE 4	EH 3
IIa	$(\frac{1}{4}\pi, \rho_1)$	\widehat{H}_{A_4}	\widehat{H}_{A_3}	2E 0	2E 4	EE 2	EH 1	CH 2	EH 3
IIb	$(\rho_1, \frac{1}{2}\pi)$			2E 0	2E 4	EH 3	EH 1	CH 2	
IIIa	$(\frac{1}{2}\pi, \rho_2)$	\widehat{H}_{B_4}	\widehat{H}_{A_3}	2H 2	2E 4	EH 3	EE 0	CH 2	EH 1
IIIb	(ρ_2, π)			2H 2	2E 4	EH 3	EE 0	EE 2	EH 1

Table 1.2: Stability (2E, 2H, etc, as explained in B.1) and Morse index (0...4) of the stationary points of \widehat{H} in (1.11). For the C_s points see § 1.5; $\rho_1 = \cos^{-1}(1/\sqrt{5})$ and $\rho_2 = \cos^{-1}(-1/\sqrt{10})$.

Proof. According to remark 1.13, it suffices to study one critical point for each of the five critical orbits of the $T_d \times \mathcal{T}$ action on $\mathbf{CP}^2(n)$. We begin by finding an appropriate local symplectic chart in the neighborhood of the critical point, and then compute the quadratic part of the Hamiltonian (1.11) in this local chart. We define the charts $(\chi_1, \chi_2, \psi_1, \psi_2)$ in terms of the polynomial invariants as described in detail in B. These charts are given in table 1.3. Note that the local coordinates (χ, ψ) are canonical only up to the constant terms in the Poisson brackets,

$$\{\chi_k, \psi_k\} = 1 + \dots, \quad \{\chi_1, \psi_2\} = 0 + \dots, \quad \{\chi_2, \psi_1\} = 0 + \dots, \quad k = 1, 2.$$

This is adequate only for the study of the linearized equations of motion. We now express Hamiltonian (1.11) in each local chart and expand it to the second

A_4^x	$\chi_1 = -\frac{1}{\sqrt{2n}}\sigma_2$ $\psi_1 = \frac{1}{\sqrt{2n}}\tau_2$	$\chi_2 = \frac{1}{\sqrt{2n}}\sigma_3$ $\psi_2 = \frac{1}{\sqrt{2n}}\tau_3$
	$\nu_1 = \delta/2$ $\nu_3 = (\sigma_2^2 + \tau_2^2)/2\delta$ $\tau_1 = (-\sigma_2\tau_3 - \tau_2\sigma_3)/\delta$ where $\delta = n + (n^2 - \sigma_2^2 - \sigma_3^2 - \tau_2^2 - \tau_3^2)^{1/2}$	$\nu_2 = (\sigma_3^2 + \tau_3^2)/2\delta$ $\sigma_1 = (\sigma_2\sigma_3 - \tau_2\tau_3)/\delta$
A_3^g	$\chi_1 = \frac{1}{2^{1/4}\sqrt{n}}(2n - 2\sigma_2 - \sigma_3)$ $\psi_1 = \frac{3}{2^{7/4}\sqrt{n}}\tau_3$	$\chi_2 = -\frac{1}{2^{1/4}\sqrt{3n}}(2n - 3\sigma_3)$ $\psi_2 = \frac{\sqrt{3}}{2^{7/4}\sqrt{n}}(2\tau_2 + \tau_3)$
	$\nu_1 = \delta/2$ $\nu_3 = (\sigma_2^2 + \tau_2^2)/2\delta$ $\tau_1 = (-\sigma_2\tau_3 - \tau_2\sigma_3)/\delta$ where $\delta = n - (n^2 - \sigma_2^2 - \sigma_3^2 - \tau_2^2 - \tau_3^2)^{1/2}$	$\nu_2 = (\sigma_3^2 + \tau_3^2)/2\delta$ $\sigma_1 = (\sigma_2\sigma_3 - \tau_2\tau_3)/\delta$
A_2^z	$\chi_1 = \frac{1}{\sqrt{n}}(\nu_2 - \frac{n}{2})$ $\psi_1 = \frac{1}{\sqrt{n}}\tau_3$	$\chi_2 = \frac{1}{\sqrt{n}}\sigma_1$ $\psi_2 = \frac{1}{\sqrt{n}}\tau_1$
	$\nu_1 = (\tau_3^2 + \delta^2)/4\nu_2$ $\sigma_2 = (-\tau_1\tau_3 + \sigma_1\delta)/2\nu_2$ $\tau_2 = (-\sigma_1\tau_3 - \tau_1\delta)/2\nu_2$ where $\delta = (4n\nu_2 - 4\nu_2^2 - \sigma_1^2 - \tau_1^2 - \tau_3^2)^{1/2}$	$\nu_3 = (\sigma_1^2 + \tau_1^2)/4\nu_2$ $\sigma_3 = \delta$
B_4^x	$\chi_1 = \frac{1}{\sqrt{n}}\sigma_1$ $\psi_1 = \frac{1}{\sqrt{n}}(\nu_3 - \frac{n}{2})$	$\chi_2 = \frac{1}{\sqrt{n}}\sigma_2$ $\psi_2 = \frac{1}{\sqrt{n}}\tau_2$
	$\nu_1 = (\sigma_2^2 + \tau_2^2)/4\nu_3$ $\sigma_3 = (\sigma_1\sigma_2 - \tau_2\delta)/2\nu_3$ $\tau_3 = (-\sigma_1\tau_2 - \sigma_2\delta)/2\nu_3$ where $\delta = (4n\nu_3 - 4\nu_3^2 - \sigma_1^2 - \sigma_2^2 - \tau_2^2)^{1/2}$	$\nu_2 = (\sigma_1^2 + \delta)/4\nu_3$ $\tau_1 = \delta$
B_3^g	$\chi_1 = \frac{1}{4\sqrt{n}}(\sqrt{3}(\sigma_2 - \sigma_3) + \tau_2 - \tau_3)$ $\psi_1 = -\frac{1}{2\sqrt{n}}(4n + 3\sigma_2 - \sqrt{3}\tau_2 - 2\sqrt{3}\tau_3)$	$\chi_2 = \frac{1}{4\sqrt{n}}(3(\sigma_2 + \sigma_3) + \sqrt{3}(\tau_2 + \tau_3))$ $\psi_2 = -\frac{1}{2\sqrt{n}}(\sqrt{3}\sigma_2 + 2\sqrt{3}\sigma_3 + 3\tau_2)$
	$\nu_1 = \delta/2$ $\nu_3 = (\sigma_2^2 + \tau_2^2)/2\delta$ $\tau_1 = (-\sigma_2\tau_3 - \tau_2\sigma_3)/\delta$ where $\delta = n - (n^2 - \sigma_2^2 - \sigma_3^2 - \tau_2^2 - \tau_3^2)^{1/2}$	$\nu_2 = (\sigma_3^2 + \tau_3^2)/2\delta$ $\sigma_1 = (\sigma_2\sigma_3 - \tau_2\tau_3)/\delta$

Table 1.3: Local coordinates at critical points on $\mathbf{CP}^2(n)$. We use these relations in order to express the Hamiltonian in each local chart and to compute the Poisson brackets of the local coordinates.

order terms. This gives

$$\begin{aligned}
H_{A^4}(\chi, \psi) &= 2n \cos \theta (\psi_1^2 + \psi_2^2) + 2n \sin \theta (\chi_1^2 + \chi_2^2), \\
H_{A^3}(\chi, \psi) &= \frac{4}{3} n^2 \sin \theta + \frac{4\sqrt{2}}{3} n (\cos \theta - \sin \theta) (\psi_1^2 + \psi_2^2) - \sqrt{2} n \sin \theta (\chi_1^2 + \chi_2^2); \\
H_{A^2}(\chi, \psi) &= n^2 \sin \theta + n ((\cos \theta - \sin \theta) \psi_1^2 + (2 \cos \theta - \sin \theta) \psi_2^2 - 4 \sin \theta \chi_1^2 + \sin \theta \chi_2^2); \\
H_{B^4}(\chi, \psi) &= n^2 \cos \theta + n (-4 \cos \theta \psi_1^2 + \sin \theta \psi_2^2 - (\cos \theta - \sin \theta) \chi_1^2 + \sin \theta \chi_2^2); \\
H_{B^3}(\chi, \psi) &= \frac{1}{3} n [(\sin \theta + 3 \cos \theta) (n - (\psi_1^2 + \psi_2^2)) - 2\sqrt{3} (\chi_1 \psi_1 + \chi_2 \psi_2) \\
&\quad - 12 \cos \theta (\chi_1^2 + \chi_2^2) + 6(\sin \theta - \cos \theta) (\chi_1 \psi_2 - \chi_2 \psi_1)].
\end{aligned}$$

(Note that in full agreement with remark 1.13, we can always find such two local charts for any two critical points in the same critical orbit, such that the respective local Hamiltonians are the same.) Using local quadratic Hamiltonians $H_\xi(\chi, \psi)$ we compute the Morse indices and the linear stability types in table 1.2. \square

Remark 1.27. Besides the linear stability type of the stationary points of \widehat{H} we can also determine that in some cases the stationary point is *orbitally stable*. This is true when the Morse index of the point is either 0 or 4.

Corollary 1.28. *The 27 equilibria of the system with Hamiltonian \widehat{H} in (1.11) which are the critical points of the $T_d \times \mathcal{T}$ action on \mathbf{CP}^2 satisfy Morse inequalities and give the right Euler characteristic for \mathbf{CP}^2 only in the region IIb when $\theta \in (\rho_1, \frac{1}{2}\pi)$. In this region \widehat{H} can be the simplest $T_d \times \mathcal{T}$ invariant Morse function. For all other values of θ this system must have other equilibria.*

Proof. Use lemma 1.16 and table 1.2. See also B.1. \square

1.5 Relative equilibria corresponding to non-critical points

In this section, we find additional equilibria of the system with Hamiltonian \widehat{H} in (1.11) predicted in corollary 1.28 for θ outside the closed interval $[\rho_1, \frac{1}{2}\pi]$. These additional equilibria ξ are likely to be created in bifurcations which take place when the value of θ leaves the interval $(\rho_1, \frac{1}{2}\pi)$.

Remark 1.29. Let c be one of the critical points of the $T_d \times \mathcal{T}$ action on \mathbf{CP}^2 described in theorem 1.12. By the theorem of Michel cited in sec. 1.1.3, c is a stationary point of $\widehat{H}(\theta)$ in (1.11). Suppose that the new stationary point ξ is created in a bifurcation of c . When considering where ξ can be found, we should take into account the following (see [42] for some of these statements):

1. The isotropy group G_ξ of ξ is a subgroup of the isotropy group G_c of c .
2. If c belongs not only in the closure of the stratum with trivial stabilizer $C_1 = \{E\}$ but also in the closure of one or several strata with nontrivial stabilizers $G', G'',$ etc, then a generic one-parameter bifurcation of the stationary point c will not break the symmetry G_c all the way down to C_1 , but G_ξ will be one of $G', G'',$ etc.

3. If such a generic bifurcation takes place, the new point stationary ξ with non-trivial stabilizer G_ξ will remain on a continuous set $\mathfrak{M} \subset \mathbf{CP}^2$ of non-critical G_ξ -invariant points. \mathfrak{M} in turn is a subset of a submanifold $M \subset \mathbf{CP}^2$ with isotropy group $G_M \subseteq G_\xi$.
4. The manifold $M \ni \xi$ can contain points c of higher isotropy; it can itself be a subspace of a larger manifold $M' \subset \mathbf{CP}^2$ with lower isotropy group $G_{M'} \subset G_M \subseteq G_\xi \subset G_c$.
5. When looking for stationary points $\xi \in M \subset M' \subset \dots \mathbf{CP}^2$ we should check if the Morse inequalities hold for all invariant submanifolds M, M' , etc.
6. Particularly interesting are situations when $P = M$, or M' , etc is also dynamically invariant because G_P is symplectic. In that case P is symplectic, and we can restrict our system on P and look for its equilibria there.
7. The action of $T_d \times \mathcal{T}$ on \mathbf{CP}^2 has several invariant submanifolds M with topology $\mathbf{S}^1, \mathbf{S}^2 \sim \mathbf{CP}^1$, and \mathbf{RP}^2 . Information on these manifolds and their intersections can be found in [2] and A.1. The 2-spheres with stabilizers of conjugacy class \mathcal{C}_s and \mathcal{C}_2 can serve as restricted phase spaces P .

1.5.1 Existence and stability of the $\mathcal{C}_s \wedge \mathcal{T}_2$ relative equilibria

Following remark 1.29(6–7), consider the \mathcal{C}_s and \mathcal{C}_2 -invariant spheres $\mathbf{S}^2 \subset \mathbf{CP}^2(n)$ described in A.1. Critical points of type A_4 and A_2 are intersection points of the two types of spheres (see figure A.2). This means that the new equilibrium points ξ created in a bifurcation of A_4 or A_2 can depart either on a \mathcal{C}_2 or a \mathcal{C}_s sphere, cf. remark 1.29(3). On the \mathcal{C}_s spheres we also find points of type B_4 , while on the \mathcal{C}_2 spheres we find points of type A_3 .

Lemma 1.30. *The $A_2, A_4,$ and B_4 equilibrium points of the system with Hamiltonian \tilde{H} in (1.11) alone do not give the right Euler characteristic for \mathbf{S}^2 on the \mathcal{C}_s spheres when $0 < \theta < \rho_1$ and $\frac{1}{2}\pi < \theta < \pi$, i.e., outside the region IIb in table 1.2; they give the right characteristic when $\rho_1 < \theta < \frac{1}{2}\pi$. Furthermore, for the same values of θ , the two points A_2 and A_4 , which lie on the same $\mathcal{C}_s \wedge \mathcal{T}_2$ -invariant circle of the \mathcal{C}_s sphere, alone do not give the correct Euler characteristic for \mathbf{S}^1 .*

Proof. We can always split local coordinates in table 1.3 in order to select a \mathcal{C}_s or \mathcal{C}_2 invariant symplectic pair. Then checking the Morse inequalities and the Euler characteristic for the \mathcal{C}_2 and \mathcal{C}_s spheres is straightforward. \square

Corollary 1.31. *In all regions in table 1.2 except IIb, the system with Hamiltonian (1.11) should have additional equilibria $\xi \in \mathbf{S}^1 \subset \mathbf{S}^2 \subset \mathbf{CP}^2(n)$, where the isotropy group of ξ and \mathbf{S}^1 is $\mathcal{C}_s \wedge \mathcal{T}_2$ and \mathbf{S}^2 has isotropy group \mathcal{C}_s .*

Lemma 1.32. *The $\mathcal{C}_s \wedge \mathcal{T}_2$ -invariant equilibria in corollary 1.31 exist only when*

$$0 < \theta < \rho_1 = \cos^{-1}(1/\sqrt{5}), \quad \text{or} \quad \frac{1}{2}\pi < \theta < \pi,$$

and have stability type *EH*. By symmetry, there should be two such equilibria on each of the six \mathcal{C}_s spheres. The original system with Hamiltonian (1.1) has 12 corresponding $\mathcal{C}_s \wedge \mathcal{T}_2$ -invariant nonlinear normal modes.

Proof. By an argument similar to that in remark 1.13, it is sufficient to study one of the six equivalent \mathcal{C}_s spheres. We chose the sphere \mathcal{C}_s^{ab} which is defined in A.1 as the set of points on $\mathbf{CP}^2(n)$ with coordinates

$$(\nu; \sigma; \tau) = n \left(\frac{1+w}{4}, \frac{1+w}{4}, \frac{1-w}{2}; \frac{u}{\sqrt{2}}, \frac{u}{\sqrt{2}}, \frac{1+w}{2}; \frac{v}{\sqrt{2}}, -\frac{v}{\sqrt{2}}, 0 \right) \quad (1.14)$$

where $u^2 + v^2 + w^2 = 1$. The $\mathcal{C}_s \wedge \mathcal{T}_2$ invariant circle on this sphere is defined by the additional equation $u = 0$. The reduced system restricted to this sphere corresponds to the original system restricted to the 4-plane in $T^*\mathbf{R}^3$ defined by $\{x = y, p_x = p_y\}$. The Poisson algebra generated by the functions (u, v, w) in (1.14) and restricted to the \mathcal{C}_s^{ab} sphere is the algebra $\mathfrak{so}(3)$ with Casimir $u^2 + v^2 + w^2$. We find the vector field of Hamiltonian (1.11) restricted to this sphere

$$\begin{aligned} \dot{u} &= -v(w+1)(\sin\theta - 4\cos\theta) - 4v\cos\theta \\ \dot{v} &= u(1-3w)\sin\theta \\ \dot{w} &= 4uv(\sin\theta - \cos\theta) \end{aligned} \quad (1.15)$$

The constant level sets of this system are shown in figure 1.3 in the coordinate system of figure A.3b with axis w aligned vertically. The equations $\dot{u} = \dot{v} = \dot{w} = 0$ for the equilibria on the sphere can be easily solved. Solutions $u = 0, v = 0, w = 1$ (North pole) and $u = 0, v = 0, w = -1$ (South pole) represent points A_2^z and A_4^z respectively; the two points A_3^a and A_3^b correspond to $u = \pm \frac{2}{3}\sqrt{2}, v = 0, w = \frac{1}{3}$. Positions of these critical points is shown in figure 1.3 for the example of $\theta = 5\pi/36$. The two new stationary points ξ_{\pm} have coordinates

$$u = 0, \quad v = \pm(1-w^2)^{1/2}, \quad w = \frac{\sin\theta}{4\cos\theta - \sin\theta}$$

This solution exists only for the values of θ specified in the lemma. From (1.14) we find the $\mathbf{CP}^2(n)$ coordinates of ξ_{\pm}

$$\xi_{\pm} = n(r, r, 1-2r; 0, 0, 2r; \pm 2\sqrt{r(1-2r)}, \pm 2\sqrt{r(1-2r)}, 0)$$

where $r = \cos\theta/(4\cos\theta - \sin\theta)$. In figure 1.3, $\theta = 5\pi/36$ (region I), ξ_{\pm} can be seen as two deep minima which lie on the $u = 0$ meridian slightly above the equatorial line and below the latitude of the A_3 points shown by a dashed line. As θ increases ξ_{\pm} move up (north). In the region IIa, they become unstable, see case $\theta = 11\pi/36$. In the region IIb ξ_{\pm} do not exist, they reappear for $\theta > \frac{1}{2}\pi$ as minima. Using the same local analysis as for other stationary points, i.e., finding a local symplectic chart and linearizing \hat{H} in this chart, we find that ξ_{\pm} are always of type *EH* (elliptic-hyperbolic). In the regions I, IIIa, and IIIb the elliptic plane is tangent to the sphere and the hyperbolic plane is orthogonal to the sphere; in the IIa region the situation is reversed. \square

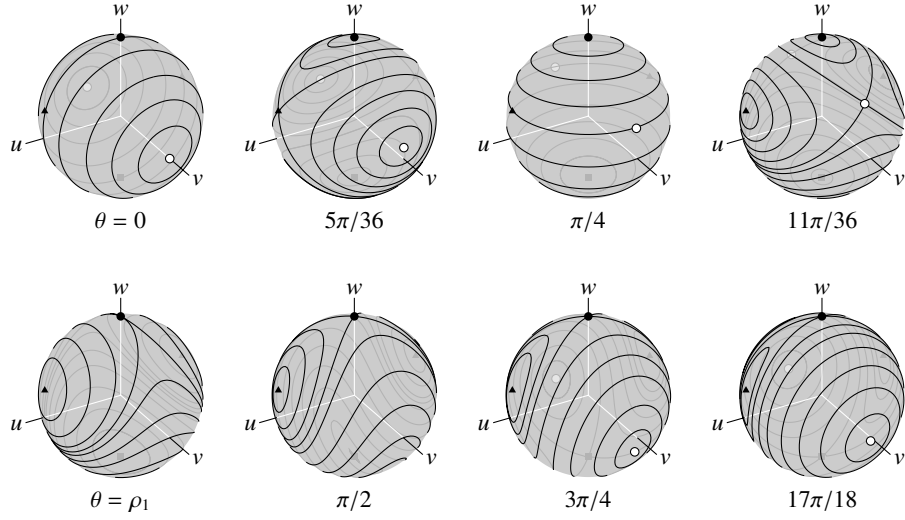


Figure 1.3: Phase portraits of the system with Hamiltonian \widehat{H} in (1.11) restricted to the \mathcal{C}_s^{ab} invariant sphere $\mathbf{S}^2 \subset \mathbf{CP}^2(n)$ for different values of the parameter θ . The location of the critical points A_2 , A_3 , and A_4 is marked by a black disc, triangle, and square respectively. The location of the \mathcal{C}_s points is marked by a white disc.

Theorem 1.33. *The reduced one-parameter Hamiltonian \widehat{H} has exactly 27 stationary points in the region $\text{Ib}(\rho_1, \frac{1}{2}\pi)$ which are the critical points of the $\mathbb{T}_d \times \mathcal{T}$ action on \mathbf{CP}^2 . In the other regions it has exactly 12 more stationary points with stabilizer $\mathcal{C}_s \wedge \mathcal{T}_2$. The only exceptional values are $\theta = 0, \frac{1}{4}\pi, \rho_1, \frac{1}{2}\pi, \rho_2, \pi$ where \widehat{H} is not a Morse function.*

Proof. The vector field $X_{\widehat{H}}$ of \widehat{H} expressed in terms of the invariants has 9 components which are quadratic polynomials:

$$\begin{aligned}
\dot{\nu}_1 &= 2(\cos \theta - \sin \theta)(\sigma_2 \tau_2 - \sigma_3 \tau_3) \\
\dot{\nu}_2 &= 2(\cos \theta - \sin \theta)(\sigma_3 \tau_3 - \sigma_1 \tau_1) \\
\dot{\nu}_3 &= 2(\cos \theta - \sin \theta)(\sigma_1 \tau_1 - \sigma_2 \tau_2) \\
\dot{\sigma}_1 &= 2(\sin \theta - \cos \theta)(\sigma_3 \tau_2 - \sigma_2 \tau_3) + 4 \cos \theta (\nu_2 - \nu_3) \tau_1 \\
\dot{\sigma}_2 &= 2(\sin \theta - \cos \theta)(\sigma_1 \tau_3 - \sigma_3 \tau_1) + 4 \cos \theta (\nu_3 - \nu_1) \tau_2 \\
\dot{\sigma}_3 &= 2(\sin \theta - \cos \theta)(\sigma_2 \tau_1 - \sigma_1 \tau_2) + 4 \cos \theta (\nu_1 - \nu_2) \tau_3 \\
\dot{\tau}_1 &= 4 \sin \theta (\nu_3 - \nu_2) \sigma_1 \\
\dot{\tau}_2 &= 4 \sin \theta (\nu_1 - \nu_3) \sigma_2 \\
\dot{\tau}_3 &= 4 \sin \theta (\nu_2 - \nu_1) \sigma_3
\end{aligned}$$

The equilibria of $X_{\widehat{H}}$ are given by the common roots of these polynomials and the polynomials Σ_k , $k = 0, \dots, 9$ (1.6). We solve this system of polynomial equations by finding its Gröbner basis using the lexicographic order $\tau_3 > \tau_2 > \tau_1 > \sigma_3 > \sigma_2 > \sigma_1 > \nu_3 > \nu_2 > \nu_1$. Such a basis can be constructed using the computer program Mathematica. Although the Gröbner basis consists of 89 polynomials it is straightforward to solve. There are two types of solutions.

27 solutions that do not depend on θ correspond to the critical stationary points of \hat{H} . 12 solutions that depend on θ correspond to the extra non-critical stationary points and are valid only when $0 < \nu_1, \nu_2, \nu_3 < n$. This condition gives that the extra stationary points do not exist in the region IIb. \square

1.5.2 Configuration space image of the $C_s \wedge \mathcal{T}_2$ relative equilibria

Remark 1.34. The evolution of the additional $C_s \wedge \mathcal{T}_2$ relative equilibria can be best seen on the interval $\theta \in [-\frac{1}{2}\pi, \rho_1]$. (The part $[-\frac{1}{2}\pi, 0]$ is equivalent to the region III $[\frac{1}{2}\pi, \pi]$ in figure 1.2 and table 1.2 up to the sign of \hat{H} , see remark 1.23.) These RE branch off the A_4 RE at $\theta = -\frac{1}{2}\pi$ and then exist continuously until their merger with the A_2 RE at $\theta = \rho_1$.

The principles of the RE representation in the configuration space $\mathbf{R}_{x,y,z}^3$ are discussed in A.4. The $C_s \wedge \mathcal{T}_2$ RE are not \mathcal{T} invariant and therefore they appear in \mathbf{R}^3 as loops. The two $C_s \wedge \mathcal{T}_2$ stationary points on the same C_s sphere, such as, for example, in figure 1.3 with $\theta = 5\pi/36$, are mapped into each other by the \mathcal{T} operation. These two points correspond to two loops running along the same closed curve in \mathbf{R}^3 in different directions. According to remark 1.34, these loops branch off one of the three A_4 orbits and merge with an A_2 orbit. Take for example the three RE A_4^z , A_2^z , and $A_2^{\bar{z}}$. The A_4^z RE is represented by a segment on axis z , while images of A_2^z and $A_2^{\bar{z}}$ lie in the planes aOb and cOd (see figure A.1 and figure 1.4, left). Note that axis z is the intersection $aOb \cap cOd$, and that the aOb and cOd planes are the configuration spaces of the restricted systems whose reduced phase spaces are the C_s^{ab} and C_s^{cd} spheres.

Without any loss to our present qualitative description, we can consider RE of the normalized system instead of those of the original system shown in figure 1.1. In the transformed space $\hat{\mathbf{R}}^3$ the A_4^z RE remains a segment of axis z , while A_2^z and $A_2^{\bar{z}}$ become segments of straight lines $x = y$ and $x = -y$ in the horizontal plane $z = 0$ as shown in figure 1.4.

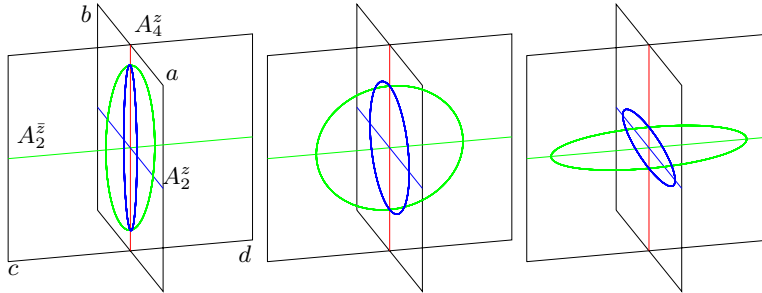


Figure 1.4: Schematic representation of the A_4^z , A_2^z , $A_2^{\bar{z}}$, and $C_s \wedge \mathcal{T}$ relative equilibria in the configuration space $\mathbf{R}_{x,y,z}^3$ of the normalized Hamiltonian (1.1).

At $\theta = \frac{1}{2}\pi$, four $C_s \wedge \mathcal{T}_2$ orbits bifurcate from A_4^z . These four RE project into two distinct closed curves in \mathbf{R}^3 . When the value of θ is only slightly above $\frac{1}{2}\pi$, the loops have a highly eccentric elliptical shape stretched along A_4^z , see figure 1.4, left. The major axis of the ellipsis is on the z axis and the ellipsis

lie in the aOb and cOd planes respectively. As θ increases, the eccentricity is reduced until the ellipses become circles at $\theta = \frac{5}{4}\pi$. At this point the elliptic and hyperbolic directions for the $\mathcal{C}_s \wedge \mathcal{T}_2$ points $\xi_{\pm} \in \mathbf{CP}^2(n)$ are interchanged. For $\theta > \frac{5}{4}\pi$ the eccentricity increases again but now the major axes lie near the intersections the $aOb \cap xOy$ and $cOd \cap xOy$ respectively. As θ approaches $\pi + \rho_1$, the two ellipses come closer to the orbits A_2^z and $A_2^{\bar{z}}$ and vanish exactly at $\theta = \pi + \rho_1$.

1.6 Bifurcations

Definition 1.35. The system with Hamiltonian (1.1) is called generic if it is ϵ^2 -generic and the corresponding principal order of the reduced Hamiltonian \hat{H} in (1.11) is a $T_d \times \mathcal{T}$ -invariant Morse function on $\mathbf{CP}^2(n)$.

Generic systems belong to one of the subfamilies in table 1.2. We have characterized the RE of these systems. In this section we comment on some of the changes of linear stability of the RE in table 1.2 and the possible bifurcations that may be happening when the parameter θ is varied. A full study of non-Morse members of the family (1.11) and bifurcations of RE requires going to higher orders of the normal form and is beyond the scope of our present work. Some of these bifurcations cannot be fully understood using the single-parameter classification scheme of sec. 1.2.

As we saw in sec. 1.5.1, several bifurcations are related to the evolution of the $\mathcal{C}_s \wedge \mathcal{T}_2$ RE. At $\theta = \frac{1}{2}\pi$ (or $-\frac{1}{2}\pi$) four $\mathcal{C}_s \wedge \mathcal{T}_2$ RE are created in the bifurcation of each of the three A_4 RE. In this bifurcation, as we go from the region IIb to IIIa in table 1.2, stability and Morse index of the A_4 RE change from 2E and 0 to 2H and 2 respectively. Since A_4 and B_4 share the same \mathcal{C}_2 -invariant subspace \mathbf{S}^2 (figure A.3, left), the Morse index change of A_4 forces the change of the Morse index of B_4 in order to preserve the right Euler characteristic of \mathbf{S}^2 . When $\theta = \pi$ and we enter region I from IIIb, the Morse index of A_4 changes from 2 to 0 (or 4, see remark 1.23). When $\theta = \rho_1$ the $\mathcal{C}_s \wedge \mathcal{T}_2$ RE collide pairwise at the A_2 RE and vanish. At this moment the A_2 RE change linear stability type from EE to EH and Morse index from 2 to 1. This bifurcation can be considered as a collision of two stationary points on the \mathcal{C}_s sphere; in systems with one degree of freedom it is often called a ‘pitchfork’ bifurcation.

The stability type of the B_3 points changes between elliptic-elliptic (EE) and complex hyperbolic (CH) at $\theta = \pi/4$ and $\theta = \rho_2$. At these values of θ the four eigenvalues of the respective Hamiltonian matrices move along the imaginary axis, collide pairwise, and then move off the axis into the complex plane. Such $EE \leftrightarrow CH$ change of linear stability is called a standard *linear Hamiltonian Hopf bifurcation*¹. It suggests that a *nonlinear* Hamiltonian Hopf bifurcation might also be taking place [85]. This important codimension-one bifurcation happens in Hamiltonian systems with two or more degrees of freedom. The $EE \leftrightarrow CH$ change is necessary but not sufficient for the standard nonlinear Hamiltonian Hopf bifurcation. The latter occurs when a family of periodic orbits either detaches from the bifurcating stationary point or shrinks to this point and

¹The name is due to the analogy with the Hopf bifurcation in dissipative systems.

disappears. We should take the nonlinearity of the system into account in order to find out if this takes place.

Unfortunately, standard theorems on the Hamiltonian Hopf bifurcation do not apply directly in our case. Thus when $\theta = \rho_2$ we can prove that the B_3 points lie on an invariant two-dimensional manifold and as a consequence, the bifurcation remains degenerate in all orders. A preliminary study using normal form techniques shows that a bifurcation of short periodic orbits which differs slightly from the Hamiltonian Hopf bifurcation takes place at $\theta = \rho_2$. At $\theta = \frac{1}{4}\pi$ the eigenvalues of the Hamiltonian matrix of the linearized equations near the B_3 equilibrium meet at 0 and then leave off to the complex plane. This means that at the moment of bifurcation the quadratic part of the local Hamiltonian is nilpotent and cannot be normalized in the standard way. We believe that both the degeneracy of the $\theta = \rho_2$ case and the nilpotency of the $\theta = \frac{1}{4}\pi$ case can be removed in the sixth (or higher) order normal form of (1.1).

A generalization of the linear Hamiltonian Hopf bifurcation is proposed in [47]. This paper describes a bifurcation of short periodic orbits that happens when a stationary point with isotropy group $\text{SO}(2) \times \mathcal{T}$ changes linear stability type from degenerate elliptic (2E) to degenerate hyperbolic (2H). In our system, the A_3 and A_4 RE change stability type from 2E to 2H at $\theta = \frac{1}{4}\pi$ and $\theta = \frac{1}{2}\pi$ respectively. Since by theorem 1.14 the A_4 and A_3 RE can only be of type 2E or 2H, the eigenvalues must become simultaneously zero when their stability changes from 2E to 2H. This degeneracy is robust under $\text{T}_d \times \mathcal{T}$ symmetric perturbations.

1.7 The 3-mode as a 3-DOF analogue of the Hénon-Heiles Hamiltonian

In [51] M. Hénon and C. Heiles introduced the Hamiltonian

$$H(x, y, p_x, p_y) = \frac{1}{2}(x^2 + p_x^2) + \frac{1}{2}(y^2 + p_y^2) + \epsilon(x^2y - \frac{1}{3}y^3), \quad (1.16)$$

which is since known as the 2-DOF (or 2D) Hénon-Heiles Hamiltonian. The specific form of its potential was chosen “because: (i) it is analytically simple; . . . (ii) at the same time, it is sufficiently complicated to give trajectories far from trivial” [51].

As Hénon and Heiles found numerically in [51], an additional integral of motion did not exist in the 2-DOF system with Hamiltonian (1.16). Their study resulted in the first illustrations of Hamiltonian chaos, and their system has since been studied extensively both numerically and analytically, see [77] for a detailed list of references. It has served not only as a model for the dynamics near the center of a galaxy but also in molecular physics where it has been used to describe doubly degenerate vibrations of molecules whose equilibrium configuration has one or several three-fold symmetry axis [78], such as H_3^+ [40], P_4 or CH_4 , and SF_6 .

The Hamiltonian (1.16) is symmetric under the action of the finite group $\mathcal{D}_3 \times \mathcal{T}$. Here \mathcal{D}_3 is the dihedral symmetry group of the equilateral triangle, and $\mathcal{T} = \{1, T\}$ is the *time reversal* or *momentum reversal* group generated by $T : (x, y, p_x, p_y) \rightarrow (x, y, -p_x, -p_y)$. Although the finite symmetry of (1.16) was not particularly emphasized in [51], it has one very important consequence, namely the *a priori* existence at low energy of eight families of periodic orbits

called *nonlinear normal modes* [17, 66, 67]. In fact, this is a property of *any* $\mathcal{D}_3 \times \mathcal{T}$ symmetric 1:1 resonant 2-oscillator.

There are many ways to introduce three degree of freedom analogues of the two degree of freedom Hénon-Heiles Hamiltonian (1.16). The most obvious is to consider the 3-DOF axisymmetric Hamiltonian

$$H(r, \theta, z, p_r, p_\theta, p_z) = \frac{1}{2}(p_r^2 + p_z^2) + \frac{p_\theta^2}{2r^2} + \frac{1}{2}(r^2 + z^2) + r^2 z - \frac{1}{3}z^3, \quad (1.17)$$

from which Hamiltonian (1.16) was deduced, see [51]. Here (r, θ, z) are cylindrical coordinates in \mathbf{R}^3 . This 3-DOF Hamiltonian has been studied in [36, 37, 94] where it is called the 3D Hénon-Heiles Hamiltonian. The reduction of the axial symmetry was done in [22] where it is shown that the reduced system is in 1:2 resonance.

We propose here a different analogue based on the extension of the discrete symmetry of (1.16) to \mathbf{R}^3 . Specifically, we propose Hamiltonian (1.1) with $K_R = 0$ as a three degree of freedom analogue of the two degree of freedom Hénon-Heiles Hamiltonian.

Comparison of the family (1.1) to the 2D Hénon-Heiles Hamiltonian (1.16).

1. Like the 2D Hénon-Heiles system, the system with Hamiltonian (1.1) is probably not integrable and hence is a genuinely three-dimensional system in the sense that the only exact first integrals are smooth functions of energy. This is in contrast to Hamiltonian (1.17) which has an axial symmetry and therefore can be reduced to a two degree of freedom system.
2. Both (1.16) and (1.1) have no compact Lie group of symmetries. Both are invariant under the action of a discrete group which includes rotations by $2\pi/3$ and the time reversal group \mathcal{T} described above. The Hamiltonian (1.1) is invariant under the action of the group $T_d \times \mathcal{T}$. This symmetry group has four conjugate subgroups $C_{3v} \times \mathcal{T}$ which are isomorphic to the symmetry group of (1.16).
3. Both (1.16) and (1.1) have principal cubic perturbation terms of the simplest possible analytic form which realize completely the respective point group symmetries D_3 and T_d . The polynomial

$$V(x, y, z) = \frac{1}{2}\mu_2 + \epsilon K_3 \mu_3 + \epsilon^2 K_4 \mu_4 + \epsilon^2 K_0 \mu_2^2 \quad (1.18)$$

is the most general T_d -invariant polynomial in (x, y, z) of degree 4.

Notice that the analysis of the fourth order normal form does not depend essentially on K_R since the latter enters only through K_t (1.13d). Therefore, all the analysis of this chapter applies also to our three degree of freedom analogue of the Hénon-Heiles Hamiltonian.

2

The hydrogen atom in crossed fields

In §0.2 we gave the Hamiltonian (0.13) which describes the hydrogen atom in crossed electric and magnetic fields. Recall here that the Hamiltonian is

$$H(Q, P) = \frac{1}{2}\mathbf{P}^2 - \frac{1}{|\mathbf{Q}|} + FQ_2 + \frac{1}{2}G(Q_2P_3 - Q_3P_2) + \frac{1}{8}G^2(Q_2^2 + Q_3^2) \quad (2.1)$$

where F and G represent the strength of the electric and the magnetic fields respectively.

2.1 Review of the Keplerian normalization

Normalization of a perturbation of the Kepler Hamiltonian with respect to Φ_0 has the problem that the potential is singular at $\mathbf{Q} = 0$ and the flow of the Kepler Hamiltonian is not complete. Therefore, in order to do the normalization we have to regularize the vector field X_{H_0} . This procedure gives a complete vector field. Many ways to achieve this have been proposed, but the most convenient for our purposes is Kustaanheimo-Stiefel regularization.

2.1.1 Kustaanheimo-Stiefel regularization

The Kustaanheimo-Stiefel regularization [54] is a standard procedure for the regularization of the Kepler vector field. We fix an energy level $E < 0$ (we are only interested in bounded motions) and introduce the new time scale $dt \rightarrow dt/|Q|$ in (2.1). The result is

$$1 = \frac{1}{2}(P^2 - 2E)|Q| + FQ_2|Q| + \frac{1}{2}G(Q_2P_3 - Q_3P_2)|Q| + \frac{1}{8}G^2(Q_2^2 + Q_3^2)|Q| \quad (2.2)$$

where the term $\frac{1}{2}(P^2 - 2E)|Q|$ comes from the Kepler Hamiltonian.

The Kustaanheimo-Stiefel regularization is defined by the transformation

$$\mathcal{KS} : T_0\mathbf{R}^4 \rightarrow T_0\mathbf{R}^3 : (q, p) \mapsto (M(q) \cdot q, \frac{1}{q^2}M(q) \cdot p) = (Q, 0, P, 0) \quad (2.3)$$

where $M(q)$ is the matrix

$$M(q) = \begin{pmatrix} q_1 & -q_2 & -q_3 & q_4 \\ q_2 & q_1 & -q_4 & -q_3 \\ q_3 & q_4 & q_1 & q_2 \\ q_4 & -q_3 & q_2 & -q_1 \end{pmatrix} \quad (2.4)$$

Notice that

$$\zeta = \frac{1}{2}(q_1 p_4 - q_2 p_3 + q_3 p_2 - q_4 p_1) = 0 \quad (2.5)$$

and that ζ generates an \mathbf{S}^1 action on $T_0\mathbf{R}^4$ called the KS symmetry. Any function defined on $T_0\mathbf{R}^4$ through the KS transformation Poisson commutes with ζ . Therefore we can treat ζ as a constant identically equal to 0.

Applying \mathcal{KS} to (2.2), scaling $(q, p) \rightarrow (q/\sqrt{\omega}, p\sqrt{\omega})$ and changing the time by $t \rightarrow \omega t$ we obtain the Hamiltonian

$$H = \frac{1}{2}(p^2 + q^2) + \frac{1}{3}f(q_1 q_2 - q_3 q_4)q^2 + \frac{1}{2}g(q_2 p_3 - q_3 p_2)q^2 + \frac{1}{8}g^2(q_1^2 + q_4^2)(q_2^2 + q_3^2)q^2 \quad (2.6)$$

where we have defined

$$\omega^2 = -2E \quad f = \frac{6F}{\omega^3} = \epsilon b \quad g = \frac{2G}{\omega^2} = \epsilon a \quad a^2 + b^2 = 1 \quad (2.7)$$

The parameters a, b characterize the relative strengths of the magnetic and electric field respectively, while ϵ characterizes the absolute strength of the fields.

2.1.2 First normalization

We normalize the Hamiltonian (2.6) with respect to the unperturbed part $H_0 = \frac{1}{2}(q^2 + p^2)$, which describes a 4-oscillator in 1:1:1:1 resonance. The result of the normalization and truncation is the Hamiltonian

$$\tilde{H} = \tilde{H}_2 + \epsilon \tilde{H}_4 + \epsilon^2 \tilde{H}_6 + \epsilon^3 \tilde{H}_8 + \epsilon^4 \tilde{H}_{10} \quad (2.8)$$

where each term \tilde{H}_j is a homogeneous polynomial of degree j in (q, p) . We do not give explicit expressions for \tilde{H} since these can be easily determined from the expressions of the reduced Hamiltonian \hat{H} (2.14) that we give later, see table 2.1.

Remark 2.1. We truncate the normal form \tilde{H} at \tilde{H}_{10} for reasons we explain at §2.6.3.

2.1.3 First reduction

The vector field X_{H_0} of $H_0 = \frac{1}{2}(p^2 + q^2)$ generates an \mathbf{S}^1 action Φ_0 on \mathbf{R}^8 . The vector field X_ζ of ζ (2.5) generates a different \mathbf{S}^1 action Φ^ζ . These actions commute since $\{H_0, \zeta\} = 0$, therefore they define a \mathbf{T}^2 action on \mathbf{R}^8 . We have that

Lemma 2.2. *The algebra $\mathbf{R}[q, p]^{\mathbf{T}^2}$ of the polynomials that are invariant under the \mathbf{T}^2 action generated by H_0 and ζ is generated by the invariant polynomials*

$$\begin{aligned}
K_1 &= \frac{1}{4}(p_2^2 + q_2^2 + p_3^2 + q_3^2 - p_1^2 - q_1^2 - p_4^2 - q_4^2) \\
K_2 &= \frac{1}{2}(p_3p_4 - q_1q_2 - p_1p_2 + q_3q_4) \\
K_3 &= -\frac{1}{2}(q_1q_3 + q_2q_4 + p_1p_3 + p_2p_4) \\
L_1 &= \frac{1}{2}(q_2p_3 - q_3p_2 + q_1p_4 - q_4p_1) \\
L_2 &= \frac{1}{2}(q_2p_4 + q_3p_1 - q_1p_3 - q_4p_2) \\
L_3 &= \frac{1}{2}(q_1p_2 + q_3p_4 - q_2p_1 - q_4p_3) \\
n &= \frac{1}{4}(p_1^2 + q_1^2 + p_2^2 + q_2^2 + p_3^2 + q_3^2 + p_4^2 + q_4^2) \\
\zeta &= \frac{1}{2}(q_1p_4 - q_2p_3 + q_3p_2 - q_4p_1)
\end{aligned} \tag{2.9}$$

which satisfy the relations

$$K^2 + L^2 = n^2 + \zeta^2 \quad K \cdot L = -n\zeta \tag{2.10}$$

Note that the vectors $K = (K_1, K_2, K_3)$ and $L = (L_1, L_2, L_3)$ are the KS transformed eccentricity and angular momentum vectors respectively.

The space of \mathbf{T}^2 orbits on $H_0^{-1}(2n) \cap \zeta^{-1}(0)$ is defined by

$$K^2 + L^2 = n^2 \quad K \cdot L = 0 \tag{2.11}$$

or equivalently

$$(K + L)^2 = n^2 \quad (K - L)^2 = n^2 \tag{2.12}$$

Therefore the space of \mathbf{T}^2 orbits on $H_0^{-1}(2n) \cap \zeta^{-1}(0)$ is $\mathbf{S}^2 \times \mathbf{S}^2$. The Poisson structure on the reduced space is

$$\{L_i, L_j\} = \sum_k \varepsilon_{ijk} L_k \quad \{K_i, K_j\} = \sum_k \varepsilon_{ijk} L_k \quad \{L_i, K_j\} = \sum_k \varepsilon_{ijk} K_k \tag{2.13}$$

We reduce the normalized Hamiltonian (2.8) with respect to the \mathbf{T}^2 action by expressing it in terms of the polynomials (2.9). The result is

$$\widehat{H} = \widehat{H}_2 + \epsilon \widehat{H}_4 + \epsilon^2 \widehat{H}_6 + \epsilon^3 \widehat{H}_8 + \epsilon^4 \widehat{H}_{10} \tag{2.14}$$

Setting $\zeta = 0$ the first terms of \widehat{H} become

$$\widehat{H}_2 = 2n \tag{2.15}$$

$$\widehat{H}_4 = n(aL_1 - bK_2) \tag{2.16}$$

The coefficients for the other terms are presented in table 2.1. Next we subtract the constant term $\widehat{H}_2 = 2n$ and then divide \widehat{H} by $n\epsilon$.

In the resulting rescaled Hamiltonian, called the *first reduced* Hamiltonian, we make the successive linear changes of variables

$$\begin{aligned}
T_1 &= aL_1 - bK_2 & T_2 &= aL_2 + bK_1 & T_3 &= L_3 \\
V_1 &= aK_1 - bL_2 & V_2 &= aK_2 + bL_1 & V_3 &= K_3
\end{aligned} \tag{2.17}$$

Coefficients of terms of $72\tilde{H}_6$		Coefficients of terms of $13824\tilde{H}_{10}$	
n^2	$-17b^2$	n^4	$1504a^2b^2 - 3563b^4$
L_3^2	$9a^2$	$n^2L_3^2$	$36a^4 + 1086a^2b^2$
L_2^2	$9a^2 + 9b^2$	L_3^4	$-351a^4 - 240a^2b^2$
K_3^2	$45a^2$	$n^2L_2^2$	$36a^4 - 1110a^2b^2 + 2970b^4$
K_2L_1	$84ab$	$L_2^2L_3^2$	$-702a^4 - 278a^2b^2$
K_2^2	$45a^2 - 51b^2$	L_2^4	$-351a^4 - 38a^2b^2 - 303b^4$
K_1L_2	$-12ab$	$n^2L_1^2$	$10224a^4 - 66192a^2b^2$
Coefficients of terms of $288\tilde{H}_8$		$L_1^2L_3^2$	$-9072a^4 + 46736a^2b^2$
n^2L_1	$337ab^2$	$L_1^2L_2^2$	$-9072a^4 + 53712a^2b^2$
$L_1L_3^2$	$-54a^3 - 102ab^2$	L_1^4	$-6768a^4 + 46976a^2b^2$
$L_1L_2^2$	$-54a^3 - 192ab^2$	$K_3L_1L_2L_3$	$12312a^3b + 120ab^3$
L_1^3	$-72a^3 - 102ab^2$	$n^2K_3^2$	$-4716a^4 + 9462a^2b^2$
$K_3L_2L_3$	$-144a^2b$	$K_3^2L_3^2$	$-12690a^4 + 48080a^2b^2$
$K_3^2L_1$	$-270a^3 - 108ab^2$	$K_3^2L_2^2$	$-2358a^4 - 2334a^2b^2$
n^2K_2	$156a^2b - 250b^3$	$K_3^2L_1^2$	$48080a^2b^2$
$K_2L_3^2$	$60a^2b$	K_3^4	$-5895a^4$
$K_2L_2^2$	$-84a^2b + 86b^3$	$n^2K_2L_1$	$-27768a^3b + 74320ab^3$
$K_2L_1^2$	$-246a^2b$	$K_2L_1L_3^2$	$-5976a^3b - 10056ab^3$
$K_2K_3^2$	$330a^2b$	$K_2L_1L_2^2$	$6336a^3b - 27312ab^3$
$K_2^2L_1$	$-270a^3 + 510ab^2$	$K_2L_1^3$	$2784a^3b - 10056ab^3$
K_2^3	$330a^2b - 250b^3$	$K_2K_3L_2L_3$	$-20664a^4 + 70888a^2b^2$
$K_1K_3L_3$	$108ab^2$	$K_2K_3^2L_1$	$-47520a^3b - 11232ab^3$
		$n^2K_2^2$	$-4716a^4 + 38978a^2b^2 - 35630b^4$
		$K_2^2L_3^2$	$-2358a^4 + 5266a^2b^2$
		$K_2^2L_2^2$	$-12690a^4 + 25740a^2b^2 + 8910b^4$
		$K_2^2K_3^2$	$-11790a^4 + 31290a^2b^2$
		$K_2^3L_1$	$-47520a^3b + 48000ab^3$
		K_2^4	$-5895a^4 + 31290a^2b^2 - 17815b^4$
		$n^2K_1L_2$	$-336a^3b - 4352ab^3$
		$K_1L_2L_3^2$	$768a^3b - 120ab^3$
		$K_1L_2^3$	$768a^3b + 744ab^3$
		$K_1K_3^2L_2$	$3720a^3b$
		$K_1K_2K_3L_3$	$-3720a^3b + 11232ab^3$

Table 2.1: Coefficients of the terms of the first normal form \tilde{H} .

and

$$\begin{aligned}
x_1 &= \frac{T_1 + V_1}{2} & x_2 &= \frac{T_2 + V_2}{2} & x_3 &= \frac{T_3 + V_3}{2} \\
y_1 &= \frac{T_1 - V_1}{2} & y_2 &= \frac{T_2 - V_2}{2} & y_3 &= \frac{T_3 - V_3}{2}
\end{aligned} \tag{2.18}$$

The variables x, y satisfy

$$x_1^2 + x_2^2 + x_3^2 = \frac{n^2}{4} \quad y_1^2 + y_2^2 + y_3^2 = \frac{n^2}{4} \tag{2.19}$$

They span the algebra $\mathfrak{so}(3) \times \mathfrak{so}(3) = \mathfrak{so}(4)$. Specifically, the Poisson structure is

$$\{x_i, x_j\} = \sum_k \varepsilon_{ijk} x_k \quad \{y_i, y_j\} = \sum_k \varepsilon_{ijk} y_k \quad \{x_i, y_j\} = 0 \tag{2.20}$$

After all these transformations the lowest order non-trivial term of the first reduced Hamiltonian becomes

$$\mathcal{H}_1 = \hat{H}_4 = x_1 + y_1 \tag{2.21}$$

We define $\mathcal{H}_j = \widehat{H}_{2j+2}$. Notice that \mathcal{H}_j is a homogeneous polynomial of degree j in (x, y, n) . The first reduced Hamiltonian can be written in terms of (x, y, n) as

$$\mathcal{H} = \mathcal{H}_1 + \epsilon \mathcal{H}_2 + \epsilon^2 \mathcal{H}_3 + \epsilon^3 \mathcal{H}_4 \quad (2.22)$$

where the terms \mathcal{H}_2 , \mathcal{H}_3 and \mathcal{H}_4 can be computed straightforwardly from table 2.1 using (2.17) and (2.18).

2.2 Second normalization and reduction

A characteristic feature of the hydrogen atom in crossed fields is that the vector field of the first term \mathcal{H}_1 of \mathcal{H} (2.22) induces an \mathbf{S}^1 action on $\mathbf{S}^2 \times \mathbf{S}^2$. We normalize and reduce \mathcal{H} with respect to this action.

2.2.1 Second normalization

\mathcal{H}_1 generates the \mathbf{S}^1 action Φ on $\mathbf{S}^2 \times \mathbf{S}^2$ given by

$$\Phi : \mathbf{S}^1 \times (\mathbf{S}^2 \times \mathbf{S}^2) \rightarrow (\mathbf{S}^2 \times \mathbf{S}^2) : (t, (x, y)) \rightarrow (x_1, R(t) \begin{pmatrix} x_2 \\ x_3 \end{pmatrix}, y_1, R(t) \begin{pmatrix} y_2 \\ y_3 \end{pmatrix}) \quad (2.23)$$

where $R(t) = \begin{pmatrix} \cos t & -\sin t \\ \sin t & \cos t \end{pmatrix}$.

We normalize the Hamiltonian \mathcal{H} (2.22) with respect to Φ . First, we define new variables

$$\begin{aligned} z_1 &= \frac{1}{2}x_1 & z_2 &= \frac{1}{2\sqrt{2}}(x_2 + ix_3) & \bar{z}_2 &= \frac{1}{2\sqrt{2}}(x_2 - ix_3) \\ w_1 &= \frac{1}{2}y_1 & w_2 &= \frac{1}{2\sqrt{2}}(y_2 + iy_3) & \bar{w}_3 &= \frac{1}{2\sqrt{2}}(y_2 - iy_3) \end{aligned} \quad (2.24)$$

Then notice that

$$\{z_1, z_2\} = \frac{z_2}{2i} \quad \{z_1, \bar{z}_2\} = -\frac{\bar{z}_2}{2i} \quad \{z_2, \bar{z}_2\} = \frac{z_1}{2i} \quad (2.25)$$

In these variables \mathcal{H}_1 becomes $\mathcal{H}_1 = 2(z_1 + w_1)$ and the action of $\text{ad}_{\mathcal{H}_1} = \{\mathcal{H}_1, \cdot\}$ on a monomial $z^a w^b = z_1^{a_1} z_2^{a_2} \bar{z}_2^{a_3} w_1^{b_1} w_2^{b_2} \bar{w}_2^{b_3}$ is diagonal:

$$\{\mathcal{H}_1, z^a w^b\} = -i(a_2 - a_3 + b_2 - b_3)z^a w^b \quad (2.26)$$

Therefore the variables z and w are particularly suitable for the application of the standard Lie series algorithm [27, 43] for the computation of the second normal form, since they trivialize the task of solving the homological equation.

Remark 2.3. Another way to perform the second normalization is to express \mathcal{H} (2.22) in terms of the original variables (q, p) . Then normalization can be performed in these variables and the result can be re-expressed in terms of the variables (x, y) .

The result of the second normalization is the Hamiltonian

$$\tilde{\mathcal{H}} = \tilde{\mathcal{H}}_1 + \epsilon \tilde{\mathcal{H}}_2 + \epsilon^2 \tilde{\mathcal{H}}_3 + \epsilon^3 \tilde{\mathcal{H}}_4 \quad (2.27)$$

where each term $\tilde{\mathcal{H}}_j$ is a homogeneous polynomial of degree j in (x, y, n) . Explicit expressions for $\tilde{\mathcal{H}}$ can be easily obtained from the expressions for the second reduced Hamiltonian $\widehat{\mathcal{H}}$ (2.32) given in table 2.2.

2.2.2 Second reduction

Lemma 2.4. *The algebra $\mathbf{R}[x, y]^\Phi$ of Φ (2.23) invariant polynomials in the variables (x, y) is generated by*

$$\begin{aligned} \pi_1 &= x_1 - y_1 & \pi_2 &= 4(x_2y_2 + x_3y_3) & \pi_3 &= 4(x_3y_2 - x_2y_3) \\ \pi_4 &= x_1 + y_1 & \pi_5 &= 4(x_2^2 + x_3^2) & \pi_6 &= 4(y_2^2 + y_3^2) \end{aligned} \quad (2.28)$$

These invariants satisfy

$$\pi_2^2 + \pi_3^2 = \pi_5\pi_6 \quad (2.29a)$$

$$\pi_5 = n^2 - (\pi_1 + \pi_4)^2 \quad (2.29b)$$

$$\pi_6 = n^2 - (\pi_1 - \pi_4)^2 \quad (2.29c)$$

$$\pi_5 \geq 0, \quad \pi_6 \geq 0 \quad (2.29d)$$

Note that $\pi_4 = \mathcal{H}_1$ is the generator of Φ .

The second reduced phase space $M_{n,c} = (\tilde{\mathcal{H}}_1|\mathbf{S}_n^2 \times \mathbf{S}_n^2)^{-1}(c)/\mathbf{S}^1$ is the semi-algebraic variety in \mathbf{R}^3 with coordinates (π_1, π_2, π_3) defined by

$$\pi_2^2 + \pi_3^2 = (n^2 - (\pi_1 + c)^2)(n^2 - (\pi_1 - c)^2) \quad (2.30a)$$

$$\pi_1 \in [n - |c|, n + |c|] \quad (2.30b)$$

Notice that in \mathbf{R}^3 the spaces $M_{n,c}$ and $M_{n,-c}$ have the same representation. The Poisson structure on $M_{n,c}$ is

$$\{\pi_1, \pi_2\} = 2\pi_3 \quad (2.31a)$$

$$\{\pi_1, \pi_3\} = -2\pi_2 \quad (2.31b)$$

$$\{\pi_2, \pi_3\} = 4\pi_1(n^2 + c^2 - \pi_1^2) \quad (2.31c)$$

Expressing $\tilde{\mathcal{H}}$ (2.27) in terms of $\pi_1, \pi_2, \pi_3, \pi_4 = c$ gives the second reduced Hamiltonian

$$\hat{\mathcal{H}} = \hat{\mathcal{H}}_1 + \epsilon\hat{\mathcal{H}}_2 + \epsilon^2\hat{\mathcal{H}}_3 + \epsilon^3\hat{\mathcal{H}}_4 \quad (2.32)$$

where

$$\hat{\mathcal{H}}_1 = \pi_4 = c \quad (2.33)$$

The coefficients of the terms $\hat{\mathcal{H}}_2, \hat{\mathcal{H}}_3$ and $\hat{\mathcal{H}}_4$ are given in table 2.2.

2.2.3 Fixed points

The \mathbf{S}^1 action Φ (2.23) is not free. It leaves fixed the points

$$p_\pm = \frac{n}{2}(\pm 1, 0, 0; \mp 1, 0, 0) \quad \text{and} \quad z_\pm = \frac{n}{2}(\pm 1, 0, 0; \pm 1, 0, 0)$$

on $\mathbf{S}^2 \times \mathbf{S}^2$. Note that we use coordinates $(x_1, x_2, x_3; y_1, y_2, y_3)$ to describe points on $\mathbf{S}^2 \times \mathbf{S}^2$. Therefore by Michel's theorem [62] these points are equilibria of any Φ invariant Hamiltonian on $\mathbf{S}^2 \times \mathbf{S}^2$. In particular, they are equilibria of $\tilde{\mathcal{H}}$ (2.27).

Notice that the equilibria p_\pm and z_\pm of $\tilde{\mathcal{H}}$ correspond to equilibria of \mathcal{H} for small enough ϵ . The problem is that the position of the equilibria of \mathcal{H} depends on n and ϵ . One can find the equilibria of \mathcal{H} directly by solving $X_{\mathcal{H}}|\mathbf{S}^2 \times \mathbf{S}^2 = 0$, using a Newton-Raphson method with p_\pm or z_\pm as initial guess.

Coefficients of terms of $72\widehat{\mathcal{H}}_2$	
π_2	$-18 a^2$
π_1^2	$9 - 18 a^2 - 18 a^4$
c^2	$-51 + 42 a^2 - 18 a^4$
n^2	$-17 + 38 a^2 + 6 a^4$
Coefficients of terms of $288\widehat{\mathcal{H}}_3$	
$\pi_2 c$	$136 a^2 - 16 a^4 - 12 a^6$
$\pi_1^2 c$	$-86 + 168 a^2 - 10 a^4 + 192 a^6 - 102 a^8$
c^3	$250 - 304 a^2 + 122 a^4 + 56 a^6 - 34 a^8$
$n^2 c$	$250 - 576 a^2 + 178 a^4 - 32 a^6 + 18 a^8$
Coefficients of terms of $13824\widehat{\mathcal{H}}_4$	
π_2^2	$-1020 a^4 + 48 a^6 + 144 a^8 - 144 a^{10}$
π_1^4	$-303 + 1252 a^2 - 304 a^4 + 996 a^6 - 3792 a^8 + 1500 a^{10} - 1500 a^{12}$
$\pi_2 n^2$	$-4908 a^2 + 8104 a^4 + 2004 a^6 + 56 a^8 - 108 a^{10}$
$\pi_1^2 \pi_2$	$1140 a^2 - 2104 a^4 - 1412 a^6 + 264 a^8 - 660 a^{10}$
$\pi_1^2 n^2$	$2970 - 11048 a^2 + 8528 a^4 - 1064 a^6 + 7640 a^8 - 1416 a^{10} + 1032 a^{12}$
$\pi_1^3 c^2$	$8910 - 19896 a^2 + 8016 a^4 - 9144 a^6 - 16608 a^8 + 27624 a^{10} - 9000 a^{12}$
$\pi_2 c^2$	$-13092 a^2 + 6136 a^4 - 996 a^6 + 1256 a^8 - 612 a^{10}$
$n^2 c^2$	$-35630 + 91624 a^2 - 54800 a^4 + 6888 a^6 + 5784 a^8 - 2568 a^{10} + 1032 a^{12}$
c^4	$-17815 + 28628 a^2 - 16320 a^4 - 1292 a^6 + 240 a^8 + 3676 a^{10} - 1500 a^{12}$
n^4	$-3563 + 13252 a^2 - 11472 a^4 - 860 a^6 - 1848 a^8 + 44 a^{10} - 44 a^{12}$

Table 2.2: Coefficients of the terms of the second reduced Hamiltonian $\widehat{\mathcal{H}}$.

2.3 Discrete symmetries and reconstruction

The original Hamiltonian (2.1) is invariant with respect to a discrete group of transformations. This group is isomorphic to $\mathbf{Z}_2 \times \mathbf{Z}_2$ and consists of the following elements

$$\begin{aligned}
g_1 &: (Q_1, Q_2, Q_3, P_1, P_2, P_3) \mapsto (-Q_1, Q_2, -Q_3, P_1, -P_2, P_3) \\
g_2 &: (Q_1, Q_2, Q_3, P_1, P_2, P_3) \mapsto (-Q_1, Q_2, Q_3, -P_1, P_2, P_3) \\
g_3 &: (Q_1, Q_2, Q_3, P_1, P_2, P_3) \mapsto (Q_1, Q_2, -Q_3, -P_1, -P_2, P_3)
\end{aligned} \tag{2.34}$$

Each g_i generates a \mathbf{Z}_2 subgroup of this group. The induced transformations on the second reduced space $M_{n,c}$ are

$$\begin{aligned}
g_1 &: (\pi_1, \pi_2, \pi_3) \mapsto (-\pi_1, \pi_2, \pi_3) \\
g_2 &: (\pi_1, \pi_2, \pi_3) \mapsto (-\pi_1, \pi_2, -\pi_3) \\
g_3 &: (\pi_1, \pi_2, \pi_3) \mapsto (\pi_1, \pi_2, -\pi_3)
\end{aligned} \tag{2.35}$$

The orbit space $V_{n,c}$ of the \mathbf{Z}_2 action on $M_{n,c}$ generated by g_1 is the image of $M_{n,c}$ under the map

$$(\pi_1, \pi_2, \pi_3) \mapsto (w = n^2 - \pi_1^2, \pi_2, \pi_3) \tag{2.36}$$

On $V_{n,c}$ define

$$\mathcal{F}_c(w, \pi_2, \pi_3) = \widehat{\mathcal{H}}((n^2 - w)^{1/2}, \pi_2, \pi_3) \tag{2.37}$$

Since $V_{n,c}$ is the orbit space of $M_{n,c}$ with respect to the \mathbf{Z}_2 symmetry generated by g_1 each point of $V_{n,c} \setminus \{w = n^2\}$ lifts to two points in $M_{n,c}$; while each point on the line $\{w = n^2\}$ lifts to one point.

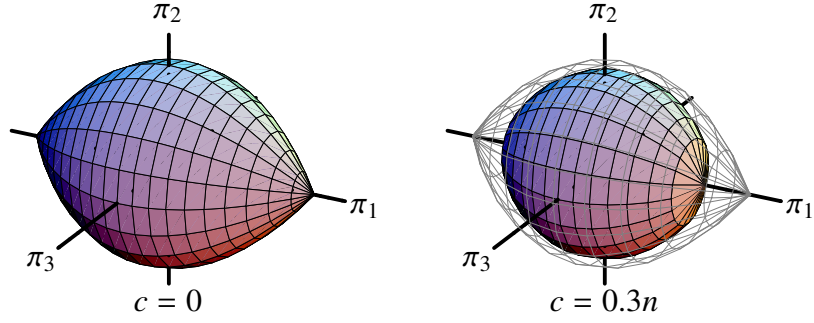


Figure 2.1: Second reduced phase spaces $M_{n,c}$.

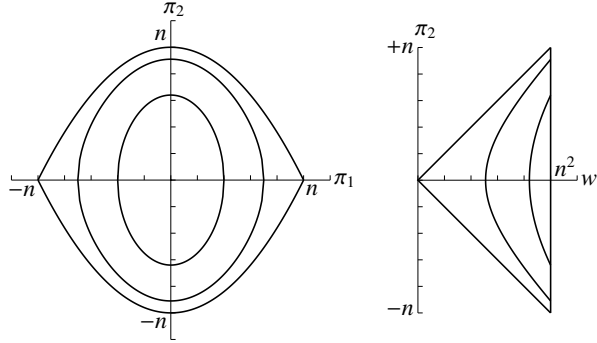


Figure 2.2: (a) Intersections $M_{n,c}^0$ of $M_{n,c}$ with the plane $\{\pi_3 = 0\}$. (b) Intersections $V_{n,c}^0$ of $V_{n,c}$ with the plane $\{\pi_3 = 0\}$. $M_{n,c}$ and $V_{n,c}$ are obtained by revolution around the π_1 and w axes respectively.

Each point of $M_{n,c}$ lifts to an \mathbf{S}^1 orbit (a topological circle) on $\mathbf{S}^2 \times \mathbf{S}^2$. The only exceptions are the singular points of $M_{n,0}$ which lift to only one point on $\mathbf{S}^2 \times \mathbf{S}^2$, and the single points $M_{n,\pm n}$, which lift to two single points. Specifically, the singular point of $M_{n,0}$ with coordinates $P_+ = (\pi_1, \pi_2, \pi_3) = (n, 0, 0)$ lifts to the point $p_+ = n/2(1, 0, 0; -1, 0, 0)$ while the point $P_- = (-n, 0, 0)$ lifts to the point $p_- = n/2(-1, 0, 0; 1, 0, 0)$. Recall that we give coordinates of points on $\mathbf{S}^2 \times \mathbf{S}^2$ as $(x_1, x_2, x_3; y_1, y_2, y_3)$. Each reduced phase space $M_{n,\pm n}$ consists of a single point with coordinates $(\pi_1, \pi_2, \pi_3) = (0, 0, 0)$. These lift to the points z_{\pm} on $\mathbf{S}^2 \times \mathbf{S}^2$ with coordinates $z_{\pm} = n/2(\pm 1, 0, 0; \pm 1, 0, 0)$. Notice that the points p_{\pm} and z_{\pm} are fixed points of the \mathbf{S}^1 action Φ (2.23) on $\mathbf{S}^2 \times \mathbf{S}^2$ and therefore they are equilibria of any Φ invariant Hamiltonian on $\mathbf{S}^2 \times \mathbf{S}^2$.

The equilibria of $\hat{\mathcal{H}}$ on $M_{n,c}$ are the points where a level curve of $\hat{\mathcal{H}}$ becomes tangent to $M_{n,c}$. Since both $\hat{\mathcal{H}}$ and $M_{n,c}$ are invariant with respect to the transformation $g_3 : \pi_3 \mapsto -\pi_3$, we expect to find all such points of tangency on the plane $\pi_3 = 0$. Therefore when looking for equilibria of $\hat{\mathcal{H}}$ we can restrict our attention to $M_{n,c}^0 = M_{n,c} \cap \{\pi_3 = 0\}$. Notice that instead of finding points of tangency between the level sets of $\hat{\mathcal{H}}$ and $M_{n,c}^0$ we can find points of tangency between the level sets of \mathcal{F}_c and $V_{n,c}^0 = V_{n,c} \cap \{\pi_3 = 0\}$.

Remark 2.5. Since $\hat{\mathcal{H}}$ is invariant with respect to $g_1 : \pi_1 \mapsto -\pi_1$, its level

curves are horizontal at $\pi_1 = 0$. This means that on the curve $M_{n,c}^0$ the points $(0, \pm c)$ (the higher and lower points) are always points of tangency between the space and a level curve of $\tilde{\mathcal{H}}$. Therefore, these points are relative equilibria of $\tilde{\mathcal{H}}$ (2.27) on $\mathbf{S}^2 \times \mathbf{S}^2$. In the orbit space $M_n = \bigcup_c M_{n,c}$ these points form the line $s \in [-n, n] \mapsto (0, s, 0)$.

Remark 2.6. It is possible to reduce completely the $\mathbf{Z}_2 \times \mathbf{Z}_2$ action by taking also into account the effect of $g_3 : \pi_3 \mapsto -\pi_3$. This is not necessary for our purposes.

2.4 The Hamiltonian Hopf bifurcations

We come now to the main result of this chapter, which is that the equilibria p_{\pm} of $\tilde{\mathcal{H}}$ go through Hamiltonian Hopf bifurcations. Notice that we work with the second normalized Hamiltonian $\tilde{\mathcal{H}}$ on $\mathbf{S}^2 \times \mathbf{S}^2$ and not with the second reduced Hamiltonian $\hat{\mathcal{H}}$ on $M_{n,c}$. We prove the following theorem.

Theorem 2.7. *The equilibria $p_{\pm} = \frac{n}{2}(\pm 1, 0, 0, \mp 1, 0, 0)$ of the second normalized Hamiltonian $\tilde{\mathcal{H}}$ (2.27) on $\mathbf{S}^2 \times \mathbf{S}^2$ undergo a supercritical Hamiltonian Hopf bifurcation at $a = a_1(n\epsilon)$ and a subcritical Hamiltonian Hopf bifurcation at $a = a_2(n\epsilon)$. Here a_1 and a_2 are functions of $\delta = n\epsilon$ given below in (2.58) and (2.59).*

Outline of the proof. The first step of the proof is to find a local chart (Q, P) on $\mathbf{S}^2 \times \mathbf{S}^2$ near the point p_+ . The symplectic form in the chart (Q, P) is in Darboux form only up to constant terms:

$$\omega = dQ_1 \wedge dP_1 + dQ_2 \wedge dP_2 + \omega_2(Q, P) + \omega_4(Q, P) + \dots \quad (2.38)$$

Here ω_2 and ω_4 are two-forms of degrees 2 and 4 respectively. In order to study the local dynamics near the equilibrium point p_+ we need to flatten the symplectic form to Darboux form at an appropriate order, using a constructive version of the Darboux theorem [20]. The result of flattening is a new chart (q, p) in which the symplectic form is

$$\omega = dq_1 \wedge dp_1 + dq_2 \wedge dp_2 + \tilde{\omega}_4(q, p) + \dots \quad (2.39)$$

After flattening the symplectic form and expressing the local Hamiltonian in the chart (q, p) , we reduce the local Hamiltonian with respect to the \mathbf{S}^1 symmetry that is induced on the local chart from Φ (2.23). The invariants of the induced \mathbf{S}^1 symmetry are generated by the quadratic polynomials M, N, T and S in the variables (q, p) ; S is the generator of the \mathbf{S}^1 symmetry and M, N generate nilpotent linear Hamiltonian vector fields X_M and X_N respectively.

The next step is to bring the quadratic part G_2 of the local Hamiltonian G into the versal normal form for the Hamiltonian Hopf bifurcation, namely

$$G_2 = \alpha M + N + \Omega S \quad \text{or} \quad G_2 = M + \beta N + \Omega S \quad (2.40)$$

We also have to check that certain transversality conditions are satisfied when $\alpha = 0$ or $\beta = 0$. This proves that the local Hamiltonian goes through a *linear* Hamiltonian Hopf bifurcation.

The final step is to normalize G with respect to X_M (or X_N) and check the sign of the coefficient of the term M^2 (or N^2) in order to determine if the Hamiltonian Hopf bifurcation is supercritical or subcritical. \square

In the next sections we fill in the details of the argument sketched above.

2.4.1 Local chart

We define a local chart on $\mathbf{S}^2 \times \mathbf{S}^2$ near the point p_+ with coordinates Q_1, Q_2, P_1, P_2 given by

$$\begin{aligned} x_1 &= \left(\frac{n^2}{4} - \frac{nQ_1^2}{2} - \frac{nP_1^2}{2} \right)^{1/2} & x_2 &= \left(\frac{n}{2} \right)^{1/2} Q_1 & x_3 &= \left(\frac{n}{2} \right)^{1/2} P_1 \\ y_1 &= -\left(\frac{n^2}{4} - \frac{nQ_2^2}{2} - \frac{nP_2^2}{2} \right)^{1/2} & y_2 &= \left(\frac{n}{2} \right)^{1/2} P_2 & y_3 &= \left(\frac{n}{2} \right)^{1/2} Q_2 \end{aligned}$$

Note that the coordinate functions Q and P are not canonically conjugate since the symplectic 2-form in these coordinates is

$$\omega = dQ_1 \wedge dP_1 + dQ_2 \wedge dP_2 + (\text{higher order terms}) \quad (2.41)$$

We make the transformation

$$\begin{aligned} Q_1 &= -\frac{1}{2}(p_1 + p_2 + q_1 - q_2) & Q_2 &= -\frac{1}{2}(p_1 - p_2 + q_1 + q_2) \\ P_1 &= \frac{1}{2}(-p_1 + p_2 + q_1 + q_2) & P_2 &= -\frac{1}{2}(p_1 + p_2 - q_1 + q_2) \end{aligned}$$

The coordinate functions q, p are not canonical either and the symplectic 2-form has the form

$$\omega = \omega_0 + \omega_2 + \omega_4 + \cdots \quad (2.42)$$

where

$$\omega_0 = dq_1 \wedge dp_1 + dq_2 \wedge dp_2 \quad (2.43)$$

and

$$\begin{aligned} \omega_2 &= \frac{1}{2n}(p_1^2 + p_2^2 + q_1^2 + q_2^2)(dq_1 \wedge dp_1 + dq_2 \wedge dp_2) \\ &\quad + \frac{1}{n}(p_1q_2 - p_2q_1)(dq_1 \wedge dq_2 + dp_1 \wedge dp_2) \end{aligned} \quad (2.44)$$

2.4.2 Flattening of the symplectic form

The first step in order to study the local behaviour of the Hamiltonian system near p_+ is to *flatten* the symplectic form ω (2.42) up to second degree terms. In other words, we need to eliminate the term ω_2 . This means that we find a near identity transformation ϕ such that

$$\phi^* \omega = \omega_0 + \tilde{\omega}_4 + \cdots \quad (2.45)$$

where the components of $\tilde{\omega}_4$ are homogeneous polynomials of degree 4 in (q, p) .

The following lemma explains why flattening ω up to the second degree terms is sufficient.

Lemma 2.8. *Consider a Hamiltonian $H = H_2 + H_3 + \cdots$ and a symplectic form $\omega = \omega_0 + \omega_j + \cdots$, which is flat to degree $j - 1$. Then the j -jet of the Hamiltonian vector field X of H with respect to ω is equal to the j -jet of the Hamiltonian vector field Y of H with respect to ω_0 .*

Proof. Write the Hamiltonian vector field X as

$$X = X_1 + X_2 + X_3 + \cdots \quad (2.46)$$

where the components of X_j are homogeneous polynomials of degree j in (q, p) . X is the solution of the equation $X \lrcorner \omega = dH$, or

$$(X_1 + X_2 + X_3 + \cdots) \lrcorner (\omega_0 + \omega_j + \cdots) = dH_2 + dH_3 + \cdots \quad (2.47)$$

Splitting this equation into terms of equal degree we get

$$\begin{aligned} X_k \lrcorner \omega_0 &= dH_{1+k}, \quad 1 \leq k \leq j \\ X_k \lrcorner \omega_0 + \sum_{l=1}^{k-j} X_l \lrcorner \omega_{j+1-l} &= dH_{1+k}, \quad k \geq j+1 \end{aligned}$$

from which the lemma follows. \square

Applying lemma 2.8 to the case at hand shows that when the first non-zero terms of the symplectic form after ω_0 are of degree 4 then we can study Hamiltonians of degree up to 5 without any more flattening, and this is exactly what we need.

Flattening of the symplectic form is done using the method described in [20]. Specifically we find a vector field X such that $\mathcal{L}_X \omega_0 + \omega_2 = 0$. An X satisfying

$$X \lrcorner \omega_0 = -\frac{1}{4} \left(q_1 \frac{\partial}{\partial q_1} + q_2 \frac{\partial}{\partial q_2} + p_1 \frac{\partial}{\partial p_1} + p_2 \frac{\partial}{\partial p_2} \right) \lrcorner \omega_2 \quad (2.48)$$

does the job. A short computation gives

$$\begin{aligned} X &= \frac{1}{8\pi} \left((-q_1(q_1^2 + q_2^2 + p_1^2 + p_2^2) - 2p_2(p_2q_1 - p_1q_2)) \frac{\partial}{\partial q_1} \right. \\ &\quad + (-q_2(q_1^2 + q_2^2 + p_1^2 + p_2^2) + 2p_1(p_2q_1 - p_1q_2)) \frac{\partial}{\partial q_2} \\ &\quad + (-p_1(q_1^2 + q_2^2 + p_1^2 + p_2^2) + 2q_2(p_2q_1 - p_1q_2)) \frac{\partial}{\partial p_1} \\ &\quad \left. + (-p_2(q_1^2 + q_2^2 + p_1^2 + p_2^2) - 2q_1(p_2q_1 - p_1q_2)) \frac{\partial}{\partial p_2} \right) \end{aligned} \quad (2.49)$$

Let \mathcal{H}^{loc} be the Taylor expansion of $\tilde{\mathcal{H}}$, expressed in the coordinates (q, p) near $(0, 0)$. The final step is to use the transformation ϕ generated by the flow of the vector field X in order to obtain the Hamiltonian $\phi^* \mathcal{H}^{\text{loc}}$ in the new coordinates in which ω is flat to terms of degree 2. We have

$$\phi^* \mathcal{H}^{\text{loc}} = \mathcal{H}_2^{\text{loc}} + (\mathcal{L}_X \mathcal{H}_2^{\text{loc}} + \mathcal{H}_4^{\text{loc}}) + \cdots \quad (2.50)$$

2.4.3 \mathbf{S}^1 symmetry

The Hamiltonian \mathbf{S}^1 action Φ (2.23) on $\mathbf{S}^2 \times \mathbf{S}^2$ induces an \mathbf{S}^1 action on the local chart. A computation shows that the action induced on the chart (q, p) is a rotation

$$\tilde{\Phi} : \mathbf{S}^1 \times \mathbf{R}^4 \rightarrow \mathbf{R}^4 : (t, (q, p)) \mapsto (R(t)q, R(t)p) \quad (2.51)$$

where $R(t) = \begin{pmatrix} \cos t & -\sin t \\ \sin t & \cos t \end{pmatrix}$.

Coefficients of terms in $1728G_2$	
M	$-432\delta + 864a^4\delta - 591\delta^3 + 1194a^2\delta^3 - 480a^4\delta^3 - 84a^6\delta^3 + 66a^8\delta^3$ $-588a^{10}\delta^3 + 492a^{12}\delta^3$
N	$-432\delta + 1728a^2\delta + 864a^4\delta - 591\delta^3 + 3078a^2\delta^3 - 3480a^4\delta^3 - 380a^6\delta^3$ $-94a^8\delta^3 - 204a^{10}\delta^3 + 492a^{12}\delta^3$
S	$-1728 - 984\delta^2 + 2448a^2\delta^2 - 1008a^4\delta^2 - 960a^6\delta^2 + 504a^8\delta^2$
Coefficients of terms in $3456G_4$	
NS	$-2064\delta + 7296a^2\delta - 624a^4\delta + 4320a^6\delta - 2448a^8\delta$
MS	$-2064\delta + 768a^2\delta + 144a^4\delta + 4896a^6\delta - 2448a^8\delta$
MN	$-864 + 1728a^2 + 1728a^4 - 576\delta^2 + 1768a^2\delta^2 - 5392a^4\delta^2 - 2360a^6\delta^2$ $+7844a^8\delta^2 - 4080a^{10}\delta^2 + 3984a^{12}\delta^2$
M^2	$432 - 864a^4 + 288\delta^2 - 1082a^2\delta^2 + 1260a^4\delta^2 + 2540a^6\delta^2 - 3978a^8\delta^2$ $+2604a^{10}\delta^2 - 1992a^{12}\delta^2$
N^2	$432 - 1728a^2 - 864a^4 + 288\delta^2 - 686a^2\delta^2 + 52a^4\delta^2 + 12a^6\delta^2 - 3290a^8\delta^2$ $+900a^{10}\delta^2 - 1992a^{12}\delta^2$
S^2	$-2016 + 1152a^2 - 1728a^4 - 6392\delta^2 + 17048a^2\delta^2 - 9000a^4\delta^2 + 616a^6\delta^2$ $-6628a^8\delta^2 + 8304a^{10}\delta^2 - 3984a^{12}\delta^2$

Table 2.3: Coefficients of $G = G_2 + \epsilon G_4$. Here $\delta = n\epsilon$ and a is defined in (2.7).

Lemma 2.9. *The algebra $\mathbf{R}[q, p]^{\tilde{\Phi}}$ of $\tilde{\Phi}$ -invariant polynomials in (q, p) is generated multiplicatively by*

$$M = \frac{1}{2}(p_1^2 + p_2^2), \quad N = \frac{1}{2}(q_1^2 + q_2^2), \quad S = q_1p_2 - q_2p_1, \quad T = q_1p_1 + q_2p_2. \quad (2.52)$$

which satisfy

$$S^2 + T^2 = 4MN, \quad M \geq 0, \quad N \geq 0. \quad (2.53)$$

Note that S is the generator of $\tilde{\Phi}$ (2.51). The Poisson structure of the algebra generated by M, N, T is

$$\{M, N\} = -T \quad (2.54a)$$

$$\{M, T\} = -2M \quad (2.54b)$$

$$\{N, T\} = 2N \quad (2.54c)$$

S is the Casimir of this algebra.

Since the second normalized Hamiltonian $\tilde{\mathcal{H}}$ is \mathbf{S}^1 invariant and the flattening vector field X (2.49) is \mathbf{S}^1 equivariant ($\mathcal{L}_X S = 0$) the local Hamiltonian \mathcal{H}^{loc} (2.50) is \mathbf{S}^1 invariant. Because of lemma 2.9 \mathcal{H}^{loc} can be expressed in terms of the invariants (2.52). Therefore truncating the local Hamiltonian to terms of degree 4, flattening and expressing the result in terms of the invariants (2.52) gives the Hamiltonian

$$G = G_2 + \epsilon G_4 \quad (2.55)$$

Here G_2 and G_4 are homogeneous polynomials of degrees 1 and 2 respectively in the invariants (2.52). Explicit expressions of G_2 and G_4 are given in table 2.3.

2.4.4 Linear Hamiltonian Hopf bifurcation

We write the quadratic in (q, p) part of G (2.55) as

$$G_2 = \delta A(a, \delta)M + \delta B(a, \delta)N + C(a, \delta)S \quad (2.56)$$

where $\delta = n\epsilon$ and the coefficients $A(a, \delta)$, $B(a, \delta)$ and $C(a, \delta)$ can be read off the first entries in table 2.3. To stress that G depends on the parameters a and $\delta = n\epsilon$ we write $G_{a,\delta}$ instead of G .

The eigenvalues of the Hamiltonian matrix of G_2 are

$$\pm i(C \pm \delta\sqrt{AB}) \quad (2.57)$$

It is obvious from (2.57) that the equilibrium at the origin changes linear stability type when either A or B change sign. Specifically, when $AB < 0$ the origin is complex hyperbolic (CH); while when $AB > 0$ it is elliptic-elliptic (EE). At $A = 0$ or $B = 0$ the eigenvalues are $(iC, iC, -iC, -iC)$ but the Hamiltonian matrix of G_2 is not semisimple.

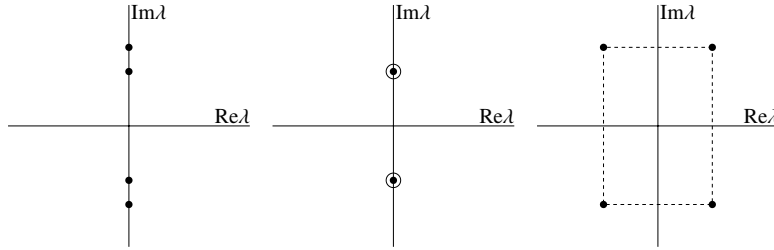


Figure 2.3: The movement of eigenvalues at a linear Hamiltonian Hopf bifurcation.

Let \mathcal{W}_A and \mathcal{W}_B be the curves on the parameter plane (a, δ) on which $A(a, \delta) = 0$ and $B(a, \delta) = 0$ respectively. Let $a_1(\delta)$ be the function that satisfies $A(a_1(\delta), \delta) = 0$ and $a_2(\delta)$ the function that satisfies $B(a_2(\delta), \delta) = 0$. For small δ , the Taylor series of the squares of these two functions are

$$a_1(\delta)^2 = \frac{1}{\sqrt{2}} + \frac{-335 + 251\sqrt{2}}{576} \delta^2 + O(\delta^4) \quad (2.58)$$

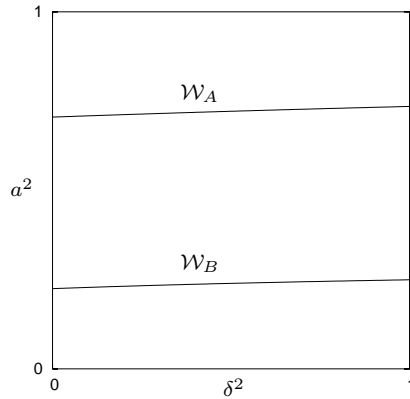


Figure 2.4: Bifurcation sets

and

$$a_2(\delta)^2 = \frac{\sqrt{6}-2}{2} + \frac{58875 - 23596\sqrt{6}}{5184} \delta^2 + O(\delta^4) \quad (2.59)$$

The curves \mathcal{W}_A and \mathcal{W}_B are depicted in figure 2.4. We note that they do not intersect.

We prove the following

Lemma 2.10. *The one-parameter family of Hamiltonians $s \mapsto G_{\mathcal{C}(s)}$ goes through a linear Hamiltonian Hopf bifurcation when the curve $\mathcal{C} : s \mapsto (a(s), \delta(s))$ crosses one of the curves \mathcal{W}_A or \mathcal{W}_B transversely at a point with $\delta > 0$.*

Proof. Consider first the case in which \mathcal{C} crosses \mathcal{W}_A transversely. This means that there is an s_1 such that $A(a(s_1), \delta(s_1)) = 0$ and $\delta(s_1) > 0$. Since \mathcal{W}_A and \mathcal{W}_B do not intersect, we can find a neighborhood U of s_1 such that for all $s \in U$ $B(a(s), \delta(s)) \neq 0$.

We rescale the Hamiltonian G (2.55) by dividing out $\delta B(a, \delta)$. Let

$$\tilde{G} = \tilde{G}_2 + \epsilon \tilde{G}_4 = \frac{G}{\delta B(a, \delta)} \quad (2.60)$$

The quadratic part of \tilde{G} is

$$\tilde{G}_2 = \alpha(a, \delta)M + N + \Omega_1(a, \delta)S \quad (2.61)$$

where $\alpha(a, \delta) = A(a, \delta)/B(a, \delta)$ and $\Omega_1(a, \delta) = C(a, \delta)/(\delta B(a, \delta))$. Clearly $\alpha(a(s_1), \delta(s_1)) = 0$. The Hamiltonian matrix of \tilde{G}_2 is

$$Y_1(a, \delta) = \begin{pmatrix} 0 & -\Omega_1(a, \delta) & 1 & 0 \\ \Omega_1(a, \delta) & 0 & 0 & 1 \\ -\alpha(a, \delta) & 0 & 0 & -\Omega_1(a, \delta) \\ 0 & -\alpha(a, \delta) & \Omega_1(a, \delta) & 0 \end{pmatrix} \quad (2.62)$$

The one-parameter family of infinitesimally symplectic matrices $s \mapsto \tilde{Y}_1(s) = Y_1(a(s), \delta(s))$ is in normal form for s near s_1 . Note that

$$\tilde{Y}_1(s_1) = \begin{pmatrix} 0 & -\Omega_1^0 & 1 & 0 \\ \Omega_1^0 & 0 & 0 & 1 \\ 0 & 0 & 0 & -\Omega_1^0 \\ 0 & 0 & \Omega_1^0 & 0 \end{pmatrix} \quad (2.63)$$

where $\Omega_1^0 = \Omega_1(a(s_1), \delta(s_1))$. A straightforward computation shows that $\Omega_1^0 \neq 0$. Because \mathcal{C} intersects \mathcal{W}_A transversely we have that

$$\left. \frac{d\alpha(a(s), \delta(s))}{ds} \right|_{s=s_1} \neq 0 \quad (2.64)$$

Therefore the family of Hamiltonians $s \mapsto \tilde{G}_2(s)$ undergoes a linear Hamiltonian Hopf bifurcation at s_1 .

The treatment of the second case is almost identical. In this case let s_2 be such that $B(a(s_2), \delta(s_2)) = 0$. We can find a neighborhood U of s_2 such that for all $s \in U$ $A(a(s), \delta(s)) \neq 0$. We rescale G dividing by $\delta A(a, \delta)$. Let

$$\hat{G} = \hat{G}_2 + \epsilon \hat{G}_4 = \frac{G}{\delta A(a, \delta)} \quad (2.65)$$

The quadratic part of \widehat{G} is

$$\widehat{G}_2 = M + \beta(a, \delta)N + \Omega_2(a, \delta)S \quad (2.66)$$

where $\beta(a, \delta) = B(a, \delta)/A(a, \delta)$ and $\Omega_2(a, \delta) = C(a, \delta)/(\delta A(a, \delta))$. Clearly $\beta(a(s_2), \delta(s_2)) = 0$.

The Hamiltonian matrix of \widehat{G}_2 is

$$Y_2(a, \delta) = \begin{pmatrix} 0 & -\Omega_2(a, \delta) & \beta(a, \delta) & 0 \\ \Omega_2(a, \delta) & 0 & 0 & \beta(a, \delta) \\ -1 & 0 & 0 & -\Omega_2(a, \delta) \\ 0 & -1 & \Omega_2(a, \delta) & 0 \end{pmatrix} \quad (2.67)$$

The one-parameter family of infinitesimally symplectic matrices $s \mapsto \widetilde{Y}_2(s) = Y_2(a(s), \delta(s))$ is already in normal form near s_2 . Notice that

$$\widetilde{Y}_2(s_0) = \begin{pmatrix} 0 & -\Omega_2^0 & 0 & 0 \\ \Omega_2^0 & 0 & 0 & 0 \\ -1 & 0 & 0 & -\Omega_2^0 \\ 0 & -1 & \Omega_2^0 & 0 \end{pmatrix} \quad (2.68)$$

where $\Omega_2^0 = \Omega_2(a(s_2), \delta(s_2))$. A straightforward computation shows that $\Omega_2^0 \neq 0$. Moreover because \mathcal{C} intersects \mathcal{W}_B transversally we have that

$$\left. \frac{d\beta(a(s), \delta(s))}{ds} \right|_{s=s_2} \neq 0 \quad (2.69)$$

Therefore the family $s \mapsto \widehat{G}_2(s)$ undergoes a linear Hamiltonian Hopf bifurcation at s_2 . \square

2.4.5 Nonlinear Hamiltonian Hopf bifurcation

In this section we normalize the rescaled Hamiltonians \widetilde{G} and \widehat{G} with respect to X_N and X_M respectively in order to study the nonlinear Hamiltonian Hopf bifurcations. We prove that

Lemma 2.11. *Any one-parameter family $s \mapsto G_{a(s), \delta(s)}$ that crosses the curve \mathcal{W}_A transversely at a point with $\delta > 0$ goes through a supercritical Hamiltonian Hopf bifurcation.*

Proof. We begin with the rescaled Hamiltonian \widetilde{G} (2.60) with quadratic part

$$\widetilde{G}_2 = \alpha(a, \delta)M + N + \Omega(a, \delta)S \quad (2.70)$$

from lemma 2.10. We have already proven that $s \mapsto \widetilde{G}_2(s)$ goes through a linear Hamiltonian Hopf bifurcation at s_1 .

We normalize the Hamiltonian \widetilde{G} (2.60) with respect to X_N using the generator

$$W = c_1NT + c_2ST + c_3MT \quad (2.71)$$

The coefficients c_i are determined by demanding that only the terms M^2 , S^2 and MS appear in the quadratic part of the normal form. Specifically, we have

$$\begin{aligned} \exp(\epsilon \mathcal{L}_W) \widetilde{G} &= (1 + \epsilon \text{ad}_W + O(\epsilon^2))(\widetilde{G}_2 + \epsilon \widetilde{G}_4 + O(\epsilon^2)) \\ &= \widetilde{G}_2 + \epsilon(\widetilde{G}_4 + \{W, \widetilde{G}_2\}) + O(\epsilon^2) \\ &= \widetilde{G}_2 + \widetilde{G}_4 + O(\epsilon^2) \end{aligned}$$

The term $\{W, \tilde{G}_2\}$ is equal to

$$\begin{aligned} \{W, \tilde{G}_2\} &= (6c_1\alpha - 6c_3)MN + (c_3 - c_1\alpha)S^2 \\ &\quad - 2c_1N^2 + 2c_3\alpha M^2 + 2c_2\alpha MS - 2c_2NS \end{aligned}$$

At the bifurcation we have $\alpha = 0$. Therefore

$$\{W, \tilde{G}_2\} = -6c_3MN + c_3S^2 - 2c_1N^2 - 2c_2NS \quad (2.72)$$

It is clear that we can ensure that \tilde{G}_4 (2.4.5) is free of terms MN , N^2 and NS by choosing c_1 , c_2 and c_3 appropriately.

A concrete computation shows that at $a = a_1(\delta)$ (2.58) we have

$$\begin{aligned} \tilde{G}_4 &= M^2(0.0922\delta + 0.0124742\delta^3) + MS(-0.135 + 0.0484\delta^2) \\ &\quad + S^2(-0.678\frac{1}{\delta} + 0.03\delta - 0.00671\delta^3) \end{aligned} \quad (2.73)$$

(the numbers given are approximate). Since the coefficient of M^2 is positive (for $\delta > 0$) the lemma follows. \square

Lemma 2.12. *Any one-parameter family $s \mapsto G_{\alpha(s), \delta(s)}$ that crosses transversely the line \mathcal{W}_B at a point with $\delta > 0$ goes through a subcritical Hamiltonian Hopf bifurcation.*

Proof. Again we begin with the rescaled Hamiltonian \hat{G} (2.65) with quadratic part

$$\hat{G}_2 = M + \beta(a, \delta)N + \Omega(a, \delta)S \quad (2.74)$$

We normalize \hat{G} (2.65) with respect to X_M using the generator

$$W = c_1NT + c_2ST + c_3MT \quad (2.75)$$

where the coefficients c_i in this case are determined by demanding that only terms N^2 , S^2 and NS appear in the normal form. We find

$$\begin{aligned} \tilde{G}_4 &= N^2(-0.0628\delta + 0.118\delta^3) + NS(0.531 - 0.822\delta^2) \\ &\quad + S^2(2.541\frac{1}{\delta} + 1.846\delta - 1.950\delta^3) + O(\delta^4) \end{aligned} \quad (2.76)$$

In this case the coefficient of N^2 is negative for small δ and we have a subcritical Hamiltonian Hopf bifurcation. \square

2.5 Hamiltonian Hopf bifurcation and monodromy

We show how the Hamiltonian Hopf bifurcation is related to qualitative features in the image of the energy-momentum map and specifically to monodromy. The energy-momentum map, is defined as

$$\mathcal{EM} : (\mathbf{S}^2 \times \mathbf{S}^2) \rightarrow \mathbf{R}^2 : z \mapsto (\tilde{\mathcal{H}}(z), \tilde{\mathcal{H}}_1(z)) \quad (2.77)$$

We denote the values of \mathcal{EM} by (h, c) . Notice that we always subtract from $\tilde{\mathcal{H}}$ terms that depend only on n and c , so that the point $(h, c) = (0, 0)$ always corresponds to p in $V_{n,0}$ and p_{\pm} in $\mathbf{S}^2 \times \mathbf{S}^2$.

Supercritical bifurcation

We show the critical values of \mathcal{EM} for $a > a_1$ in figure 2.5a and a blow up of a small region around the point $(0, 0)$ in figure 2.5b. The large structure in figure 2.5a corresponds to the relative equilibria discussed in remark 2.5. This is also true in all the other cases.

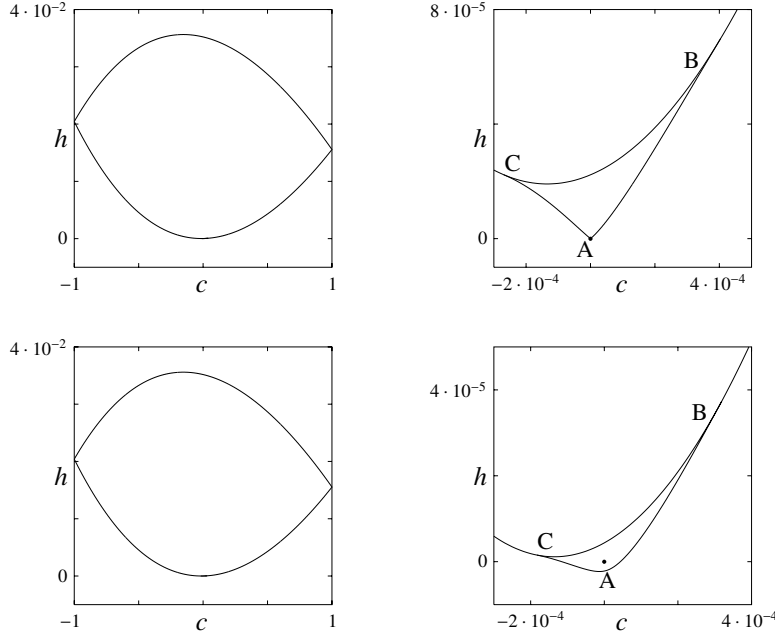


Figure 2.5: Image of \mathcal{EM} for values of a near the supercritical bifurcation value $a = a_1(0.1)$. Top row: $a = a_1 + 10^{-4}$. Bottom row: $a = a_1 - 2 \cdot 10^{-4}$.

In figure 2.5b we see that $(0, 0)$ is connected to a family of critical values. These lift to relative equilibria in $\mathbf{S}^2 \times \mathbf{S}^2$. Each point inside the small ‘triangular’ region, marked ABC, lifts to two disjoint \mathbf{T}^2 . For this reason we consider that the region ABC consists of two leaves. A point (h, c) on one leaf lifts to a \mathbf{T}^2 and the same point on the second leaf lifts to another \mathbf{T}^2 . Notice that the fact that regular values of \mathcal{EM} near $(0, 0)$ lift to two \mathbf{T}^2 is a consequence of the discrete symmetries of the problem, and more specifically of the fact that the dynamics around p_+ and p_- are the same.

Points inside the range of \mathcal{EM} and above the curve BC lift to one \mathbf{T}^2 . Points on BC lift to two \mathbf{T}^2 joined along a relative equilibrium (figure 2.6c). In order to explain this, we represent qualitatively in figure 2.6a some level curves of $\widehat{\mathcal{H}}_{c=0}$. The dashed level curve corresponds to the point on the curve BC with $c = 0$, but the situation is qualitatively the same for all points on BC. The dashed level curve intersects $M_{n,0}$ along a curve which is a figure-8 (figure 2.6): two topological circles joined at one point. This point is an unstable equilibrium of $\widehat{\mathcal{H}}_{c=0}$. It lifts to an unstable relative equilibrium in $\mathbf{S}^2 \times \mathbf{S}^2$. The rest of the figure-8 lifts to the stable and unstable manifolds of this relative equilibrium (figure 2.6c).

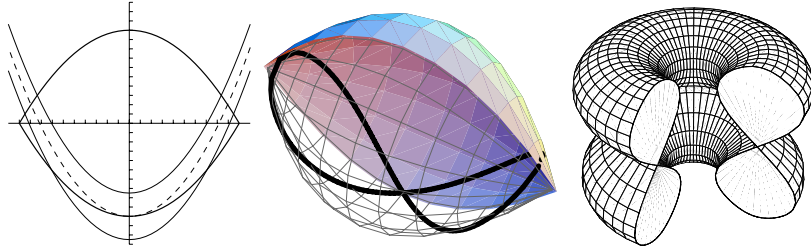


Figure 2.6: (a) Schematic representation of the projection to the plane (π_1, π_3) of intersections of level curves of $\widehat{\mathcal{H}}_{c=0}$ with $M_{n,0}$. (b) The intersection of a level curve of $\widehat{\mathcal{H}}_{c=0}$ with M_n lifts to (c) two glued tori.

We see that for $a < a_1$ (figure 2.5c,d) $(0,0)$ is detached from the family of critical values and is isolated. It lifts to two disjoint singly pinched 2-tori. Regular values of \mathcal{EM} inside the region ABC lift to two disjoint \mathbf{T}^2 . In this case also, we consider that the region ABC consists of two leaves.

In order to compute monodromy we consider a path on one of the leaves around the representative of $(0,0)$ on the same leaf. Since the latter point lifts to *one* singly pinched torus the monodromy matrix is $\begin{pmatrix} 1 & 1 \\ 0 & 1 \end{pmatrix}$. Therefore as the system goes through a supercritical Hamiltonian Hopf bifurcation it acquires monodromy, as described in [85].

An alternative way to understand this situation is to consider a closed path Γ inside ABC around the point $(0,0)$ without distinguishing between different leaves. The path lifts to *two* disjoint \mathbf{T}^2 bundles over Γ . The monodromy matrix for each bundle is $\begin{pmatrix} 1 & 1 \\ 0 & 1 \end{pmatrix}$. By considering each leaf separately we essentially consider only one bundle at a time.

Subcritical bifurcation

The critical values of \mathcal{EM} for $a > a_2$ are shown in figure 2.7. The point $(0,0)$ is a critical value which lifts to a doubly pinched torus in $\mathbf{S}^2 \times \mathbf{S}^2$. Points around $(0,0)$ are regular values of \mathcal{EM} which lift to a single \mathbf{T}^2 . Therefore, the monodromy matrix for a path going around $(0,0)$ is $\begin{pmatrix} 1 & 2 \\ 0 & 1 \end{pmatrix}$.

When a becomes smaller than a_2 , a small ‘triangle’ ABC of critical values is created (figure 2.7d), with $(0,0)$ at the vertex A. Points on the curves AB and AC lift to elliptic relative equilibria. Points on the curve BC lift to three tori joined along two hyperbolic relative equilibria (figure 2.8b).

In figure 2.8a we show some level curves of $\widehat{\mathcal{H}}_{c=0}$ and the reduced phase space $M_{n,0}$. The dashed curve is tangent to $M_{n,0}$ at two points and corresponds to the point on the curve BC with $c = 0$. The two points of tangency are unstable equilibria on the reduced phase space and lift to unstable periodic orbits on $\mathbf{S}^2 \times \mathbf{S}^2$. The dashed level curve intersects $M_{n,0}$ along a braid with two nodes. The nodes are the unstable equilibria, while the rest of the braid represents their stable and unstable manifolds. The braid lifts to the two unstable relative equilibria together with its stable and unstable manifolds (figure 2.8b).

Each regular point inside the region ABC lifts to *three* disjoint \mathbf{T}^2 . This can be deduced from figure 2.8a if we consider a level curve of $\widehat{\mathcal{H}}_{c=0}$ slightly below

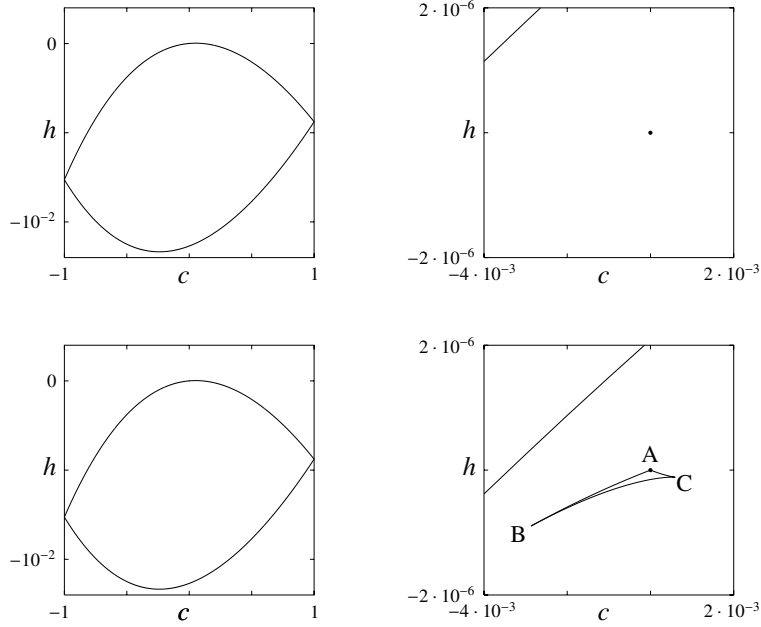


Figure 2.7: Image of \mathcal{EM} for values of a near the subcritical bifurcation value $a = a_2(0.1)$. Top row: $a = a_2 + 10^{-6}$. Bottom row: $a = a_2 - 25 \cdot 10^{-6}$.

the dashed level curve. We have not drawn such level curve for practical reasons but it is clear that such a curve will intersect $M_{n,0}$ along three disjoint circles, which lift to three disjoint \mathbf{T}^2 . Two of these circles are near the singular points while the third lies between them. Therefore the region ABC is composed of three leaves. The first ‘big’ leaf extends beyond the region ABC and covers the whole image of \mathcal{EM} . The other two leaves are restricted in the region ABC. The three leaves join along the curve BC where the three tori join.

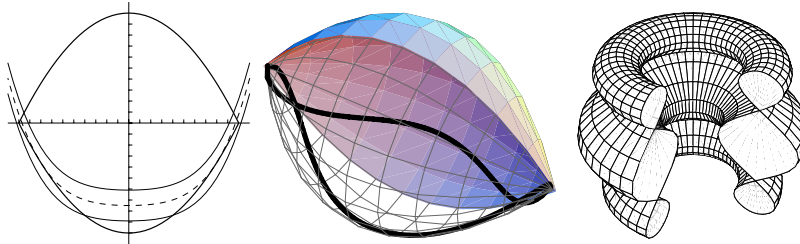


Figure 2.8: (a) Schematic representation of the intersections of the level curves of $\widehat{H}_{c=0}$ with $M_{n,c}$. (b) The intersection of the dashed level curve of $\widehat{H}_{c=0}$ with $M_{n,0}$ lifts to (c) three glued tori joined along two relative equilibria.

We consider monodromy along a path on the ‘big’ leaf that goes around BC. The two leaves are deformations of the isolated critical value that exists for $a > a_2$. For this reason, the monodromy matrix remains the same as for

$a > a_2$ i.e. $\begin{pmatrix} 1 & 2 \\ 0 & 1 \end{pmatrix}$. This type of monodromy in which we consider a path around a curve along which two or more different leaves join is called *leaf* monodromy (see also chapter 3).

Remark 2.13. Let us consider for a moment what would happen if we had not considered the separation into leaves. Consider first a simple closed path Γ of regular values of \mathcal{EM} that goes around the region ABC. Γ lifts to a \mathbf{T}^2 bundle, which has monodromy matrix $\begin{pmatrix} 1 & 2 \\ 0 & 1 \end{pmatrix}$. Consider now another path Γ' that goes around BC but enters and then exits the region ABC crossing AB and AC. Let γ denote the part of Γ inside the region ABC. Then $\mathcal{EM}^{-1}(\Gamma')$ consists of a \mathbf{T}^2 bundle over Γ' (which is homotopic to $\mathcal{EM}^{-1}(\Gamma) \rightarrow \Gamma$) and two disjoint \mathbf{S}^3 . The 3-spheres are obtained from γ .

We see that the subcritical Hamiltonian Hopf bifurcation is related to monodromy both before and after the bifurcation. Before the bifurcation i.e. when the equilibria p_{\pm} are EE ($a < a_2$) each one of them is attached to a family of relative equilibria. In this case we have leaf monodromy. After the bifurcation, the equilibria p_{\pm} become complex hyperbolic and the family of relative equilibria disappears. In this case we have standard monodromy.

2.6 Description of the Hamiltonian Hopf bifurcation on the fully reduced space

In §2.7 we proved the existence of Hamiltonian Hopf bifurcations working with \mathcal{H} (2.27) on $\mathbf{S}^2 \times \mathbf{S}^2$. In this section we discuss the appearance of these bifurcations on the fully reduced spaces introduced in §2.3.

A geometric criterion for the existence of Hamiltonian Hopf bifurcations and the determination of their type is given in [45, 47, 48]. This criterion is based on the behaviour of the level sets of the energy with respect to the fully reduced phase space. In order to apply this criterion, the reduced phase space must have a conical singularity that lifts to the equilibrium that undergoes the Hamiltonian Hopf bifurcation. Moreover, the stratification of the orbit space by reduced phase spaces must be locally equivalent to the standard case. If these are true then we can deduce the type of Hamiltonian Hopf bifurcation by considering how the energy level curve that passes through the singular point bends with respect to the cone. We begin by reviewing the standard case.

2.6.1 The standard situation

Consider a two degree of freedom Hamiltonian H which is invariant with respect to the \mathbf{S}^1 action generated by $S = q_1 p_2 - q_2 p_1$ and for which the point $(q, p) = 0$ is an equilibrium. By lemma 2.9 H can be expressed in terms of the invariant polynomials M, N, S and T , which satisfy $S^2 + T^2 = 4MN$ and $M \geq 0, N \geq 0$.

M, N, T span a Lie algebra isomorphic to $\mathfrak{sl}(2, \mathbf{R})$ with Casimir $4MN - T^2$. The reduced phase space $P_s = S^{-1}(s)/\mathbf{S}^1 \subset \mathbf{R}^3$ is the semialgebraic variety defined by $s^2 + T^2 = 4MN, M \geq 0, N \geq 0$. For $s \neq 0$, P_s is a hyperboloid. P_0 is a cone with vertex at $(M, N, T) = (0, 0, 0)$ (see figure 2.9a where we show intersections of P_s with the plane $\{T = 0\}$ for different s). The vertex of the cone lifts to $(q, p) = 0$.

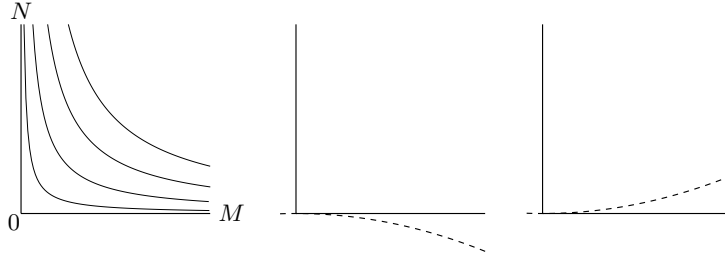


Figure 2.9: (a) The fibration of the orbit space near the conical singularity for the standard case. (b) The level curves of the Hamiltonian at the supercritical case bend outwards. (c) In the subcritical case they bend inwards.

We denote by \widehat{H}_s the reduced Hamiltonian on P_s . According to [48] the universal unfolding of \widehat{H}_s is

$$\widehat{H}_s = N + \nu M + \alpha M^2 \quad (2.78)$$

where $\nu = 0$ at the bifurcation and the sign of α determines the type of the bifurcation. Specifically, if $\alpha > 0$ we have a supercritical Hamiltonian Hopf bifurcation, while for $\alpha < 0$ we have a subcritical Hamiltonian Hopf bifurcation.

The equilibria of \widehat{H}_s are the points of tangency between the level curves of \widehat{H}_s and the reduced phase space P_s . Since \widehat{H}_s does not depend on T these points lie on the plane $\{T = 0\}$. Therefore when looking for equilibria of \widehat{H}_s we can restrict our attention to $P_s^0 = P_s \cap \{T = 0\}$.

Note that $\widehat{H}_{s=0}^{-1}(0)$ is the level curve of $\widehat{H}_{s=0}$ that passes through the vertex of P_0^0 . Exactly at the bifurcation, i.e. when $\nu = 0$, it is given by $N = -\alpha M^2$. Therefore, the sign of α determines how $\widehat{H}_{s=0}^{-1}(0)$ is bent with respect to P_0^0 . If $\alpha > 0$, then $\widehat{H}_{s=0}^{-1}(0)$ stays outside P_0^0 (figure 2.9b), while when $\alpha < 0$ it goes inside (figure 2.9c). Notice that these correspond to the supercritical and the subcritical case respectively. The case $\alpha = 0$ is degenerate since in that case $H^{-1}(0)$ stays on the boundary of P_0^0 and any arbitrarily small change of α can move us either to the subcritical or the supercritical case.

2.6.2 The hydrogen atom in crossed fields

Recall from §2.3 that in the fully reduced phase space $V_{n,0}$, the point p with coordinates $(w, \pi_2) = (0, 0)$ corresponds to the points p_{\pm} on $\mathbf{S}^2 \times \mathbf{S}^2$ undergoing Hamiltonian Hopf bifurcations. $V_{n,0}$ has a conical singularity at p . The orbit space near p is stratified in exactly the same way as in the standard situation, as a comparison between figures 2.2b and 2.9a immediately shows. Therefore we can apply the geometric criterion of [47] in our case.

Recall that in the supercritical Hamiltonian Hopf bifurcation a family of periodic orbits (which in our case are relative equilibria) detaches from an equilibrium as the latter loses stability, while in the subcritical case a family of periodic orbits disappears. Recall, also that relative equilibria of $\widetilde{\mathcal{H}}$ on $\mathbf{S}^2 \times \mathbf{S}^2$ correspond to equilibria of \mathcal{F}_c on $V_{n,c}$, while the equilibria p_{\pm} on $\mathbf{S}^2 \times \mathbf{S}^2$ that go through the Hamiltonian Hopf bifurcations correspond to the vertex p of $V_{n,0}$. Therefore, we conclude that in the orbit space $V_n = \cup_c V_{n,c}$ the supercritical bifurcation appears as the detachment from p of a family of equilibria, while

the subcritical bifurcation appears as the disappearance of a family of relative equilibria that shrinks into p .

In this section we do not provide proofs since our purpose here is mainly to illustrate the Hamiltonian Hopf bifurcation on the reduced space, and not to prove again that the bifurcation is actually taking place. In the following computations we fix $n = 1$, $\epsilon = 1/10$. For these values of n , ϵ the system goes through the supercritical bifurcation at $a_1 = a_1(0.1) \simeq 0.841102$ and the subcritical bifurcation at $a_2 = a_2(0.1) \simeq 0.4744664$.

Supercritical bifurcation

When a passes through a_1 we have a supercritical Hamiltonian Hopf bifurcation that is depicted in figures 2.10a-d. In order to show better the family of equilibria we have used coordinates $\sigma_1 = (w - \pi_2)/2$ and $\sigma_2 = (w + \pi_2)/2$. In figures 2.10a,c we show $V_{n,0}^0$ and the level curves of $\mathcal{F}_{c=0}$ (2.37). It is clear that the latter ‘bend outwards’ and according to the geometric criterion this corresponds to a supercritical Hamiltonian Hopf bifurcation, in accordance with theorem 2.7.

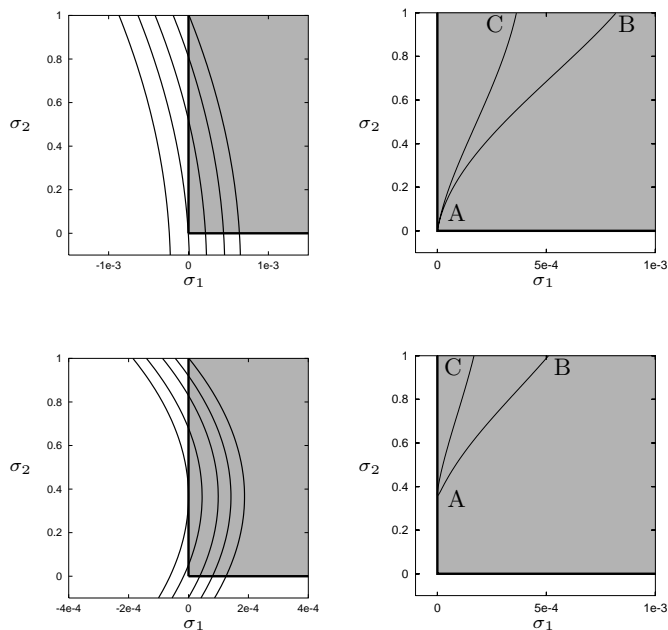


Figure 2.10: Supercritical bifurcation. Top row: $a = a_1 + 10^{-4}$. Bottom row: $a = a_1 - 2 \cdot 10^{-4}$. (a,c) Level curves of $\mathcal{F}_{c=0}$. (b,d) Family of equilibria of \mathcal{F}_c . In these figures the coordinates are $\sigma_1 = (w - \pi_2)/2$ and $\sigma_2 = (w + \pi_2)/2$. The vertical axis $\sigma_1 = 0$ corresponds to the line $w = \pi_2$ of $V_{n,0}^*$. The horizontal axis $w = -\pi_2$ corresponds to the line $w = -\pi_2$ of $V_{n,c}^*$.

We now check into more detail what happens as the system goes through the bifurcation. For $a > a_1$ the points p_{\pm} are elliptic-elliptic. In this case on the

orbit space V_n a family of equilibria parametrized by c emanates from p . These equilibria are shown in figure 2.10b. Each point on this curve corresponds to an equilibrium on a different fully reduced space $V_{n,c}$. The branch AB corresponds to $c > 0$ while the branch AC corresponds to $c < 0$. The two branches do not coincide, even though $V_{n,c}^0$ and $V_{n,-c}^0$ are identical, because $\mathcal{F}_c \neq \mathcal{F}_{-c}$.

For $a < a_1$ the points p_{\pm} on $\mathbf{S}^2 \times \mathbf{S}^2$ become complex hyperbolic. The family of equilibria on V_n detaches from p and moves away. The situation is depicted in figure 2.10d where again the two branches AB and AC correspond to different signs of c .

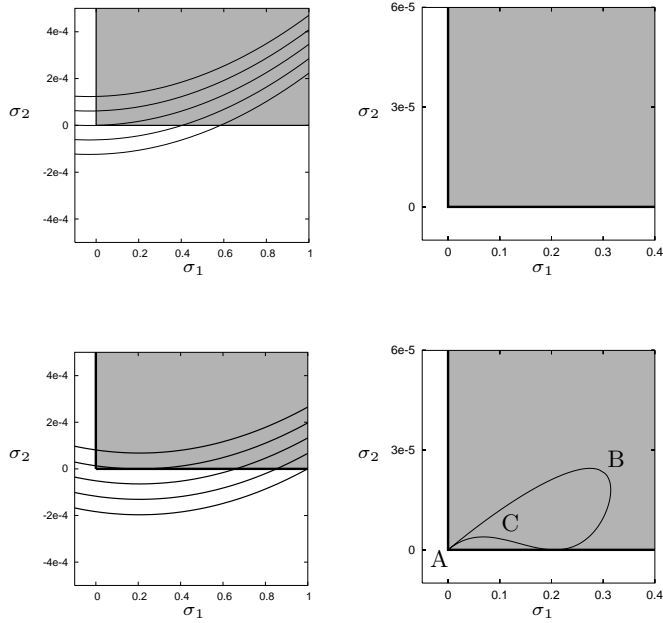


Figure 2.11: Subcritical bifurcation. Top row: $a = a_2 + 10^{-6}$. Bottom row: $a = a_2 - 25 \cdot 10^{-6}$. (a,c) Level curves of $\mathcal{F}_{c=0}$. (b,d) Family of equilibria of \mathcal{F}_c . The family of equilibria does not exist in (b) for $a = a_2 + 10^{-6}$.

Subcritical bifurcation

In the case of the subcritical bifurcation the level set $\mathcal{F}_{c=0}^{-1}(0)$ becomes tangent to the line $w = -\pi_2$. In figures 2.11a,c we show the level curves of the Hamiltonian which ‘bend inwards’. According to the geometric criterion this corresponds to a subcritical Hamiltonian Hopf bifurcation, in accordance to theorem 2.7.

We now check into more detail what happens as we cross the value $a = a_2$ going from smaller to larger values of a . For $a < a_2$, a family of equilibria is attached to p (figure 2.11d). This family corresponds to a family of relative equilibria on $\mathbf{S}^2 \times \mathbf{S}^2$. The points ABC in figure 2.11d correspond to the points ABC in figure 2.7d. Notice that the segments AB, AC in figure 2.11d correspond to elliptic equilibria, while the segment BC corresponds to hyperbolic

Part of \mathcal{F}_c	Allowed terms
$\mathcal{F}_{c,1}$	c
$\mathcal{F}_{c,2}$	w, π_2, c^2, n^2
$\mathcal{F}_{c,3}$	wc, π_2c, c^3, n^2c
$\mathcal{F}_{c,4}$	$w\pi_2, \pi_2^2, \pi_2c^2, \pi_2n^2, w^2, wc^2, wn^2, c^4, n^2c^2, n^4$

Table 2.4: Terms compatible with the $\mathbf{Z}_2 \times \mathbf{Z}_2$ symmetry.

equilibria, whose stable and unstable manifolds form the glued tori of figure 2.8b. As a approaches a_2 from below the family of equilibria shrinks towards p . Exactly at $a = a_2$ the family disappears and does not exist for $a \leq a_2$.

2.6.3 Degeneracy

We close this chapter with an explanation of why we had to compute the first normal form \tilde{H} (2.8) to order 10 in (q, p) .

The discrete $\mathbf{Z}_2 \times \mathbf{Z}_2$ symmetry (see §2.3) imposes certain restrictions on the types of terms that can appear in the fully reduced Hamiltonian \mathcal{F}_c (2.37). The allowed terms appear in table 2.4, where $\mathcal{F}_{c,j}$ is the part of \mathcal{F}_c that comes from $\tilde{\mathcal{H}}_j$, i.e. from the part of $\tilde{\mathcal{H}}$ of degree j .

Therefore if we consider \mathcal{F}_c only up to $\mathcal{F}_{c,3}$ its level curves will appear in the plane (w, π_2) as straight lines. These lines change slope and for some values of the parameter a they coincide either with the line $w = \pi_2$ or with the line $w = -\pi_2$. Thus we have a degenerate situation, since an arbitrarily small change of the Hamiltonian can change the shape of the level curves to either the ‘outwards’ or ‘inwards’ cases. In order to resolve this degeneracy \mathcal{F}_c must contain terms quadratic in (w, π_2) .

The first term of \mathcal{F}_c that contains quadratic terms is $\mathcal{F}_{c,4}$. Tracing this back to the first normal form we find that it corresponds to terms of degree 10 in (q, p) .

3

Quadratic spherical pendula

3.1 Generalities

We describe and analyze the family of quadratic spherical pendula. Our approach in this chapter is heavily influenced by the study of the spherical pendulum in [20].

3.1.1 Constrained equations of motion

We consider the motion of a particle on the surface of a sphere of unit radius

$$\mathbf{S}^2 = \{x \in \mathbf{R}^3 : x^2 = 1\}$$

The sphere is placed in a force field determined by the potential function $V(x)$. The archetypical problem of this kind is the spherical pendulum for which $V(x) = x_3$. The phase space of the system with potential $V(x)$ is the tangent bundle of the sphere defined as

$$T\mathbf{S}^2 = \{(x, y) \in T\mathbf{R}^3 : x^2 - 1 = 0 \text{ and } xy = 0\} \quad (3.1)$$

The unconstrained Hamiltonian system $(H, T\mathbf{R}^3, \omega)$ where $\omega = \sum_i dx_i \wedge dy_i$ and

$$H(x, y) = \frac{1}{2}(y_1^2 + y_2^2 + y_3^2) + V(x) \quad (3.2)$$

describes a particle that moves in \mathbf{R}^3 under the influence of the potential $V(x)$.

We need to take into account the constraint of the system and compute the vector field of $H|T\mathbf{S}^2$ with respect to the symplectic form $\omega|T\mathbf{S}^2$.

Remark 3.1. Usually (see for example [41]) such problems are studied introducing spherical coordinates (θ, ϕ) and expressing the Hamiltonian in terms of (θ, ϕ) and their conjugate momenta (p_θ, p_ϕ) . The problem with spherical coordinates is that they are singular at the ‘north’ and ‘south’ poles of the sphere. Therefore, they are not the best choice for studying trajectories that pass through these points and for making a global study of the system.

We can proceed in two ways. Although the content of both approaches is essentially the same, they give emphasis on the computation of different

quantities. Therefore, each one is suitable in different circumstances. The first approach, is to define a modified Hamiltonian H^* such that $X_{H^*}|_{TS^2} = X_H|_{TS^2}$. Check [20] for details. The second approach, which is the one that we use here, is to define the Dirac-Poisson bracket $\{, \}^*$ on $T\mathbf{R}^3$ such that the vector field $X_H^*|_{TS^2}$ of H with respect to the Dirac-Poisson bracket is equal to $X_H|_{TS^2}$ [13, 20]. These two approaches are related since

$$\{F, G\}^*|_{TS^2} = \{F^*, G^*\}|_{TS^2}$$

We proceed using the second approach, which has the obvious advantage that we compute once and for all the modified Dirac-Poisson structure $\{, \}^*$. Another advantage that will become apparent later, is that based on the Dirac-Poisson structure we will be able to define the appropriate Poisson structure on local charts that we introduce on TS^2 in order to study local features of the equilibria of the system.

Lemma 3.2. *The Dirac-Poisson structure $\{, \}^*|_{TS^2}$ is*

	x_1	x_2	x_3	y_1	y_2	y_3
x_1	0	0	0	$1 - x_1^2$	$-x_1x_2$	$-x_1x_3$
x_2		0	0	$-x_2x_1$	$1 - x_2^2$	$-x_2x_3$
x_3			0	$-x_3x_1$	$-x_3x_2$	$1 - x_3^2$
y_1				0	$x_2y_1 - x_1y_2$	$x_3y_1 - x_1y_3$
y_2					0	$x_3y_2 - x_2y_3$
y_3						0

with Casimirs $c_1(x, y) = x^2 - 1$ and $c_2(x, y) = xy$.

Proof. In order to write the equations of motion for the constrained system we use the modified Dirac brackets. The phase space TS^2 is given as a subset of $T\mathbf{R}^3$ by the constraints

$$c_1(x, y) = x^2 - 1 = 0 \quad \text{and} \quad c_2(x, y) = xy = 0 \quad (3.3)$$

The Dirac-Poisson brackets are given by the relation

$$\{F, G\}^* = \{F, G\} + \sum_{i,j} C_{ij} \{F, c_i\} \{G, c_j\} \quad (3.4)$$

where C_{ij} are the elements of the inverse of the matrix with elements $\{c_i, c_j\}$. In our case

$$C = \frac{1}{2x^2} \begin{pmatrix} 0 & -1 \\ 1 & 0 \end{pmatrix} \quad (3.5)$$

The result follows from a simple computation. \square

Lemma 3.3. *The constrained equations on TS^2 are given by*

$$\begin{aligned} \frac{dx}{dt} &= y \\ \frac{dy}{dt} &= -\nabla V(x) - x(y^2 - x\nabla V(x)) \end{aligned} \quad (3.6)$$

Proof. Compute the equations of motion for the Hamiltonian function (3.2) with respect to the Dirac-Poisson bracket and then restrict the resulting vector field to TS^2 . \square

Remark 3.4. In Newtonian mechanics, equations (3.6) can be obtained as follows. $F = -\nabla V(x)$ is the force exerted to the particle by the field, and $N = -xy^2 - x(xF)$ is the reaction force exerted by the surface of the sphere that compensates the normal component $F_n = x(xF)$ of F and gives the centripetal force $-xy^2$.

We restrict our attention to the class of axially symmetric potentials i.e. potentials that depend only on x_3 . Such potentials are invariant with respect to rotations

$$R(t) = \begin{pmatrix} \cos t & -\sin t & 0 \\ \sin t & \cos t & 0 \\ 0 & 0 & 1 \end{pmatrix}$$

about the x_3 axis. The cotangent lift of $R(t)$ gives an \mathbf{S}^1 action on TS^2

$$\Phi : \mathbf{S}^1 \times TS^2 \rightarrow TS^2 : (t, (q, p)) \mapsto (R(t)q, R(t)p) \quad (3.7)$$

The Hamiltonian and the Dirac-Poisson structure are invariant under Φ and the corresponding vector field is equivariant. The generator of Φ is

$$J(x, y) = x_1 y_2 - x_2 y_1 \quad (3.8)$$

i.e. the component of the angular momentum along the x_3 axis. We can check that

$$\{J, H\}^* | TS^2 = 0$$

that is, J is an integral of motion. As a result we have

Lemma 3.5. *The Hamiltonian systems that describe particles constrained to move on the surface of a sphere under the influence of an axisymmetric potential are Liouville integrable.*

The energy-momentum map is defined as

$$\mathcal{EM} : TS^2 \rightarrow \mathbf{R}^2 : \mathcal{EM}(z) = (H(z), J(z)) \quad (3.9)$$

3.1.2 Reduction of the axial symmetry

Φ (3.7) is not free; it leaves fixed the points $(0, 0, \pm 1, 0, 0, 0)$ on TS^2 . Therefore we can not perform regular reduction. We do *singular reduction* [20] which was developed by Cushman in order to deal with cases like this one.

Lemma 3.6. *The algebra $\mathbf{R}[x, y]^\Phi$ of Φ invariant polynomials in (x, y) is generated by*

$$\begin{aligned} \sigma_1 &= x_3 & \sigma_2 &= y_3 & \sigma_3 &= y_1^2 + y_2^2 + y_3^2 \\ \sigma_4 &= x_1 y_1 + x_2 y_2 & \sigma_5 &= x_1^2 + x_2^2 & \sigma_6 &= x_1 y_2 - x_2 y_1 \end{aligned} \quad (3.10a)$$

subject to the relations

$$\sigma_4^2 + \sigma_6^2 = \sigma_5(\sigma_3 - \sigma_2^2) \quad \sigma_3 - \sigma_2^2 \geq 0 \quad \sigma_5 \geq 0 \quad (3.10b)$$

Proof. See [20]. □

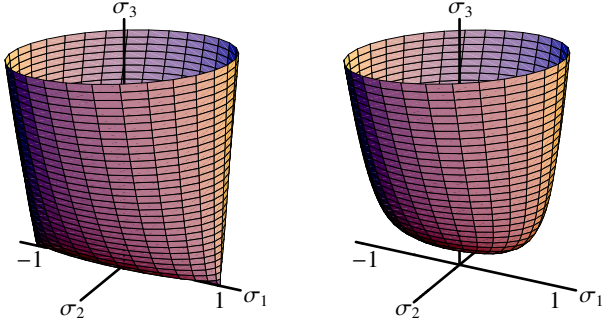


Figure 3.1: (a) Singular reduced phase space M_0 , it is called the canoe. (b) Regular reduced phase space M_j for $j \neq 0$.

Restriction from $T\mathbf{R}^3$ to $T\mathbf{S}^2$ imposes the extra relations

$$\sigma_5 + \sigma_1^2 = 1 \quad \sigma_4 + \sigma_1\sigma_2 = 0 \quad (3.11)$$

We rewrite the relations (3.10b) by eliminating σ_4 and σ_5 , using (3.11), and setting $\sigma_6 = j$. We find

$$\Psi = \sigma_3(1 - \sigma_1^2) - \sigma_2^2 - j^2 = 0, \quad \sigma_1^2 \leq 1, \quad \sigma_3 - \sigma_2^2 \geq 0 \quad (3.12)$$

The reduced phase space $M_j = J^{-1}(j)/\mathbf{S}^1$ is the semialgebraic variety defined by (3.12). For $j = 0$ the reduced phase space M_0 (figure 3.1a) has two singular points at $p_{\pm} = (\pm 1, 0, 0)$. These correspond to the points $P_{\pm} = (0, 0, \pm 1; 0, 0, 0)$ on $T\mathbf{S}^2$. For $j \neq 0$, M_j is diffeomorphic to \mathbf{R}^2 (figure 3.1b).

Lemma 3.7. *The Poisson structure of the polynomial algebra generated by σ_1 , σ_2 and σ_3 is*

$$\{\sigma_1, \sigma_2\} = 1 - \sigma_1^2 \quad \{\sigma_2, \sigma_3\} = -2\sigma_1\sigma_3 \quad \{\sigma_3, \sigma_1\} = -2\sigma_2 \quad (3.13)$$

Notice that Ψ is a Casimir of this algebra.

The dynamics of the reduced system is described by the *reduced* Hamiltonian

$$H_j = \frac{1}{2}\sigma_3 + V(\sigma_1) \quad (3.14)$$

The reduced equations of motion on M_j are

$$\begin{aligned} \dot{\sigma}_1 &= \{\sigma_1, H_j\} = \sigma_2 \\ \dot{\sigma}_2 &= \{\sigma_2, H_j\} = -\sigma_1\sigma_3 - (1 - \sigma_1^2)V'(\sigma_1) \\ \dot{\sigma}_3 &= \{\sigma_3, H_j\} = -2\sigma_2V'(\sigma_1) \end{aligned}$$

Moreover, notice that an orbit of H_j with energy h and momentum j lies on the curve $\gamma_{h,j}$ defined by the intersection of the level curve $\{H_j = h\}$ with M_j . Note that if $\gamma_{h,j}$ is singular then it might not be a single orbit.

3.2 Classification of quadratic spherical pendula

We restrict our attention to axisymmetric *quadratic* potentials of the form

$$V(x) = \frac{1}{2}bx_3^2 + cx_3 + d \quad (3.15)$$

We classify these systems in terms of the qualitative features of their bifurcation diagrams i.e. the set of critical values of the energy-momentum map \mathcal{EM} . This classification is summarized in figure 3.2 (page 94).

3.2.1 Critical values of the energy-momentum map

In this section we study the critical values of the energy-momentum map of the family of Hamiltonians (3.2) with potential (3.15). Our main result is a complete description of the set of critical values of \mathcal{EM} for all values of b , c and d . We prove first

Lemma 3.8. *For fixed values of the parameters b, c, d the set of critical values of \mathcal{EM} is the set $\Delta_{b,c,d}$ of values (h, j) for which the polynomial*

$$\begin{aligned} P_{h,j}^{(b,c,d)}(\sigma_1) &= 2(h - V(\sigma_1))(1 - \sigma_1^2) - j^2 \\ &= b\sigma_1^4 + 2c\sigma_1^3 - (b + 2(h - d))\sigma_1^2 - 2c\sigma_1 + (2(h - d) - j^2) \end{aligned} \quad (3.16)$$

has a double root in $[-1, 1]$. We call $\Delta_{b,c,d}$ the discriminant locus of the polynomial $P_{h,j}^{(b,c,d)}$.

We usually suppress h, j and/or b, c, d from $P_{h,j}^{(b,c,d)}$.

Remark 3.9. Critical values (h, j) of \mathcal{EM} correspond to pairs (h, j) for which the level curve $H_j = h$ is tangent to the reduced phase space M_j or it goes through one or both of the singular points p_{\pm} on M_0 . Since, H_j does not depend on σ_2 , the points where the level curve $\{H_j = h\}$ can be tangent to M_j can only be on the plane $\{\sigma_2 = 0\}$. Therefore, we look for such points on the curve $M_j^0 = M_j \cap \{\sigma_2 = 0\}$.

Proof of lemma 3.8. Consider first the case $j \neq 0$. The level curve $\{H_j = h\}$ is the graph of the function $\ell_h(\sigma_1) = 2(h - V(\sigma_1))$ while M_j^0 is the graph of the function $m_j(\sigma_1) = \frac{j^2}{1 - \sigma_1^2}$. The two curves are tangent when the function $f_{h,j}(\sigma_1) = \ell_h(\sigma_1) - m_j(\sigma_1)$ has a double root i.e. when for some $\sigma_1 = z$ we have $f_{h,j}(z) = f'_{h,j}(z) = 0$. Notice that $P_{h,j}(\sigma_1) = (1 - \sigma_1^2)f_{h,j}(\sigma_1)$. It is easy to show that for $j \neq 0$ the functions $f_{h,j}$ and $P_{h,j}$ have the same double roots. The argument is based on the fact that for $j \neq 0$, σ_1 can not be ± 1 .

Consider now the case $j = 0$ and notice that $P_{h,0}(\sigma_1) = (1 - \sigma_1^2)\ell_h(\sigma_1)$. We need to prove that the curve $\ell_h(\sigma_1)$ becomes tangent to the line segment $\sigma_3 = 0$, $|\sigma_1| \leq 1$ or passes through the points $(\sigma_1, \sigma_3) = (\pm 1, 0)$ if and only if $P_{h,0}(\sigma_1)$ has a double root in $[-1, 1]$. The ‘only if’ part is trivial. The ‘if’ is slightly more involved. Let $z \in [-1, 1]$ be a double root of $P_{h,0}$, i.e. $P_{h,0}(z) = P'_{h,0}(z) = 0$. These two equations become

$$\begin{aligned} (1 - z^2)\ell_h(z) &= 0 \\ (1 - z^2)\ell'_h(z) - 2z\ell_h(z) &= 0 \end{aligned}$$

We obtain the solutions (a) $z = 1$, $\ell_h(1) = 0$ (b) $z = -1$, $\ell_h(-1) = 0$ and (c) $\ell_h(z) = \ell'_h(z) = 0$. This proves the lemma. \square

Lemma 3.10. *The polynomials $P_{h,j}^{(b,c,d)}$ and $P_{h,j}^{(b,-c,d)}$ have the same discriminant loci.*

Proof. If z is a double zero of $P_{h,j}^{(b,c,d)}$ it is easy to see that $-z$ is a double zero of $P_{h,j}^{(b,-c,d)}$. \square

Lemma 3.11. *When $c > 0$, Δ is parametrized by*

$$2(h-d) = 2bs^2 + 3cs - cs^{-1} - b \quad (3.17a)$$

$$j^2 = -s^{-1}(bs+c)(1-s^2)^2 \quad (3.17b)$$

where

Case O. $s \in [-1, 0) \cup \{1\}$ when $0 < |b| \leq c$.

Case I. $s \in [-1, 0) \cup [-\frac{c}{b}, 1]$ when $0 < c < -b$.

Case II. $s \in \{-1\} \cup [-\frac{c}{b}, 0) \cup \{1\}$ when $0 < c < b$.

When $c = 0$, Δ is the union of the curve

$$2(h-d) = j^2 \quad (3.18)$$

and the point $(h, j) = (b/2, 0)$ when $b > 0$, or the curve $2(h-d) = -|b| \pm 2\sqrt{|b|}j$ with $|j| \leq -b$ and $2(h-d) \geq b$ when $b < 0$.

Proof. We begin with the case $b \neq 0$. If $P(z)$ has a double root in $[-1, 1]$ it can be factored as

$$P(z) = b(z-s)^2(z^2 - 2uz + v) \quad (3.19)$$

with $s \in [-1, 1]$. Collecting powers of z and equating coefficients in the two expressions we find

$$2(h-d) - j^2 - bs^2v = 0 \quad (3.20a)$$

$$2(h-d) + bs^2 + 4bsu + bv + b = 0 \quad (3.20b)$$

$$s(su + v) = c/b \quad (3.20c)$$

$$s + u = -c/b \quad (3.20d)$$

When $c \neq 0$, equation (3.20c) gives that $s \neq 0$. The solution of the system of equations (3.20) becomes

$$2(h-d) = 2bs^2 + 3cs - cs^{-1} - b \quad (3.21a)$$

$$j^2 = -s^{-1}(bs+c)(1-s^2)^2 \quad (3.21b)$$

Notice that the right hand side of equation (3.21b) must be non-negative. This gives a permissible region for s for which we already have that it belongs in $[-1, 1] \setminus \{0\}$. A small amount of algebra gives the three cases O, I and II of the lemma.

We deal now with the case $c = 0$. In this case the equations (3.20) become

$$2(h - d) - j^2 - bs^2v = 0 \quad (3.22a)$$

$$2(h - d) + bs^2 + 4bsu + bv + b = 0 \quad (3.22b)$$

$$s(su + v) = 0 \quad (3.22c)$$

$$s + u = 0 \quad (3.22d)$$

Equation (3.22d) gives $u = -s$, and substituting into (3.22c) we get $s = 0$ or $v = s^2$. If $s = 0$ we get $2(h - d) = j^2$. If $v = s^2$ we get at the end $j^2 = -b(1 - s^2)^2$. If $b > 0$ then $s = \pm 1$, and this gives $j = 0$ and $2(h - d) = b$. On the other hand if $b < 0$, s can take any value in $[-1, 1]$. In that case $2(h - d) = -|b| \pm 2\sqrt{|b|}j$ with $|j| \leq -b$.

We did not deal with the case $b = 0$. In this case our system is equivalent to the spherical pendulum which has been studied in [20]. It is easy following the proof of the case $b \neq 0$, $c \neq 0$ to prove that this case is characterized by the same equations (3.21) with $b = 0$. □

The cases O, I and II of lemma 3.11 correspond to the types O, I and II introduced in §0.3.2 (page 33). The form of the loci of critical values of \mathcal{EM} are shown in figure 3.2.

3.2.2 Reconstruction

Recall that the orbit of energy h and momentum j of the vector field of H_j on the reduced phase space M_j is geometrically the intersection $\gamma_{h,j}$ of the level curve $\{H_j = h\}$ with the space M_j . All the points of M_j lift to an \mathbf{S}^1 orbit in the original phase space $T\mathbf{S}^2$ under the inverse of the reduction map $\sigma = (\sigma_1, \sigma_2, \sigma_3)$. The only exceptions are the singular points $(\pm 1, 0, 0)$ of M_0 which lift to the respective point in $T\mathbf{S}^2$ with coordinates $(x, y) = (0, 0, \pm 1; 0, 0, 0)$. Using these facts we can deduce the type of $\mathcal{EM}^{-1}(h, j)$ for all (h, j) in the image of the \mathcal{EM} map. We do not give proofs for our results since these can be easily proved using arguments similar to that in [20]. The following result is from [20].

Lemma 3.12. *If $\gamma_{h,j}$ is diffeomorphic to a circle, it lifts to a \mathbf{T}^2 . If it consists of a single non singular point it lifts to a topological \mathbf{S}^1 . If it consists of a single singular point then it lifts to a single point in $T\mathbf{S}^2$. Finally, if $\gamma_{h,j=0}$ is a topological circle that contains one or both of the singular points, then it lifts to a singly or doubly pinched torus respectively (figure 3.3).*

Notice that lemma 3.12 does not cover all the possible cases.

Having the preceding lemma in hand we discuss each qualitative type individually. Notice that the level curve $H_j = h$ is the set of points that satisfy the equation

$$H_j = \frac{1}{2}\sigma_3 + \frac{1}{2}b\sigma_1^2 + c\sigma_1 + d = h \quad (3.23)$$

which we solve for σ_3 to get

$$\sigma_3 = -b\sigma_1^2 - 2c\sigma_1 + 2(h - d) \quad (3.24)$$

Therefore the level curve $H_j = h$ is a parabola that is turned *upwards* when $b < 0$ and *downwards* when $b > 0$, and its extremum is at $\sigma_1 = -c/b$.

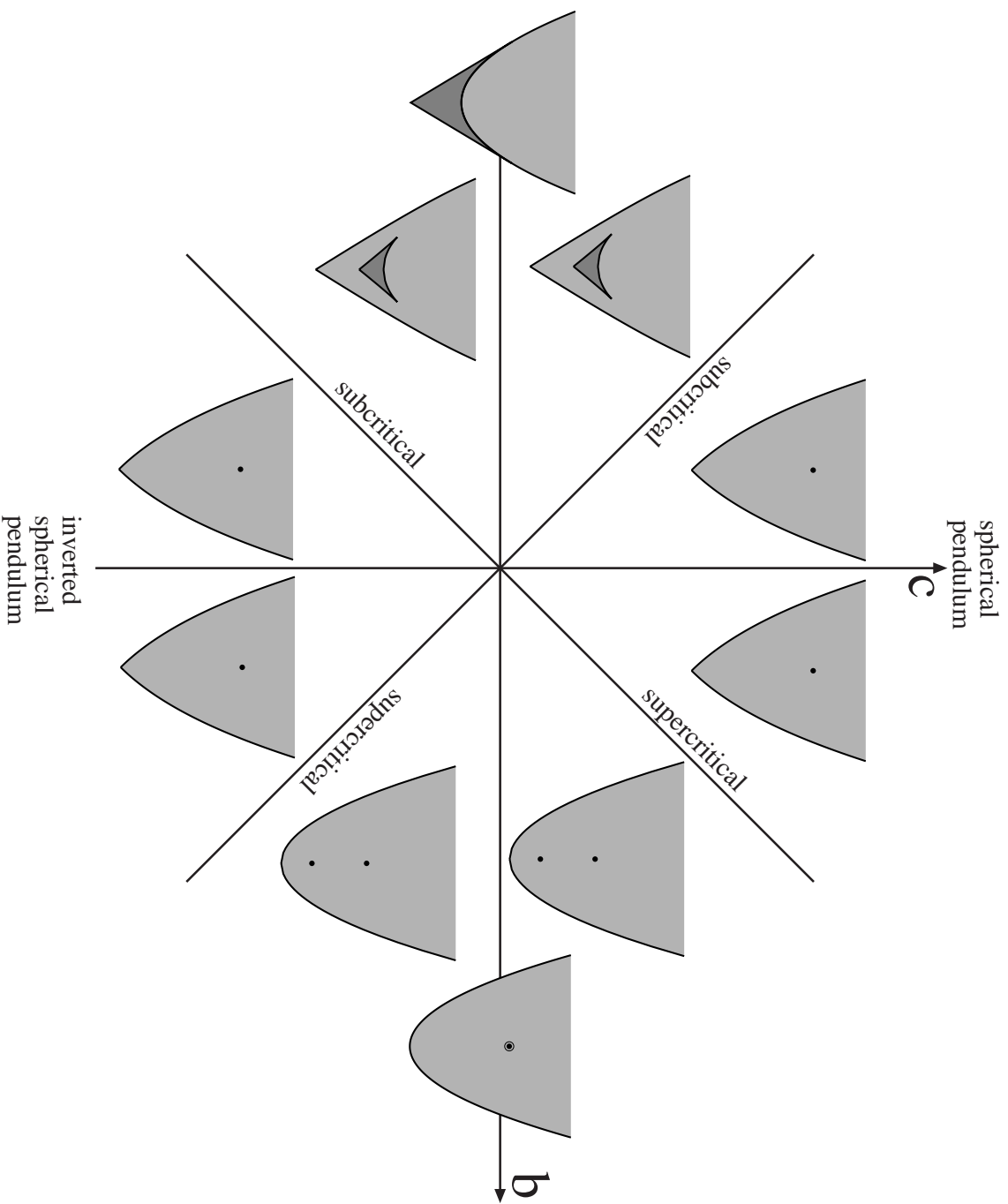


Figure 3.2: Global diagram of the image of \mathcal{EM} for the family of quadratic potentials. We show the image of \mathcal{EM} for representative values of the parameters b and c . For each image the vertical axis represents the energy and the horizontal axis represents the momentum.

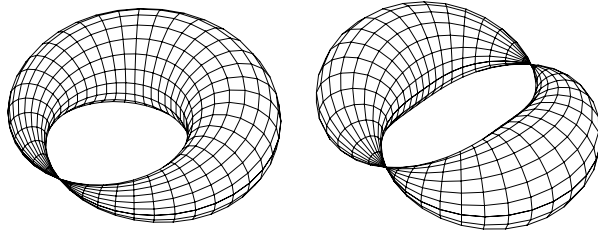


Figure 3.3: Representations of a single and a double pinched torus in \mathbf{R}^3 .

Type O systems

Systems of this type are characterized by the existence of a single isolated critical value of \mathcal{EM} with coordinates $(h_c, j_c) = (b/2 + |c|, 0)$ which lifts to a singly pinched torus. The spherical pendulum belongs in this category. In this case the level curves of H_j are parabolas whose extremum (maximum or minimum) lies outside the interval $[-1, 1]$.

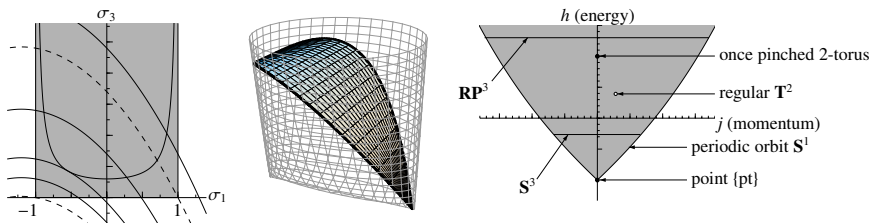


Figure 3.4: Reconstruction of type O systems.

In figure 3.4b we show the projection of some level curves of H_j and spaces M_j on the plane (σ_1, σ_3) . Notice that the projection map $\rho : (\sigma_1, \sigma_2, \sigma_3) \mapsto (\sigma_1, \sigma_3)$ sends two points of M_j to the same point, except for points on the *fold curve* M_j^0 .

The upper dashed level curve in figure 3.4b goes through one of the critical points. Its intersection with M_0 is a topological circle (figure 3.4c). This corresponds to the isolated critical value of \mathcal{EM} and lifts to a singly pinched torus in $T\mathbf{S}^2$.

The other dashed level curve consists only of the other singular point and lifts to a single point in $T\mathbf{S}^2$. Points of tangency between a level curve $H_j = h$ and a reduced space M_j lift to an \mathbf{S}^1 . Finally, all other intersections are diffeomorphic to a circle and each one of them lifts to a \mathbf{T}^2 .

Type II systems

The energy-momentum map of type II systems for $c \neq 0$ has two isolated critical values with coordinates $(h, j) = (b/2 \pm |c|, 0)$. These lift to two singly pinched tori. When $c = 0, b > 0$ there is only one critical value which lifts to a doubly pinched torus. The level curves of H_j in this case are parabolas turned downwards with their maximum inside $(-1, 1)$.

In figure 3.5b we show the projection of some level curves of H_j and spaces M_j on the plane (σ_1, σ_3) . The two dashed curves in figure 3.5b pass through one

singular point each and they intersect M_0 in a topological circle (figure 3.5c). Each one of them lifts to a singly pinched torus. All the other intersections $\gamma_{h,j}$ lift either to \mathbf{S}^1 or to \mathbf{T}^2 .

When $c = 0$ (figure 3.5d,e,f) the level curves are symmetric with respect to $\sigma_1 \mapsto -\sigma_1$. Therefore the same dashed level curve (figure 3.5e) goes through both singular points. The intersection of this level curve with M_0 is a topological circle with two singularities (figure 3.5f). It lifts to a doubly pinched torus.

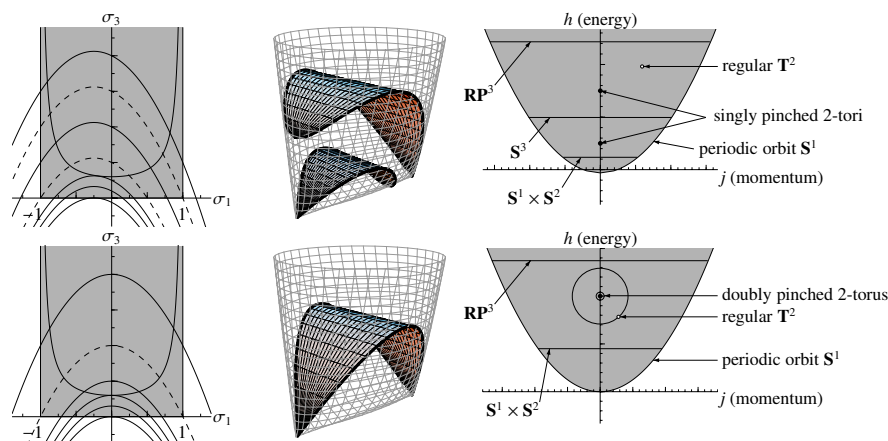


Figure 3.5: (a) Reconstruction of generic type II systems. (b) The degenerate case $c = 0$ with the doubly pinched torus.

Type I systems

Type I systems are characterized by the existence of the ‘triangular’ set ABC of critical values of \mathcal{EM} (figure 3.6a). In this case the level curves of H_j are parabolas that are turned upwards and their minimum is inside the interval $[-1, 1]$.

In figure 3.6b we see that there are two level curves of H_j (represented by dashed lines) that pass through the two singular points of M_0 . The lower of these curves has only one point in common with M_0 and therefore it lifts to a single point in \mathbf{TS}^2 . It corresponds to the lowest point in the image of \mathcal{EM} with coordinates $(b/2 - |c|, 0)$.

The upper dashed curve touches M_0 at the singular point but has also a disjoint intersection with M_0 which is diffeomorphic to a circle and lifts to a \mathbf{T}^2 . It corresponds to the point A in the image of \mathcal{EM} .

Level curves of H_j a little above the upper dashed curve intersect M_0 (and M_j for $|j|$ close to 0) at two disjoint circles. These lift to two disjoint \mathbf{T}^2 .

The thick level curve is tangent to M_0 . Its intersection with M_0 is a ‘figure-8’ (figure 3.6c). In \mathbf{TS}^2 it lifts to two singular tori joined along a cycle. This cycle is an unstable relative equilibrium and the rest of the the two tori are its stable and unstable manifolds (figure 3.6d).

For even higher level curves the intersection with M_0 is a single circle and therefore we now have a single \mathbf{T}^2 .

The values (h, j) for which we have two disjoint tori form the interior of the region ABC in figure 3.6a. Points along AB and AC lift to the disjoint union of an \mathbf{S}^1 and a \mathbf{T}^2 while the point A itself lifts to the disjoint union of a single point and a \mathbf{T}^2 . Points on BC lift to unstable periodic orbits with their stable and unstable manifolds.

Therefore, one can view the image of \mathcal{EM} as consisting of two leaves. The first leaf L_1 is the light gray part of figure 3.6a and it covers the whole image of \mathcal{EM} . The second leaf L_2 lies over leaf L_1 (and therefore hides part of it). It is represented by the dark gray leaf i.e. the triangular region ABC in figure 3.6a. Each point inside each leaf lifts to a single torus in TS^2 .

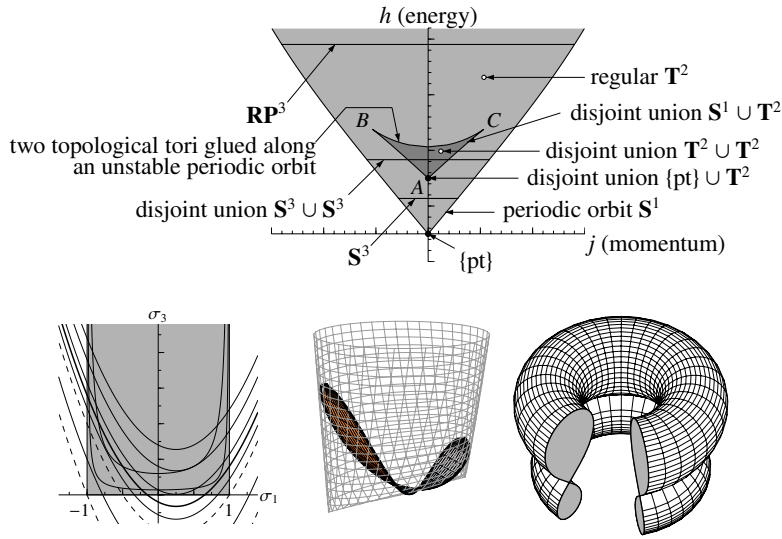


Figure 3.6: Image of \mathcal{EM} for type I systems. Reconstruction for type I systems.

3.3 Monodromy in the family of quadratic spherical pendula

We use two qualitative arguments in order to deduce the monodromy matrix for all members of the family of quadratic spherical pendula. The first is the *geometric monodromy theorem* [21, 97] which in our case reduces to the statement that

Theorem 3.13. *If p is an isolated critical value of \mathcal{EM} which lifts to a k -pinched torus then the monodromy matrix for a path Γ around p is $\begin{pmatrix} 1 & k \\ 0 & 1 \end{pmatrix}$ in an appropriate basis.*

The second is a deformation argument:

Lemma 3.14. *Let $s \in [0, 1] \mapsto \Gamma_s$ be a smooth family of closed paths and $s \in [0, 1] \mapsto \mathcal{EM}_s$ a smooth family of energy-momentum maps $\mathcal{EM}_s : \mathbf{R}^4 \rightarrow \mathbf{R}^2$ such that $\Gamma_s \subseteq \mathcal{R}_s$ for all $s \in [0, 1]$, where \mathcal{R}_s is the set of regular values of \mathcal{EM}_s . Then the \mathbf{T}^2 bundles $\mathcal{EM}_0^{-1}(\Gamma_0) \rightarrow \Gamma_0$ and $\mathcal{EM}_1^{-1}(\Gamma_1) \rightarrow \Gamma_1$ are isomorphic.*

It is known from [20] and [14] that the monodromy matrix for the spherical pendulum $V(z) = z$ is $\begin{pmatrix} 1 & 1 \\ 0 & 1 \end{pmatrix}$ while the monodromy matrix for the spherical pendulum $V(z) = z^2$ is $\begin{pmatrix} 1 & 2 \\ 0 & 1 \end{pmatrix}$. We will use the geometric monodromy theorem and deformation arguments in order to deduce the monodromy matrix for all the members of the family of quadratic spherical pendula.

3.3.1 Monodromy in type O and type II systems

Recall that type O systems are characterized by the existence of a single isolated critical value of \mathcal{EM} with coordinates $(h, j) = (b/2 + |c|, 0)$ which lifts to a singly pinched torus.

Lemma 3.15. *The monodromy matrix around a path Γ that encircles the unique isolated critical value of \mathcal{EM} in type O systems is $\begin{pmatrix} 1 & 1 \\ 0 & 1 \end{pmatrix}$.*

Proof. This is a direct consequence of theorem 3.13. \square

Monodromy in type II systems has been studied in [14, 26]. Recall that the energy-momentum map of type II systems for $c \neq 0$ has two isolated critical values $(b/2 - |c|, 0)$ and $(b/2 + |c|, 0)$. Each critical value lifts to a singly pinched torus. When $b > 0, c = 0$ \mathcal{EM} has only one isolated critical value which lifts to a double pinched torus. Therefore from theorem 3.13 (see also [14]) we have

Lemma 3.16. *The monodromy matrix around a path that encircles the unique isolated critical value of \mathcal{EM} for $b > 0, c = 0$ is $\begin{pmatrix} 1 & 2 \\ 0 & 1 \end{pmatrix}$.*

In the case of type II systems with $c \neq 0$ we prove

Lemma 3.17. *The monodromy matrix around a path Γ that encircles each of the isolated critical values of \mathcal{EM} in type II systems is $\begin{pmatrix} 1 & 1 \\ 0 & 1 \end{pmatrix}$. The monodromy matrix around a path that encircles both isolated critical values is $\begin{pmatrix} 1 & 2 \\ 0 & 1 \end{pmatrix}$.*

Remark 3.18. This result is contained in [14]. One can also use the *monodromy addition theorem* [26] to prove the part about paths going around both critical values. Here we use a deformation argument for this part.

Proof. The monodromy for paths that go around one of the critical values is a direct consequence of theorem 3.13.

Consider now a path Γ that encircles both critical values of \mathcal{EM} . If we keep b fixed and reduce c to 0 then the two critical values merge to a single critical value that lifts to a doubly pinched torus. From lemma 3.16 we know that the monodromy matrix around this value is $\begin{pmatrix} 1 & 2 \\ 0 & 1 \end{pmatrix}$. From lemma 3.14 we obtain that the monodromy matrix around both isolated critical values is also $\begin{pmatrix} 1 & 2 \\ 0 & 1 \end{pmatrix}$. \square

3.3.2 Non-local monodromy

Lemma 3.19. *The monodromy for a path Γ on leaf L_1 that goes around the curve of critical values BC is $\begin{pmatrix} 1 & 1 \\ 0 & 1 \end{pmatrix}$.*

Proof. Consider a type O system i.e. a system with one isolated critical value of \mathcal{EM} and a path Γ that goes around this critical value. As we saw in the previous section, in this case the monodromy matrix is $\begin{pmatrix} 1 & 1 \\ 0 & 1 \end{pmatrix}$. We deform

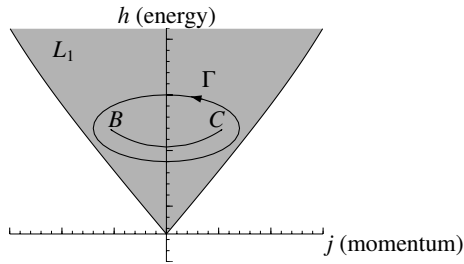


Figure 3.7: The path Γ around the curve BC on the leaf L_1 lifts under $\mathcal{EM}^{-1}|_{L_1}$ to a \mathbf{T}^2 bundle over Γ .

smoothly this system and the path Γ until we obtain a type I system in such a way that the path Γ is not crossed by any critical values of \mathcal{EM} during this deformation. Then according to lemma 3.14 the monodromy matrix for Γ for the type I system is also $\begin{pmatrix} 1 & 1 \\ 0 & 1 \end{pmatrix}$. Notice that the condition imposed on the path means that in the type I system the path does not intersect the region ABC .

Moreover, we can consider a path Γ' that goes around the line of critical values BC but enters into the region ABC . Notice that on the leaf L_1 the path Γ' and the path Γ that goes around ABC are homotopic. Since the monodromy matrix for the \mathbf{T}^2 bundle over Γ is already known to be $\begin{pmatrix} 1 & 1 \\ 0 & 1 \end{pmatrix}$ we deduce that this is the case also for the \mathbf{T}^2 bundle over Γ' . \square

We call this type of monodromy *non-local monodromy*.

Remark 3.20. An interesting and still open question is whether we can define in a meaningful way monodromy for a path that *crosses* the line BC . Consider such a path and begin at a point outside the region ABC . This point lifts to a torus. Suppose that the path enters ABC through BC . As we enter the island the single torus breaks into two tori. For this reason, I believe that it is not possible to define *classical* monodromy for any path Γ that crosses the line BC . Nevertheless, it may be possible to define *quantum* monodromy for such paths¹.

3.4 Quantum monodromy in the quadratic spherical pendula

A short introduction to quantum monodromy and its relation with classical monodromy is given in appendix C.2.

Quantum monodromy is a characteristic of the joint spectrum of the quantum operators

$$\mathcal{H} = -\hbar^2 \left(\frac{1}{\sin \theta} \frac{\partial}{\partial \theta} \left(\sin \theta \frac{\partial}{\partial \theta} \right) + \frac{1}{\sin^2 \theta} \frac{\partial^2}{\partial \phi^2} \right) + V(\cos \theta) \quad (3.25)$$

$$\mathcal{J} = -i\hbar \frac{\partial}{\partial \phi} \quad (3.26)$$

which correspond to the classical Hamiltonian H and momentum J respectively on $T\mathbf{S}^2$.

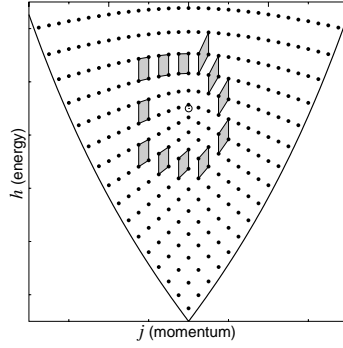


Figure 3.8: Quantum monodromy in the spherical pendulum and other type O systems.

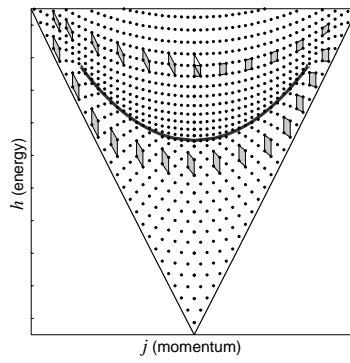


Figure 3.9: Quantum monodromy in the case of type I systems.

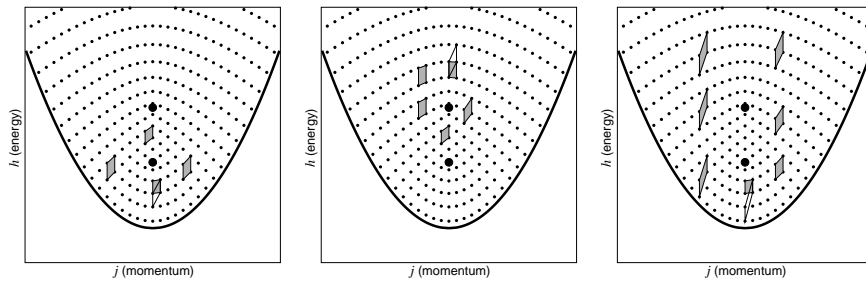


Figure 3.10: Quantum monodromy in the case of type II systems.

The spherical harmonics $\{Y_{lm}\}$ with fixed m and $l \geq |m|$ form a linear \mathcal{H} -invariant subspace of the Hilbert space while they are eigenvectors of \mathcal{J} with the same eigenvalue m . The spectrum of \mathcal{H} for fixed m is the set of eigenvalues of the matrix $\langle Y_{l',m} | \mathcal{H} | Y_{l,m} \rangle$ where $l, l' \geq |m|$. Since this matrix is infinite we truncate it at a large value of l .

Recall that the monodromy matrix is then computed by considering a small cell spanned by vectors k_1, k_2 and transporting it around the path Γ . If we denote by k'_1, k'_2 the vectors that span the lattice when we come back to the original point we have $k'_1 = k_1 + mk_2$ and $k'_2 = k_2$. Then the monodromy matrix is $\begin{pmatrix} 1 & m \\ 0 & 1 \end{pmatrix}$.

The quantum lattices for type O systems which are qualitatively the same as the linear spherical pendulum, and type I and II systems, are shown in figures 3.8, 3.9 and 3.10 respectively. We can easily read the monodromy matrix for each case from these figures.

3.5 Geometric Hamiltonian Hopf bifurcations

In this section we prove that the equilibria located at the ‘north’ and ‘south’ poles of the sphere go through two qualitatively different geometric Hamiltonian Hopf bifurcations and we relate these bifurcations to monodromy.

Consider the one-parameter family

$$H(x, y) = \frac{1}{2}(y_1^2 + y_2^2 + y_3^2) + \frac{1}{2}b_\theta x_3^2 + c_\theta x_3 \quad (3.27)$$

where $b_\theta = \cos \theta$ and $c_\theta = \sin \theta$.

Recall that $P_\pm = (0, 0, \pm 1; 0, 0, 0)$ are the two equilibria of H (3.2) on TS^2 .

Theorem 3.21. *P_- is elliptic-elliptic for $\theta \in (\pi/4, 5\pi/4)$ and hyperbolic-hyperbolic for $\theta \in (-3\pi/4, \pi/4)$. At $\theta = \pi/4$ P_- goes through a supercritical geometric Hamiltonian Hopf bifurcation. At $\theta = 5\pi/4$ it goes through a subcritical geometric Hamiltonian Hopf bifurcation.*

Theorem 3.22. *P_+ is elliptic-elliptic for $\theta \in (3\pi/4, 7\pi/4)$ and hyperbolic-hyperbolic for $\theta \in (-\pi/4, 3\pi/4)$. At $\theta = -\pi/4$ P_+ goes through a supercritical geometric Hamiltonian Hopf bifurcation. At $\theta = 3\pi/4$ it goes through a subcritical geometric Hamiltonian Hopf bifurcation.*

We will prove only the theorem for P_- , since the theorem for P_+ can then be obtained by flipping the sphere upside down and changing $c \mapsto -c$.

First let us clarify what we mean by geometric Hamiltonian Hopf bifurcation. Recall that the Hamiltonian Hopf bifurcation is related to the behaviour of a family of periodic orbits with respect to an equilibrium that loses linear stability. In particular, when an equilibrium is elliptic-elliptic, a family of periodic orbits emanates from it. In the case of a standard Hamiltonian Hopf bifurcation the equilibrium loses stability by becoming complex hyperbolic. What is interesting is the nonlinear behaviour of the system. In the case of a standard supercritical Hamiltonian Hopf bifurcation the family of periodic orbits detaches from the equilibrium, while in the subcritical case the family shrinks to the equilibrium and disappears.

¹Private communication with Boris Zhilinskii.

In the family of quadratic spherical pendula we prove that the equilibria P_{\pm} can be only degenerate elliptic (2E) or degenerate hyperbolic (2H). Nevertheless, the nonlinear behaviour of the family of periodic orbits that emanates from P_+ or P_- when it is 2E is the same as in the case of the standard Hamiltonian Hopf bifurcation. For this reason we call this a *geometric Hamiltonian Hopf bifurcation*. The case of a geometric Hamiltonian Hopf bifurcation has been discussed in [46] for the 3D Hénon-Heiles family.

Remark 3.23. Notice that when P_- goes through a supercritical Hamiltonian Hopf bifurcation we have no monodromy when P_- is 2E and standard monodromy when P_- is 2H. When it goes through a subcritical Hamiltonian Hopf bifurcation we have non-local monodromy when it is 2E and standard monodromy when it is 2H. Recall that we saw a similar situation in chapter 2.

Local chart

We define a local chart on TS^2 near P_- using the relations

$$\begin{aligned} x_1 &= q_1 & x_2 &= q_2 & x_3 &= -(1 - q_1^2 - q_2^2)^{1/2} \\ y_1 &= p_1 & y_2 &= p_2 & y_3 &= \frac{q_1 p_1 + q_2 p_2}{(1 - q_1^2 - q_2^2)^{1/2}} \end{aligned}$$

The Poisson structure in the local chart is

	q_1	q_2	p_1	p_2
q_1	0	0	$1 - q_1^2$	$-q_1 q_2$
q_2		0	$-q_1 q_2$	$1 - q_2^2$
p_1			0	$q_2 p_1 - q_1 p_2$
p_2				0

The corresponding symplectic structure is

$$\begin{aligned} \omega &= \frac{1}{1 - q_1^2 - q_2^2} \left((1 - q_2^2) dq_1 \wedge dp_1 + (1 - q_1^2) dq_2 \wedge dp_2 \right. \\ &\quad \left. + (p_2 q_1 - q_2 p_1) dq_1 \wedge dq_2 + q_1 q_2 (dq_1 \wedge dp_2 + dq_2 \wedge dp_1) \right) \end{aligned} \quad (3.28)$$

The \mathbf{S}^1 action Φ (3.7) induces a local \mathbf{S}^1 action Φ_{local} on the chart (q, p) . This action is

$$\Phi_{\text{local}} : \mathbf{S}^1 \times \mathbf{R}^4 \rightarrow \mathbf{R}^4 : t, (q, p) \mapsto (R_t q, R_t p) \quad (3.29)$$

where $R_t = \begin{pmatrix} \cos t & \sin t \\ -\sin t & \cos t \end{pmatrix}$.

Notice that this exactly the same action as (2.51). Therefore lemma 2.9 holds. We recall that lemma here.

Lemma 3.24. *The algebra $\mathbf{R}[q, p]^{\mathbf{S}^1}$ of polynomials invariant with respect to the local \mathbf{S}^1 action are $S = q_1 p_2 - q_2 p_1$, $N = \frac{1}{2}(q_1^2 + q_2^2)$, $M = \frac{1}{2}(p_1^2 + p_2^2)$ and $T = q_1 p_1 + q_2 p_2$ related by $T^2 = 4MN - S^2$.*

Linear stability

The linear stability of the equilibria can be computed taking into account just the constant term of the symplectic form. In our case this is

$$\omega_0 = dq_1 \wedge dp_1 + dq_2 \wedge dp_2 \quad (3.30)$$

We express the Hamiltonian (3.2) in terms of the local chart (q, p) and we Taylor expand it around 0. The result is a local Hamiltonian function in variables (q, p) that we denote again by H and which has the form

$$H = H_2 + H_4 + H_6 + \dots \quad (3.31)$$

where each term H_{2k} is a polynomial of degree $2k$ in (q, p) .

Since the local Hamiltonian is invariant with respect to the \mathbf{S}^1 action Φ_{local} (3.29) we deduce that the quadratic part H_2 must have the form $H_2 = a_1 M + a_2 N + a_3 S + a_4 T$. But notice that the original Hamiltonian (3.2) is also invariant with respect to the time-reversal group \mathcal{T} which is generated by $y \mapsto -y$. This means that the local Hamiltonian H (3.31) is invariant under the transformation $p \mapsto -p$. The action of time reversal on the \mathbf{S}^1 invariants is $(M, N, S, T) \mapsto (M, N, -S, -T)$. Therefore the only $\mathbf{S}^1 \times \mathcal{T}$ invariants are M and N and the most general $\mathbf{S}^1 \times \mathcal{T}$ invariant Hamiltonian H_2 must be of the form

$$H_2 = a_1 M + a_2 N = \frac{a_1}{2}(p_1^2 + p_2^2) + \frac{a_2}{2}(q_1^2 + q_2^2) \quad (3.32)$$

The frequencies of such Hamiltonian are $\pm(-a_1 a_2)^{1/2}$ (twice). Therefore P_- can only be 2E or 2H for *any* initial Hamiltonian of the form (3.2) with an axisymmetric potential $V(x_3)$. Therefore the only way with which P_- can lose stability is by becoming 2H. In the presence of symmetry this is non-generic in general bifurcation has become generic.

Remark 3.25. This type of analysis is in the same spirit as the analysis in [1] of the possible types of linear stability of the critical points of the $\mathbb{T}_d \times \mathcal{T}$ action on $\mathbb{C}\mathbf{P}^2$.

Here in particular, the quadratic part of the local Hamiltonian is

$$H_2 = \frac{1}{2}(p_1^2 + p_2^2) + \frac{1}{2}(c - b)(q_1^2 + q_2^2) = M + (c - b)N \quad (3.33)$$

The linear stability of P_- can be easily deduced from H_2 . Specifically, the frequencies are $\pm(b - c)^{1/2}$ (twice). This means that P_- is degenerate elliptic (2E) for $b - c < 0$ and degenerate hyperbolic (2H) for $b - c > 0$. P_- changes linear stability type when $c = b$. The movement of eigenvalues is shown in figure 3.11.

Nonlinear Hamiltonian Hopf bifurcation

The symplectic form ω can be Taylor expanded in the form

$$\omega = \omega_0 + \omega_2 + \omega_4 + \dots \quad (3.34)$$

where

$$\omega_0 = dq_1 \wedge dp_1 + dq_2 \wedge dp_2 \quad (3.35)$$

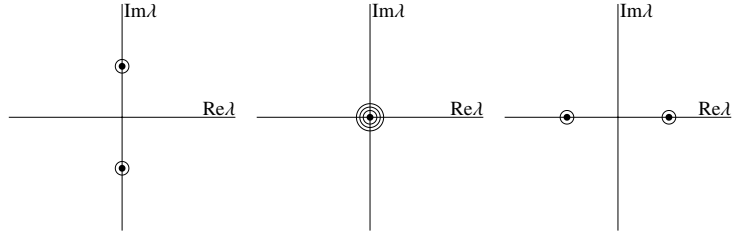


Figure 3.11: Movement of eigenvalues in the $\mathbf{S}^1 \times \mathcal{T}$ equivariant geometric Hamiltonian Hopf bifurcation.

is the standard symplectic form. Each term ω_{2k} contains terms of degree $2k$ in (q, p) . Specifically, the second term is

$$\begin{aligned} \omega_2 = & q_1^2 dq_1 \wedge dp_1 + q_2^2 dq_2 \wedge dp_2 \\ & + (p_2 q_1 - q_2 p_1) dq_1 \wedge dq_2 + q_1 q_2 (dq_1 \wedge dp_2 + dq_2 \wedge dp_1) \end{aligned} \quad (3.36)$$

In order to flatten the symplectic form we use the method described in [20] and in the previous chapter. Specifically, we use the transformation ϕ induced in time 1 by the vector field

$$\begin{aligned} X = & -\frac{1}{4}q_1(q_1^2 + q_2^2)\frac{\partial}{\partial q_1} - \frac{1}{4}q_2(q_1^2 + q_2^2)\frac{\partial}{\partial q_2} \\ & - \frac{1}{4}(q_1(q_1 p_1 + q_2 p_2) + q_2(q_1 p_2 - q_2 p_1))\frac{\partial}{\partial p_1} \\ & - \frac{1}{4}(-q_1(q_1 p_2 - q_2 p_1) + q_2(q_1 p_1 + q_2 p_2))\frac{\partial}{\partial p_2} \end{aligned} \quad (3.37)$$

Notice that X is Φ_{local} equivariant. This means that the ϕ transformed Hamiltonian

$$\phi^* H = H_2 + \mathcal{L}_X H_4 \quad (3.38)$$

is Φ_{local} invariant. It is expressed in terms of the invariants (M, N, S, T) as

$$\phi^* H = M + (c - b)N + \frac{1}{2}(2b - c)N^2 + MN \quad (3.39)$$

Recall that the equilibrium changes linear stability when $c = b$ i.e. when the coefficient of N in H_2 becomes 0. The last step is normalization with respect to N which kills all terms of order higher than 4 which contain M or T . We do this normalization using the Lie series method with the generator $W = NT/6$. The result is the normalized Hamiltonian

$$\tilde{H} = M + (c - b)N + \frac{1}{6}S^2 + \frac{1}{6}(4b - c)N^2 \quad (3.40)$$

Exactly at the bifurcation $b = c$, the coefficient of N^2 becomes $c/2$. Therefore we have a supercritical Hamiltonian Hopf bifurcation when $c > 0$ and a subcritical one when $c < 0$.

3.6 The LiCN molecule

Recall that in §0.3 we introduced the family of quadratic spherical pendula as a family that includes the simple model of the LiCN molecule. In this section

we discuss LiCN without taking into account the approximation that Li moves on the surface of a sphere.

Recall that in floppy molecules of type XAB we have two stretching motions characterized by the distance r between the atoms AB and the distance R between the center of mass and X. We also have the bending motion characterized by the bending angle γ . In molecules like CO₂ there is an 1:2 resonance between the stretching and bending motions but no such prominent resonance exists between these two modes in HCN or LiCN. Therefore we can average the two stretching motions (for LiCN in particular r is considered fixed). This gives a surface $R(\gamma)$, on which X moves in the averaged system and where R depends considerably on γ . The potentials in both cases are given by *ab initio* calculations [32, 49, 87].

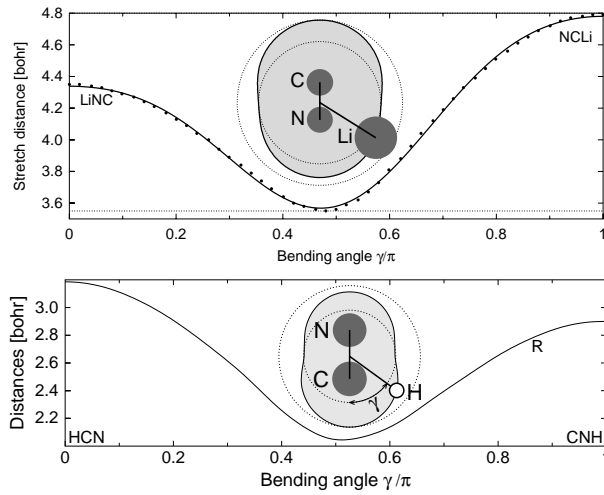


Figure 3.12: The functions $R(\gamma)$ for LiCN and HCN.

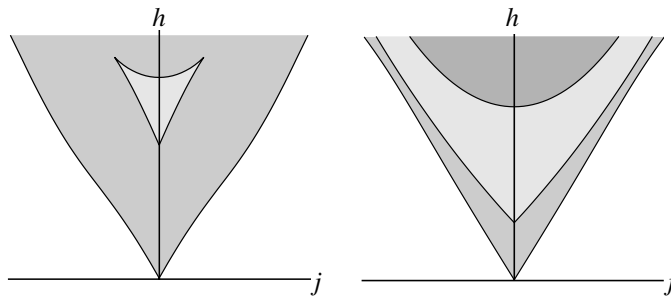


Figure 3.13: The image of \mathcal{EM} for LiCN and HCN.

The functions $R(\gamma)$ for HCN and LiCN are shown in figure 3.12. The main difference between these cases is that the surface on which the Li atom moves in LiCN is convex but for the HCN it is not. This affects remarkably the qualitative features of the image of \mathcal{EM} for the two systems. This is shown in

figure 3.13. We can clearly see that the LiCN molecule has the main qualitative features of type I quadratic spherical pendula.

On the other hand, the image of \mathcal{EM} for HCN is completely different qualitatively. It consists of three leaves L_1 , L_2 and L_3 which join along the upper side of L_1 and L_2 and the lower side of L_3 . The leaves L_1 and L_2 overlap partially. Values (h, j) of \mathcal{EM} inside the overlap lift to two disjoint \mathbf{T}^2 in phase space. For more details see [5] and [52].

4

Fractional monodromy

In this chapter we study monodromy in $m:-n$ resonances. First, we demonstrate that the $1:-1$ resonance has regular monodromy. Most of this chapter is about the analytic proof of fractional monodromy in the $1:-2$ resonance. Recall that fractional monodromy is a generalization of regular monodromy [72, 73]. Finally, we give some conjectures about fractional monodromy in higher $m:-n$ resonances.

4.1 The $1:-1$ resonance

We begin with a brief discussion of the $1:-1$ resonance. Recall from §0.4 that in this case the invariants of the \mathbf{S}^1 action generated by the $1:-1$ resonance are

$$\begin{aligned} J &= \frac{1}{2}((q_1^2 + p_1^2) - (q_2^2 + p_2^2)) \\ \pi_1 &= \frac{1}{2}((q_1^2 + p_1^2) + (q_2^2 + p_2^2)) \\ \pi_2 &= q_1 q_2 - p_1 p_2 \\ \pi_3 &= q_1 p_2 + q_2 p_1 \end{aligned}$$

Notice that the momentum J is the generator of the oscillator symmetry. The Hamiltonian is defined as

$$H(q, p) = q_1 p_2 + q_2 p_1 + \epsilon(q_1^2 + p_1^2)(q_2^2 + p_2^2) \quad (4.1)$$

The reduced Hamiltonian H_j on $J^{-1}(j)/\mathbf{S}^1$ is

$$H_j = \pi_3 + \epsilon(\pi_1^2 - j^2)$$

The term of order ϵ has been introduced in the Hamiltonian in order to compactify the common level sets $H^{-1}(h) \cap J^{-1}(j)$.

The energy-momentum map is $\mathcal{EM} : \mathbf{R}^4 \rightarrow \mathbf{R}^2 : z \mapsto (H(z), J(z))$. The set of critical values of \mathcal{EM} is shown in figure 4.1. It consists of the line $h = -\frac{1}{4\epsilon}$ each point of which lifts to an \mathbf{S}^1 and the isolated critical value $(0, 0)$. The latter lifts to a singly pinched torus. By the geometric monodromy theorem we have that the monodromy matrix for paths that go around the isolated critical value is $\begin{pmatrix} 1 & 1 \\ 0 & 1 \end{pmatrix}$.

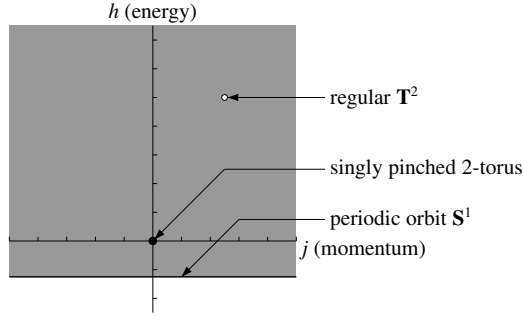


Figure 4.1: Image of the \mathcal{EM} map of the 1:–1 resonance

4.2 The 1:–2 resonance

We define the 1:–2 resonance system and give the set of critical points of its energy-momentum map.

4.2.1 The energy-momentum map

Consider the functions

$$\begin{aligned} H : \mathbf{R}^4 \rightarrow \mathbf{R} : z = (q_1, q_2, p_1, p_2) \mapsto H(z) = \\ = \sqrt{2}((q_1^2 - p_1^2)p_2 + 2q_1q_2p_1) + 2\epsilon(q_1^2 + p_1^2)(q_2^2 + p_2^2) \end{aligned} \quad (4.2)$$

where ϵ is positive and sufficiently small, and

$$J : \mathbf{R}^4 \rightarrow \mathbf{R} : z \mapsto J(z) = \frac{1}{2}(q_1^2 + p_1^2) - (q_2^2 + p_2^2) \quad (4.3)$$

The flow of the linear Hamiltonian vector field X_J is

$$\phi^J : \mathbf{S}^1 \times \mathbf{R}^4 \rightarrow \mathbf{R}^4 : (t, z) \mapsto \begin{pmatrix} \cos t & 0 & -\sin t & 0 \\ 0 & \cos 2t & 0 & \sin 2t \\ \sin t & 0 & \cos t & 0 \\ 0 & -\sin 2t & 0 & \cos 2t \end{pmatrix} z \quad (4.4)$$

ϕ^J defines an \mathbf{S}^1 action on \mathbf{R}^4 which is in 1:–2 resonance. H is ϕ^J -invariant. Hence

$$\mathcal{EM} : \mathbf{R}^4 \rightarrow \mathbf{R}^2 : z \mapsto (H(z), J(z)) \quad (4.5)$$

is the energy-momentum map of a Liouville integrable Hamiltonian system. Because the quartic terms are positive definite, H is a proper function. Consequently the fibers of \mathcal{EM} are compact. Let \mathcal{R} denote the set of regular values of \mathcal{EM} which lie in its range. For each $(h, j) \in \mathcal{R}$, each connected component of the fiber $\mathcal{EM}^{-1}(h, j)$ is a smooth two dimensional torus $\mathbf{T}_{h,j}^2$ by the Arnol'd-Liouville theorem.

4.2.2 The integrable foliation

In this section we study the geometry of the singular foliation defined by the the level sets of H (4.2) and J (4.3). The geometry of an equivalent foliation is obtained in [72] (see §4.3.1 for more details).

First, we reduce the \mathbf{S}^1 symmetry (4.4). Since the \mathbf{S}^1 action ϕ^J has \mathbf{Z}_2 isotropy on $\{q_1 = p_1 = 0\}$ and thus is not free, we need singular reduction. We use invariant theory.

Recall from §0.4 that the algebra of ϕ^J -invariant polynomials is generated by the polynomials

$$\begin{aligned} J(q_1, q_2, p_1, p_2) &= \frac{1}{2}(q_1^2 + p_1^2) - (q_2^2 + p_2^2) \\ \pi_1(q_1, q_2, p_1, p_2) &= \frac{1}{2}(q_1^2 + p_1^2) + (q_2^2 + p_2^2) \\ \pi_2(q_1, q_2, p_1, p_2) &= \sqrt{2}((q_1^2 - p_1^2)q_2 - 2q_1p_1p_2) \\ \pi_3(q_1, q_2, p_1, p_2) &= \sqrt{2}((q_1^2 - p_1^2)p_2 + 2q_1q_2p_1) \end{aligned}$$

subject to the relation

$$\Psi = \pi_2^2 + \pi_3^2 - (\pi_1 - J)(\pi_1 + J)^2 = 0 \quad (4.6)$$

and $\pi_1 \geq |J|$.

The space $\mathbf{R}^4/\mathbf{S}^1$ of \mathbf{S}^1 -orbits is defined by (4.6) and is the image of the \mathbf{S}^1 -orbit map

$$\rho : \mathbf{R}^4 \rightarrow \mathbf{R}^4 : z \mapsto (J(z), \pi_1(z), \pi_2(z), \pi_3(z))$$

The reduced phase space $P_j = J^{-1}(j)/\mathbf{S}^1$ (see figure 0.11) is the image of $J^{-1}(j)$ under the reduction map $\rho_j = \rho|_{J^{-1}(j)}$ and is defined by

$$\pi_2^2 + \pi_3^2 = (\pi_1 - j)(\pi_1 + j)^2, \quad \pi_1 \geq |j| \quad (4.7)$$

Since H (4.2) is invariant under ϕ^J , it induces on P_j a smooth function

$$H_j : P_j \subseteq \mathbf{R}^3 \mapsto \mathbf{R} : \pi = (\pi_1, \pi_2, \pi_3) \mapsto H_j(\pi) = \pi_3 + \epsilon(\pi_1^2 - j^2) \quad (4.8)$$

called the reduced Hamiltonian.

The space of smooth functions on the reduced phase space P_j has a Poisson structure. A straightforward calculation shows that its skew symmetric structure matrix has nonzero entries

$$\begin{aligned} \{\pi_1, \pi_2\} &= -2 \frac{\partial \Psi}{\partial \pi_3} = -4\pi_3 \\ \{\pi_2, \pi_3\} &= -2 \frac{\partial \Psi}{\partial \pi_1} = 2(\pi_1 + j)(3\pi_1 - j) \\ \{\pi_3, \pi_1\} &= -2 \frac{\partial \Psi}{\partial \pi_2} = -4\pi_2 \end{aligned}$$

J and Ψ are Casimirs of this algebra. The equations of motion for the reduced Hamiltonian H_j (4.8) are

$$\dot{\pi}_1 = \{\pi_1, H_j\} = 4\pi_2 \quad (4.9a)$$

$$\dot{\pi}_2 = \{\pi_2, H_j\} = 2(\pi_1 + j)(3\pi_1 - j) + 8\epsilon \pi_1 \pi_3 \quad (4.9b)$$

$$\dot{\pi}_3 = \{\pi_3, H_j\} = -8\epsilon \pi_1 \pi_2 \quad (4.9c)$$

Next we describe the discriminant locus Δ of \mathcal{EM} (4.5), that is, the set of critical values of \mathcal{EM} which lie in its range.

Lemma 4.1. Δ is the union of the image of the two curves

$$\mathcal{C}_1 : [0, \infty) \rightarrow \mathbf{R}^2 : s \mapsto (h(s), j(s)) = (0, -s) \quad (4.10)$$

and

$$\begin{aligned} \mathcal{C}_2 : [\frac{1}{2\epsilon^2}, \infty) \rightarrow \mathbf{R}^2 : s \mapsto (h(s), j(s)) = \\ = (4s(2\epsilon^2s - 1)(\sqrt{2}(8\epsilon^2s - 1)\sqrt{s(2\epsilon^2s - 1)} - 2\epsilon s(8\epsilon^2s - 3)), \\ s(3 - 8\epsilon^2s + 4\epsilon\sqrt{2s(2\epsilon^2s - 1)})) \end{aligned} \quad (4.11)$$

which join at the point $P = (0, -\frac{1}{2\epsilon^2})$ in a C^1 but not C^2 fashion.

Proof. See §4.3.6. □

Definition 4.2. The image of the curve $\mathcal{C}_1|(0, \frac{1}{2\epsilon^2})$ is called the *critical line* \mathcal{C} .

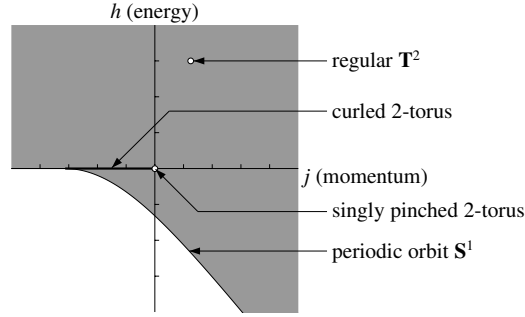


Figure 4.2: The set of critical values Δ of \mathcal{EM} . The range of \mathcal{EM} is shaded.

We now discuss the topology of the fibers of the reduced Hamiltonian H_j (4.8) on the reduced space P_j (4.7).

Lemma 4.3. For points $(h, j) \in \mathcal{C}_2 \cup \mathcal{C}_1|(\frac{1}{2\epsilon^2}, \infty)$ (the boundary of the \mathcal{EM} image) $H_j^{-1}(h)$ is a single point. For points $(h, j) \in \mathcal{C}$, $H_j^{-1}(h)$ is a circle with one conical singularity. For the point $(h, j) = (0, 0)$, $H_j^{-1}(h)$ is a circle with one cusp. For all other points $(h, j) \in \mathcal{R}$, $H_j^{-1}(h)$ is a smooth circle.

Proof. From figure 4.2 we see that the boundary of the image of \mathcal{EM} is the union of the images of $\mathcal{C}_1|[\frac{1}{2\epsilon^2}, \infty)$ and \mathcal{C}_2 and corresponds to the critical values where H_j has an absolute minimum on P_j . Therefore, for nearby regular values $(h, j) \in \mathcal{R}$, the h -level set of H_j is a smooth circle. From the facts that $\mathcal{EM}|\mathcal{EM}^{-1}(\mathcal{R}) : \mathcal{EM}^{-1}(\mathcal{R}) \mapsto \mathcal{R}$ is a proper surjective submersion and \mathcal{R} is connected and simply connected, it follows that for every $(h, j) \in \mathcal{R}$ the level set $H_j^{-1}(h)$ is a smooth circle. Next we look at those level sets where (h, j) lies on the critical curve \mathcal{C} . In this case $H_j^{-1}(h)$ is defined by

$$\begin{cases} \pi_3 + \epsilon(\pi_1^2 - j^2) = h = 0, & j < 0 \\ \pi_2^2 + \pi_3^2 = (\pi_1^2 - j^2)(\pi_1 - |j|), & \pi_1 \geq |j|. \end{cases}$$

Eliminating π_3 shows that $H_j^{-1}(h)$ is the image of the curve

$$\begin{aligned} \mathcal{D} : [|j|, \infty) \rightarrow \mathbf{R}^3 : \\ \pi_1 \mapsto (\pi_1, \pm\epsilon(\pi_1 - |j|)\sqrt{(\pi_1 + |j|)(\frac{1}{\epsilon^2} - |j| - \pi_1)}, \epsilon(\pi_1^2 - j^2)). \end{aligned}$$

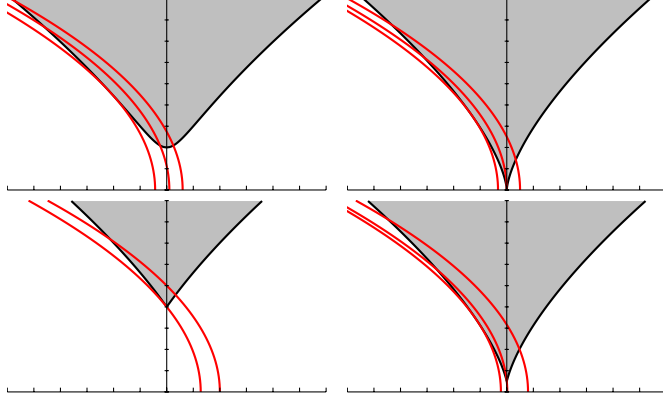


Figure 4.3: Projections of the intersections $P_j \cap \{H_j = h\}$ on the plane (π_3, π_1) . The level sets $\{H_j = h\}$ are shown by bold solid curves. From top to bottom: $j > 0$, $j = 0$, $j < 0$ with $|j|$ large, $j < 0$ with $|j|$ small.

Choose ϵ so that $\epsilon \in (0, \frac{1}{\sqrt{1+|j|}})$. Then $(\pi_1 + |j|)(\frac{1}{\epsilon^2} - |j| - \pi_1) \geq 0$ if and only if $\pi_1 \in [|j|, \frac{1}{\epsilon^2} - |j|]$. Hence $H_j^{-1}(h)$ is a compact one dimensional manifold, which is smooth except at the point $Q = (|j|, 0, 0)$ where it has a conical singularity. Hence $H_j^{-1}(h)$ is homeomorphic (but *not* diffeomorphic) to a circle. \square

Remark 4.4. We can obtain the result of lemma 4.3 pictorially by studying the intersections of level sets $\{H_j = h\}$ and the reduced phase spaces P_j , see figure 4.3.

We now carry out reconstruction.

Lemma 4.5. For points $(h, j) \in \mathcal{C}_2 \cup \mathcal{C}_1 | (\frac{1}{2\epsilon^2}, \infty)$ (the boundary of the \mathcal{EM} image) $\mathcal{EM}^{-1}(h, j)$ is a smooth circle. For points $(h, j) \in \mathcal{C}$, $\mathcal{EM}^{-1}(h, j)$ is a curled torus. For the point $(h, j) = (0, 0)$, $\mathcal{EM}^{-1}(0, 0)$ is curled pinched torus. For all other points $(h, j) \in \mathcal{R}$, $H_j^{-1}(h)$ is a smooth two-torus $\mathbf{T}_{h,j}^2$.

Proof. In the original phase space \mathbf{R}^4 the level set $H_j^{-1}(h)$ on P_j reconstructs to $\mathcal{EM}^{-1}(h, j) = H^{-1}(h) \cap J^{-1}(j)$. When $H_j^{-1}(h)$ is a smooth circle, $\mathcal{EM}^{-1}(h, j)$ is a smooth two dimensional torus $\mathbf{T}_{h,j}^2$. When (h, j) lies on the boundary of the image of \mathcal{EM} , $H_j^{-1}(h)$ is a point and $\mathcal{EM}^{-1}(h, j)$ is a smooth circle. When (h, j) lies on the critical line \mathcal{C} , the singular point $(0, 0, |j|)$ of P_j reconstructs to a periodic orbit $\gamma_{h,j}$ of X_H , which is given by

$$\{q_1 = p_1 = 0, q_2^2 + p_2^2 = |j|\}.$$

$\gamma_{h,j}$ is hyperbolic and has primitive period π . Since its linear Poincaré map is $\varphi_\pi^J = -\text{id}$, the orbit $\gamma_{h,j}$ is hyperbolic with reflection. Thus $H_j^{-1}(h)$ for $(h, j) \in \mathcal{C}$ reconstructs to $\gamma_{h,j}$ together with its stable and unstable manifolds. The latter are twisted so that $\mathcal{EM}^{-1}(h, j)$ is not orientable. In other words, for (h, j) on the critical curve \mathcal{C} , $\mathcal{EM}^{-1}(h, j)$ is a *curled 2-torus*; namely, a cylinder

on a figure eight with the ends of the cylinder identified after performing a half twist. Here $\gamma_{h,j}$ is the curve formed from the crossing point of the figure eight after making the identification. When $j = h = 0$, the curve $\gamma_{h,j}$ collapses to a point and $\mathcal{EM}^{-1}(h,j)$ is a *pinched curled 2-torus*. \square

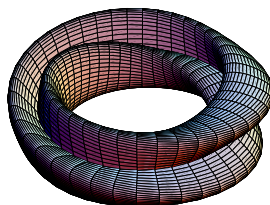


Figure 4.4: Curled torus

This completes the description of the geometry of the singular foliation $\mathcal{EM}^{-1}(h,j)$ where (h,j) ranges over the image of \mathcal{EM} .

4.3 Fractional monodromy in the 1:–2 resonance

We come now to the crux of this chapter, which is the analytical computation for the 1:–2 resonance of the generalized type of monodromy introduced in [73]. In [73] the authors defined the notion of fractional monodromy and then computed the fractional monodromy in a 1:–2 resonance system studying directly the behaviour of the cycles basis of the first homology group. We give here the first analytic computation of fractional monodromy based on the period lattice approach of [29] and [20].

4.3.1 From regular to fractional monodromy

Regular monodromy

Let us recall briefly how we can prove analytically the existence of monodromy in the regular situation [20, 29]. Consider a closed path Γ in the image of \mathcal{EM} . All the points on Γ are regular values of \mathcal{EM} , and Γ encloses one or more critical values of \mathcal{EM} . The monodromy matrix is defined as a linear automorphism on $H_1(\mathbf{T}_{h_0, j_0}^2, \mathbf{Z})$ where (h_0, j_0) is the starting point of Γ . The period lattice $\mathcal{P}(h,j)$ of $\mathbf{T}_{h,j}^2$ is the set $\{(T_1, T_2) \in \mathbf{R}^2 : \phi_J^{T_1} \phi_H^{T_2}(z) = z, \text{ for } z \in \mathbf{T}_{h,j}^2\}$. These points form a lattice in \mathbf{R}^2 that is generated by the vectors $v_1 = (2\pi, 0)$ and $v_2 = (-\Theta(h,j), T(h,j))$. The period lattice bundle over Γ is isomorphic to the H_1 bundle over Γ . Therefore, we can study the former instead of the latter. If the linear automorphism that identifies $\mathcal{P}(h_0, j_0)$ after going once around Γ is not the identity then the system has monodromy.

Fractional monodromy

The main difference between the regular situation described above and the 1:–2 resonance is that in the latter case the path Γ must cross the critical line \mathcal{C} . Specifically, we consider a path Γ with starting point a regular value

(h_0, j_0) of \mathcal{EM} that goes around the point $(0, 0)$ and crosses \mathcal{C} once before coming back to (h_0, j_0) , see figure 4.5. This causes three problems that we must resolve in order to compute, and even define, monodromy in this case within the framework of the analytical approach based on period lattices.

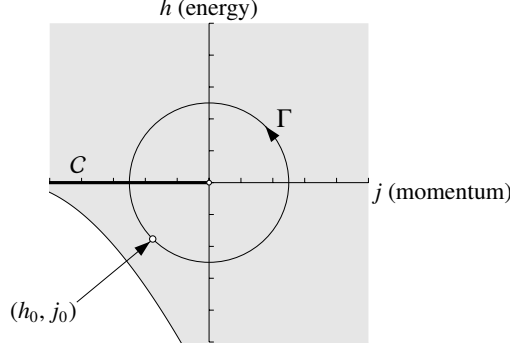


Figure 4.5: Path Γ in the case of 1: -2 resonance.

The first problem, is that near \mathcal{C} the first return time $T(h, j)$ of X_H goes to infinity. We overcome this problem by rescaling the vector field X_H . The rescaled vector field \hat{X} defines a modified first return time $\hat{T}(h, j)$ on $\mathbf{T}_{h,j}^2$. We prove that $\hat{T}(h, j)$ remains finite as $h \rightarrow 0$ and that $\lim_{h \rightarrow 0^+} \hat{T}(h, j) = \lim_{h \rightarrow 0^-} \hat{T}(h, j)$ for $j < 0$. The introduction of \hat{X} gives a modified period lattice $\hat{\mathcal{P}}(h, j)$ on $\mathbf{T}_{h,j}^2$ generated by $v_1 = (2\pi, 0)$ and $v_2 = (-\Theta(h, j), \hat{T}(h, j))$.

The second problem is that $\Theta(h, j)$ is discontinuous at \mathcal{C} and we obtain that

$$\lim_{h \rightarrow 0^+} \Theta(h, j) - \lim_{h \rightarrow 0^-} \Theta(h, j) = \pi \quad (4.12)$$

We cover Γ with open sets U^α , $\alpha = 1, \dots, \ell$ such that $(h_0, j_0) \in U^1 \cap U^\ell$, $U^\alpha \cap U^{\alpha+1} \neq \emptyset$ and $U^a \cap U^b \cap U^c = \emptyset$ for any triplet of (different) a, b, c . Let Θ^α be defined as the continuous function on U^α , for which $\Theta^1 = \Theta|_{U^1}$ and $\Theta^j = \Theta|_{U^j} +$ (some piecewise constant function on Γ) where Θ is given by the integral (4.21). When Γ crosses \mathcal{C} , we have by (4.12) that $\Theta^\ell(h_0, j_0) = \Theta^1(h_0, j_0) + \pi$. This means that $\hat{\mathcal{P}}^1(h_0, j_0)$ is spanned by vectors $v_1^1 = (2\pi, 0)$ and $v_2^1 = (-\Theta^1(h_0, j_0), \hat{T}^1(h_0, j_0))$. When we follow Γ back to (h_0, j_0) the new modified period lattice $\hat{\mathcal{P}}^\ell(h_0, j_0)$ is formally spanned by $v_1^\ell = (2\pi, 0)$ and $v_2^\ell = (-\Theta^\ell(h_0, j_0), \hat{T}^\ell(h_0, j_0)) = (-\Theta^1(h_0, j_0) - \pi, \hat{T}^1(h_0, j_0)) = v_2^1 - \frac{1}{2}v_1^1$. Notice that this can not be true because

$$\varphi_{X_j}^{-\Theta^\ell} \varphi_{\hat{X}}^{\hat{T}^\ell}(z) = \varphi_{X_j}^{-\pi} \varphi_{X_j}^{-\Theta^1} \varphi_{\hat{X}}^{\hat{T}^1}(z) = \varphi_{X_j}^{-\pi}(z) \neq z$$

Therefore by keeping the rotation number continuous we arrive at a lattice that is *not* a period lattice.

Moreover, since the transformation between the two bases (v_1^1, v_2^1) and (v_1^ℓ, v_2^ℓ) is not unimodular, they span different lattices. Nevertheless, both lattices have a common sublattice $\tilde{\mathcal{P}}(h_0, j_0)$ spanned by $v_1^1, 2v_2^1$ or equivalently by $v_1^\ell, 2v_2^\ell$. Therefore, although it does not make sense to study monodromy for the whole modified lattice $\hat{\mathcal{P}}$ we can study monodromy for the sublattice $\tilde{\mathcal{P}}$. Observe that for points $(T_1, T_2) \in \tilde{\mathcal{P}}$ we always have $\varphi_{X_j}^{T_1} \varphi_{\hat{X}}^{T_2}(z) = z$.

Notice, that now we must restrict our attention from the first homology group $H_1(\mathbf{T}_{h,j}^2, \mathbf{Z})$ to a subgroup $\tilde{H}_1(\mathbf{T}_{h,j}^2, \mathbf{Z})$ as it was also done in [72]. We discuss this point later.

The final problem is quite subtle. Monodromy is related to the behaviour of the basis cycles of $\tilde{H}_1(\mathbf{T}_{h,j}^2, \mathbf{Z})$ as we follow Γ . Instead of studying directly \tilde{H}_1 we study $\tilde{\mathcal{P}}$ the behaviour of which we can compute analytically. We have defined $\tilde{\mathcal{P}}$ in such a way that its basis vectors change continuously when Γ crosses \mathcal{C} . The question is if the basis cycles of \tilde{H}_1 also change continuously in that case. We demonstrate that this is indeed the case.

With these problems out of the way, we prove that the monodromy matrix for the \tilde{H}_1 bundle over Γ (or equivalently for the $\tilde{\mathcal{P}}$ bundle) expressed in the basis $[\gamma_1], 2[\gamma_2]$ is $\begin{pmatrix} 1 & 1 \\ 0 & 1 \end{pmatrix}$. Expressing this formally in the basis $[\gamma_1], [\gamma_2]$ of H_1 we find the matrix $\begin{pmatrix} 1 & 1/2 \\ 0 & 1 \end{pmatrix}$. This is the origin of the ‘fractional’ characterization for this type of monodromy. Nevertheless, notice that the latter matrix is only formal. *In reality, the meaning of fractional monodromy is that we have to consider instead of the whole first homology group, some appropriate subgroup* (see [72, 73]).

Relation to the 1:-2 resonance system of [73]

In [73] the authors study geometrically the fractional monodromy in the 1:-2 resonance using instead of the Hamiltonian (4.8), the Hamiltonian

$$\tilde{H}(z) = \sqrt{2}((q_1^2 - p_1^2)p_2 + 2q_1q_2p_1) + \epsilon(\frac{1}{2}(q_1^2 + p_1^2) + (q_2^2 + p_2^2))^2 \quad (4.13)$$

which reduces to

$$\tilde{H}_j = \pi_3 + \epsilon\pi_1^2 \quad (4.14)$$

We want to uncover the relation between (4.8) and (4.14) and explain why in this work we had to choose (4.8). Note that the definitions of the invariants in [73] differ by a scale factor but this does not affect this discussion.

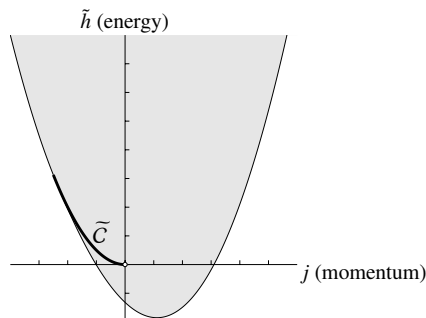


Figure 4.6: Energy-momentum map of the modified 1:-2 resonance

The energy-momentum map in [73] is

$$\widetilde{\mathcal{EM}}(z) = (\tilde{H}(z), J(z)) = (H(z) + \epsilon J(z)^2, J(z)) = \Psi \circ \mathcal{EM}(z)$$

where Ψ is the diffeomorphism $(h, j) \mapsto (h + \epsilon j^2, j)$. Since the two energy-momentum maps are related through a diffeomorphism they define the same

foliation of \mathbf{R}^4 . Therefore, qualitatively the two systems are the same. The image of \mathcal{EM} is depicted in figure 4.6.

The crucial difference is that the rotation number for $\widetilde{\mathcal{EM}}$ goes to infinity as we approach the critical curve $\widetilde{\mathcal{C}}$. Specifically the computation of the rotation number $\widetilde{\Theta}$ of $X_{\widetilde{H}}$ shows that

$$\widetilde{\Theta} \circ \Psi(h, j) = \Theta(h, j) - 2\epsilon j T(h, j)$$

The last expression isolates the part of $\widetilde{\Theta}$ that causes the blow-up behaviour near $\widetilde{\mathcal{C}}$, which is $-2\epsilon j T(h, j)$. In order to account for this term we have ‘corrected’ the Hamiltonian \widetilde{H} by subtracting the term ϵJ^2 , that gives H (4.8).

4.3.2 Rotation angle and first return time

In this section we describe the dynamics of X_H on the toric leaves of the foliation of \mathbf{R}^4 defined by \mathcal{EM} corresponding to regular values of \mathcal{EM} .

Let z be a point on $\mathbf{T}_{h,j}^2 = \mathcal{EM}^{-1}(h, j)$, where $(h, j) \in \mathcal{R}$, and consider the integral curve $t \mapsto \varphi_H^t(z)$ of X_H on $\mathbf{T}_{h,j}^2$. This integral curve reaches the circle on $\mathbf{T}_{h,j}^2$ traced out by the integral curve $s \mapsto \varphi_J^s(z)$ of X_J for the first positive time at $T(h, j)$. This time is called the *first return time*. Since the image of $t \mapsto \varphi_H^t(p)$ under the reduction mapping is precisely the integral curve of the reduced vector field X_{H_j} whose image is the circle $H_j^{-1}(h)$, $T(h, j)$ is the period of the orbit of X_{H_j} on $H_j^{-1}(h) \cap P_j$. Since the trajectory $H_j^{-1}(h)$ lies on P_j , we have that $\pi_2^2 = Q_{h,j}(\pi_1)$ where

$$Q_{h,j}(\pi_1) = (\pi_1 - j)(\pi_1 + j)^2 - (h - \epsilon(\pi_1^2 - j^2))^2 \quad (4.15)$$

is obtained from (4.7) by substitution of π_3 through the relation $H_j = h$ (4.8). The projection of this trajectory on the π_1 -axis is the closed interval $[\pi_1^-, \pi_1^+]$. Here π_1^- and π_1^+ are the two real roots of the polynomial $Q_{h,j}(\pi_1)$ in the interval $[[j], +\infty)$ with $\pi_1^+ > \pi_1^-$. The period $T(h, j)$ of the trajectory $H_j^{-1}(h)$ on P_j is

$$T(h, j) = \int_0^{T(h,j)} dt = 2 \int_{\pi_1^-}^{\pi_1^+} \frac{d\pi_1}{\dot{\pi}_1} = \frac{1}{2} \int_{\pi_1^-}^{\pi_1^+} \frac{d\pi_1}{\pi_2}. \quad (4.16)$$

The last equality in (4.16) follows from (4.9a). Hence the integral (4.16) becomes

$$T(h, j) = \frac{1}{2} \int_{\pi_1^-}^{\pi_1^+} \frac{d\pi_1}{\sqrt{Q_{h,j}(\pi_1)}} \quad (4.17)$$

As (h, j) approaches a point c on the critical curve \mathcal{C} , the period $T(h, j)$ goes to infinity, because $\mathcal{EM}^{-1}(c)$ is a hyperbolic periodic orbit with its stable and unstable manifolds.

Next we determine the rotation angle of the flow of X_H on $\mathbf{T}_{h,j}^2$. Let $\theta = \tan^{-1}(q_1/p_1)$. The (multivalued) function θ is canonically conjugate to J , as is easily seen by computing

$$\{\theta, J\} = \mathcal{L}_{X_J}\theta = 1$$

The time derivative of θ along an integral curve of X_H is

$$\dot{\theta} = \mathcal{L}_{X_H}\theta = \frac{q_1\dot{p}_1 - p_1\dot{q}_1}{q_1^2 + p_1^2} \quad (4.18)$$

From Hamilton's equations for the integral curves of X_H we obtain \dot{p}_1 and \dot{q}_1 . The function $\dot{\theta}$ is ϕ^J -invariant, since

$$\{J, \dot{\theta}\} = \{J, \{\theta, H\}\} = -\{\theta, \{H, J\}\} - \{H, \{\theta, J\}\} = -\{H, 1\} = 0.$$

Therefore we can express $\dot{\theta}$ in terms of the invariants J , π_1 , π_2 and π_3 . A short computation gives

$$\dot{\theta} = \frac{2h}{j + \pi_1} \quad (4.19)$$

Define the *rotation angle* $\Theta(h, j)$ of the flow of X_H on $\mathcal{EM}^{-1}(h, j)$ by

$$\Theta(h, j) = \int_0^{\Theta(h, j)} d\theta = \int_0^{T(h, j)} \dot{\theta} dt \quad (4.20)$$

Then

$$\Theta(h, j) = 2 \int_{\pi_1^-}^{\pi_1^+} \frac{2h}{j + \pi_1} \frac{d\pi_1}{\dot{\pi}_1} = h \int_{\pi_1^-}^{\pi_1^+} \frac{1}{j + \pi_1} \frac{d\pi_1}{\sqrt{Q_{h, j}(\pi_1)}}, \quad (4.21)$$

using (4.9a).

The rotation angle $\Theta(h, j)$ of X_H on $\mathcal{EM}^{-1}(h, j)$, where $(h, j) \in \mathcal{R}$ has a limit when h converges to 0 from above or below. More precisely, we find

Lemma 4.6. *For $j < 0$ and $\epsilon|2j|^{1/2} < 1$ we have*

$$\lim_{h \rightarrow 0^+} \Theta(h, j) = \frac{\pi}{2} + \sin^{-1}(\epsilon(2|j|)^{1/2}) \quad (4.22)$$

and

$$\lim_{h \rightarrow 0^-} \Theta(h, j) = -\frac{\pi}{2} + \sin^{-1}(\epsilon(2|j|)^{1/2}) \quad (4.23)$$

Proof. See §4.3.6. □

4.3.3 The period lattice

In this section we define a suitable notion of period lattice for the singular foliation defined by the level set of H (4.2) and J (4.3).

Definition 4.7. The period lattice $\mathcal{P}(h, j)$ of $\mathbf{T}_{h, j}^2$ is the set

$$\{(T_1, T_2) \in \mathbf{R}^2 : \varphi_{X_J}^{T_1} \varphi_{X_H}^{T_2}(z) = z \text{ for } z \in \mathbf{T}_{h, j}^2\}$$

We define the smooth vector fields

$$\begin{aligned} X_1(z) &= 2\pi X_J(z) \\ X_2(z) &= -\Theta(\mathcal{EM}(z)) X_J(z) + T(\mathcal{EM}(z)) X_H(z) \end{aligned}$$

on $\mathbf{T}_{h, j}^2$. These are linearly independent and have periodic flows of period 1. At a given point $z \in \mathbf{T}_{h, j}^2$ they span $\mathcal{P}(h, j)$. The period lattice does not depend on the choice of z , because the \mathbf{T}^2 -action defined by the composition of the flows $\varphi_{X_J}^t$ and $\varphi_{X_H}^t$ is transitive. Since $T(h, j)$ does *not* remain finite as (h, j) approaches the critical line \mathcal{C} , we cannot speak of a limiting period lattice on \mathcal{C} .

In order to resolve this difficulty, we rescale time to ensure that the new period is finite. Specifically, let

$$\widehat{X}(z) = \frac{1}{q_1^2 + p_1^2} X_H(z)$$

\widehat{X} is a smooth vector field on $\mathbf{R}^4 \setminus \{q_1 = p_1 = 0\}$. The image of an integral curve of \widehat{X} through $z \in \mathbf{T}_{h,j}^2$ is the same as the image of an integral curve of X_H through z . It follows that $\mathbf{T}_{h,j}^2$ is an invariant manifold of \widehat{X} . Hence $\widehat{X}|_{\mathbf{T}_{h,j}^2}$ is a smooth nonvanishing vector field on $\mathbf{T}_{h,j}^2$. Because the function $(q_1, q_2, p_1, p_2) \mapsto p_1^2 + q_1^2$ is invariant under the flow of X_J , the vector fields $\widehat{X}|_{\mathbf{T}_{h,j}^2}$ and $X_J|_{\mathbf{T}_{h,j}^2}$ commute.

Lemma 4.8. *The modified first return time $\widehat{T}(h, j)$ of the vector field $\widehat{X}|_{\mathbf{T}_{h,j}^2}$ is finite.*

Proof. See §4.3.6. □

We note that the *modified rotation angle* $\widehat{\Theta}(h, j)$ of the vector field $\widehat{X}|_{\mathbf{T}_{h,j}^2}$ is equal to the rotation angle $\Theta(h, j)$ (4.21), because

$$\widehat{\Theta}(h, j) = \int_0^{\widehat{T}(h,j)} \frac{d\theta}{ds} ds = \int_0^{T(h,j)} \frac{d\theta}{ds} \frac{ds}{dt} dt = \int_0^{T(h,j)} \frac{d\theta}{dt} dt = \Theta(h, j).$$

We now return to our discussion of the period lattice.

Definition 4.9. The modified period lattice $\widehat{\mathcal{P}}(h, j)$ of $\mathbf{T}_{h,j}^2$ is the set

$$\{(T_1, T_2) \in \mathbf{R}^2 : \varphi_{X_J}^{T_1} \varphi_{\widehat{X}}^{T_2}(z) = z \text{ for } z \in \mathbf{T}_{h,j}^2\}$$

Define the smooth vector fields

$$\begin{aligned} Y_1(z) &= 2\pi X_J(z) \\ Y_2(z) &= -\Theta(\mathcal{E}\mathcal{M}(z))X_J(z) + \widehat{T}(\mathcal{E}\mathcal{M}(z))\widehat{X}(z) \end{aligned} \tag{4.24}$$

on $\mathbf{T}_{h,j}^2$. They are linearly independent, they commute and they have period 1. For fixed $z_0 \in \mathbf{T}_{h,j}^2$ the vectors $(Y_1(z_0), Y_2(z_0))$ span $\widehat{\mathcal{P}}(h, j)$ on $\mathbf{T}_{h,j}^2$. Because the \mathbf{T}^2 -action on $\mathbf{T}_{h,j}^2$ generated by the composition of the flows of X_J and \widehat{X} is transitive, the modified period lattice $\widehat{\mathcal{P}}(h, j)$ does *not* depend on the choice of z_0 .

Observe that the modified period lattice $\widehat{\mathcal{P}}(0^\pm, -|j|)$ is defined by continuation for $(0, -|j|)$ on the critical curve \mathcal{C} because the limits of the modified first return time $\widehat{T}(h, -|j|)$ are finite and equal as $h \rightarrow 0^\pm$ and the limit of the rotation angle $\Theta(h, j)$ of the modified period lattice $\widehat{\mathcal{P}}(h, j)$ as $h \rightarrow 0^\pm$ is finite by lemma 4.6.

4.3.4 Going through the critical line with the period lattice

We have defined the modified period lattice $\widehat{\mathcal{P}}(h, j)$ that can, at least formally, go through \mathcal{C} . Let us look at what happens to the period lattice in order to understand why this is not enough.

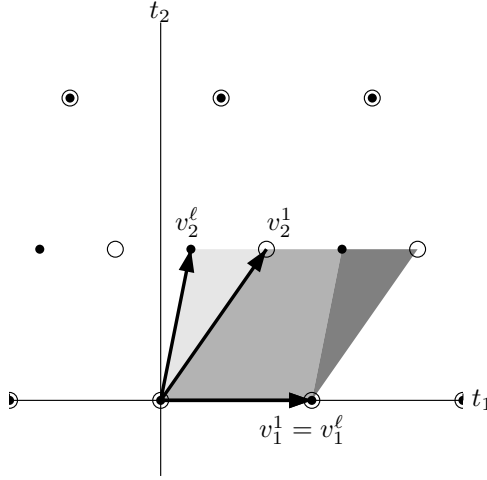


Figure 4.7: Period lattices $\widehat{\mathcal{P}}^1(h_0, j_0)$ (represented by open circles) and $\widehat{\mathcal{P}}^\ell(h_0, j_0)$ (represented by black dots). The common sublattice $\widetilde{\mathcal{P}}^1(h_0, j_0) = \widetilde{\mathcal{P}}^\ell(h_0, j_0)$ represented by black circled dots.

First recall from §4.3 that we introduced a covering of Γ by open sets U^α , $\alpha = 1, \dots, \ell$ and $(h_0, j_0) \in U^1 \cap U^\ell$. The period lattice $\widehat{\mathcal{P}}^1(h_0, j_0)$ is generated by the vectors $v_1^1 = (2\pi, 0)$ and $v_2^1 = (-\Theta^1(h_0, j_0), \widehat{T}^1(h_0, j_0))$. When we follow the path Γ and come back to (h_0, j_0) the rotation number increases by π . Therefore the new lattice (which as we explained before is not a period lattice) is spanned by $v_1^\ell = (2\pi, 0)$ and $v_2^\ell = (-\Theta^1(h_0, j_0) - \pi, \widehat{T}^1(h_0, j_0))$. The two sets of basis vectors do not define the same lattice (see figure 4.7). Their common points form a *sublattice* of both of these lattices. This sublattice, that we denote $\widetilde{\mathcal{P}}^\alpha(h_0, j_0)$ $\alpha = 1, \dots, \ell$, is generated by v_1^α and $2v_2^\alpha$.

When we come back to the starting point (h_0, j_0) of Γ the rotation number increases by π . Therefore, $\widetilde{\mathcal{P}}(h_0, j_0)$ which was initially spanned by $v_1^1 = (2\pi, 0)$ and $2v_2^1 = (-2\Theta(h_0, j_0), 2\widehat{T}(h_0, j_0))$ is now spanned by $v_1^\ell = (2\pi, 0) = v_1$ and $2v_2^\ell = (-2\Theta^1(h_0, j_0) - 2\pi, 2\widehat{T}^1(h_0, j_0)) = 2v_2 - v_1$. Therefore in the basis $(v_1, 2v_2)$ we have $(M^{-1})^\dagger = \begin{pmatrix} 1 & 0 \\ -1 & 1 \end{pmatrix}$, and the monodromy matrix is $M = \begin{pmatrix} 1 & 1 \\ 0 & 1 \end{pmatrix}$.

Consider now the first homology groups $H_1^1(\mathbf{T}_{h_0, j_0}^2, \mathbf{Z})$ and $H_1^\ell(\mathbf{T}_{h_0, j_0}^2, \mathbf{Z})$. A basis for the first are the cycles $[\gamma_1^1] = [t \in [0, 1] : \phi_{Y_1^1}^t(z)]$ and $[\gamma_2^1] = [t \in [0, 1] : \phi_{Y_2^1}^t(z)]$. Here $Y_2^1(z) = -\Theta^1(\mathcal{E}\mathcal{M}(z))X_J(z) + \widehat{T}^1(\mathcal{E}\mathcal{M}(z))\widehat{X}(z)$ where $z \in \mathbf{T}_{h_0, j_0}^2$. Assume that we want to define a basis for the homology group $H_1^\ell(\mathbf{T}_{h_0, j_0}^2, \mathbf{Z})$ in the same way. In that case we should have that $Y_2^\ell(z) = -\Theta^\ell(\mathcal{E}\mathcal{M}(z))X_J(z) + \widehat{T}^\ell(\mathcal{E}\mathcal{M}(z))\widehat{X}(z) = Y_2^1(z) - \pi X_J(z)$. Notice that Y_2^ℓ has primitive period 2. In particular, in time 1 the flow of $Y_2^\ell(z)$ will bring an initial point $z \in \mathbf{T}_{h_0, j_0}^2$ to the point $\varphi_{X_J}^{-\pi}(z)$. This means in particular that $\gamma_2^\ell = (t \in [0, 1] : \phi_{Y_2^\ell}^t(z))$ is not a cycle.

This shows that both at the level of the homology groups and the level of the period lattice the increase of the rotation number by π creates some problems. For the period lattice these problems can be solved by considering instead of the lattice $\widehat{\mathcal{P}}^\alpha$ spanned by v_1^α, v_2^α the sublattice $\widetilde{\mathcal{P}}^\alpha$ spanned by

$v_1^\alpha, 2v_2^\alpha$. In the case of the homology groups we can solve these problems by considering instead of the group H_1^α generated by $[\gamma_1^\alpha] = [t \in [0, 1] : \phi_{Y_1^\alpha}^t(z)]$ and $[\gamma_2^\alpha] = [t \in [0, 1] : \phi_{Y_2^\alpha}^t(z)]$, its subgroup \tilde{H}_1^α generated by $[\tilde{\gamma}_1^\alpha] = [\gamma_1^\alpha]$ and $[\tilde{\gamma}_2^\alpha] = [t \in [0, 2] : \phi_{Y_2^\alpha}^t(z)]$, $\alpha = 1, \dots, \ell$. Notice that when $\Theta^\alpha = \Theta$ we have $[\tilde{\gamma}_2^\alpha] = 2[\gamma_2^\alpha]$, but the last relation does not make sense when $\Theta^\alpha = \Theta + \pi$ because then $[\gamma_2^\alpha]$ is not properly defined.

On each U^α , $\alpha = 1, \dots, \ell$, the isomorphism between $\tilde{P}^\alpha(h, j)$ and $\tilde{H}_1^\alpha(\mathbf{T}_{h,j}^2, \mathbf{Z})$ is

$$n(2\pi, 0) + 2m(-\Theta^\alpha(h, j), \hat{T}^\alpha(h, j)) \mapsto [t \in [0, 1] \mapsto \varphi_{Y_1^\alpha}^{nt} \varphi_{Y_2^\alpha}^{2mt}(z)] = n[\tilde{\gamma}_1^\alpha] + m[\tilde{\gamma}_2^\alpha]$$

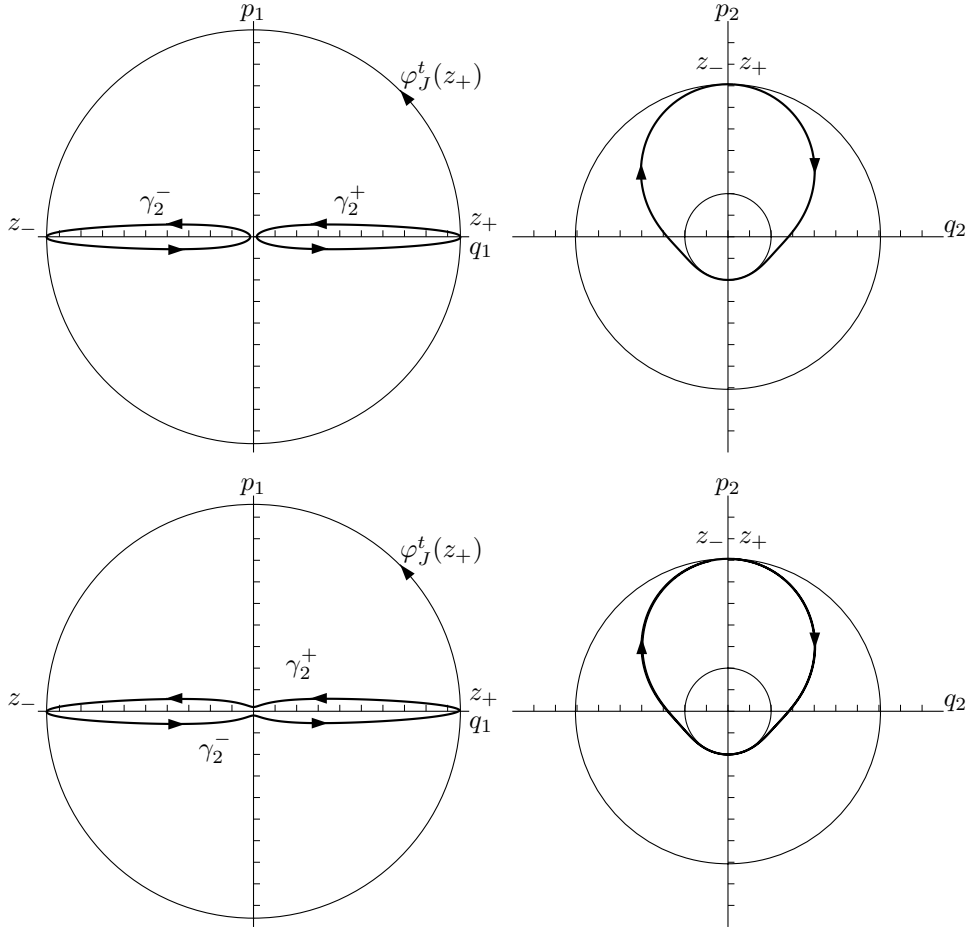


Figure 4.8: Limits of the basis cycles. Projections of the cycles γ_2^+ and γ_2^- for $h > 0$ (upper row) and $h < 0$ (bottom row) to the planes $q_1 - p_1$ and $q_2 - p_2$. The circles represent the projections of X_J orbits.

This isomorphism is valid everywhere, except on \mathcal{C} . As we mentioned before as Γ crosses \mathcal{C} the sublattice $\tilde{P}^\delta(h, j)$ changes continuously. Here, U^δ is by definition the set of the covering U^α , $\alpha = 1, \dots, \ell$ which contains the intersection of Γ with \mathcal{C} . It is possible to imagine that the same does not hold for the basis of $\tilde{H}_1^\delta(\mathbf{T}_{h,j}^2, \mathbf{Z})$. We prove that this is not the case.

For that we consider representatives of the basis elements $[\widehat{\gamma}_2^\delta]$ above and below the critical line and show that they have the same limit as we approach \mathcal{C} from both directions (see figure 4.8). Consider the orbit segments $\gamma_2^\pm = t \in [0, 1] \mapsto \varphi_{Y_2^\delta}^t(z_\pm)$ where z_+ and z_- are defined as the unique points on $\mathbf{T}_{h,j}^2$ with coordinates (q_1, q_2, p_1, p_2) where

$$q_1 = \pm \sqrt{\pi_1^+ + j} \quad q_2 = p_1 = 0 \quad p_2 = -\frac{h - \epsilon((\pi_1^+)^2 - j^2)}{\sqrt{2}(\pi_1^+ + j)}$$

Here π_1^+ is the maximum value that π_1 attains on the reduced orbit $\gamma_{h,j}$. The choice of signs \pm for q_1 corresponds to the two points z_\pm .

Notice that for $h > 0$ we have $\Theta^\delta(h, j) = \Theta(h, j)$. In this case the two orbit segments correspond to two homotopic cycles and their sum is a representative of the class $[\widehat{\gamma}_2^\delta]$.

For $h < 0$ we have $\Theta^\delta(h, j) = \Theta(h, j) + \pi$. In this case, neither γ_2^+ nor γ_2^- are cycles, since as we explained the vector field Y_2^δ becomes periodic with primitive period 2. Nevertheless, we have that $\varphi_{Y_2^\delta}^1(z_\pm) = z_\mp$. Therefore, the ending point of γ_2^+ is the starting point of γ_2^- and vice versa. The result is that the two orbit segments traversed one after the other correspond to the orbit segment $t \in [0, 2] : \phi_{Y_2^\delta}^t(z_+)$ which is a cycle on the torus.

We prove that $\gamma_2 = \gamma_2^+ + \gamma_2^-$ goes through \mathcal{C} continuously. Specifically, for two 1-dimensional sets c_1 and c_2 in \mathbf{R}^4 that are unions of disjoint piecewise smooth curves define their distance $d(c_1, c_2)$ as

$$d(c_1, c_2) = \sup_{z_1 \in c_1} \inf_{z_2 \in c_2} \|z_1 - z_2\| \quad (4.25)$$

Denote $c^a(h)$ the union of γ_2^+ and γ_2^- above the critical line ($h > 0$) and $c^b(h)$ the curve obtained by going first along γ_2^+ and then along γ_2^- below the critical line ($h < 0$). Then we have the following lemma.

Lemma 4.10. *With respect to the distance d we have*

$$\lim_{h \rightarrow 0^+} d(c^a(h), c^0) = \lim_{h \rightarrow 0^-} d(c^b(h), c^0) = 0 \quad (4.26)$$

where c^0 is a curve given in the proof.

Figure 4.8 provides a numerical verification of the lemma.

Proof. Consider the situation for $h = 0$. Notice that $\mathcal{T} = \mathcal{EM}^{-1}(h = 0, j < 0)$ contains the circle $q_2^2 + p_2^2 = -j$, $q_1 = p_1 = 0$ where \widehat{X} and therefore Y_2 are not defined. Let $\phi^t = \varphi_{Y_2^\delta}^t$. The flow ϕ^t brings the point z_+ which for $h = 0$ has coordinates $q_1 = (2j + \epsilon^{-2})^{1/2}$, $p_1 = q_2 = 0$, $p_2 = (\sqrt{2}\epsilon)^{-1}$ to this circle in time $1/2$. This means in particular that Y_2 is not complete.

We study in more detail the dynamics on \mathcal{T} . Consider the orbit of the vector field \widehat{X} with initial point z_+ . Then it is easy to prove that this orbit is given by the parametric equations

$$\begin{aligned} q_1(t) &= \left(2j + \frac{1}{2\epsilon^2}(1 + \cos(4\epsilon t))\right)^{1/2} \\ p_1(t) &= 0 \\ q_2(t) &= \frac{1}{2\sqrt{2}\epsilon} \sin(4\epsilon t) \\ p_2(t) &= \frac{1}{2\sqrt{2}\epsilon}(1 + \cos(4\epsilon t)) \end{aligned}$$

Notice that $q_1(t)$ becomes zero in finite time

$$t_* = \frac{1}{4\epsilon} \cos^{-1}(-1 - 4\epsilon^2 j) = \frac{1}{2} \widehat{T}(0, j) = \frac{1}{2} \lim_{h \rightarrow 0} \widehat{T}(h, j)$$

This proves that the orbit of Y_2 with initial point z_+ reaches $q_1 = p_1 = 0$ at time $1/2$.

Consider the space \mathcal{K} of smooth curves $t \in [0, \frac{1}{2}] \mapsto c(t) \in \mathbf{R}^4$ with the metric

$$d'(c_1, c_2) = \sup_{t \in [0, 1/2]} \|c_1(t) - c_2(t)\| \quad (4.27)$$

We construct the 1-dimensional curve c^0 of the lemma in the following way. Let $g_+ = (t \in [0, \frac{1}{2}] \mapsto \phi^t(z_+))$, $g'_+ = (t \in [0, \frac{1}{2}] \mapsto \phi^{-t}(z_+))$, $g_- = (t \in [0, \frac{1}{2}] \mapsto \phi^t(z_-))$ and $g'_- = (t \in [0, \frac{1}{2}] \mapsto \phi^{-t}(z_-))$ where ϕ^t is the flow of Y_2^δ for $h = 0, j < 0$. Then we define

$$c^0 = g_+ \cup g'_+ \cup g_- \cup g'_-$$

Note that in the last relation we do not assign any orientation to c^0 but we consider it only as a 1-dimensional subset of \mathbf{R}^4 .

Consider now the situation for $h > 0$. Recall that in this case the curve $t \in [0, 1] \mapsto \phi^t(z_+)$ defines a cycle on the torus $\mathbf{T}_{h,j}^2$. Let $f_+(h) = (t \in [0, \frac{1}{2}] \mapsto \phi^t(z_+))$, $f'_+(h) = (t \in [0, \frac{1}{2}] \mapsto \phi^{-t}(z_+))$, $f_-(h) = (t \in [0, \frac{1}{2}] \mapsto \phi^t(z_-))$ and $f'_-(h) = (t \in [0, \frac{1}{2}] \mapsto \phi^{-t}(z_-))$ where ϕ^t is the flow of Y_2^δ for $h > 0$ and z_\pm depend on h . Then $f_+(h) \cup f'_+(h)$ is one cycle on $\mathbf{T}_{h,j}^2$ (taking into account the correct direction of traversal) while $f_-(h) \cup f'_-(h)$ is a second homotopic cycle. Then we have that

$$c^a(h) = f_+(h) \cup f'_+(h) \cup f_-(h) \cup f'_-(h)$$

Since Y_2^δ is smooth, and $z_\pm(h)$ depend smoothly on h for h close to 0 (either positive or negative) we obtain that the curves $f_+(h)$ change continuously with respect to d' and in particular that $\lim_{h \rightarrow 0^+} d'(f_+(h), g_+) = 0$. Notice that we can not extend this result for times greater than $1/2$ because for $h = 0$ the orbit hits $q_1 = p_1 = 0$. The situation is analogous for the other curve segments from which $c^a(h)$ and c^0 . Therefore, we have

$$\lim_{h \rightarrow 0^+} d(c^a(h), c^0) = 0$$

The situation for $h < 0$ is similar. We obtain

$$\lim_{h \rightarrow 0^-} d(c^b(h), c^0) = 0$$

□

4.3.5 Quantum fractional monodromy

We finish the discussion on the fractional monodromy of the 1: - 2 resonance with a brief discussion of the quantum manifestation of this phenomenon. For more details see [72, 73]. In figure 4.9 we show the joint spectrum of the quantum operators that correspond to the classical functions H and J for the 1: - 2 resonance. Consider a single cell (not drawn in figure 4.9) just above

the critical line \mathcal{C} and pass it through \mathcal{C} going downwards. Doing the same with a neighbouring single cell produces a different result. The only way to get consistent results is to consider a *double cell* (dark gray in figure 4.9). Then when we move the double cell around the point $(0, 0)$ we find that the quantum monodromy matrix is $M = \begin{pmatrix} 1 & 1/2 \\ 0 & 1 \end{pmatrix}$. Going formally to a single cell we find the matrix $\begin{pmatrix} 1 & 1/2 \\ 0 & 1 \end{pmatrix}$.

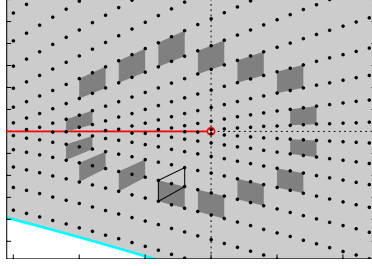


Figure 4.9: Crossing the critical line with a double cell.

4.3.6 Technical proofs

Proof of lemma 4.1

The set Δ of critical values of \mathcal{EM} is the set of $(h, j) \in \mathbf{R}^2$ such that the level set $\{H_j = h\}$ is tangent to the reduced phase space P_j at some point, or goes through the singular point $(0, 0, |j|)$ of P_j for $j \leq 0$. Recall, that for $j > 0$, P_j is smooth at $(0, 0, |j|)$. Eliminating π_3 from (4.7) using $H_j = h$, we obtain

$$\pi_2^2 - Q_{h,j}(\pi_1) = 0 \quad (4.28)$$

where

$$Q_{h,j}(\pi_1) = (\pi_1^2 - j^2)(\pi_1 + j) - (h - \epsilon(\pi_1^2 - j^2))^2, \quad \pi_1 \geq |j| \quad (4.29)$$

We can prove, exactly as we did for the spherical pendula in §3.2.1, that $(h, j) \in \Delta$ if and only if the polynomial $Q_{h,j}(\pi_1)$ has a multiple root in $[|j|, \infty)$. This happens if and only if we can write

$$Q_{h,j}(\pi_1) = -(\pi_1 - s)^2(\epsilon^2\pi_1^2 + u\pi_1 + v), \quad (4.30)$$

for $s \in [j, \infty)$ and $u, v \in \mathbf{R}$. Equating coefficients of the same power of π_1 in (4.29) and (4.30) gives

$$\begin{aligned} u - 2s\epsilon^2 &= -1 \\ v - 2su + s^2\epsilon^2 &= -2\epsilon h - j - 2\epsilon^2 j^2 \\ s^2 u - 2sv &= j^2 \\ s^2 v &= h^2 + j^3 + 2\epsilon h j^2 + \epsilon^2 j^4 \end{aligned} \quad (4.31)$$

Eliminating u and v from equations (4.31) gives

$$2h^2 + 2j^3 + j^2 s + s^3 - 2\epsilon^2 s^4 = 0 \quad (4.32a)$$

$$-4\epsilon s h + (j - s)^2 - 4s^2(1 - s\epsilon^2) = 0 \quad (4.32b)$$

We now show how to parametrize the solution set of (4.32). If $s = 0$ then $j = h = 0$. Suppose $s \neq 0$. Then from (4.32b) we get

$$h = \frac{1}{4\epsilon s}(j+s)(j-3s-4\epsilon^2 s(j-s)) \quad (4.33)$$

Using (4.33) to eliminate h from (4.32a) we find

$$(j+s)^2((j-3s)^2 + 16\epsilon^2 s^2(j-s)) = 0 \quad (4.34)$$

where $s \geq |j|$. We have three cases depending on the discriminant $\delta = 128\epsilon^2 s^3(2\epsilon^2 s - 1)$ of the quadratic factor in (4.34).

CASE 1. When $0 < s < \frac{1}{2\epsilon^2}$ we have $\delta < 0$. In this case (4.34) has only one real linear factor. Hence $j = -s$. From (4.33) we find that $h = 0$. This gives the critical curve \mathcal{C}_1 .

CASE 2. When $s = \frac{1}{2\epsilon^2}$, equation (4.34) becomes $(j + \frac{1}{2\epsilon^2})^4 = 0$ that is, $j = -\frac{1}{2\epsilon^2}$. From equation (4.33), we obtain $h = 0$. This gives the point P where \mathcal{C}_2 joins \mathcal{C}_1 .

CASE 3. When $s > \frac{1}{2\epsilon^2}$, we have $\delta > 0$. In this case (4.34) has three real linear factors which give rise to three real solution branches of (4.32); namely

$$\begin{aligned} j &= -s \\ h &= 0 \end{aligned} \quad (4.35)$$

or

$$\begin{aligned} j &= s(3 - 8\epsilon^2 s + 4\epsilon\sqrt{2s(2\epsilon^2 s - 1)}) \\ h &= 4s(2\epsilon^2 s - 1)(\sqrt{2}(8\epsilon^2 s - 1)\sqrt{s(2\epsilon^2 s - 1)} - 2\epsilon s(8\epsilon^2 s - 3)) \end{aligned} \quad (4.36)$$

or

$$j = s(3 - 8\epsilon^2 s - 4\epsilon\sqrt{2s(2\epsilon^2 s - 1)}) \quad (4.37a)$$

$$h = 4s(2\epsilon^2 s - 1)(-\sqrt{2}(8\epsilon^2 s - 1)\sqrt{s(2\epsilon^2 s - 1)} - 2\epsilon s(8\epsilon^2 s - 3)) \quad (4.37b)$$

From (4.37a) and using that $s > \frac{1}{2\epsilon^2}$ we obtain that $|j| > s$. Therefore (4.37) must be excluded.

Proof of lemma 4.6

Fix $\epsilon > 0$ and choose $j < 0$ so that $\epsilon|2j|^{1/2} < 1$. Let $u = \pi_1 + j$. Then (4.21) becomes

$$\Theta(h, j) = h \int_{u_-}^{u_+} \frac{1}{u} \frac{du}{\sqrt{Q_{h,j}(u)}}, \quad (4.38)$$

where $u_{\pm} = \pi_1^{\pm} + j$. Notice that since $\pi_1 \geq |j| = -j$, we have $u \geq 0$.

We first express the roots u_{\pm} of $Q_{h,j}(u)$ as a power series in h around $h = 0$. For $h < 0$ we obtain

$$u_- = \frac{h}{|2j|^{1/2}(\epsilon|2j|^{1/2} - 1)} + O(h^2) = \alpha_- h + O(h^2) \quad (4.39)$$

while for $h > 0$ we get

$$u_- = \frac{h}{|2j|^{1/2}(\epsilon|2j|^{1/2} + 1)} + O(h^2) = \alpha_+ h + O(h^2). \quad (4.40)$$

In both cases

$$u_+ = \frac{1 - 2\epsilon^2|j|}{\epsilon^2} + O(h). \quad (4.41)$$

First we consider the case $h > 0$. Set $u = hv$. Then

$$\Theta(h, j) = \int_{u_-/h}^{u_+/h} \frac{dv}{v\sqrt{S_{h,j}(v)}}, \quad (4.42)$$

where

$$\begin{aligned} S_{h,j}(v) &= Q_{h,j}(hv)/h^2 \\ &= -\epsilon^2 h^2 v^4 + (1 + 4\epsilon^2 j)h^3 v^3 + (-2j - 4\epsilon^2 j^2 + 2\epsilon h)v^2 - 4\epsilon jv - 1 \end{aligned} \quad (4.43)$$

Taking the limit as h approaches the critical curve $\mathcal{C} : h = 0, j \in (-1/(2\epsilon^2), 0)$ from above we find that

$$\lim_{h \rightarrow 0^+} \Theta(h, j) = \int_{\alpha_+}^{\infty} \frac{dv}{v\sqrt{S_{0,j}(v)}}$$

Substituting $v = 1/z$ gives

$$\lim_{h \rightarrow 0^+} \Theta(h, j) = \int_0^{\alpha_+} \frac{dz}{\sqrt{-z^2 - 4\epsilon jz - 4j^2\epsilon^2 - 2j}} = \int_0^{\alpha_+} \frac{dz}{\sqrt{2|j| - (z - 2\epsilon|j|)^2}}$$

Hence

$$\lim_{h \rightarrow 0^+} \Theta(h, j) = \frac{\pi}{2} + \sin^{-1}(\epsilon\sqrt{2|j|}) \quad (4.44)$$

When $h < 0$, we follow the same procedure keeping track of all the minus signs. The result is

$$\lim_{h \rightarrow 0^-} \Theta(h, j) = -\frac{\pi}{2} + \sin^{-1}(\epsilon\sqrt{2|j|}) \quad (4.45)$$

This proves the lemma.

Proof of lemma 4.8

We now compute the *modified first return time* $\widehat{T}(h, j)$ of the vector field $\widehat{X}|\mathbf{T}_{h,j}^2$. Since $\widehat{X}|\mathbf{T}_{h,j}^2$ is invariant under the flow of X_J , it induces a vector field \widehat{X}_j on the reduced space P_j . Using (4.9), we see that the integral curves of \widehat{X}_j satisfy

$$\begin{aligned} \frac{d\pi_1}{ds} &= \frac{dt}{ds} \frac{d\pi_1}{dt} = \frac{1}{\pi_1 + j} \frac{d\pi_1}{dt} = \frac{4\pi_2}{\pi_1 + j} \\ \frac{d\pi_2}{ds} &= \frac{1}{\pi_1 + j} \frac{d\pi_2}{dt} = 2(3\pi_1 - j) + \frac{8\epsilon\pi_1\pi_2}{\pi_1 + j} \\ \frac{d\pi_3}{ds} &= \frac{1}{\pi_1 + j} \frac{d\pi_3}{dt} = -\frac{8\epsilon\pi_1\pi_2}{\pi_1 + j}. \end{aligned}$$

Hence the period $\widehat{T}(h, j)$ of \widehat{X}_j on $H_j^{-1}(h)$, which is the first return time of $\widehat{X}|_{\mathbf{T}_{h,j}^2}$, is

$$\begin{aligned}\widehat{T}(h, j) &= \int_0^{\widehat{T}(h, j)} ds = 2 \int_{\pi_1^-}^{\pi_1^+} \frac{d\pi_1}{\frac{d\pi_1}{ds}} = \frac{1}{2} \int_{\pi_1^-}^{\pi_1^+} (\pi_1 + j) \frac{d\pi_1}{\pi_2} \\ &= \frac{1}{2} \int_{\pi_1^-}^{\pi_1^+} \frac{(\pi_1 + j) d\pi_1}{\sqrt{Q_{h,j}(\pi_1)}}.\end{aligned}$$

For $|h|$ sufficiently small, the polynomial $Q_{h,j}$ has four distinct real roots, two of which are strictly greater than $|j|$ when $j < 0$. Using the new variable $u = \pi_1 + j$ we can write $Q_{h,j}$ as

$$\begin{aligned}Q_{h,j}(u) &= -\epsilon^2 u^4 + (1 - 4\epsilon^2 |j|)u^3 + (2|j| - 4\epsilon^2 j^2 + 2\epsilon h)u^2 + 4\epsilon |j| h u - h^2 \\ &= -\epsilon^2 \prod_{i=1}^4 (u - u_i).\end{aligned}$$

Here $u^- = u_3$ and $u^+ = u_4$ are strictly positive. Hence

$$\widehat{T}(h, j) = \int_{u^-}^{u^+} \frac{u du}{\sqrt{-\epsilon^2 \prod_{i=1}^4 (u - u_i)}} = \int_{u^-}^{u^+} \omega.$$

We note that ω is a differential form of the second kind on the complex affine elliptic curve $E : v^2 = -\epsilon^2 \prod_{i=1}^4 (u - u_i)$. The 1-form ω is holomorphic on E with a double pole at ∞ , see [84, p.296–297]. Because the roots of $Q_{h,j}(u)$ are distinct, when $h = 0$ and $j < 0$, it follows that as functions of (h, j) the roots $u_i(h, j)$ are holomorphic in \mathcal{N} , which is a product of a complex neighborhood where $|h|$ is sufficiently small and a complex strip neighborhood of the nonpositive real axis. Thus the differential form ω is holomorphic as a function of $(h, j) \in \mathcal{N}$. Let Λ be a loop in the complex plane, which encircles the roots u^\pm for all $(h, j) \in \mathcal{N}$. Then $\widehat{T}(h, j) = \int_\Lambda \omega$ is a holomorphic function of $(h, j) \in \mathcal{N}$.

4.4 Fractional monodromy in other resonances

I have not studied yet any other resonances $m : -n$. Nevertheless, I would like to mention that Zhilinskiĭ¹ through the study of fractional monodromy as a lattice defect (see [96]) has suggested the following conjectures

Conjecture 4.11. *The formal monodromy matrix in a $1 : -n$ resonance system, where $n \geq 2$, is*

$$M_{1:-n} = \begin{pmatrix} 1 & \frac{1}{n} \\ 0 & 1 \end{pmatrix}$$

Conjecture 4.12. *The formal monodromy matrix in a $m : -n$ resonance system, where $m, n \geq 2$ and relatively prime, is*

$$M_{m:-n} = \begin{pmatrix} 1 & \frac{1}{m} + \frac{1}{n} \\ 0 & 1 \end{pmatrix}$$

¹Private communication

Here the precise meaning of the formal monodromy matrix is that we should consider a sublattice of the period lattice (or equivalently a subgroup of the homology group) generated by v_1 and mnv_2 . Then in this basis the monodromy matrix is

$$M_{m:-n} = \begin{pmatrix} 1 & m+n \\ 0 & 1 \end{pmatrix}$$

5

Conclusions

We collect here the results that we obtained for each system that we studied in this work and some questions and possible future lines of research.

5.1 Triply degenerate vibrational mode of tetrahedral molecules

The main objective for the triply degenerate vibrational modes of tetrahedral molecules was the classification of generic members of the Hamiltonian family (0.9) in terms of their nonlinear normal modes. Recall that (0.9) is $T_d \times \mathcal{T}$ invariant. In chapter 1 we obtained all the nonlinear normal modes based on the study of the fourth order normal form approximation of the Hamiltonian (0.9).

Considering only the number of relative equilibria we discovered that generically there are two qualitatively different forms of (0.9), one with 27 RE, which is the minimum number compatible with the $T_d \times \mathcal{T}$ symmetry, and one with 39 RE. If we consider also the classification in terms of the types of linear stability of these RE we find that the parameter space is made up from 5 different regions, which are given in table 1.2 and are shown in figure 1.2.

Many of these results were obtained using only symmetry arguments, that is, the action of $T_d \times \mathcal{T}$ on \mathbf{CP}^2 and therefore they apply to any $T_d \times \mathcal{T}$ invariant Hamiltonian on \mathbf{CP}^2 . On the other hand the exact type of linear stability of these RE and the proof that we found all of them were based on the specific study of the family (0.9).

Questions

1. The bifurcations of the relative equilibria of type B_3 from EE to CH in the original Hamiltonian (0.9) probably corresponds to a Hamiltonian Hopf bifurcation. This can probably be proven if we consider a higher order normal form of (0.9).
2. The relative equilibria A_4 and A_3 change linear stability type from 2E to 2H. As we saw in chapter 3 this situation may correspond to a generalized Hamiltonian Hopf bifurcation. Again we need a higher order normal form in order to study these bifurcations.

3. It would be interesting to have a description of the dynamics for the non-integrable normalized system. Based on such a description we could later study diffusion phenomena in the original 3-DOF system.

5.2 The hydrogen atom in crossed fields

The main objective for the hydrogen atom in crossed fields was to prove that the system goes through two Hamiltonian Hopf bifurcations as we tune it from the Stark to the Zeeman limit. We used second normalization to bring the system to an integrable form on $\mathbf{S}^2 \times \mathbf{S}^2$ and we proved the existence of these bifurcations using standard techniques. Finally, we explained how the Hamiltonian Hopf bifurcations are represented in the image of the energy-momentum map and the second reduced phase space and we related these bifurcations to standard and non-local monodromy.

Questions

1. Very close to the value of the parameter for which we have the subcritical Hamiltonian Hopf bifurcation there is a second bifurcation that we did not describe. A complete study of the system should include this bifurcation.
2. Is there a way to observe the manifestation of the Hamiltonian Hopf bifurcations in the experimentally observed spectrum of the hydrogen atom in crossed fields?
3. The two normalizations that we used gave a completely integrable system. Nevertheless, the original Hamiltonian is non-integrable. Is it interesting to study the effects of this non-integrability to the global dynamics of the system.

5.3 Quadratic spherical pendula

The objective for the family of quadratic spherical pendula was the study of the generalized Hamiltonian Hopf bifurcation that appear and their relation to monodromy. In chapter 3 we classified the quadratic spherical pendula in terms of the qualitative features of the image of the energy-momentum map. Specifically, we found three different types, that we called type O, I, and II. The energy-momentum map for type O and II systems has respectively one and two isolated critical values. The image of the energy-momentum map for type I systems consists of two leaves.

We studied monodromy in each case and especially for type I systems which have non-local monodromy. We proved that as the type of the system changes from O to II or I the system goes through a generalized Hamiltonian Hopf bifurcation.

Questions

1. Can we define monodromy in type I systems for paths that cross the curve of critical values?

2. How does the image of the energy-momentum map change for higher order potentials (cubic, quartic, etc.)? How does monodromy change and what kinds of bifurcations happen?

5.4 Fractional monodromy

The objective here was to give an analytic proof, based on the notion of the period lattice, of the result of [72, 73] according to which the $1: -2$ resonance system has fractional monodromy. This was done in chapter 4.

Questions

1. What is the situation for higher order resonances? Are the conjectures of §4.4 true?
2. Are there other methods to prove fractional monodromy?
3. Can we find analogues of fractional monodromy in other areas of mathematics, eg. complex analysis?

A

The tetrahedral group

A.1 Action of the group $T_d \times T$ on the spaces \mathbf{R}^3 and $T^*\mathbf{R}^3$

The symmetry group $T_d \subset O(3)$ of the tetrahedron is a group of point transformations of the physical 3-space, see figure A.1. As an abstract group it is isomorphic to the permutation group of 4 elements. We assume that the coordinate functions (x, y, z) in the configuration space \mathbf{R}^3 of (1.1) span a three dimensional *vector* representation of T_d , that is, T_d acts on (x, y, z) as on the coordinates in the physical 3-space. Let O be the origin $(0, 0, 0) \in \mathbf{R}^3$, and

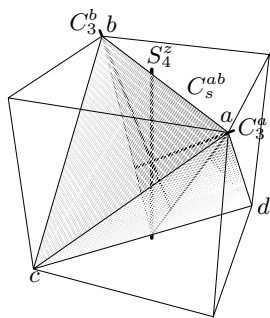


Figure A.1: Symmetry axes and planes of a tetrahedron

let Ox , Oy and Oz be the directed semi-axes of the coordinate system in \mathbf{R}^3 . Consider also the 4 directed semi-axes Oa , Ob , Oc and Od in figure A.1, where $a = (1, 1, 1)$, $b = (-1, -1, 1)$, $c = (1, -1, -1)$ and $d = (-1, 1, -1)$. Any pair of semi-axes $(O\alpha, O\beta)$ defines a 2-plane $\alpha O\beta$ passing through O . Table A.1 gives explicit definition of some basic operations in T_d which we further explain below.

S_4 Operation S_4^x combines the counterclockwise rotation by $2\pi/4 = \frac{1}{2}\pi$ about Ox and the reflection in the plane $yOz \perp Ox$. Similar operations S_4^y and S_4^z involve axes Oy and Oz respectively. The conjugacy class S_4 in

T_d also contains the elements $(S_4^\alpha)^{-1}$, $\alpha = x, y, z$; elements $C_2^\alpha = (S_4^\alpha)^2$ form the conjugacy class C_2 .

C_3 Operations C_3^a , C_3^b , C_3^c and C_3^d are counterclockwise rotations by $2\pi/3$ about axes Oa , Ob , Oc and Od respectively. The conjugacy class C_3 also includes $(C_3^a)^2$, $(C_3^b)^2$, $(C_3^c)^2$ and $(C_3^d)^2$.

C_s Reflection in each of the six planes $\{aOb, cOd, aOd, bOc, aOc, bOd\}$, which we denote as C_s^{ab} , C_s^{cd} , C_s^{ad} , C_s^{bc} , C_s^{ac} and C_s^{bd} , leaves the tetrahedron invariant. These operations form the conjugacy class C_s .

R	Rx	Ry	Rz	R	Rx	Ry	Rz	R	Rx	Ry	Rz
S_4^x	$-x$	$-z$	y	C_3^a	z	x	y	C_s^{ab}	y	x	z
S_4^y	z	$-y$	$-x$	C_3^b	$-z$	x	$-y$	C_s^{cd}	$-y$	$-x$	z
S_4^z	$-y$	x	$-z$	C_3^c	$-z$	$-x$	y	C_s^{ad}	z	y	x
				C_3^d	z	$-x$	$-y$	C_s^{bc}	$-z$	y	$-x$
								C_s^{ac}	x	z	y
								C_s^{bd}	x	$-z$	$-y$

Table A.1: The action of some elements of T_d on the representation spanned by x, y, z .

The extension of the T_d action described above to the phase space $T^*\mathbf{R}^3$ of (1.1) uses the following lemma.

Lemma A.1. *If the matrices M_q and M_p in $GL(\mathbf{R}, 3)$ acting on the coordinates $q = (x, y, z)$ and the conjugate momenta $p = (p_x, p_y, p_z)$ respectively define a linear symplectic transformation in $T^*\mathbf{R}^3$, then $M_p = (M_q^{-1})^T$.*

It follows that $M_q = M_p$ for $M_q \in T_d \subset O(3)$, that is, (x, y, z) and (p_x, p_y, p_z) transform according to the *same* representation of T_d . The action of the full symmetry group $T_d \times \mathcal{T}$ on $T^*\mathbf{R}^3$ is obtained by combining the action of T_d and the momentum reversal $T : (q, p) \rightarrow (q, -p)$.

A.2 Fixed points of the action of $T_d \times \mathcal{T}$ on \mathbf{CP}^2

The projection of the $T_d \times \mathcal{T}$ action on \mathbf{CP}^2 has been discussed in detail in [79, 95] and [1, 2]. We give only the information that is useful for our study. The action of $T_d \times \mathcal{T}$ on the invariants (1.5) can be found straightforwardly using the action of $T_d \times \mathcal{T}$ on $T^*\mathbf{R}^3$. Table A.2 gives the results. Zhilinskii described the critical orbits of the T_d action on \mathbf{CP}^2 in [95]. The action of the full group $T_d \times \mathcal{T}$ has the same 5 critical orbits [1, 2] which we characterize in tables 1.1 and A.3. Observe that points of types A and B transform differently with respect to T : A_4 , A_3 , and A_2 are T -invariant, while B_4 and B_3 are not, because T maps each B -type point to another, for example $B_4^z \rightarrow B_4^{\bar{z}}$.

R	$R\nu_1$	$R\nu_2$	$R\nu_3$	$R\sigma_1$	$R\sigma_2$	$R\sigma_3$	$R\tau_1$	$R\tau_2$	$R\tau_3$
C_2^x	ν_1	ν_2	ν_3	σ_1	$-\sigma_2$	$-\sigma_3$	τ_1	$-\tau_2$	$-\tau_3$
S_4^x	ν_1	ν_3	ν_2	$-\sigma_1$	$-\sigma_3$	σ_2	τ_1	τ_3	$-\tau_2$
C_3^a	ν_3	ν_1	ν_2	σ_3	σ_1	σ_2	τ_3	τ_1	τ_2
C_s^{ab}	ν_2	ν_1	ν_3	σ_2	σ_1	σ_3	$-\tau_2$	$-\tau_1$	$-\tau_3$
T	ν_1	ν_2	ν_3	σ_1	σ_2	σ_3	$-\tau_1$	$-\tau_2$	$-\tau_3$

Table A.2: Action of some elements of $T_d \times \mathcal{T}$ on \mathbf{CP}^2

A.3 Subspaces of \mathbf{CP}^2 invariant under the action of $T_d \times \mathcal{T}$

The action of $T_d \times \mathcal{T}$ on \mathbf{CP}^2 has a number of invariant subspaces M of topology \mathbf{RP}^2 , $\mathbf{CP}^1 \sim \mathbf{S}^2$, and \mathbf{S}^1 [2]. The points of M are non-isolated fixed points of the action of the stabilizer $G_M \subset T_d \times \mathcal{T}$ of M . The invariant manifolds of points with stabilizers \mathcal{C}_2 and \mathcal{C}_s are 2-spheres \mathbf{S}^2 which are symplectic. Moreover these spheres remain invariant under the flow of any $T_d \times \mathcal{T}$ -invariant Hamiltonian \hat{H} . According to [95], the 27 critical points and the spheres intersect in \mathbf{CP}^2 as shown in figure A.2. We discuss these spheres in more detail.

Consider specifically the action of $\mathcal{C}_2^x \subset T_d$ on $\mathbf{CP}^2(n)$. Using table A.2 we find that fixed points of this action are of the form $(\nu_1, \nu_2, \nu_3; \sigma_1, 0, 0; \tau_1, 0, 0)$. Taking the relations (1.6) into account we find that the subset of $\mathbf{CP}^2(n)$ with stabilizer \mathcal{C}_2^x is the disjoint union of A_2^x and the \mathbf{S}^2 sphere $(0, \nu_2, n - \nu_2; \sigma_1, 0, 0; \tau_1, 0, 0)$ with $\sigma_1^2 + \tau_1^2 + (2\nu_2 - n)^2 = n^2$. In the coordinates $u = \sigma_1 n^{-1}$, $v = \tau_1 n^{-1}$ and $w = 2\nu_2 n^{-1} - 1$, its equation is $u^2 + v^2 + w^2 = 1$. There are three \mathcal{C}_2 spheres corresponding to the three axes \mathcal{C}_2 . On each sphere we find six critical points, two of type A_4 , two of type A_2 and two of type B_4 . Specifically, on the \mathcal{C}_2^x sphere we find the points $A_4^y, A_4^z, A_2^x, A_2^{\bar{x}}, B_4^x$, and $B_4^{\bar{x}}$ (figure A.3a).

The same analysis for the action of $\mathcal{C}_s^{ab} \subset T_d$ shows that the set of $\mathbf{CP}^2(n)$ points fixed under this action is the disjoint union of A_2^z and the \mathbf{S}^2 sphere $(\nu_1, \nu_1, n - 2\nu_1; \sigma_1, \sigma_1, 2\nu_1; \tau_1, -\tau_1, 0)$ with $2\sigma_1^2 + 2\tau_1^2 + (4\nu_1 - n)^2 = n^2$ and coordinates $u = \sqrt{2}\sigma_1 n^{-1}$, $v = \sqrt{2}\tau_1 n^{-1}$ and $w = 4\nu_1 n^{-1} - 1$. There are six such spheres, one for each \mathcal{C}_s plane. On each \mathcal{C}_s sphere we find four critical points, one of type A_4 , one of type A_2 , and two of type A_3 . Specifically, on the \mathcal{C}_s^{ab} sphere we find the points A_2^z, A_4^z, A_3^a , and A_3^b (figure A.3b).

The action of the group $T_d \times \mathcal{T}$ on each \mathcal{C}_s sphere is reduced to the action of a $C_{2v} = \mathbf{Z}_2 \times \mathbf{Z}_2$ group generated by the transformations $u \rightarrow -u$ and $v \rightarrow -v$. The orbit space of this action is defined by the invariants $U = u^2$, $V = v^2$ and w subject to the relations $U + V + w^2 = 1$, $U > 0$ and $V > 0$. Because of the relation between the invariants we can use only two of them to describe the orbit space. We choose U and w . The orbit space is depicted in figure A.3(c).

Point	Isotropy	
A_4^x	$D_{2d}^x \times \mathcal{T}$	$\{1, S_4^x, C_2^x, (S_4^x)^{-1}, C_2^y, C_2^z, C_s^{ac}, C_s^{bd}\} \times \mathcal{T}$
A_4^y	$D_{2d}^y \times \mathcal{T}$	$\{1, S_4^y, C_2^y, (S_4^y)^{-1}, C_2^x, C_2^z, C_s^{ad}, C_s^{bc}\} \times \mathcal{T}$
A_4^z	$D_{2d}^z \times \mathcal{T}$	$\{1, S_4^z, C_2^z, (S_4^z)^{-1}, C_2^x, C_2^y, C_s^{ab}, C_s^{cd}\} \times \mathcal{T}$
A_3^a	$C_{3v}^a \times \mathcal{T}$	$\{1, C_3^a, (C_3^a)^2, C_s^{ab}, C_s^{ac}, C_s^{ad}\} \times \mathcal{T}$
A_3^b	$C_{3v}^b \times \mathcal{T}$	$\{1, C_3^b, (C_3^b)^2, C_s^{ab}, C_s^{bc}, C_s^{bd}\} \times \mathcal{T}$
A_3^c	$C_{3v}^c \times \mathcal{T}$	$\{1, C_3^c, (C_3^c)^2, C_s^{ac}, C_s^{bc}, C_s^{cd}\} \times \mathcal{T}$
A_3^d	$C_{3v}^d \times \mathcal{T}$	$\{1, C_3^d, (C_3^d)^2, C_s^{ad}, C_s^{bc}, C_s^{cd}\} \times \mathcal{T}$
A_2^x	$C_{2v}^x \times \mathcal{T}$	$\{1, C_2^x, C_s^{ac}, C_s^{bd}\} \times \mathcal{T}$
$A_2^{\bar{x}}$	$C_{2v}^x \times \mathcal{T}$	$\{1, C_2^x, C_s^{ac}, C_s^{bd}\} \times \mathcal{T}$
A_2^y	$C_{2v}^y \times \mathcal{T}$	$\{1, C_2^y, C_s^{ad}, C_s^{bc}\} \times \mathcal{T}$
$A_2^{\bar{y}}$	$C_{2v}^y \times \mathcal{T}$	$\{1, C_2^y, C_s^{ad}, C_s^{bc}\} \times \mathcal{T}$
A_2^z	$C_{2v}^z \times \mathcal{T}$	$\{1, C_2^z, C_s^{ab}, C_s^{cd}\} \times \mathcal{T}$
$A_2^{\bar{z}}$	$C_{2v}^z \times \mathcal{T}$	$\{1, C_2^z, C_s^{ab}, C_s^{cd}\} \times \mathcal{T}$
B_4^x	$S_4^x \wedge T_2^y$	$\{1, S_4^x, C_2^x, (S_4^x)^{-1}, C_2^y T, C_2^z T, C_s^{ac} T, C_s^{bd} T\}$
$B_4^{\bar{x}}$	$S_4^x \wedge T_2^y$	$\{1, S_4^x, C_2^x, (S_4^x)^{-1}, C_2^y T, C_2^z T, C_s^{ac} T, C_s^{bd} T\}$
B_4^y	$S_4^y \wedge T_2^z$	$\{1, S_4^y, C_2^y, (S_4^y)^{-1}, C_2^x T, C_2^z T, C_s^{ad} T, C_s^{bc} T\}$
$B_4^{\bar{y}}$	$S_4^y \wedge T_2^z$	$\{1, S_4^y, C_2^y, (S_4^y)^{-1}, C_2^x T, C_2^z T, C_s^{ad} T, C_s^{bc} T\}$
B_4^z	$S_4^z \wedge T_2^x$	$\{1, S_4^z, C_2^z, (S_4^z)^{-1}, C_2^x T, C_2^y T, C_s^{ab} T, C_s^{cd} T\}$
$B_4^{\bar{z}}$	$S_4^z \wedge T_2^x$	$\{1, S_4^z, C_2^z, (S_4^z)^{-1}, C_2^x T, C_2^y T, C_s^{ab} T, C_s^{cd} T\}$
B_3^a	$C_3^a \wedge T_s^{ab}$	$\{1, C_3^a, (C_3^a)^2, C_s^{ab} T, C_s^{ac} T, C_s^{ad} T\}$
$B_3^{\bar{a}}$	$C_3^a \wedge T_s^{ab}$	$\{1, C_3^a, (C_3^a)^2, C_s^{ab} T, C_s^{ac} T, C_s^{ad} T\}$
B_3^b	$C_3^b \wedge T_s^{ab}$	$\{1, C_3^b, (C_3^b)^2, C_s^{ab} T, C_s^{bc} T, C_s^{bd} T\}$
$B_3^{\bar{b}}$	$C_3^b \wedge T_s^{ab}$	$\{1, C_3^b, (C_3^b)^2, C_s^{ab} T, C_s^{bc} T, C_s^{bd} T\}$
B_3^c	$C_3^c \wedge T_s^{cd}$	$\{1, C_3^c, (C_3^c)^2, C_s^{ac} T, C_s^{bc} T, C_s^{cd} T\}$
$B_3^{\bar{c}}$	$C_3^c \wedge T_s^{cd}$	$\{1, C_3^c, (C_3^c)^2, C_s^{ac} T, C_s^{bc} T, C_s^{cd} T\}$
B_3^d	$C_3^d \wedge T_s^{cd}$	$\{1, C_3^d, (C_3^d)^2, C_s^{ad} T, C_s^{bc} T, C_s^{cd} T\}$
$B_3^{\bar{d}}$	$C_3^d \wedge T_s^{cd}$	$\{1, C_3^d, (C_3^d)^2, C_s^{ad} T, C_s^{bc} T, C_s^{cd} T\}$

Table A.3: Critical points of the $T_d \times \mathcal{T}$ action on \mathbf{CP}_n^2 . In the second column $\mathcal{T}_2 = \{1, C_2 T\}$ and $\mathcal{T}_s = \{1, C_s T\}$.

A.4 Action of $T_d \times \mathcal{T}$ on the projections of nonlinear normal modes in the configuration space \mathbf{R}^3

Like in the 2D Hénon-Heiles system, it is quite convenient to represent the nonlinear normal modes of the 3D system with Hamiltonian (1.1) by their projections in the configuration space $\mathbf{R}_{x,y,z}^3$ shown in figure 1.1. The qualitative “shape” of each projection can be derived from the symmetry properties (isotropy group) of the mode using a set of simple principles which we formulate below as lemmas.

Lemma A.2. *Projections $\Gamma \subset \mathbf{R}_{x,y,z}^3$ of periodic orbits of the system with Hamiltonian H in (1.1) can be of two types: (i) closed curves; (ii) curved line segments (degenerate closed curves).*

Lemma A.3. *The action of an element $g \in T_d$ on the projection Γ is found*

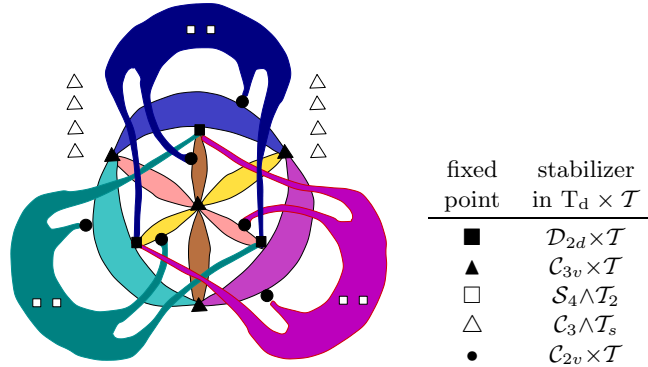


Figure A.2: Orbits of the T_d and $T_d \times T$ group action on \mathbf{CP}^2 according to [95]. Colored areas represent the three C_2 -invariant and the six C_s -invariant spheres.

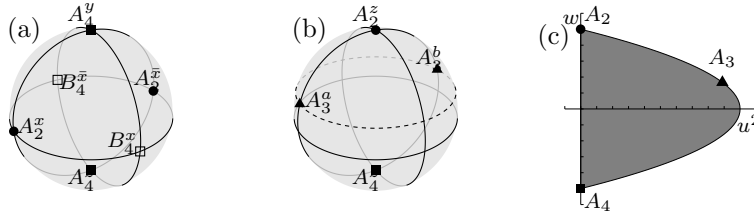


Figure A.3: The C_2^x invariant sphere (a) and the C_s^{ab} invariant sphere (b) in the ambient space \mathbf{R}^3 with coordinates (u, v, w) adapted for each case (see text). Solid lines represent the intersections of the spheres with the planes $\{u = 0\}$, $\{v = 0\}$ and $\{w = 0\}$. In (b) the dashed line represents the intersection of the sphere with the plane $\{w = 1/3\}$. (c) Orbit space of the $C_{2v} = \mathbf{Z}_2 \times \mathbf{Z}_2$ action on the C_s sphere which is used as a chart in figure 1.3.

straightforwardly from the action of g on each point $m \in \Gamma \subset \mathbf{R}^3$.

Lemma A.4. *In order to study the action of the time reversal operation T on the closed curve projections Γ , we should consider the latter as directed closed curves, or loops. The two periodic orbits which project into the same closed curve Γ correspond to two loops Γ_+ and Γ_- with different directions. The T operation changes direction, i.e., $T : \Gamma_+ \leftrightarrow \Gamma_-$. A segment projection represents one T -invariant periodic orbit.*

Lemma A.5. *Let Γ be an image of a periodic orbit defined according to lemma A.4, and $G \subset T_d \times T$ be its isotropy group. Then each operation $g \in G$ maps Γ into itself as a whole, but points $m \in \Gamma$ are not necessarily fixed points of g . On the other hand, if $g \notin G$ (but $g \in T_d \times T$) then g defines a 1:1 map $\Gamma \rightarrow \Gamma'$ where Γ' is an image of another periodic orbit in the same group orbit.*

It follows from lemma A.4 that the T -invariant modes A_4 , A_3 , and A_2 project into segments (degenerate loops). Furthermore, the action of the D_{2d} stabilizers on \mathbf{R}^3 is such that the A_4 modes must project onto the symmetry axes (Ox, Oy, Oz), e.g., A_4^z is represented by a segment of axis Oz (see figs. 1.1

and A.1). Similarly, the A_3 modes project onto the C_3 axes (Oa, Ob, Oc, Od). The spatial isotropy group of the A_2 modes is the group C_{2v} , whose C_2 axis is one of the (Ox, Oy, Oz). These modes project into curved line segments lying in the symmetry planes of the C_{2v} group. For example, the images of the periodic orbits A_2^z and $A_2^{\bar{z}}$ lie in the planes aOb (the plane $x = y$) and cOd (the plane $x = -y$) respectively near the intersections of these planes with the horizontal plane xOy . The images do not intersect: A_2^z passes above the xOy plane while $A_2^{\bar{z}}$ lies below it, see figure 1.1.

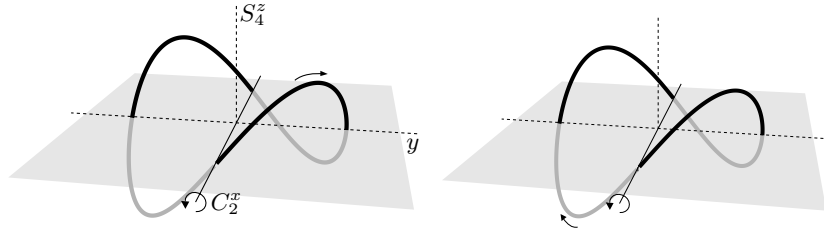


Figure A.4: Two B_4^z nonlinear normal modes related by the T and C_2 operations. Compared to figure 1.1 the z axis (vertical) scale is zoomed.

On the other hand, the modes B_3 and B_4 are not T -invariant. They project into closed curves in figure 1.1. According to lemma A.4, each such closed curve accommodates two orbits. As an instructive example, consider the two B_4^z modes in figure A.4. In accordance with the spatial symmetry of these orbits S_4^z , their projection resembles a wobbled square whose two pairs of opposing smoothed vertexes are lifted and lowered out of the plane xOy . It is easy to see from figure A.4 that both operations C_2^x and T preserve this projection geometrically but change the direction of the mode, so that $B_{4+}^z \leftrightarrow B_{4-}^z$. At the same time, the modes are invariant with regard to the combination $T_2 = C_2 \circ T$ where $C_2 = C_2^x$ or C_2^y .

B

Local properties of equilibria

B.1 Stability of equilibria

In order to determine the possible types of linear stability of the fixed points of the action of \mathcal{C}_k on \mathbf{CP}^2 under the flow of the reduced \mathcal{C}_k -invariant Hamiltonian \widehat{H}_ϵ , we need to compute the eigenvalues of the corresponding linearized vector field (the frequencies) at the fixed point. If one of the frequencies is $\lambda \in \mathbf{C}$, then $-\lambda$, $\bar{\lambda}$ and $-\bar{\lambda}$ are also frequencies. Therefore there are generically four types of linear stability depending on the arrangement of the frequencies on the complex plane (see fig. B.1).

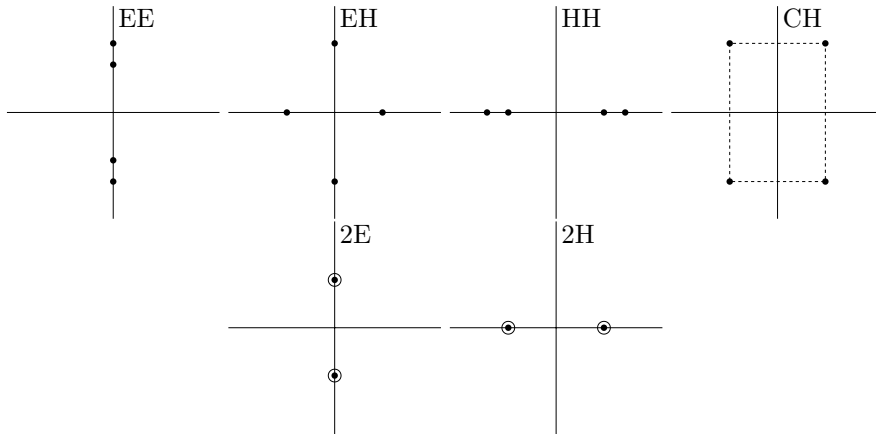


Figure B.1: Types of linear stability for an equilibrium of a 2 degree of freedom Hamiltonian. Starting at the upper left EE, EH, HH, CH, 2E, 2H.

- a. Elliptic-elliptic (EE) when all the frequencies are on the imaginary axis.
- b. Elliptic-hyperbolic (EH) when two of the frequencies are real and two are imaginary.
- c. Hyperbolic-hyperbolic (HH) when all frequencies are real.

- d. Complex hyperbolic (CH) when λ is neither real nor imaginary and the frequencies form a quadruplet $\lambda, -\lambda, \bar{\lambda}, -\bar{\lambda}$.

There are also other nongeneric cases in the space of all possible quadratic Hamiltonians. We are interested mainly in the following two cases:

- e. Two pairs of equal frequencies on the imaginary axis $\pm i\lambda$ (twice) with $\lambda \in \mathbf{R}$. We denote this case by 2E and we call it *degenerate elliptic*.
- f. Two pairs of equal frequencies on the real axis $\pm\lambda$ (twice) with $\lambda \in \mathbf{R}$. We denote this case by 2H and we call it *degenerate hyperbolic*.

As we will see later, some of these nongeneric cases become generic in the presence of particular symmetries.

B.2 Morse inequalities and the Euler characteristic

A function f defined on a manifold M is called a Morse function if all its stationary points $m \in M$ are nondegenerate, i.e., the determinant of the Hessian at m is not zero, $\det \partial^2 f(m) \neq 0$. The *Morse index* j of a nondegenerate stationary point m of f is defined as the number of negative eigenvalues of $\partial^2 f(m)$. Stationary points of a Morse function f must obey certain relations, called *Morse inequalities*, that are expressed in terms of the *Betti numbers*. The $\dim M + 1$ Betti numbers b_j , $j = 0, \dots, \dim M$, are nonnegative integers that depend only on topological properties of M . These numbers and the *Euler characteristic* $B_{\dim M} = \sum_{j=0}^{\dim M} (-1)^j b_j$ for the spaces encountered in our work are given below.

manifold M	$\dim M$	Betti numbers	$B_{\dim M}$
\mathbf{CP}^2	4	$b_0 = 1, b_1 = 0, b_2 = 1, b_3 = 0, b_4 = 1$	3
$\mathbf{CP}^1 \sim \mathbf{S}^2$	2	$b_0 = 1, b_1 = 0, b_2 = 1$	2
\mathbf{S}^1	1	$b_0 = 1, b_1 = 1$	0

If c_j is the number of stationary points of f with Morse index j , and

$$\begin{aligned} C_j &= c_j - C_{j-1} \text{ for } j = 1, \dots, \dim M, \text{ and } C_0 = c_0, \\ B_j &= b_j - B_{j-1} \text{ for } j = 1, \dots, \dim M, \text{ and } B_0 = b_0, \end{aligned}$$

then the Morse inequalities are

$$C_j \geq B_j \text{ for } j = 0, \dots, n-1, \text{ and } C_{\dim M} = B_{\dim M}. \quad (\text{B.1})$$

Specifically, in the case of \mathbf{CP}^2 the inequalities (B.1) become

$$\begin{aligned} c_0 &\geq 1, & c_1 - c_0 &\geq -1, & c_2 - c_1 + c_0 &\geq 2, \\ c_3 - c_2 + c_1 - c_0 &\geq -2, & c_4 - c_3 + c_2 - c_1 + c_0 &= 3. \end{aligned} \quad (\text{B.2})$$

Remark B.1. The minimal number of stationary points of a Morse function h on \mathbf{CP}^2 in the absence of symmetries is three. When h has just three stationary points, Morse inequalities (B.2) become equalities and h is called a *perfect* Morse function.

In a 1-DOF system the correspondence between the two stability types and the Morse index is simple: a stable point can be of index 0 or 2, while an unstable point has Morse index 1.

Lemma B.2. *In 2-DOF Hamiltonian systems we have the following relation of possible linear stability types and Morse indices.*

Morse index	0 or 4	1 or 3	2
Stability type	EE	EH	EE, HH, CH

Proof. Consider normal forms of quadratic Hamiltonians for 2-DOF systems [91] and compute possible Morse indices for each one of them. \square

B.3 Linearization near equilibria on \mathbf{CP}^2

We explain how to compute linearized equations of motion in a local symplectic chart $T^*\mathbf{R}^2(\xi)$ at the stationary point $\xi \in \mathbf{CP}^2(n)$ in order to determine linear stability of ξ . Note that even though different local charts can be chosen, the linear stability type of ξ or the Morse index of ξ do not depend on the choice of coordinates.

We denote invariants in (1.5) as π_j , $j = 1, \dots, 9$, and use four of these invariants as coordinates α_k , $k = 1, \dots, 4$, in $T^*\mathbf{R}^2(\xi)$. If α 's are chosen correctly then it should be possible to express the remaining five invariants β_l , $l = 1, \dots, 5$ near ξ in terms of α 's and n using relations Σ_i , $i = 0, \dots, 9$ in (1.6). We assure this requirement by means of the implicit function theorem. We take the 9×10 Jacobian matrix $\partial\Sigma_i/\partial\pi_j$ evaluated at ξ , where $i = 0, \dots, 9$ and $j = 1, \dots, 9$, and select 5 rows and 5 columns of this matrix so that the determinant of the resulting 5×5 submatrix is non-zero. Invariants β_1, \dots, β_5 correspond to the selected columns, and relations $\tilde{\Sigma}_m(\beta; \alpha, n)$, $m = 1, \dots, 5$, correspond to the selected rows; note that $\Sigma_0 \in \{\tilde{\Sigma}\}$. We can now solve the relations $\{\tilde{\Sigma}_m\}$ for β_l in terms of α_k and n . If the choice of $\{\beta\}$ and $\{\tilde{\Sigma}\}$ is not unique, we aim at such choice that yields the simplest possible expressions $\beta_l(\alpha, n)$.

In order to study the system near ξ , we introduce the displacements $\delta\alpha_k$ of α_k from their values $\alpha_k(\xi)$, i.e., $\delta\alpha_k = \alpha_k - \alpha_k(\xi)$. The local coordinates $\delta\alpha = (\delta\alpha_1, \dots, \delta\alpha_4)$ are not necessarily canonical coordinates in $T^*\mathbf{R}^2(\xi)$. However, it is always possible to find such linear transformation

$$(\chi, \psi) = (\chi_1, \chi_2, \psi_1, \psi_2) = B \cdot \delta\alpha$$

that the variables (χ, ψ) are canonical at $(\chi, \psi) = 0$. The Poisson brackets of these variables evaluated near $(\chi, \psi) = 0$ are $\{\chi_1, \chi_2\} = \{\psi_1, \psi_2\} = \{\chi_1, \psi_2\} = \{\chi_2, \psi_1\} = \mathcal{O}(\chi, \psi)$ and $\{\chi_1, \psi_1\} = \{\chi_2, \psi_2\} = 1 + \mathcal{O}(\chi, \psi)$.

C

Classical and quantum monodromy

C.1 Classical monodromy

Consider a two degree of freedom Hamiltonian system with Hamiltonian H , that is invariant with respect to a Hamiltonian \mathbf{S}^1 action generated by the momentum J . In other words, J is a first integral of X_H . Moreover, we assume that J and H are functionally independent. The energy-momentum map \mathcal{EM} is defined as

$$\mathcal{EM} : \mathbf{R}^4 \rightarrow \mathbf{R}^2 : p \mapsto (H(p), J(p))$$

Let \mathcal{R} be the set of regular values of \mathcal{EM} . The following famous result provides a characterization of the compact regular fibers of \mathcal{EM} .

Theorem C.1 (Arnol'd-Liouville). *If $(h, j) \in \mathcal{R}$ and $\mathcal{EM}^{-1}(h, j)$ is compact, then $\mathcal{EM}^{-1}(h, j)$ is a disjoint union of \mathbf{T}^2 . Moreover, in an open region U around $\mathcal{EM}^{-1}(h, j)$ there exist action-angle variables (I, θ) such that $\dot{I}_i = 0$ and $\dot{\theta}_i = \omega_i(I)$, $i = 1, 2$.*

Consider a closed path Γ in \mathcal{R} , and assume that for each point $(h, j) \in \mathcal{R}$, $\mathcal{EM}^{-1}(h, j)$ is a single \mathbf{T}^2 . $\mathcal{EM}^{-1}(\Gamma)$ is a \mathbf{T}^2 bundle over Γ . We say that the bundle $\mathcal{EM}^{-1}(\Gamma)$ is *trivial* if it is diffeomorphic to $\mathbf{S}^1 \times \mathbf{T}^2$.

Definition C.2. A system has *monodromy* if there is a path Γ for which the bundle $\mathcal{EM}^{-1}(\Gamma)$ is not trivial.

The importance of monodromy is due to the following theorem by Duistermaat [29].

Theorem C.3 (Duistermaat). *A system with monodromy has no globally defined action-angle variables.*

Let (h_0, j_0) denote a point on a closed path Γ . The classifying map of the \mathbf{T}^2 bundle $\mathcal{EM}^{-1}(\Gamma) \rightarrow \Gamma$ induces a linear automorphism on the first homology group $H_1(\mathcal{EM}^{-1}(h_0, j_0), \mathbf{Z})$ of $\mathcal{EM}^{-1}(h_0, j_0)$. The matrix of this automorphism is called the *monodromy* matrix. A system has monodromy when the monodromy matrix is not the identity.

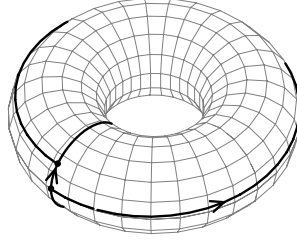


Figure C.1: The flow of X_H and X_J on a torus and the definition of the first return time.

Usually, instead of studying directly the linear automorphism induced to the first homology group we study the period lattice:

Definition C.4. The *period lattice* $P_{h,j}$ of the regular torus $\mathcal{EM}^{-1}(h,j)$ is the set of points $(t_1, t_2) \in \mathbf{R}^2$ for which $\phi_J^{t_1} \circ \phi_H^{t_2}(p) = p$, where ϕ_J^t, ϕ_H^t are the flows of the vector fields X_J and X_H respectively and $p \in \mathcal{EM}^{-1}(h,j)$.

Consider the flow of X_H and X_J on each torus. The flow of X_J gives closed orbits of period 2π . This means that $2\pi J$ can be considered an action variable I_1 . The flow of X_H gives orbits that are in general not closed. The situation is depicted in figure C.1.

In order to define a second action variable I_2 , consider an orbit γ of X_H that begins at a point p on the torus $\mathcal{EM}^{-1}(h,j)$. Consider also the orbit γ_1 of $X_{I_1} \equiv X_J$ that begins at the same point p . γ intersects γ_1 after time $T(h,j)$ at a point p' . $T(h,j)$ is called the first return time. The time it takes for the orbit γ_1 to go from p to p' is called the rotation number $\Theta(h,j)$. Define the vector field

$$X_{I_2} = -\Theta(h,j)X_J + T(h,j)X_H$$

It is easy to prove that an orbit γ_2 of X that begins at p will come back at the same point after time 2π . Therefore γ_1 and γ_2 are basis cycles for $H_1(\mathcal{EM}^{-1}(h,j), \mathbf{Z})$. The second action I_2 is defined by $X_{I_2} \lrcorner \omega = dI_2$.

It is easy to see that the period lattice $P_{h,j}$ is spanned by the vectors $v_1 = (2\pi, 0)$ and $v_2 = (-\Theta(h,j), T(h,j))$. The importance of the period lattice is due to the following result

Lemma C.5. *The bundle $\bigcup_{(h,j) \in \Gamma} P_{h,j} \rightarrow \Gamma$ is isomorphic to the bundle $\bigcup_{(h,j) \in \Gamma} H_1(\mathcal{EM}^{-1}(h,j), \mathbf{Z}) \rightarrow \Gamma$.*

This means that the classifying map of the \mathbf{T}^2 bundle over Γ induces the same linear automorphism to P_{h_0, j_0} as it does to $H_1(\mathcal{EM}^{-1}(h_0, j_0), \mathbf{Z})$. Therefore, instead of studying directly the homology group we can study the period lattice and in particular the behaviour of the rotation number and the first return time.

C.2 Quantum monodromy

Monodromy can be visualized in the joint quantum spectrum of a Liouville integrable system. In this section we consider the semiclassical approximation.

The joint spectrum is defined as the points $(h, j) \in \mathbf{R}^2$ for which the actions I_i on the torus $\mathcal{EM}^{-1}(h, j)$ satisfy the condition

$$I_i = \hbar(n_i + \mu_i) \quad (\text{C.1})$$

where $n_i \in \mathbf{Z}$ and μ_i are the Maslov indices.

This defines a lattice on the image of \mathcal{EM} . If we consider a cell of the lattice and we transport along a path we find that when we return to the initial point the cell may have changed (see figure C.2 for the case of the linear spherical pendulum). In this case we have *quantum* monodromy.

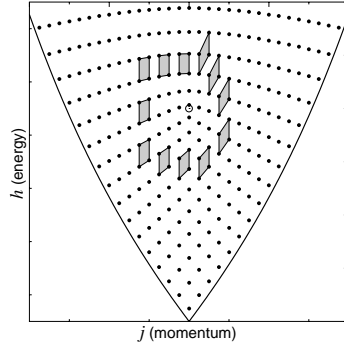


Figure C.2: Quantum monodromy in the spherical pendulum. The elementary cell is transported along a path around the critical point. The path begins above the critical point and goes anticlockwise. When the cell returns to the original point it has changed.

The relation between classical and quantum monodromy was proven in [88]. We give here an informal discussion of this relation.

Consider the integrable foliation defined by two integrals $F_1 = J$ and $F_2 = H$. Suppose that a cell of the lattice is spanned by the vectors k_1 and k_2 . Then, to first order, we have that

$$k_i dI_j = \hbar \delta_{ij} \quad (\text{C.2})$$

where

$$dI_j = \left(\frac{\partial I_j}{\partial F_1}, \frac{\partial I_j}{\partial F_2} \right) \quad (\text{C.3})$$

Assume that after a tour around the critical point the actions change according to the linear transformation $(M^{-1})^T$, i.e.

$$\begin{pmatrix} I'_1 \\ I'_2 \end{pmatrix} = (M^{-1})^T \begin{pmatrix} I_1 \\ I_2 \end{pmatrix} \quad (\text{C.4})$$

Then the cycles γ_1, γ_2 transform according to

$$\begin{pmatrix} \gamma'_1 \\ \gamma'_2 \end{pmatrix} = (M^{-1})^T \begin{pmatrix} \gamma_1 \\ \gamma_2 \end{pmatrix} \quad (\text{C.5})$$

This means in particular that the linear automorphism of $H_1(\mathbf{T}^2, \mathbf{Z})$ is given by the matrix M .

When we transport the initial cell spanned by the vectors k_1, k_2 along a path we obtain a new cell spanned by the vectors k'_1, k'_2 . Then we can easily prove using the relations $k'_i dI'_j = \hbar \delta_{ij}$ and (C.4), that the two pairs of vectors are related by the monodromy matrix

$$\begin{pmatrix} k'_1 \\ k'_2 \end{pmatrix} = M \begin{pmatrix} k_1 \\ k_2 \end{pmatrix} \quad (\text{C.6})$$

This means that we can see the existence of monodromy by considering a cell of the joint spectrum lattice and transporting it around a path. Because of the previous relations the result is exact in the limit $\hbar \rightarrow 0$. Notice that in order to compute practically the quantum monodromy, \hbar should be small enough with respect to the dimensions of the image of \mathcal{EM} in order to have a large enough number of cells to be able to move the cell around.

Personal papers

- [1] K. Efstathiou, D. A. Sadovskii, and R. H. Cushman. Linear Hamiltonian Hopf bifurcation for point group invariant perturbations of the 1:1:1 resonance. *Proc. Roy. Soc. London, Ser. A*, 459:2997–3019, 2003.
- [2] K. Efstathiou, D. A. Sadovskii, and B. I. Zhilinski. Analysis of rotation-vibration relative equilibria on the example of a tetrahedral four atom molecule. *SIAM J. Appl. Dyn. Syst. (SIADS)*, 2004. in print.
- [3] K. Efstathiou, R. H. Cushman, and D. A. Sadovskii. Hamiltonian hopf bifurcation of the hydrogen atom in crossed fields. *Physica D*, 2004. in print.
- [4] K. Efstathiou and D. A. Sadovskii. Perturbations of the 1:1:1 resonance with tetrahedral symmetry: a three degree of freedom analogue of the two degree of freedom Hénon-Heiles Hamiltonian. *Nonlinearity*, 17:415–446, 2004.
- [5] K. Efstathiou, M. Joyeux, and D. A. Sadovskii. Does the $\text{HCN} \leftrightarrow \text{CNH}$ molecule have monodromy or global bending quantum number? *Phys. Rev. A*, 2004. in print.
- [6] K. Efstathiou and D. A. Sadovskii. Monodromy in the hydrogen atom in crossed fields as a result of Hamiltonian Hopf bifurcation. in preparation.
- [7] K. Efstathiou and D. A. Sadovskii. Quadratic deformations of the spherical pendulum. in preparation.
- [8] K. Efstathiou, R. H. Cushman, and D. A. Sadovskii. Fractional monodromy in the 1: – 2 resonance. in preparation.

Bibliography

- [9] R. Abraham and J. Marsden. *Foundations of Mechanics*. Addison-Wesley, Reading Mass., 2nd edition, 1978.
- [10] V. I. Arnol'd. Proof of a theorem of A.N. Kolmogorov on the invariance of quasi-periodic motions under small perturbations of the hamiltonian. *Russian Math. Surveys*, 18(5):9–36, 1963.
- [11] V. I. Arnol'd. *Mathematical methods of classical mechanics*, volume 60 of *Graduated Texts in Mathematics*. Springer-Verlag, New York, 2nd edition, 1989. Translated by K. Vogtmann and A. Weinstein; original Russian edition *Matematicheskie Metody Klassicheskoi Mekhaniki*. Nauka, Moscow, 1974.
- [12] V. I. Arnol'd. *Huygens and Barrow, Newton and Hooke*. Springer, 1990.
- [13] V. I. Arnol'd, V. V. Kozlov, and A. I. Neishtadt. *Mathematical Aspects of Classical and Celestial Mechanics*. Springer-Verlag New York Inc., 2 edition, 1996.
- [14] L. Bates and M. Zou. Degeneration of Hamiltonian monodromy cycles. *Nonlinearity*, 6:313–335, 1993.
- [15] G. D. Birkhoff. *Dynamical Systems*. AMS, Providence, RI, 1927.
- [16] D. Buchanan. Trojan satellites—limiting case. *Trans. R. Soc. Canada*, 35:9–25, 1941.
- [17] R. C. Churchill, M. Kummer, and D. L. Rod. On averaging, reduction and symmetry in Hamiltonian systems. *J. Diff. Eqns.*, 49:359–414, 1983.
- [18] R. C. Churchill, G. Pecelli, and D. L. Rod. A survey of the Hénon-Heiles Hamiltonian with applications to related examples. In G. Casati and J. Ford, editors, *Stochastic behavior in classical and quantum Hamiltonian systems*, volume 93 of *Lecture Notes in Physics*, pages 76–136, Berlin, 1979. Springer.
- [19] R. H. Cushman. A survey of normalization techniques applied to perturbed Keplerian systems. In K. Jones et al, editor, *Dynamics Reported*, volume 1 of *new series*, pages 54–112, New York, 1991. Springer-Verlag.
- [20] R. H. Cushman and L. Bates. *Global aspects of classical integrable systems*. Birkhäuser, 1997.

- [21] R. H. Cushman and J. J. Duistermaat. Non-Hamiltonian monodromy. *J. Diff. Eqs.*, 172:42–58, 2001.
- [22] R. H. Cushman, R. Ferrer, and H. Hanßmann. Singular reduction of axially symmetric perturbations of the isotropic harmonic oscillator. *Nonlinearity*, 12:389–410, 1999.
- [23] R. H. Cushman and D. A. Sadovskii. Monodromy perturbed Kepler systems: hydrogen atom in crossed fields. *Europhysics Letters*, 47:1–7, 1999.
- [24] R. H. Cushman and D. A. Sadovskii. Monodromy in the hydrogen atom in crossed fields. *Physica D*, 142:166–196, 2000.
- [25] R. H. Cushman and J. C. van der Meer. The Hamiltonian Hopf bifurcation in the Lagrange top. In *Lecture Notes in Mathematics*, volume 1416, pages 26–38. 1991.
- [26] R. H. Cushman and S. Vu Ngoc. Sign of the monodromy for Liouville integrable systems. *Ann. Henri Poincaré*, 3:883–894, 2002.
- [27] A. Deprit. Canonical transformations depending on a small parameter. *Cel. Mech.*, 1:12–30, 1969.
- [28] A. Deprit and J. Henrard. A manifold of periodic orbits. *Adv. Astron. Astroph.*, 6:2–124, 1968.
- [29] J. J. Duistermaat. On global action-angle coordinates. *Comm. Pure Appl. Math.*, 33:687–706, 1980.
- [30] J. J. Duistermaat. Bifurcations of periodic solutions near equilibrium points of Hamiltonian systems. preprint 300, Dept. of Mathematics, University of Utrecht, August 1983. 6 lectures given at the CIME course on *Bifurcation theory and applications*, Montecatini Terme, Italy, 1983.
- [31] J. J. Duistermaat. The monodromy in the Hamiltonian Hopf bifurcation. *Z. Angew. Math. Phys.*, 49:156–161, 1998.
- [32] R. Essers, J. Tennyson, and P. E. S. Wormer. An SCF potential energy surface for Lithium Cyanide. *Chem. Phys. Lett.*, 89:223–227, 1982.
- [33] D. Farrelly and K. Krantzman. Dynamical symmetry of the quadratic Zeeman effect in hydrogen: Semiclassical quantization. *Phys. Rev. A*, 43:1666–1668, 1991.
- [34] D. Farrelly and J. A. Milligan. Action-angle variables for the diamagnetic Kepler problem. *Phys. Rev. A*, 45:8277–8279, 1992.
- [35] D. Farrelly, T. Uzer, P. E. Raines, J. P. Skelton, and J. A. Milligan. Electronic structure of Rydberg atoms in parallel electric and magnetic fields. *Phys. Rev. A*, 45:4738–4751, 1992.
- [36] S. Ferrer, M. Lara, J. Palacián, J. F. San Juan, A. Viartola, and P. Yanguas. The Hénon and Heiles problem in three dimensions. I. Periodic orbits near the origin. *Int. J. Bif. Chaos*, 8:1199–1213, 1998.

- [37] S. Ferrer, M. Lara, J. Palacián, J. F. San Juan, A. Viartola, and P. Yanguas. The Hénon and Heiles problem in three dimensions. II. Relative equilibria and bifurcations in the reduced system. *Int. J. Bif. Chaos*, 8:1215–1229, 1998.
- [38] E. Flöthmann, J. Main, and K. H. Welge. The Kepler ellipses of the hydrogen atom in crossed electric and magnetic fields. *J. Phys. B*, 27(13):2821–2833, 1994.
- [39] E. Flöthmann and K. H. Welge. Crossed-field hydrogen atom and the three-body Sun-Earth-Moon problem. *Phys. Rev. A*, 54:1884–1888, 1996.
- [40] N. Fulton, J. Tennyson, D. A. Sadovskii, and B. I. Zhilinskií. Nonlinear normal modes and localized vibrations of H_3^+ and D_3^+ . *J. Chem. Phys.*, 99:906–918, 1993.
- [41] H. Goldstein. *Classical Mechanics*. Addison-Wesley Publishing Company, Inc., 2nd edition, 1980.
- [42] M. Golubitsky, I. Stewart, and D. Schaeffer. *Singularities and Groups in Bifurcation Theory*, volume 69 of *Appl. Math. Sciences*. Springer Verlag, 1988.
- [43] W. Gröbner. *Die Lie-Reihen und ihre Anwendungen*. Deutscher Verlag der Wissenschaftern, Berlin, 1960.
- [44] M. C. Gutzwiller. *Chaos in Classical and Quantum Mechanics*. Springer Verlag, 1991.
- [45] H. Hanßmann and J. C. van der Meer. On non-degenerate Hamiltonian Hopf bifurcations in 3DOF systems. preprint.
- [46] H. Hanßmann and J. C. van der Meer. On the Hamiltonian Hopf bifurcations in the 3D Hénon-Heiles family. *Journal of Dynamics and Diff. Equations*, 14:657–695, 2002.
- [47] H. Hanßmann and J. C. van der Meer. On the Hamiltonian Hopf bifurcations in the 3D Hénon-Heiles family. *Journal of Dynamics and Diff. Equations*, 14:657–695, 2002.
- [48] H. Hanßmann and J. C. van der Meer. Algebraic methods for determining Hamiltonian Hopf bifurcations in three-degree-of-freedom systems. Technical Report RANA 03-14, Technische Universiteit Eindhoven, 2003.
- [49] G. J. Harris, O. L. Polyansky, and J. Tennyson. Ab initio spectroscopy of HCN/HNC. *Spectrochimica Acta A*, 58:673–690, 2002.
- [50] K. T. Hecht. Vibration-rotation energies of tetrahedral XY_4 molecules. I. Theory of spherical top molecules. *J. Mol. Spectrosc.*, 5:355–389, 1960.
- [51] M. Hénon and C. Heiles. The applicability of the third integral of motion: some numerical experiments. *Astron. J.*, 69:69–73, 1964.
- [52] M. Joyeux, D. A. Sadovskii, and J. Tennyson. Monodromy of the LiNC/NCLi molecule. *Chem. Phys. Lett.*, 2003. in print.

- [53] K. D. Krantzman, J. A. Milligan, and D. Farrelly. Semiclassical mechanics of the quadratic Zeeman effect. *Phys. Rev. A*, 45:3093–3103, 1992.
- [54] P. Kustaanheimo and E. Stiefel. Perturbation theory of Kepler motion based on spinor regularization. *J. Reine Angew. Math.*, 219:204–219, 1965.
- [55] M. Kuwata, A. Harada, and H. Hasegawa. Derivation and quantisation of Solov’ev’s constant for the diamagnetic Kepler motion. *J. Phys. A*, 23(14):3227–3244, 1990.
- [56] T. Levi-Civita. Sur la régularisation du problème des trois corps. *Acta Mathematica*, 42:99–144, 1920.
- [57] E. N. Lorentz. Deterministic nonperiodic flow. *J. Atmos. Sci.*, 20:130–141, 1963.
- [58] J. D. Louck and H. W. Galbraith. Eckart vectors, Eckart frames and polyatomic molecules. *Rev. Modern Phys.*, 48:69–106, 1976.
- [59] J. Marsden and A. Weinstein. Reduction of symplectic manifolds with symmetry. *Rep. Math. Phys.*, 5:121–130, 1974.
- [60] K. R. Meyer and G. R. Hall. *Introduction to Hamiltonian Dynamical Systems and the N-Body Problem*, volume 90 of *Applied Mathematical Sciences*. Springer-Verlag, New York, 1991.
- [61] K. R. Meyer and D. S. Schmidt. Periodic orbits near l_4 for mass ratios near the critical mass ratio of Routh. *Cel. Mech.*, 4:99–109, 1971.
- [62] L. Michel. Points critiques des fonctions invariantes sur une G -variété. *C. R. Acad. Sci. Paris*, 272:433–436, 1971.
- [63] L. Michel and B. I. Zhilinskiĭ. Symmetry, invariants, topology. Basic tools. *Physics Reports*, 341:11–84, 2001.
- [64] J. W. Milnor. *Morse Theory*. Princeton University Press, 1969.
- [65] J. Montaldi and T. Ratiu, editors. *Mechanics and Symmetry Summer School*, 1999.
- [66] J. Montaldi, M. Roberts, and I. Stewart. Periodic solutions near equilibria of symmetric Hamiltonian systems. *Phil. Trans. R. Soc. London, Ser. A*, 325:237–293, 1988.
- [67] J. Montaldi, M. Roberts, and I. Stewart. Existence of nonlinear normal modes of symmetric Hamiltonian systems. *Nonlinearity*, 3:695–730, 1990.
- [68] M. Morse and S. S. Cairns. *Critical point theory and differential topology*. Academic Press, New York, 1969.
- [69] J. Moser. On invariant curves of area-preserving mappings of an annulus. *Nachr. Akad. Wiss. Göttingen Math.-Phys. Kl.*, II:1–20, 1962.
- [70] D. Mumford. *Algebraic Geometry. I Complex Projective Varieties*, volume 221 of *Grundlehren*. Springer Verlag, Berlin, 1976.

- [71] N. N. Nekhoroshev. An exponential estimate of the time of stability of nearly integrable hamiltonian systems. *Russian Math. Surveys*, 32(6):1–65, 1977.
- [72] N. N. Nekhoroshev, D. A. Sadovskii, and B. I. Zhilinskiĭ. Fractional monodromy. in preparation.
- [73] N. N. Nekhoroshev, D. A. Sadovskii, and B. I. Zhilinskiĭ. Fractional monodromy of resonant classical and quantum oscillators. *Comptes Rendus Academie des Sciences*, ??–?, 2002.
- [74] J. I. Palmore. *Numerical Experimentation Into Effects of Varying the Mass Ratio on Periodic Solutions of the Restricted Problem of Three Bodies*. PhD thesis, Yale University, 1967.
- [75] C. W. Patterson. Quantum and semiclassical description of a triply degenerate anharmonic oscillator. *J. Chem. Phys.*, 83:4618–4632, 1985.
- [76] H. Poincaré. *Les méthodes nouvelles de la mécanique céleste*, volume 1–3. Gauthier-Villars, 1899.
- [77] D. L. Rod and R. C. Churchill. A guide to the Hénon-Heiles Hamiltonian. In S. N. Pnevmatikos, editor, *Singularities and Dynamical Systems*, pages 385–395, New York, 1985. Elsevier.
- [78] D. A. Sadovskii. Normal forms, geometry, and dynamics of atomic and molecular systems with symmetry. In D. Bambusi, M. Cadoni, and G. Gaeta, editors, *Symmetry and Perturbation Theory (Proceedings of the international conference SPT2001)*, pages –, Singapore, 2001. World Scientific.
- [79] D. A. Sadovskii and B. I. Zhilinskiĭ. Group theoretical and topological analysis of localized vibration-rotation states. *Phys. Rev. A*, 47:2653–2671, 1993.
- [80] D. A. Sadovskii and B. I. Zhilinskiĭ. Tuning the hydrogen atom in crossed fields between the Zeeman and Stark limits. *Phys. Rev. A*, 57:2867–2884, 1998.
- [81] D. A. Sadovskii, B. I. Zhilinskiĭ, and L. Michel. Collapse of the Zeeman structure of the hydrogen atom in an external electric field. *Phys. Rev. A*, 53:4064–4067, 1996.
- [82] G. Schwarz. Smooth functions invariant under the action of a compact Lie group. *Topology*, 14:63–68, 1975.
- [83] J. M. Souriau. *Structure des Systèmes Dynamiques*. Dunod, Paris, 1970.
- [84] G. Springer. *Introduction to Riemann surfaces*. Addison-Wesley, Reading, MA, 1957.
- [85] J. C. van der Meer. *The Hamiltonian Hopf bifurcation*, volume 1160 of *Lecture Notes in Mathematics*. Springer, New York, 1985.

- [86] J. C. van der Meer and R. H. Cushman. Orbiting dust under radiation pressure. In H. D. Doebner and J. D. Henning, editors, *Proc. of the XV Intl. Conference on Differential Geometric Methods in Theoretical Physics*, pages 403–414, Singapore, 1987. World Scientific.
- [87] T. van Mourik, G. J. Harris, O. L. Polyansky, J. Tennyson, A. G. Császár, and P. J. Knowles. Ab initio global potential, dipole, adiabatic and relativistic correction surfaces for the HCN/HNC system. *J. Chem. Phys.*, 115:3706–3718, 2001.
- [88] S. Vu Ngoc. Quantum monodromy in integrable systems. *Comm. Math. Phys.*, 203:465–479, 1999.
- [89] H. Waalkens, A. Junge, and H. R. Dullin. Quantum monodromy in the two-centre problem. *J. Phys. A*, 36:L307–L314, 2003.
- [90] A. Weinstein. Normal modes for nonlinear Hamiltonian systems. *Invent. Math.*, 20:47–57, 1973.
- [91] J. Williamson. On an algebraic problem concerning the normal forms of linear dynamical systems. *Amer. J. Math.*, 58:141–163, 1936.
- [92] E. Wilson, J. Decius, and P. Cross. *Molecular vibrations*. Mc-Graw Hill, New York, 1955.
- [93] N. Woodhouse. *Geometric quantization*. Oxford, 2nd edition, 1991.
- [94] P. Yanguas. *Integrability, Normalization and Symmetries of Hamiltonian Systems in 1–1–1 Resonance*. PhD thesis, Universidad Pública de Navarra, 1998.
- [95] B. I. Zhilinskií. Qualitative analysis of vibrational polyads: N mode case. *Chem. Phys.*, 137:1–13, 1989.
- [96] B. I. Zhilinskií. Hamiltonian monodromy as lattice defect. In *Workshop on Topology in Condensed Matter Physics*, 2003. in preparation.
- [97] N. T. Zung. A note on focus-focus singularities. *Diff. Geom. and Appl.*, 7:123–130, 1997.